

Investigation of Design Parameters for Increased Solar Potential of
Dwellings and Neighborhoods

Caroline Hachem

A Thesis
In the Department
of
Building, Civil, and Environmental Engineering

Presented in Partial Fulfillment of the Requirements
For the Degree of
Doctor of Philosophy (Building Engineering) at
Concordia University
Montreal, Quebec, Canada

September 2012

© Caroline Hachem, 2012

**CONCORDIA UNIVERSITY
SCHOOL OF GRADUATE STUDIES**

This is to certify that the thesis prepared

By: Caroline Hachem

Entitled: Investigation of Design Parameters for Increased Solar Potential of Dwellings and Neighborhoods

and submitted in partial fulfillment of the requirements for the degree of

Doctor of Philosophy (Building Engineering)

complies with the regulations of the University and meets the accepted standards with respect to originality and quality.

Signed by the final examining committee:

<u>Dr. Y. Shehine</u>	Chair
<u>Dr. I. Ugursal</u>	External Examiner
<u>Dr. A. Hammad</u>	External to Program
<u>Dr. R. Zmeureanu</u>	Examiner
<u>Dr. A. Bagshi</u>	Examiner
<u>Dr. A. Athienitis and Dr. P. Fazio</u>	Thesis Supervisor

Approved by

Chair of Department or Graduate Program Director

Dean of Faculty

ABSTRACT

Investigation of Design Parameters for Increased Solar Potential of Dwellings and Neighborhoods

Caroline Hachem, PhD

Concordia University, 2012

Neighborhoods can be designed to achieve net-zero energy consumption by addressing key design parameters for optimal solar collection, while allowing flexibility of building designs.

The current study comprises a comprehensive investigation of key parameters of dwelling shapes and neighborhood patterns for increased solar potential. Key findings and recommendations related to the solar potential and energy consumption of these dwellings and their assemblages are presented. Solar potential include the capture of solar radiation incident on, and transmitted by windows of near equatorial facing facades, and energy generation by building integrated photovoltaic systems covering complete near equatorial facing roof surfaces. The design parameters studied include geometric shapes of individual units, density of units and site layouts. Dwelling shapes include basic geometries and variations on these geometrical shapes. Density effect is analyzed through different assemblages of detached and attached housing units, as well as of parallel rows of units. Site layouts include straight road configurations and semi-circular road patterns, with the curve facing south or north. Roof designs are

investigated independently to explore concepts offering an increased electrical/ thermal energy generation potential of integrated photovoltaic/thermal systems.

The analysis employs the EnergyPlus simulation package to simulate configurations consisting of combinations of values of parameters in order to assess the effects of these parameters on the solar potential, as well as heating and cooling demand/consumption of dwellings and neighborhoods. Effects are evaluated as the change of the energy generation and energy demand/consumption, relative to reference configurations. The reference shape is a rectangle, the reference density is detached units and the reference layout is a straight road. The weather data for Montreal, Canada (45°N) are employed to represent a northern mid-latitude climate zone.

An evaluation procedure is proposed as decision-aiding tool to assess the performance of design alternatives. The evaluation is based on design parameter effects and weights assigned to different performance criteria. A holistic design methodology is developed to support the design and analysis of solar optimized residential neighborhoods. This methodology may be employed to assist the design of net-zero energy communities while allowing for different dwelling shapes, roads and density patterns.

ACKNOWLEDGMENTS

I would like to express my deepest gratitude to my supervisors, Dr. Andreas Athienitis and Dr. Paul Fazio, for their invaluable support and guidance. Through their material support and encouragement I was exposed to a broad range experiences including participation in numerous international conferences, becoming a member of the international energy agency (IEA) task 41- Solar Energy and Architecture, and assisting in different workshops and seminars.

I convey my sincere and deep gratitude to Dr. Ariel Hanaor, for his guidance, his support and his patience in revising and editing this work.

Recognition is due to a great number of individuals in Concordia University, particularly to Mrs. Lyne Dee for her valuable assistance, Mrs. Olga Soares, and the administrative staff in general.

This project was made possible through the major Alexander Graham Bell Scholarship of the Natural Sciences and Engineering Research Council of Canada (NSERC), ASHRAE grant-in aid award and from NSERC discovery grants held by Dr. Athienitis and Dr. Fazio and by the Faculty of Engineering and Computer Science of Concordia University. Their financial supports to this project are greatly appreciated.

This work was also partly supported by the NSERC Smart Net-zero Energy Buildings Strategic Research Network.

TABLE OF CONTENTS

List of Figures.....	ix
List of Tables.....	xii
Nomenclatures.....	xiv
Introduction.....	1
Chapter I: Literature Survey.....	8
1.1. Energy Efficient and Net Zero Energy Housing.....	8
1.1.1. Energy Efficient Houses.....	10
1.1.2 Active Solar Technologies.....	19
1.2. Energy Performance of Buildings and Neighborhoods.....	29
1.2.1. Energy and Building Shapes.....	30
1.2.2. Effects of Urban Design.....	34
1.2.3. Case studies.....	39
1.3. Tools.....	46
1.3.1. Modeling of Net-Zero Energy Solar Houses.....	46
1.3.2. Tools for Simulations of Urban Areas.....	48
Chapter II: Design and Methodology of the investigation.....	51
2.1. Outline of the Investigation.....	51
2.1.1 Background.....	51
2.1.2. Objectives and Scope.....	54
2.2. Methodology.....	56
2.2.1. Shape Study.....	57
2.2.2. Neighborhood Study.....	60
2.2.3. Roof Study.....	64
2.2.4. Design Methodology for Solar Neighborhoods.....	66
2.3. Tools.....	67
2.3.1. Selection of Simulation Software.....	67
2.3.2. Modeling and Simulations.....	69
Chapter III: Dwelling Shapes.....	73
3.1. Shape Design and Investigation.....	73
3.1.1 Basic Design Assumptions.....	74
3.1.2 Shape of Dwelling Units.....	75
3.1.3 Parametric Investigation.....	80
3.2 Presentation and Analysis of Results.....	85
3.2.1. Effects of Basic Shape Design.....	86
3.2.2. Variations of Basic Shapes.....	92

3.2.3. Energy Balance of Basic Shapes	103
Chapter IV: Neighborhood design	106
4.1 Design Parameters	106
4.1.1. Neighborhood Characteristics	107
4.1.2 Shading Effects.....	108
4.1.3 Neighborhood Design Parameters and their Values	110
4.1.4 Summary of Parametric Investigation	116
4.2 Presentation and Analysis of Results	118
4.2.1. Shading Effect	119
4.2.2 Density Effect.....	124
4.2.3. Effect of Site Layout.....	134
4.2.4. Evaluation of Energy Balance of Neighborhoods	143
Chapter V: Roofs	146
5.1. BIPV/T systems	147
Approximate Model.....	147
5.2. Basic Surface Parameters and their Effect	153
5.2.1. Effect of Tilt Angle.....	153
5.2.2. Effect of Orientation Angle	154
5.2.3. Combination of Tilt and Orientation Angles	157
5.3. Design of Roofs	158
5.3.1. Hip Roofs.....	159
5.3.2. Advanced Roof Design.....	160
5.3.3 Redesign of Units	164
5.4 Presentation and Analysis of Results	165
5.4.1. Roof Morphology Effect	165
5.4.2 Redesign of Units	172
5.4.3 Evaluation of Energy Balance	173
Chapter VI: Guidelines for Design of Solar Housing Units and Neighborhoods	176
6.1. Summary of Design Parameters and their Effects	176
6.1.1. Shape Parameters.....	176
6.1.2. Neighborhood Parameters	180
6.1.3. Roof Parameters	182
6.1.4. Tables of Performance.....	183
6.1.5 Design Considerations and Evaluation of Energy Performance	191
6.2. Solar Neighborhood Design Methodology	203
Chapter VII: Conclusion.....	215
References	230
Appendix A.....	242
Appendix B.....	244

Appendix C.....	248
Glossary.....	258

LIST OF FIGURES

Figure (i), Energy use per sector in Canada, based on data by NRCan (2010)	1
Figure (ii), Tree-Diagram representing the investigation of design parameters	7
Figure 1.1, Schematic illustrating major principles of a net –zero energy solar house for a cold (relatively sunny) climate.	10
Figure 1.2 Energy use in residential buildings, based on data by NRCan (2010)... ..	16
Figure 1.3, (a) Shingle PV, (b) PV Tiles (c) PV slates (Uni-Solar, 2011), (d) PV laminates (Solar Power Panels, 2011).	25
Figure 1.4, (a) Solar sandwich (Best Solar Energy, 2011), b) solar roof system (Systaic, 2011).....	25
Figure 1.5, (a) GreenPix Media Wall, (Beijing, China (© Simone Giostra & Partners/Arup); (b) Solar decathlon (façade from Onyx).	26
Figure 1.6, (a) PV panels as window shutters, (Colt international, 2011); (b) Solar awnings, (Solar Awning inbalance-energy.co.uk).....	27
Figure 1.7, PV cost index per cumulative production (Breyer and Gerlach, 2010).....	28
Figure 1.8, Aerial view of the Clarum houses (Clarum houses, 2003).....	40
Figure 1.9, Solarsiedlung am Schlierberg, Freiburg (Breisgau) (a) view of multi-story buildings and terrace houses, of Mixed-function development, (b) plan view, (c) detail of the overhang of a terrace house, (d) terrace house (Hagemann, 2007).	41
Figure 1.10, PV integration in Nieuwland, (a) on the roof of a parking lot; (b) in sport complex, (c) noise wall houses, (d) Prefab PV roofs (PV UPSCALE: Nieuwland, 2008).....	42
Figure 1.11 Jo-Town Kanokodai (MSK corporation, IEA PVPS-Task 10: Japan: Jo-Town Kanokodai)	43
Figure 2.1, Basic shapes.	58
Figure 2.2, Shape parameters.	59
Figure 2.3, Hip roof of a rectangular plan layout.	59
Figure 2.4, Roof shapes.	60
Figure 2.5, Overall site designs	62
Figure 2.6, Illustration of the density parameters.	63
Figure 2.7, Sample neighborhood configurations.....	63
Figure 2.8, Sample modified roof shapes for rectangular housing unit: a) split surface; b) folded plate.	66
Figure 3.1, Basic shapes.	77
Figure 3.2, Roof layouts of basic designs: a) Single ridge design for convex shapes; b) Double ridge designs in L, T; c) Roofs of U and H shapes.	80
Figure 3.3, Irregular roof shapes and PV integration. PV integrated surfaces are shown hatched. a) and b) represent roofs of V-WS60- variant and obtuse angle O-S, c) and d) represent V-EN60 and O-N. Basic shapes.	84
Figure 3.4, Transmitted radiations of windows in south façades for a WDD and for a SDD.	87
Figure 3.5, Window annual heat gain of all shapes associated with different south window areas.	88
Figure 3.6, WDD peak electricity generation and annual electricity generation for all basic shapes	89

Figure 3.7, Correlation between building envelope area and heating load for varying ratios of window areas.....	90
Figure 3.8, Effect of window size on annual energy consumption for heating of basic shapes	92
Figure 3.9, Relation between heating and cooling loads and aspect ratio of rectangular shape.....	93
Figure 3.10, Effect of orientation on transmitted radiation over a summer and winter design day (SDD and WDD).....	94
Figure 3.11, Heating load of rectangular units with various orientations.....	95
Figure 3.12, Annual energy production of selected L variants, (a) South Facing (V-ES and V-WS), (b) North Facing (V-EN and V-WN).	100
Figure 3.13, electricity generation for L shape with wing rotation (kW/m ²), (a) WDD, (b) SDD.	102
Figure 3.14, Annual heating and cooling of selected L and L variant shapes (a) South facing, (b) North facing.....	103
Figure 3.15, Energy use and energy supply of all basic shapes.	105
Figure 4.1, POA concept, shading and shaded units are represented by solid colour; shaded unit is in the centre of the circle; (a) and (b) single shading unit with different , (c) and (d) two shading units.....	109
Figure 4.2, 3-D view of the POA concept, (a) one shaded unit, (b) 2 shaded units	110
Figure 4.3, variation of site I, (a) south facing rectangle, (b) rectangles oriented to the street, (c) L-variants (V)	111
Figure 4.4, Configurations of shapes in different site layouts: a) site I; b) Site II; c) Site III.	112
Figure 4.5, Illustration of the POA concept for L variant in site II	112
Figure 4.6, Attached units in sites I, II and III. Site I: a) rectangular, b) L shape, c) L variants; Site II: d) trapezoid; e) obtuse-angle; f) L variants. Site III: g) trapezoid; h) obtuse-angle; i) L variants	114
Figure 4.7, row configurations of all studied shapes; (a) detached configurations; (b) attached configurations.....	116
Figure 4.8, Shading effect on annual solar radiation of a rectangular shape, (a) single shading unit-radiation as function of POA, (b) single shading unit- radiation as function of distance (d), (c) two shading units- radiation as function of POA, (d) two shading unit- radiation as function of distance (d).....	121
Figure 4.9, Shading effect on heating load of rectangular shape, a) single shading unit- heating load as function of POA, (b) single shading unit- heating load as function of distance (d), (c) two shading units- heating load as function of POA, (d) two shading unit- heating load as function of distance (d)	123
Figure 4.10, Comparison of heating and cooling demand between isolated units and detached units in a neighborhood.....	127
Figure 4.11, Heating consumption at different spacing between units	128
Figure 4.12 Reduction in transmitted radiation due to row effect for WDD U1, U2 and U3 are the units of the shaded row, U2 is the mid unit: a) Effect on selected configurations at 5m row separation; b) Effect on detached rectangular units, at separations of 5, 10 and 20 m	130
Figure 4.13, Detached units (a) Heating load of two rows relative to isolated rows, (b) Heating load of the two rows of detached units.....	132
Figure 4.14, Comparison of the row effect in site I – R1 exposed row, R2 obstructed row: (a) Comparison to isolated row, (b) Heating loads of the two rows	133
Figure 4.15, Ratio of heating load of the obstructed row to the unobstructed row as function of the minimal distance required to avoid shading	134
Figure 4.16, Comparisons of heating/ cooling loads and land use area of all configurations of the inclined road sites.....	137

Figure 4.17, Hourly electricity generation (from 4-6 AM to 6-8 PM) (kW) for site II, on a WDD: a) on the total south roof of attached rectangular (trapezoid); b) on the hip of L variants of detached L variants; c) on the hip of L variants of attached L variants	142
Figure 4.18, Heating and cooling loads of sites II and III relative to site I	143
Figure 4.19, Energy demand and production for isolated units of different shapes: a) Shapes of sites I and II; b) Shapes of site III.....	144
Figure 5.1, a) Cross-section illustrating an open loop BIPV/T system , b) schematic illustrating the thermal network in one control volume of the BIPV/T system	149
Figure 5.2, a) Q_u/Q_e for 45° tilt angle roof for one sunny day of each month, over a year; b) Q_u/Q_e for WDD of roofs with different tilt angles	152
Figure 5.3, Relation between air velocity and the average air change temperature in the cavity (ΔT), on a WDD.	152
Figure 5.4, Monthly electricity generation for different tilt angles	154
Figure 5.5, Effect of the angle of orientation on: (a) the electricity generation, (b) heat generation over the period between mid-October and mid-April.....	155
Figure 5.6, Effect of the angle of orientation on the monthly electricity generation of the BIPV/T systems.	156
Figure 5.7, Effect of the angle of orientation on the electricity generation, (a) 30° for the WDD, (b) 60° for the WDD, (c) 30° for the SDD, (d) 60° for the SDD.	157
Figure 5.8, Ratio of energy generation of different configurations to south facing BIPV/T system with 45 ° tilt angle.	158
Figure 5.9, Illustration of hip roofs of basic shapes	160
Figure 5.10, Split-surface roof designs: (a) configuration 1, side plates with 15° orientation from south; (b) configuration 2, side plates with 30° orientation from south.	162
Figure 5.11, Folded plate roof designs, (a) configuration 1 – basic 4-plate with 15° orientation of the central plates; (b) Configuration 2 – two basic 4-plate units with 30° orientation, (c) Configuration 3 – two basic 3-plate roof with 30° orientation.	163
Figure 5.12, Split- roof option with: (a) rectangular shape, (b) redesigned south facing façade.	164
Figure 5.13, Folded plates roof option with: (a) rectangular shape, (b) redesigned south facing façade.	165
Figure 5.14, Annual electricity generation of roofs with differing tilt-side angles and shapes (MWh)	168
Figure 5.15, Peak electricity generations (kW): a) Tilt angle 30°; b) Tilt angle 45°.	169
Figure 5.16, Electricity generation on design days for the plates of the 30°(E,W), 40° split-surface roof option, (a) SDD, (b) WDD.....	170
Figure 5.17, Energy consumption and production of rectangular units with different roof designs	174
Figure 6.1, Keys for color shades expressing the performance of design parameters; (a) Solar potential, (b) Energy demand.	184
Figure 6.2, Flow chart illustrating the design process of energy efficient residential neighborhoods.....	214

LIST OF TABLES

Table 1.1, Summary of case studies	44
Table 3.1, Main Characteristics and Electric Loads of Housing Units.....	75
Table 3.2, shape design parameters for basic cases.....	78
Table 3.3. Variations of L shapes	83
Table 3.4, Parameter combinations	85
Table 3.5, Energy performance of basic shapes	90
Table 3.6, Effect of window size on annual heating and cooling loads of basic shapes.....	91
Table 3.7, Effect of depth ratio on incident and transmitted radiation of L and U shapes	97
Table 3.8, Effect of DR on solar potential and energy performance	98
Table 3.9, Comparison of annual electricity generation of selected L variants to the reference case	100
Table 3.10, Energy consumption for all basic units	105
Table 4.1, Characteristics of the studied neighborhoods	107
Table 4.2, Some design characteristics of the site layouts.....	113
Table 4.3, Configurations simulated – Parameter combinations	117
Table 4.4, Design parameters of the neighborhood study	118
Table 4.5, Density effect on electricity generation in sites II and III for summer and winter design days (SDD and WDD), and annually	126
Table 4.6, Summary of the results analysis of the inclined road configurations	138
Table 4.7. Site layout effect on average electricity generation for summer and winter design days (SDD and WDD), and annually	140
Table 4.8, Ratio of energy production to consumption	145
Table 4.9, Ratio of energy production to total energy consumption of all configurations	145
Table 5.1, Electricity generation, heat generation and combined generation of various combinations	158
Table 5.2, Design Consideration Split- Roofs and Folded Plates’ Roofs	163
Table 5.3, Ratio of annual electricity generation of different variants of roofs, to the optimum roof (gable roof).....	167
Table 5.4, Yearly energy and heat generation of all hip roof options	168
Table 5.5, Comparison of Multi-Faceted Roof Design Options to the Gable Roof	171
Table 5.6, Energy Potential of the Multi-Faceted Roof Design Options.....	171
Table 5.7, Comparison of the Effect of Roof Shapes on Heating and Cooling, for the Rectangular Shape and the Redesigned Shapes.....	173
Table 5.8, Energy Production, Consumption and Energy Balance.....	175
Table 6.1, Shape Parameters and their Effects	185
Table 6.2, POA and Distance	186
Tables 6.3, Neighborhood patterns; 6.3 a- Straight layout	187
Table 6.3b- Layout with south facing curved road.....	189

Table 6.3c- Layout with north facing curved road	190
Table 6.4, Considerations for solar neighborhood design	191
Table 6.5a, Scenario #1, weights and grades of design objectives	197
Table 6.5b, Scenario #2, weights and grades of design objectives (including shift of peak timing generation as a performance criterion)	197
Table 6.6a, Evaluation of housing units' shapes- scenario 1	199
Table 6.6b, Evaluation of housing units' shapes- scenario 2.....	199
Table 6.7a, Sample evaluation of neighborhood design- scenario 1	201
Table 6.7b, Sample evaluation of neighborhood design- scenario 2	202

NOMENCLATURES

Symbols

A	Surface area
C_{air}	Specific heat of air
G	Solar irradiation
H	Total height of the shading building
h_c	Convective heat transfer coefficient in the cavity
M	Mass flow rate of air
Q_e	Electricity generation by the BIPV/T system
q_i	Heat source at the node i
Q_u	Heat carried by the air flow
SL	Shadow length
T	Temperature
U	Heat transfer coefficient
W	Air cavity width of the BIPV/T system
w	Width of the shading building
Greek Letters	
α	Solar altitude
ΔT	Difference between inlet and outlet air temperature of the BIPV/T system
η_{PV}	Electrical efficiency of the BIPV/T system
$\eta_{thermal}$	Thermal efficiency of the BIPV/T system
ψ	Azimuth of the surface
ϕ	Solar azimuth
Shapes	
β	Angle between the wings of L-variant shape
O-N	Variant of L shape with an obtuse angle between the wings, where the wings are north facing
O-S	Variant of L shape with an obtuse angle between the wings, where the wings are south facing
R	Rectangular shape
L-WS	L shape with the branch attached to the west end of the main wing towards the south
L-WN	L shape with the branch attached to the west end of the main wing towards the north
V-EN(#)	L variant with a branch attached to the east end of the main wing, facing

	north
V-WS	a variant with a branch attached to the west end of the main wing, facing south
SE (orientation)	South east
SW (orientation)	South west

Abbreviations and Acronyms

ACH	Air Change per Hour
AR	Aspect ratio
ASHRAE	American Soc. of Heating, Refrigerating and Air-Conditioning Engineers
BIPV	Building Integrated Photovoltaic
BIPV/T	Building Integrated Photovoltaic/Thermal
CEUD	Comprehensive Energy Use Database
CMHC	Canada Mortgage and Housing Corporation
COP	Coefficient of Performance of Heat Pump
CWEC	CWEC – Canadian Weather For Energy Calculations
DD	Degree Days
DHW	Domestic Hot Water
DR	Depth ratio
ECBCS	Energy Conservation in Buildings and Community Systems
ESP-r	Energy systems performance research-program
HDD	Heating Degree Days
HVAC	Heating, Ventilating and Air Conditioning
IEA	International Energy Agency
NZEB	Net- Zero Energy Buildings
NZESH	Net-Zero Energy Solar Houses
POA	Planar obstruction angle
PV	Photovoltaics
SDD	Summer Design Day
SHGC	Solar Heat Gain Coefficient
WDD	Winter Design Day

INTRODUCTION

Energy consumption in buildings accounts for 30% of Canada’s total energy consumption, and over 50% of Canada’s electricity consumption (Comprehensive Energy Use Database (CEUD), 2003). Residential buildings are responsible for 16% of Canada’s total energy consumption (Fig. (i)).

Implementation of energy efficiency measures in buildings enables reduction of energy consumption by up to 35% (ECBCS, 2011)). Energy efficiency measures are not sufficient, however, to address an expected increase in future energy demand of the building sector. Coupling energy efficiency measures with increased renewable energy production techniques (for example, cogeneration of heat and power), enables the generation of some or all of buildings’ energy consumption, thus reducing dependence on fossil fuel.

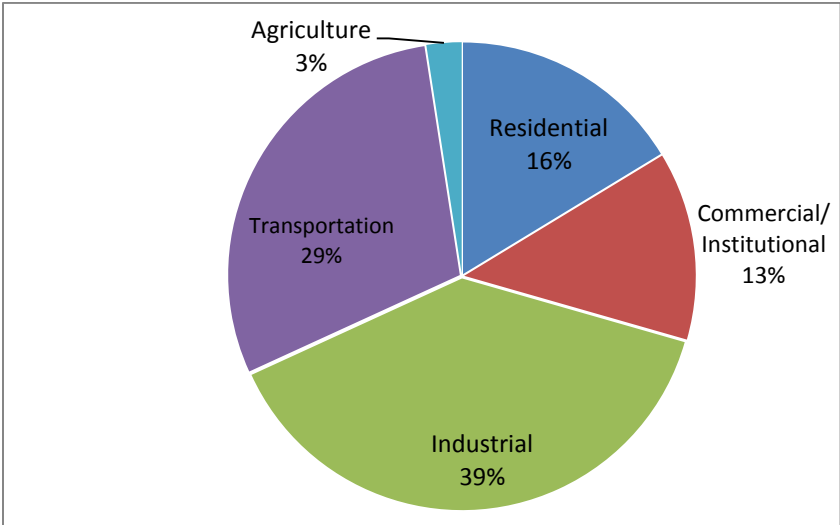


Figure (i), Energy use per sector in Canada, based on data by NRCan (2010)

Several international initiatives are aiming at achieving net zero energy buildings. These are buildings that generate energy to counterbalance their consumption (Torcellini and Crawley, 2006). Initiatives to implement stringent energy efficiency measures and to enhance energy production are starting to take shape, internationally (ECSBC News, 2011, ASHRAE Vision 2020 report, 2008). Policymakers around the world are embracing the concept of net zero energy buildings as a vital strategy to meet energy and carbon emission goals (Crawley et al, 2009, European Parliament 2009).

The principle of net zero energy can be applied on a larger scale than the individual building to achieve overall net-zero energy neighborhoods. This has the advantage of economy of scale, since some technologies are more efficient and economic when applied on a large scale than to individual projects (cogeneration of heat and power, geothermal technologies, solar technologies etc.). The design of energy efficient solar communities can potentially provide opportunities for seasonal storage, implementation of smart grids for power sharing between housing units, controlling peak electricity production and reducing utility peak demand. Additional advantages of expanding net zero concepts to the neighborhood scale include enabling design flexibility and increasing of rooftop surfaces for the integration of photovoltaic systems.

Notwithstanding the general interest in applying solar design principles in buildings and urban areas, there are still obstacles that hinder the implementation of solar technologies, and passive solar design principles, especially in urban planning. For instance, the effects of design parameters of buildings and neighborhoods on solar capture and utilization are not well defined. Existing design guidelines for passive solar

buildings or districts do not provide quantified data on the effects of key design parameters on the overall energy performance.

Design guidelines for passive solar energy efficient houses are limited largely to rectangular shapes. Lack of flexibility of design can deter architects and the public from integration of solar systems in buildings. Extending the range of energy efficient building shapes requires the understanding of the penalties and advantages associated with various shapes regarding energy performance. On the level of urban areas and neighborhood design, there is no systematic integrated design approach for passive solar design. Such approach should consider the interaction between individual units and methods of assemblage of these units in varying density configurations and site layouts.

Scope

This research investigates means for achieving net zero energy dwellings and neighborhoods through maximizing solar potential of dwelling units, isolated and in assemblages. In this study, solar potential refers to passive and active exploitation of solar radiation. Passive potential involves irradiation and transmission of heat and daylighting by fenestration of near-equatorial-facing facades. Active potential consists of generation of both electricity and thermal energy employing building integrated photovoltaic and photovoltaic/thermal systems (BIPV and BIPV/T). Neighborhood patterns are characterized by the density of dwelling units and the site layout, in addition to the units' shapes. The pilot location for the research is Montreal, Canada (latitude 45°N), representing mid-latitude locations in a northern climate.

The main contribution of this research consists of developing an innovative holistic design methodology to support the design and analysis of solar optimized residential buildings and neighborhoods. This design methodology is based on systematic investigation of design parameters of dwelling geometries and neighborhood patterns that govern their overall energy performance, separately and in combinations. The design methodology can serve as foundation for the development of comprehensive design guidelines and procedures for optimized net- zero energy communities, and can assist in shaping policies to realize such neighborhoods.

Overview of the Thesis

The thesis is divided into two main parts, an analytical part which investigates design parameters for increased solar potential of dwellings and neighborhoods, and a synthesis part presenting a methodology of design of such neighborhoods based on the aforementioned investigation. The first part, including Chapters III, IV and V is illustrated in a Tree-diagram (Fig. ii). The design methodology is presented in detail in Chapter VI (Flowchart of Figure 6.2). A brief outline of the six chapters forming the main body of this presentation is given below.

Chapter I is a survey of the pertinent literature. The chapter is divided into three main sections: introduction to energy efficient and net zero solar energy buildings, energy performance of buildings and neighborhoods, and building simulation tools. The first section includes a summary of energy efficiency measures and building integrated solar technologies. The focus of the second part is the effect of building shape on energy performance and potential to capture and utilize solar energy. The effect of urban design on energy performance and solar potential is discussed as well. The third part is dedicated

to simulation tools employed in the design process of net zero energy buildings and solar neighborhoods.

Chapter II presents the objectives, scope and methodology of the investigation. The general approach applied in each stage of the research is defined, and assumptions and limitations of each of these stages are discussed. The approach includes the design methodology employed in defining the dwelling' shape study, the neighborhood patterns as well as the roof design. Modeling and simulations employed in the analysis of the effects of parameters are also summarized.

Chapter III details the housing units' shape investigation. Details of the design parameters employed in the investigation are presented. Basic shapes of dwelling units and variations of some of these shapes are studied. The investigation includes the effects of key design parameters of these shapes on energy performance, which consists of solar potential and energy consumption, as well as the balance between energy supply from building integrated photovoltaics and the total energy consumption.

Chapter IV presents the neighborhood study. The objective of this chapter is to assess the effects of parameters associated with residential neighborhood design on the solar potential and energy balance of the neighborhood and of the individual dwelling units. The selection of dwelling shapes for the neighborhood investigation is based on results obtained in the study of shape effects (Chapter III).

Results of the simulation analysis are presented in terms of the effects of the design parameters on energy potential and generation and energy consumption of units in a neighborhood and the energy performance of the neighborhood as a whole.

Chapter V is a detailed analysis of roof design for increased potential of building integrated photovoltaic thermal (BIPV/T) systems. This chapter presents in depth-study of roof design and its effect on the combined electrical/thermal performance of the BIPVT systems, and the application of such roofs to actual housing units. The chapter includes the presentation of a numerical model employed to establish a correlation between the thermal and electrical energy production by the BIPV/T system. The effect on energy consumption for heating and cooling of redesigning rectangular units to fit the modified roof design is also investigated.

Chapter VI provides a summary of the main effects of the design parameters of dwellings and neighborhoods on their energy performance. This summary is presented in a matrix that relates design parameters to performance criteria. An evaluation method is demonstrated for selection among design alternatives. The chapter concludes with a proposed design methodology for solar optimized residential neighborhoods. This methodology details the main stages suggested to be implemented in the design process of such neighborhoods.

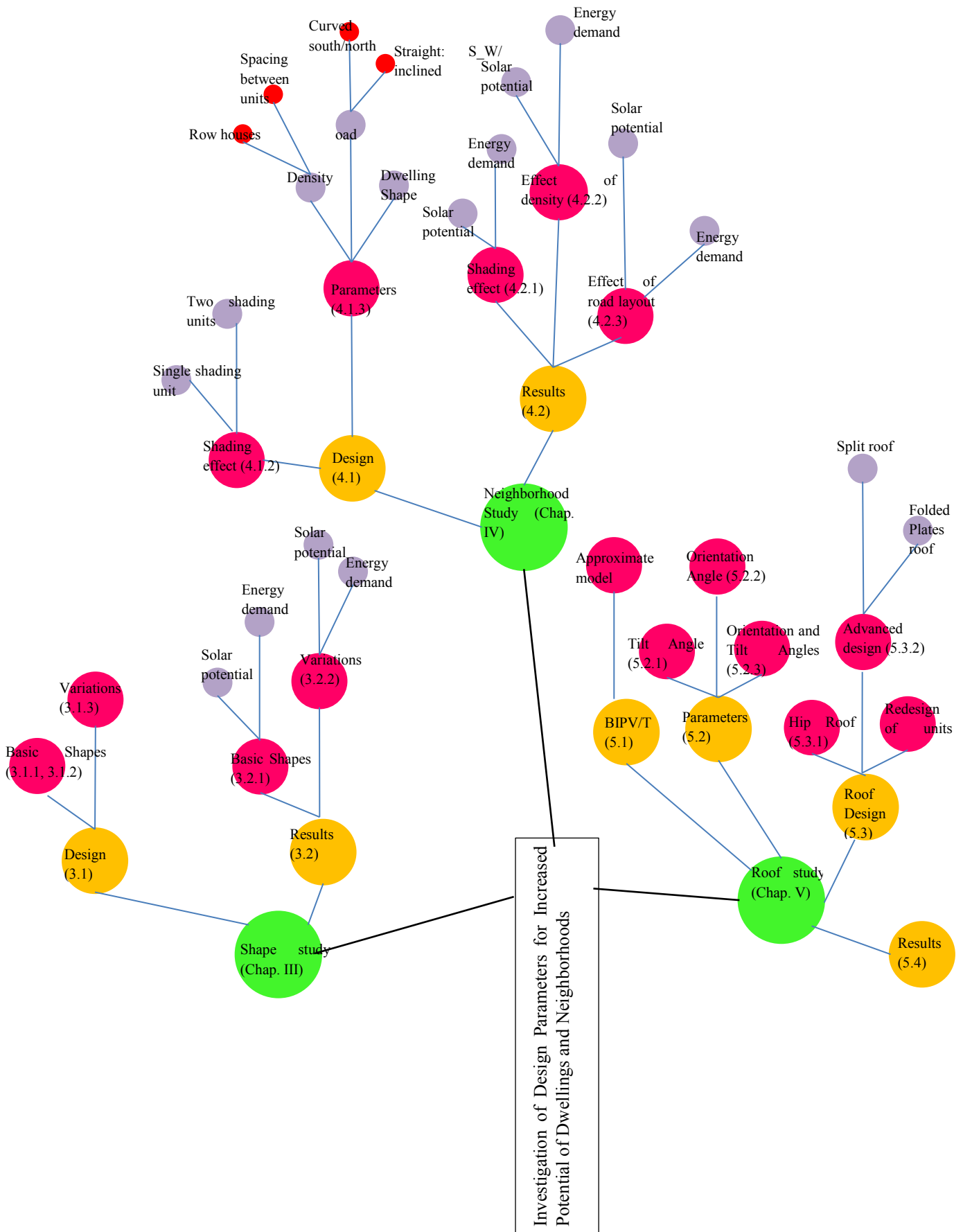


Figure (ii), Tree-Diagram representing the investigation of design parameters.

CHAPTER I: LITERATURE SURVEY

This chapter includes three main parts – energy efficient and net zero energy solar buildings; energy performance of buildings and neighborhoods; and building simulation tools. The first section provides a general introduction to energy efficient and net-zero solar energy buildings. The second part presents the effects of building shape on energy performance and its potential to capture and utilize solar energy, as studied in the literature, as well as the effects of urban form on energy consumption and solar potential. The third part outlines simulation tools that are employed in the design process of net zero energy buildings and in solar neighborhood design.

1.1 Energy Efficient and Net Zero Energy Housing

A net zero energy house can be defined as a house that generates as much energy as its overall load over a typical year (Torcellini and Crawley, 2006). A net zero energy *solar* house (NZESH) utilizes solar technologies to generate the energy required to reach the net zero energy status. Grid connected solar houses purchase electricity from the utility company to supply their demand during periods of limited availability of solar radiation, and counterbalance this energy debt by selling excess electricity production to the utility at high solar radiation periods.

The NZESH design concept relies on a two-fold approach: implementation of energy efficiency measures to minimize energy demand, and use of solar energy technologies (e.g. photovoltaic system (BIPV) and solar thermal collectors) to balance energy requirements on an annual basis (Pellant and Poissant, 2006). The realization of

NZESH especially on the level of communities, should consider the implementation of smart grids which communicate with smart building systems (including net metering technologies and control systems) to optimize electricity flows from/to these houses (Holmberg & Bushby, 2009).

Various indicators are employed to assess NZESH performance, for instance net energy consumption on site, net primary energy consumption, net energy costs, carbon emissions (Torcellini and Crawley, 2006; Tsoutsos et al., 2010). A relevant indicator is the Estimated Net Energy Produced (ENEP) (Iqbal, 2004; Parker, 2009), which is computed as the excess of energy generated by renewable sources over a period of time, after deducting the energy consumption of the building, over the same period (Kolokotsa et al, 2010). Applications of energy efficient and net zero energy buildings are reported in various sources (e.g. Hamada et al., 2003; Charon, 2009; Crawley et al., 2009).

Figure 1.1 is a schematic illustration of the key principles of a net zero solar energy house (or energy plus house). Passive design principles, such as the use of thermal mass and large glazed area, are applied together with building integrated photovoltaic thermal system (BIPV/T). In addition to electricity generation, BIPV/T systems allows heat capture from the rear part of the PV panels to be employed for space and/or water heating, so as to facilitate reaching net-zero energy status.

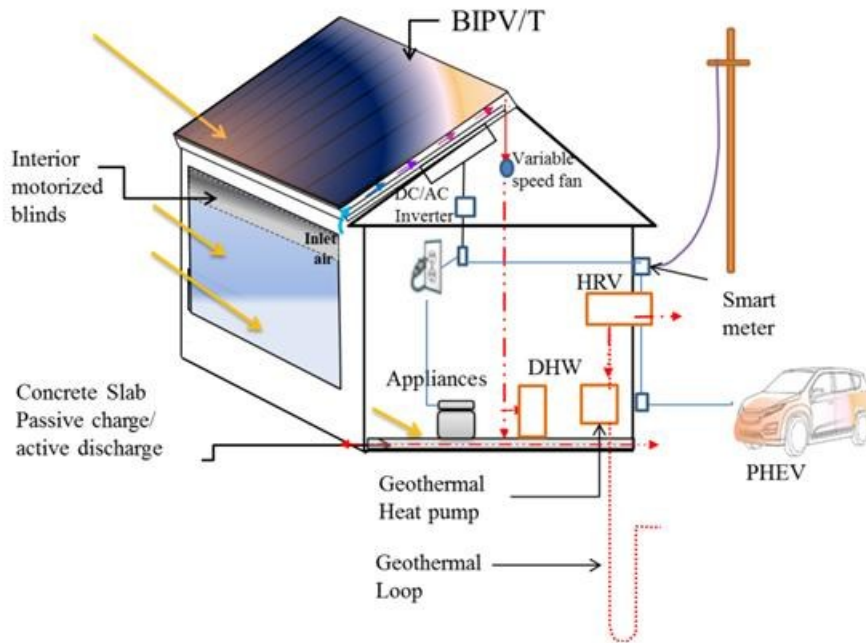


Figure 1.1, Schematic illustrating major principles of a net –zero energy solar house for a cold (relatively sunny) climate.

Following is a summary of passive and active solar design principles.

1.1.1. Energy Efficient Houses

Major technical developments have been implemented recently to achieve high energy efficiency buildings. New standards have been introduced in different parts of the world, aiming at reducing the total energy consumption of buildings, including heating, cooling, lighting and appliances loads. “PassivHaus” in Germany (Straube, 2009) and “Minergie” (Minergie, 2011) in Switzerland are successful examples of such standards.

In Canada the R-2000 program is an effective implementation of low-energy standards (NRCAN, 2009a). The R-2000 program in Canada typically achieves about 30% overall total reduction of energy consumption relative to standard housing. Energy

efficiency measures of the R-2000 Standard comprise requirements for energy efficient building envelope, design of mechanical systems and heat recovery ventilators, and upgrade of domestic hot water (DHW) systems. Requirements for energy efficient building envelope include thermal insulation level, airtightness, and window performance.

Energy efficient buildings utilize passive solar techniques in conjunction with other energy efficiency measures. The design of such buildings relies on an optimal passive solar design, to reduce heating and cooling load, in addition to the use of energy efficient appliances, lighting, DHW and auxiliary heat supply.

Passive Design Principles

Passive solar design involves the following strategies:

- Employing a holistic approach that relies on the integration of a building's architecture, envelope design and construction materials, together with the mechanical systems for heating and cooling, in both design and operation (Robertson and Athienitis, 2007).
- The collection, storage and redistribution of solar energy (Lechner, 2001).
- Cutting heat loss, maximizing solar heat gains in winter and passive cooling in summer, and providing daylighting, thus reducing the overall energy consumption (Hastings, et al., 2007).
- Daylighting management is another energy-efficient strategy that depends on the availability of solar radiation, and incorporates several technologies and design approaches. Daylighting can improve the quality of light in a space and it reduces

the energy required for artificial (ECSB Annex 29, 2010) .Geometrical shape of the building and windows' location and orientation, play an important role in daylight design of a building (Lechner 2001).

A well designed passive solar building may provide 45% to 100% of heating requirements, on a sunny winter day (ASHRAE, 2007). Principles of passive solar design are summarized in different sources (e.g. Arasteh et al., 2007; Athienitis and Santamouris, 2002, Pitts 1994). Key passive solar design principles include location and orientation of the building, building envelope design and characteristics, window size, orientation and properties (glazing), shading devices, and thermal mass. Characteristics of these parameters are summarized in the following.

Building Orientation

Building orientation constitutes the first and most fundamental step in passive solar design. The building should be oriented with the long axis running east-west, so as to have the largest facade equatorial facing (south facing in the northern hemisphere). This is due to the fact that east- and west-facing buildings can be potentially subjected to overheating during the cooling season, and to reduced heat gain during the heating season (Robertson and Athienitis, 2007).

Building Envelope

The R-2000 and Passivhaus standards demonstrate that improvement of the building envelope can reduce energy demand for space heating by 30% to 85% (Charon, 2005). Heat loss through the building envelope is due mainly to poor insulation, thermal bridges and air infiltration. Significant improvement to the building envelope can be

achieved through highly insulated wall and windows (including frames), and improved air tightness. Window effects on heat loss and characteristics are detailed below.

Heat loss from air infiltration is highly significant. The level of air tightness of a house is described by air changes per hour (ACH) at a 50 Pa pressure difference across the envelope. Air tightness in passive buildings should be in the order of 0.6 ACH (Klingenberg et al., 2008). This value is, however, usually hard to realize. High air tightness level can be achieved through appropriate construction methods that implement air barrier, sealants, and weather stripping (US DOE: EERE, 2011).

Glazing

Windows constitute the most critical surfaces of the building envelope, representing a significant heat loss source. Heat loss occurs through both glazing and framing of windows (Arasteh et al., 1989, Winkelmann, 2001). High insulated windows (low U-value), including glazing and frame, should be selected as a fundamental step to achieve energy efficient design.

The design of the near- equatorial facing windows should balance between low U-value of glazing and high solar heat gain coefficient (SHGC) and high visible transmittance, in order to optimize net energy gains. SHGC represents the portion of solar radiation transmitted and absorbed by the glazing; it is usually used to measure glazing's ability to transmit solar gains.

The glazing area on the equatorial facing facade depends on building characteristics, thermal control systems and local climate (Charron and Athienitis, 2006). In mid-latitudes, to optimize the solar potential of a building, equatorial facing windows

should cover 30% to 50% of wall area. Glazing on the other facades is minimized to reduce heat losses in winter and overheating in summer. Chiras (2002) recommends minimizing non-south facing glass to at most 4% of total floor space, for passive solar design in cold climates.

Thermal Mass

Thermal mass in a building can provide thermal storage and regulate diurnal temperature swing, providing thus better thermal comfort. Thermal mass absorbs daytime solar radiation and passively (or actively) releases the heat gain during the night (Athienitis and Santamouris, 2002). Thermal mass is usually implemented using large, concrete surface of high heat capacity.

The amount of thermal mass required in a building depends on the amount of glazing, as well as on the material properties of the mass. For instance, glazing area equal to 7% to 12% of the floor area requires a concrete slab thickness of about 100 mm to 150 mm (Chiras, 2002). The percentage of glazing can be increased by up to 20% when combination of solar design features such as solar spaces, thermal mass and controlled shading are implemented (Charron and Athienitis, 2006, CMHC 1998, Chiras, 2002).

Shading Devices

Appropriate solar shading devices can control indoor illumination, glare and solar heat gains, while saving energy demand for heating and lighting (Laouadi, 2009). For instance, highly reflective interior blinds can reduce heat gain by around 45% (WBDG, 2011). Shading devices are divided into two main categories, static and dynamic. Static devices are simple but they have limited capability of controlling solar gains.

Dynamic shading has more potential in controlling heat gains, and adapting this gain to the need. Extensive studies have examined the potential in energy savings of dynamic shading devices (manually or mechanically operated) including internal blinds (Foster and Oreszczyn, 2001; Tzempelikos and Athienitis, 2007), retractable awnings (Athienitis and Santamouris, 2002) and rollshutters (Laouadi, 2009).

Exterior insulated roll-shutters are found to be very effective under Canada's climate. Roll-shutters can reduce heating and cooling energy demand and summer electricity peak demand, as well as improve thermal conditions near windows (Laouadi, 2009). Retractable awnings on the other hand, enable the reduction by 80% of summer solar gains, although this is associated with reduced daylighting (Athienitis and Santamouris, 2002).

Energy Efficiency Measures

Energy efficiency measures implemented together with optimized passive solar design can assist in reducing the total energy demand in dwellings. Figure 1.2 presents energy consumption in residential buildings for various domestic functions in Canada. A summary of the main energy efficiency strategies that can be considered for the improvement of energy efficiency in buildings is presented below.

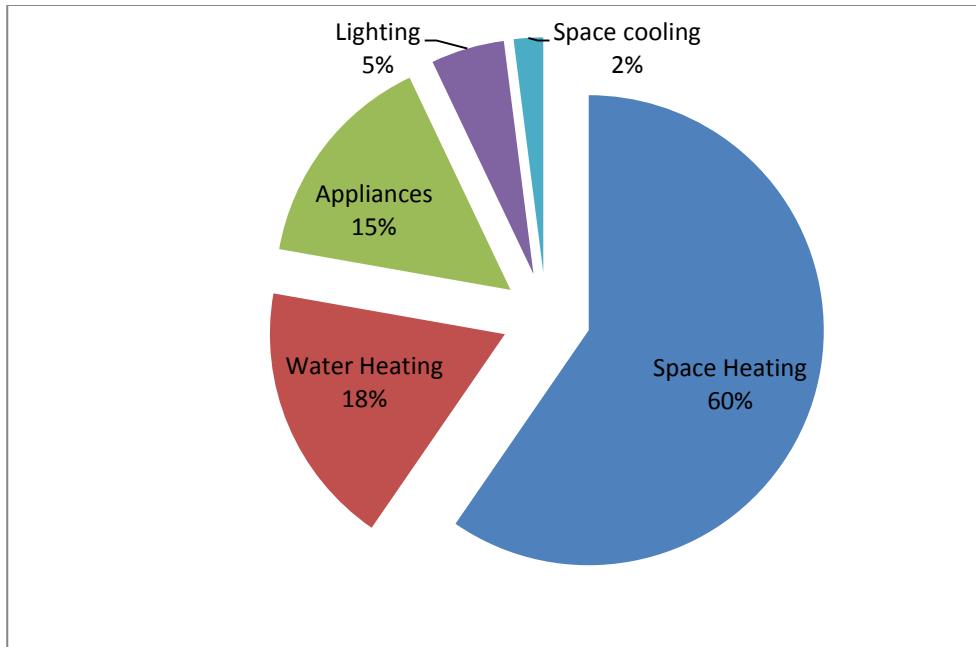


Figure 1.2 Energy use in residential buildings, based on data by NRCan (2010).

Incorporation of high efficiency HVAC equipment

Energy use for space heating represents 60% of the total energy consumption in houses, in Canada, as shown in Figure 1.2 (NRCan, 2010). Considerable energy, cost savings and emission reduction can be achieved by the implementation of HVAC efficiency measures in conjunction with integrated building design. These measures include the installation of energy efficient equipment such as heat pumps, combined with geothermal energy, solar collectors, heat recovery ventilators, solar air-conditioning, and effective distribution and controls.

Heat pumps (GSHPs) can supply heat of up to quadruple the energy of the electricity they consume, by using ground extracted heat (NRCan, 2008). Heating or cooling of fresh air supply can be minimized by employing a heat recovery ventilator (HRV), which further reduces energy consumption for space heating/cooling (NRCan, 2009b).

Smart control management systems enable preheating or precooling the house before the peak hours. Preheating and precooling can be readily applied in net zero houses through strategic exploitation of thermal mass, highly efficient building envelope and controllable mechanical ventilation (Christian et al., 2007).

Domestic Hot Water, Lighting and Appliances

Solar thermal collectors can provide around 55% of the DHW demand for residential applications (Kemp, 2006). A typical solar hot water system consists of a solar collector, circulating system to transfer heat from the collector to the preheated insulated storage water tank and a backup water heating system. Insulated storage tanks should be used to eliminate heat losses.

Low-energy appliances can reduce electricity demand in the range of 10%-50% (as in ENERGY STAR appliances; Pellant and Poissant, 2006).

Appliances, DHW and lighting loads for NZEH

Various sources list the energy load for major and minor appliances for household in Canada. Major appliances include refrigeration equipment (freezer and refrigerator), dishwasher, washing machine, clothes dryer and cooking appliances. Minor appliances include wide range of appliances used in the kitchen and for entertainment purposes.

Armstrong et al. (2009) determined the annual consumption targets for three typical Canadian detached households - Low, medium and high energy households. A total energy load of 4813 kwh/y was computed for a low energy household of 141m².

Charon (2007) determined average electricity consumption for household appliances. The study included energy efficient and Energy Star appliances. A total

electricity consumption of about 1450kWh/y was computed for minor appliances and about 2000kWh/y for major appliances.

Analysis of a Canadian NZESH (Pohgarian, 2008) assumed a total of 3 kWh /day (about 1095 kWh/y) for minor appliances, and about 1600 kWh/y for major appliances. This shows a significant reduction (28%) relative to the figure given by Armstrong et al (2009), demonstrating that energy efficient appliances can significantly reduce the electricity consumption.

Sartori et al (2010) indicated that NZESHs should limit electricity consumption for all appliances and plug-loads to 800kWh/y or less, per occupant. Electricity consumption for lighting, estimated as 1100 kWh/year in a typical low energy Canadian house, should be reduced to less than 400 kWh/year. In fact this study proposes to restrict the lighting consumption to about 3kWh/m²/y for a NZESH in mid-latitude locations. This value of lighting consumption is based on the assumption that a ZESH is expected to optimize daylight use.

Sartori et al (2010) recommend limiting hot water energy consumption to a daily average of 2.75 kWh per occupant, based on the assumption of hot water usage of 50L/day/person. The 50L/person is based, first on reference numbers suggested by various studies (e.g. EN 15316 (66.6 L/person) and the Canadian Equilibrium Initiative (56.25L/person)), and on the assumption that it is possible to reduce significantly the DHW consumption, using different methods (such as using low-flow showerheads).

1.1.2 Active Solar Technologies

Active solar systems refer to systems that convert solar energy to usable energy by means of solar collectors. Solar collectors include thermal collectors that can be used for domestic hot water (DHW) and space heating, as well as photovoltaic (PV) or hybrid photovoltaic/ thermal (PV/T) systems.

Photovoltaic systems are emerging as an important part of the trend towards energy source diversification (Wiginton, 2010; Neuhoff, 2005; Pearce, 2002). PV technology implementation is still limited however; constituting less than 1% of global energy production (Wiginton, 2010). In Canada, building integrated photovoltaic systems (BIPV) are estimated to have the potential of providing 46% of the total residential energy needs (Pelland and Poissant, 2006). This figure is determined based on a conservative methodology which estimates the available area of roofs and facades for integration of grid connected PV systems, while accounting for architectural and solar constraints (Technical Report IEA-PVPS T7-4, 2002).

Building Integrated Photovoltaic Systems

PV systems can be used as an add-on over the building envelope (building add-on photovoltaic system (BAPV)), or integrated into the envelope system (BIPV). BAPV requires additional mounting systems while the BIPV system is an integral part of the building envelope construction and has therefore the potential to meet all its requirements (such as mechanical resistance, weather protection, etc.). BIPV and BIPV/T systems, referred to as building integrated hybrid photovoltaic/thermal systems, are assumed in this research.

Introduction to PV

The electricity generated by a PV system constitutes only a fraction of the solar radiation absorbed by the system surface, referred to as the electrical conversion efficiency of the PV modules. The remaining energy is partly converted to heat (Poissant and Kherani 2008).

Existing electrical efficiency of some of the commonly used PV modules such as polycrystalline and monocrystalline silicon ranges currently between 20% and 25% while the electrical efficiency of amorphous silicon (a-Si) PV reaches 10% (Green et al, 2011). Thin film silicon modules are being developed with increasing efficiency, currently reaching some 16%. The electrical conversion efficiency is measured under standard conditions (solar irradiation of 1000 W/m^2 and cell temperature of 25°C) (Green et al, 2011).

The performance of a PV system depends mainly on the tilt angle and azimuth of the collectors, local climatic conditions, the collector efficiency, and the operating temperature of the cells. During the winter months, the insolation can be maximized by using a surface tilt angle that exceeds the latitude of the location by $10\text{-}15^\circ$. In summer an inclination of $10\text{-}15^\circ$ less than the site latitude maximizes the insolation (Duffie and Beckman, 1991). The PV system is commonly mounted at an angle equal to the latitude of the location, to reach a balance between winter and summer production (Kemp, 2006). In locations where snow accumulation is an issue, the tilt angle should be selected to take into account this factor.

The orientation of the PV panels affects both the electricity generation and the time of peak generation. PV system orientation can be selected to better match the grid

peak load (Holbert, 2009). This can affect the annual return value of the produced electricity, especially in locations where electricity value changes with time of use (Borenstein, 2008).

Hybrid photovoltaic /thermal systems (PV/T)

Hybrid photovoltaic/thermal systems (PV/T) combine PV modules and heat extraction devices to produce simultaneously power and heat (Tripanagnostopoulos, 2001). Heat extraction from the PV rear surface is usually achieved using the circulation of a fluid (air or water) with low inlet temperature. The extraction of thermal energy serves two main functions. It is exploited for space heating and solar hot water applications, and it serves for cooling the PV modules, thus increasing the total energy output of the system (Charron and Athienitis, 2006).

The total electrical and thermal energy output of the PV/T systems depends on several factors including solar energy input, ambient temperature, wind speed, and heat extraction mode. For locations with large space heating requirements, air based PV/T systems can be particularly advantageous and cost effective (Tripanagnostopoulos et al, 2001).

Integration of PV in the Building Envelope

Integration of PV panels into the building design as BIPV is gaining much attention. For instance, the International Agency of Energy (IEA) has launched IEA Task 41- Solar Energy and Architecture (IEA Task 41, 2009) to investigate the architectural integration of solar collectors in buildings. The mission of this task includes the identification of barriers for integration of solar collectors, providing guidelines for

integration and identification of successful examples of architectural integration of PV systems and solar thermal collectors, around the world.

Advantages of building-integrated photovoltaic systems include architectural, technical and financial aspects. Some of these advantages are summarized in the following:

- The electricity is produced on site, thus reducing the cost and impact of transport and distribution (Mueller, 2005).
- Elimination of the structural framework required to support free standing solar collectors. This can help in offsetting the cost associated with the additional support structure, as well as the cost of multiple roof penetrations for the supports (Pearsall and Hill, 2001).
- BIPV panels are designed to substitute the external skin of the building envelope (i.e. PV as a cladding), or to substitute the whole technological sandwich (e.g. semitransparent glass-glass modules as skylights), and therefore it can counterbalance the price of the building materials and systems it replaces (Pearsall and Hill, 2001).
- No additional land area is required, since the building surfaces are used to mount the system, thus allowing its application in dense urban areas (Pearsall and Hill, 2001).
- PV systems have generally a long life span and require no maintenance (Mueller, 2005).

- PV systems offer a multitude of architectural design solutions, ranging from urban planning scale to specific building components (e.g. shading devices, spandrels, etc.) (Kaan and Reijenga, 2004).

BIPV systems have few disadvantages as compared to add on PV modules (BAPV), the most significant is its higher cost (Pearsall and Hill, 2001). This cost however is continuously decreasing (see below). The application of BIPV systems is more suitable for new buildings than to retrofitted buildings.

Aspects of Integration

A multidisciplinary approach is required to achieve a successful integration of BIPV systems. Several aspects should be considered including architectural, functional and technical aspects. A summary of some of these considerations is presented below.

- Architectural/ aesthetic integration: Several ways of architectural integration have been identified (IEA Task 7, 2000). These include neutral integration, where the system does not contribute to the appearance of the building, or prominent integration, where the BIPV system is distinguished from the total building design. An important criterion of a good architectural integration is the overall coordination with the design of the building.
- Functional integration: Solar collectors can be engineered to serve multiple functions. Examples include passive solar design elements (awnings, light shelves, etc., see below) and as roof and façade cladding materials (Keoleian and Lewis, 2003).

- Technical integration: This refers to the integration with the building systems, such as the structural, mechanical and electrical systems. For instance, the integration of the BIPV/T system with the building HVAC system can contribute to energy savings by preheating fresh air intake. Electrical integration includes voltage and current requirements, wiring methods, in addition to the utility integration.

Building envelope incorporating BIPV systems must be designed to resist water infiltration that may penetrate the framework into the BIPV interlayers, must provide a weather seal and control thermal transfer. In addition, the BIPV systems must be able to withstand the stresses that a building envelope is subjected to, including thermal expansion.

Methods of Integration of PV in the Building Envelope

BIPV systems can be designed to cover a part or total area of roofs or facades, or as added components on these surfaces.

Roofs:

- There is an intense interest to integrate PV systems in the roofs especially in residential or low rise buildings, since it can provide an ideal exposure to solar radiation. BIPV products are becoming commercially available, that can substitute some types of traditional roof claddings such as tiles, shingles and slates (Fig. 1.3). These BIPV products are developed to match existing building products and are therefore compatible with their mounting systems.

- Prefabricated roofing systems (insulated panels) with integrated thin film laminates (Fig. 1.4) are starting to penetrate the market as well. These PV “sandwiches” constitute complete PV systems that comprise PV modules with mounting and interface components. Such products often include dummy elements to facilitate the aesthetical integration.

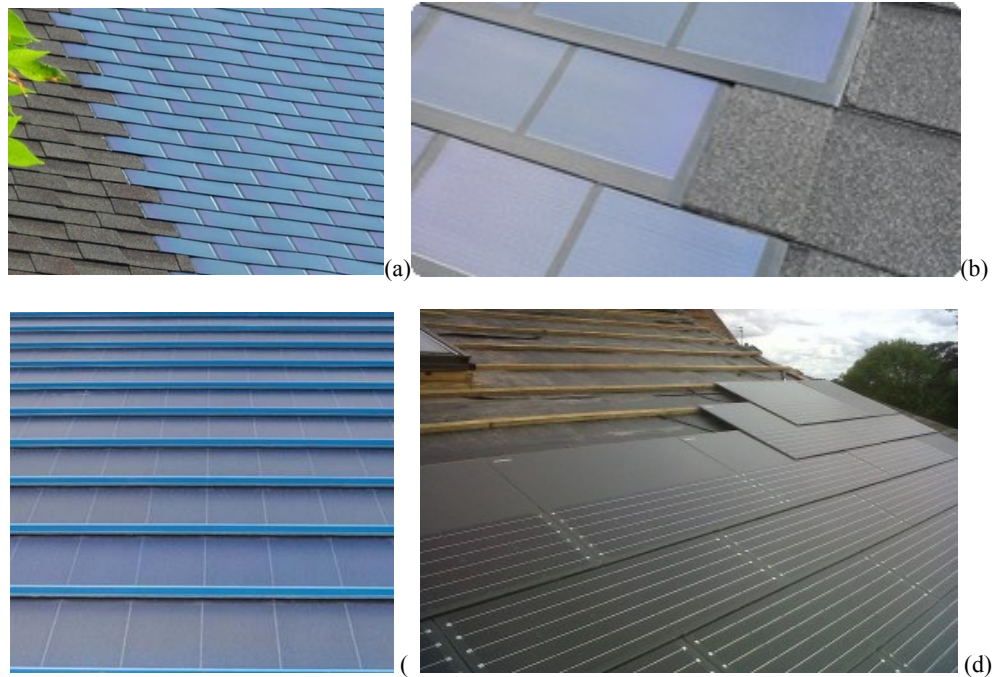


Figure 1.3, (a) Shingle PV, (b) PV Tiles (c) PV slates (Uni-Solar, 2011), (d) PV laminates (Solar Power Panels, 2011).

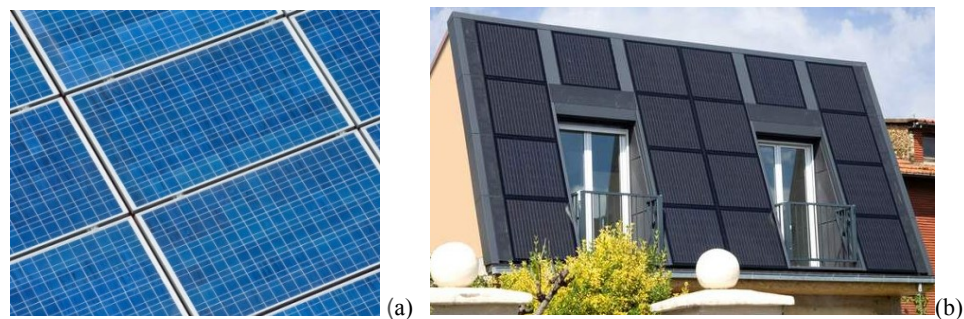


Figure 1.4, (a) Solar sandwich (Best Solar Energy, 2011), (b) solar roof system (Systaic, 2011).

Semi-transparent PV systems can be used in skylights, where semi-transparent crystalline or translucent thin film panels are most commonly employed.

Façades:

- A PV system can substitute the external layer of façades, as a cladding component, or it can substitute the whole façade system (e.g. curtain walls – opaque or translucent). In the case of PV as external cladding, the back is usually ventilated, to avoid overheating of the panels and lowering the electrical efficiency of the system. The heated air can be employed for space or water heating. Different curtain wall structures can offer a multitude of architectural appearances (Fig. 1.5).

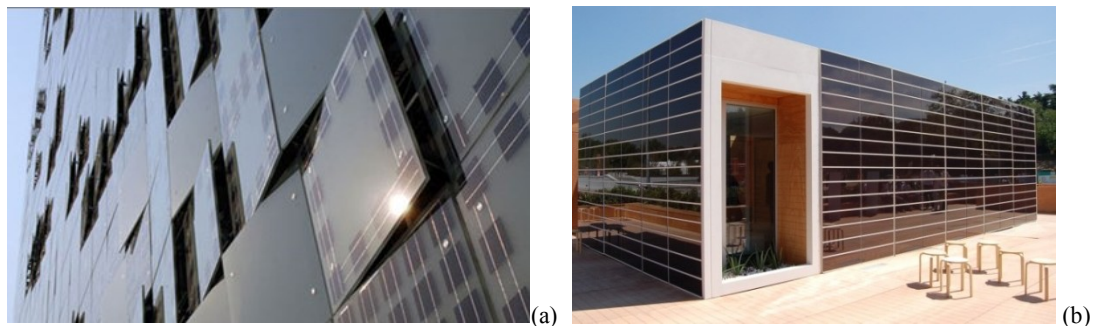


Figure 1.5, (a) GreenPix Media Wall, (Beijing, China (© Simone Giostra & Partners/Arup); (b) Solar decathlon (façade from Onyx).

External Components:

PV panels can be employed as external components to serve various functions such as shading devices, spandrels or balcony parapets. Figure 1.6 shows examples of BIPV systems as window shutters and awnings.

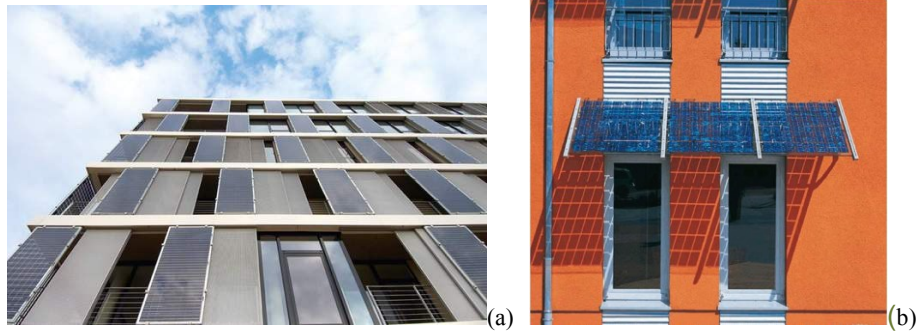


Figure 1.6, (a) PV panels as window shutters, (Colt international, 2011); (b) Solar awnings, (Solar Awning imbalance-energy.co.uk).

Cost of PV Systems

The average price of PV is currently around 3\$ per Watt peak (Wp) (Solarbuzz, 2011). Due to market extension and the increased production volume, prices are dropping steadily (Fig.1.7). A feasible long term cost potential of PV module that ranges between 0.3 USD/Wp and 0.6USD/Wp is estimated (Curtright, et al. 2008; Pietzcker et al., 2009). At this price, it could be economical to integrate PV systems not only on the equatorial facing roofs and /or facades, but also on west and east sides of the building. Figure 1.2 depicts the cost of PV systems over the last 30 to 40 years.

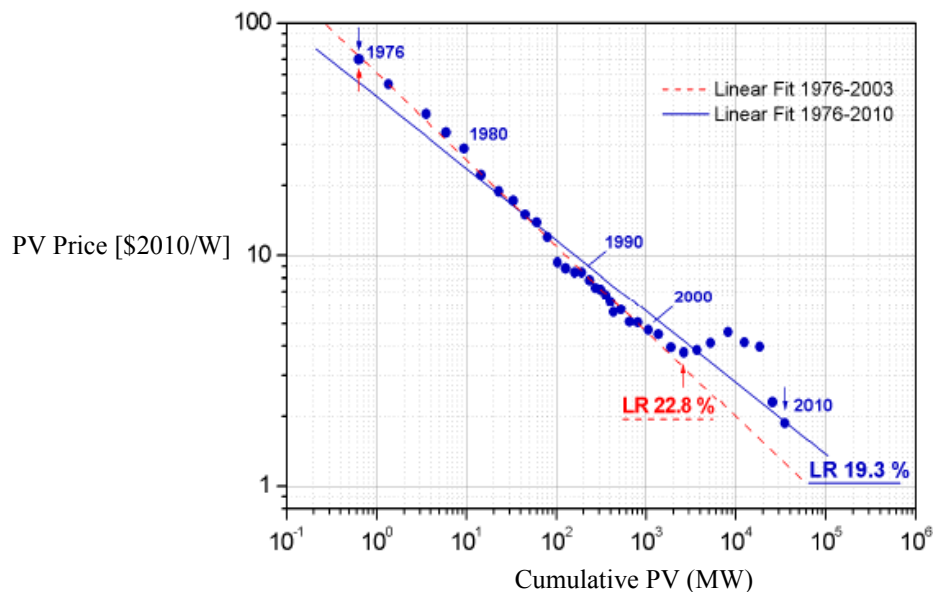


Figure 1.7, PV cost index per cumulative production (Breyer and Gerlach, 2010).

PV price depends directly on the Watt - peak capacity of a panel. *Watt Peak* is defined as the power a module can deliver under standard test conditions (solar irradiation of 1000 W/m^2 , and temperature of cells at 25°C). Consequently, it is possible, given a predetermined budget, to cover different surface areas of roofs or façades by using different available technologies. For instance the decision maker can opt for a small PV area (used as overhangs or other similar functions), where the PV system has high electrical efficiency and high price, or to a large surface area, with low electrical efficiency and low cost.

The financial return of PV electricity generation can be broken into two main parts: 1) Initial immediate return through subsidies (see below), and 2) Energy saving and selling to the utility (Holbert, 2009). Immediate return on the cost of PV systems is usually obtained through utility and governmental incentives that provide investment subsidies. In these cases the authorities refund part of the cost of installation of the system, as well as offering the owners (in commercial and residential projects) a premium price for all the renewable power produced at their site.

Moreover, selling the excess electricity to the grid can reduce the payback period for the original cost of PV systems. Currently, there are several incentives that buy the electricity at a price that can significantly reduce the payback period. These incentives include feed-in tariffs (FIT), and time of use (TOU). These are summarized below.

- Feed-in tariffs/net metering: the electricity utility buys PV electricity from the producer under a multiyear contract at a guaranteed rate. The solar buyback rate can be large enough to cover the cost for the remaining electricity need at the

going residential rate. Currently in Canada, only Ontario offers significant incentive through the feed-in tariff program for renewable energy employed to encourage installation of PV systems for renewable energy generation (CMHC, 2010).

- Time of use plans: According to this plan, the cost of electricity varies as a function of time and day (due to demand variations). When demand is high the electricity price is high and vice versa. In locations where prices of electricity vary with TOU, annual return on energy produced may be a more important object than the amount of energy produced. Favorable timing of the PV electricity generation can increase its value by up to 20%. This premium value of PV can be improved by 30-50% when price responsive demand and peaking prices strategies are used (Borenstein, 2008).

1.2. Energy Performance of Buildings and Neighborhoods

Energy use in a community is not restricted to building operations, but encompasses industry, vehicles, and infrastructure. Carlisle (2009) defines a zero-energy community as a community where the total energy needs for vehicles, thermal, and electrical energy within the community, is met by renewable energy. This research is however restricted to two-storey dwellings within small scale residential neighborhoods. This research can be considered as the first stage in the process of studying net zero energy neighborhoods.

1.2.1. Energy and Building Shapes

Building shape plays a major role in governing energy consumption and can provide advantages in capturing solar energy (Ouarghi and Krarti, 2006). The following section presents a survey of the main literature addressing building shape effects on solar capture and energy performance.

Effects of Building Shapes on Solar Potential and Energy Consumption

Studies that approach methodically the effect of building shape on its potential to capture and utilize solar energy are rather scarce. The existing examples in literature focus primarily on the dimensional proportions of rectangular buildings, on orientation of the building, or on vertical self-shading of the building (e.g. due to overhangs) (Olgyay, 1963; Knowels, 1981 & 2003; Capeluto, 2001). Very few studies deal with buildings of non-rectangular floor plans and their effect on total insolation. For instance Ling et al. (2007) studied the effect of high-rise buildings of two convex geometric shapes – rectangular and oval, with different relative dimensions on the total insolation. The goal of the study is to identify the optimum shape in minimizing total solar insolation in low latitude regions.

Research into the effects of building shape on energy performance, as distinct from solar potential, has been quite extensive. Two main approaches are employed in these investigations. The first approach consists of studying the effect of changing a few geometrical parameters and building envelope characteristics on the energy performance of a pre-defined shape. The second approach applies optimization methods to generate energy efficient building shapes.

Shape and Envelope Effects

Rectangular Shape

The first approach – evaluating the effect of shape on energy performance – is mostly limited to the study of variations of rectangular shape. These variations consist mainly of studying the effect of compactness of the building or relative dimensions of the equatorial façade to the perpendicular façade (see *aspect ratio* below). Simple numeric indicators that focus on building's geometric compactness are usually applied (Heindl and Grilli, 1991; Mahdavi and Gurtekin, 2002). Compactness is usually represented by what is termed a *shape coefficient*, defined as the ratio of the overall building envelop surface to the inner volume of the building. For instance, Depecker et al. (2001) established a linear dependence between compactness and heating demand based on 14 buildings derived from the same basic rectangular module.

A significant parameter in the design of the dimensions of rectangular solar buildings is the *aspect ratio*, defined as the ratio of the equatorial-facing façade width to that of the lateral façade. The aspect ratio is emphasized in various studies as an important factor in energy efficient building designs, under different climate conditions. In cold climate, the optimal aspect ratio for a rectangular shape solar house design ranges from 1.3 to 1.5 (Chiras, 2002; Charron and Athienitis, 2006).

Understanding the limitations of the compactness factor as representative of building shape, a number of studies venture beyond the rectangular shape. For instance, Pessenlehner and Mahdavi (2003) analyzed the influence of additional parameters including the overall geometry of the building, the glazing area and the orientation.

Multiple shapes were generated, employing a modular geometry system based on elementary cube. Their research demonstrates that compactness and the portion of glazing of the building envelope significantly impact the thermal performance of various residential building shapes. They concluded that simple geometrical indicators such as the shape coefficient (presented above) are incapable of capturing non-rectangular geometries, and therefore of predicting phenomena such as the risk of overheating of buildings.

Non-rectangular shapes

Ouarghi and Krarti (2006) correlated the annual energy consumption of office buildings with their relative compactness. Two building shapes studied in this investigation are rectangular and L shapes. Al-Anzi et al. (2009) further developed the method introduced by Ouraghi et al (2006). Applying linear regression, they developed a correlation model to predict the impact of building shape of office buildings on energy efficiency for various window areas and glazing types. Several high rise building shapes were investigated in their study, including rectangular shape, L-shape, T-shape, Cross-shape, H-shape, and U-shape. To obtain various dimensions of the studied shape configurations, they changed the bounding rectangles of each shape while preserving the same floor area. The main results of their study indicate that three factors have major effect on total building energy consumption - relative compactness, window-to-wall ratio, and glazing type,.

Shape Optimization

In the second approach – shape optimization for energy performance – several research projects employ multiple optimization criteria. In most of these investigations simple convex geometrical forms such as rectangular or polygonal shapes are employed to represent the building. Some investigations consider several geometric variables in their optimizations, like wall lengths, building height, walls angles, window sizes and the thermal resistance of external walls (Adamski and Marks 1993, Jedrzejuk and Marks 1994). The optimization of the volume of a building in arbitrary and polygonal plan is also considered in a few studies (Marks, 1997; Jedrzejuk and Marks, 2002; and Adamski, 2007). However, the issue of design, including functional aspects, is not raised in any of these studies.

More recently, Yi and Malkawi (2009) developed an optimization method to generate shapes based on their thermal performance. The method enables generating sophisticated shapes with multi-surface envelopes and irregular plans. EnergyPlus program was employed as the engine for the simulations. Results of simulations conducted in a specific location demonstrate that during summer, the optimized form should have more shaded surface areas resulting in concave building enclosure especially on its south, east and west surfaces. These concave surfaces should not be too deep, so as to avoid shade during the winter period.

Although this is an interesting approach, the functionality and cost of the design are not addressed. Functionality can be a major issue especially for dwellings, where the utilization of spaces and their partitioning are of primary importance.

1.2.2. Effects of Urban Design

Neighborhood design is governed by three main factors: land use, density of development and arrangement of streets. These parameters are usually prescribed for a given site. Solar neighborhood designed for exploitation of useful solar radiation for heating, daylight and electricity generation, require consideration of additional parameters, such as building geometry, roof shapes, the arrangement of housing units along streets and the configuration to match the required density (e.g. attached units, rows). These design parameters, which have substantial impact on passive solar gain, daylighting and the feasibility and performance of photovoltaic systems, can be manipulated to achieve net zero energy neighborhood. High density development is associated with low energy use per capita (Steenmerris, 2003). On the other hand, high density may reduce solar access and consequently solar energy utilization potential. Solar access and solar radiation distribution should be considered from the earliest planning stages to ensure that the majority of buildings on a site, in the northern hemisphere, are oriented between south east and south west in order to have good solar access (Erley and Jaffe, 1979). Size and shape of a site, as well as the layout of streets within this site can influence orientation of buildings and therefore their accessibility to solar radiations (Knowles, 1981).

Solar Potential in Urban Areas

Solar radiation in the urban context has been extensively studied over the past few decades. Techniques have been developed for building specifications to minimize mutual shading by buildings and to determine insolation or shading in a given urban area. For

instance, Arumi (1979) established a model to define the maximum allowed height of a building to avoid overshadowing its surrounding.

Knowles (1981) suggested a method termed *solar envelope*, to assure solar access to each residence unit in a community. The solar envelope consists of an imaginary boundary based on the sun's relative motion. Buildings contained within this envelope do not jeopardize the solar rights of their neighboring buildings during critical periods of solar access.

Compagnon (2004) proposed a methodology for estimating the amount of solar energy available to a building of arbitrary shape, taking into account obstructions due to the surrounding landscape and associated reflections. Montavon et al. (2004) and Scartezzini et al. (2002) developed a procedure to produce histograms of irradiation as a function of built portion in a specific urban area.

Several studies have focused on the distribution of solar radiation on different surfaces in a built environment (e.g. Ouarghi and Krarti, 2006; Stasinopoulos, 2002; Leveratto, 2002), as well as the availability of solar energy and its optimization, at the urban scale.

Mardaljevic and Rylatt (2000) computed irradiation in complex urban environments using the ray tracing program RADIANCE. RADIANCE has also been applied to study the periodic (annual or winter) solar distribution as a function of built area (Compagnon, 2004; Mardaljevic, and Rylatt, 2000; and Cheng et al., 2006).

Ghosh and Vale (2006) determined the solar energy potential for a New Zealand neighborhood by using geographic information system (GIS) to calculate the roof area

suitable for solar thermal and solar PV (Ghosh, et al., 2006). GIS system is usually employed for mapping and analysis of geographic data.

Energy Consumption in Urban Areas

Extensive research has been conducted to estimate the energy consumption of urban areas as large as whole cities. Various methods are developed to determine the effect of urban form on energy demand of buildings.

Ratti et al. (2005) used Digital Elevation Models (DEM) – a 3-D representation of a terrain surface created from its elevation data, including building elevations – to determine the effects of urban texture on energy consumption. The DEM method is employed to refine the “solar envelope” method (Knowels, 1981, see above) so it reflects accurately the solar radiation over a large urban area and simplifies the calculations of this solar envelope.

Christensen et al (2008) propose a computerized Subdivision Energy Analysis Tool (SEAT), which allows an interactive design of street layouts while receiving feedback on energy impact.

The urban energy consumption simulator CitySim is under development, based on multiple physical models. CitySim can compute an estimation of the on-site energy use for heating, cooling and lighting (Perez et al. 2011).

Other investigations have focused on establishing approaches to minimize energy use in various built environments. For instance, Kampf et al (2010) developed a methodology to reduce energy demand of buildings in an urban area employing multiobjective evolutionary algorithm to maximize incident solar irradiation whilst

accounting for thermal losses. The shapes of three commonly used urban forms are optimized in this study – terrace flat roofs, slab sloped roofs and terrace courts.

Cheng et al. (2006) conducted a parametric study of 18 different models, representing various combinations of built form and density. The trial and error method they employed was unlikely to identify an optimal geometric form in terms of maximizing the solar irradiation potential, given the small number of cases tested.

Pol et al. (2011) summarized the main findings of the impact of urban morphology on energy needs in the built environment. The study shows that there is no common basis allowing for a generalization of the knowledge available.

Solar Parameters of Urban Design (Neighborhoods)

Two approaches are adopted to analyze energy performance of urban areas. The first approach uses models representative of real urban design morphologies. These cases are usually limited in their ability to generalize the findings, unless the studied morphologies can represent ubiquitous prototypes.

The second approach is based on simplified urban morphological archetypes which can be easily parameterized, both for performing sensitivity analyses and for urban morphology optimization. The major problem of this approach is the risk of not representing realistic urban design forms. The most frequently assessed archetypes are pavilions (Morello and Ratti, 2009; Morello et al. 2009), including shape variations for high-rise buildings (Leung and Steemers, 2009), courtyard configurations (Kämpf and Robinson, 2010), row houses (Jabareen, 2006) and urban street canyons (Ali-Toudert, 2009).

The urban morphology parameters most widely investigated can be divided into three categories, depending on whether they describe (1) building form only; (2) the morphological surrounding of a given building; (3) the morphological patterns of an entire neighborhood (Pol et al., 2011).

1) Individual building parameters include: wall surface area, ratio of envelope area to floor area, building orientation, and ratio of passive to non-passive floor area. Passive solar floor area is defined as the area of the floor adjacent to the equatorial façade, having a total width of about double the interior height (measured from floor to ceiling). This method is used to estimate the solar radiation penetration (Baker and Steemers, 2000).

2) The parameters characterizing the direct environment of a building include: *obstruction angle* defined as “the smallest angle with the horizontal under which the sky can be seen from the lower edge of a vantage point, usually an opening in a building” (Morello and Ratti, 2009); *urban horizon angle* which combines: orientation, elevation of the obstruction and elevation of the sun (depends on the latitude of the urban area) (Baker and Steemers, 2000); *sky view factor* is defined as the ratio of the radiation received (or emitted) by a planar surface to the radiation emitted (or received) by the entire hemispheric environment (Watson and Johnson, 1987); and the ratio of the building height to its width (H/W) ratio.

3) Parameters characterizing a neighborhood consist of the *site coverage* defined as the portion of a site occupied by any building or structure for human occupancy, and the typology (including heights) of clusters of buildings (Pol et al, 2011).

1.2.3. Case studies

Under current market conditions financial incentives on the part of governments and/or the utility companies are essential to make the implementation of solar technology viable at the urban scale. Most urban-scale PV projects to date have obtained some level of capital funding subsidy.

A growing number of projects related to application of BIPV systems at an urban scale are reported in different locations in the world. Examples of these applications are presented by the International Energy Agency - IEA PVPS Task 10 (IEA-PVPS-Task 10). Some of the most advanced countries in design and application of solar urban projects include Germany, the Netherlands, Japan and the United States. In general, these projects try to maximize total electricity production. A few examples of urban solar projects are presented below, accompanied by a discussion of some of the main characteristics related to form optimization, urban planning issues and technologies employed (PV, combined heat and power etc.). None of the reported projects, however, includes methodic approach to the design of solar energy efficient communities/neighborhoods, aiming at achieving net zero energy status.

Clarum Homes – Vista Montana (USA)

Vista Montana is one of many zero energy home developments by the Clarum Homes Development Company, in the United States (Clarum Houses, 2003). A PV system is installed on the roof of each housing unit (Fig. 1.8). The PV system electricity generation together with energy efficiency features, result in reduction of overall net energy demand by some 90%, compared to conventional houses. The layout of the development ensures an economical land use.



Figure 1.8, Aerial view of the Clarum houses in the USA(Clarum houses, 2003).

Solarsiedlung am Schlierberg, Freiburg, (Germany)

Solarsiedlung am Schlierberg is a mixed-function development that comprises residential and commercial buildings. Large areas of photovoltaic modules are installed in a plane above the south facing roofs of the various buildings. Asymmetrical gable roofs and shed roofs are adopted to increase the area of the roofs for PV installation (Fig. 1.9d) (Hagemann, 2007). Both roof styles have large overhangs on the south face and therefore provide shading on these facades in summer, while further increasing the roof surface for PV integration. An air-gap of 16 cm is designed between the roof and the PV plane. Although structurally and functionally the PV array and roofing systems are separate, the two systems form a well-integrated feature of the roof complex.

The energy generation is complemented by energy efficiency measures.

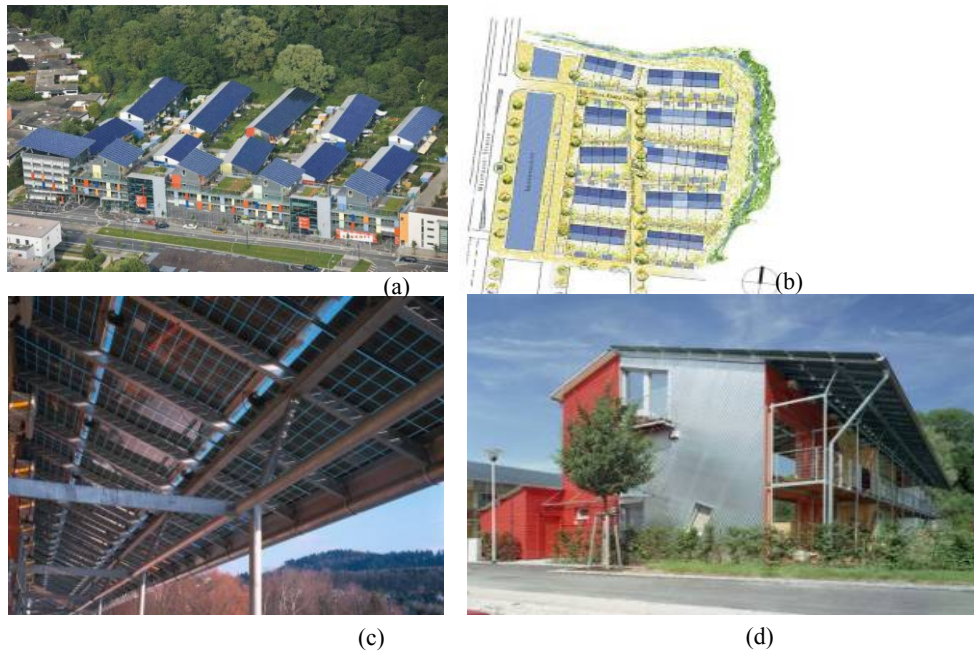


Figure 1.9, Solarsiedlung am Schlierberg, Freiburg (Breisgau) (a) view of multi-story buildings and terrace houses, of Mixed-function development, (b) plan view, (c) detail of the overhang of a terrace house, (d) terrace house (Hagemann, 2007).

The Nieuwland (Netherlands)

The Nieuwland 1 MW PV project involves the implementation of PV systems on a large scale. The solar electricity contributes about 54% of total energy consumption.

The urban planning consisted originally of east-west oriented houses. This original planning was subsequently modified so as to optimize the development for solar radiation access. This allowed the development to achieve a target level of 20 m² PV per household. The land was parceled to maximize the roof surface areas that are suitable for PV integration, to reach the level of 1 MW_{peak}.

The houses were developed using recognized concepts for technical integration of PV panels, taking into consideration the orientation, inclination and ventilation. The resulting architectural design shows a great variety of building integrated PV systems,

oriented between SE and SW, with tilt angles ranging between 20° and 90° (Figs. 1.10 a-d). Solar modules are used as roofing tiles, facade cladding and as sunshades. The watertightness of the PV roofs was guaranteed by a watertight layer under the solar modules. Some unforeseen issues such as shading and non-optimal orientation and tilt angle caused 5 to 16% underperformance in electricity generation (SECURE: Nieuwland solar energy project).

The utility company owns the PV systems; therefore the electricity generated is fed directly into the public grid.



Figure 1.10, PV integration in Nieuwland, (a) on the roof of a parking lot; (b) in sport complex, (c) noise wall houses, (d) Prefab PV roofs (PV UPSCALE: Nieuwland, 2008).

Kanokodai (Japan)




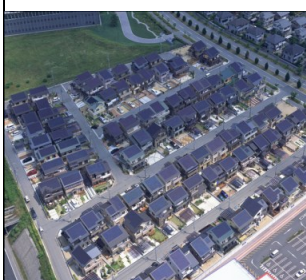
The community has 95 houses equipped with BIPV systems. To create a well-designed appearance of the houses and a harmonized streetscape as a community (Fig.1.11), PV roof tiles were selected for the PV systems. The houses were customized to the inhabitants' requirements.

The PV system received a governmental subsidy. A net-metering scheme was applied so that excess of electricity generation is sold to the utility company, at a price that equals the residential electric tariff (IEA PVPS-Task 10: Japan: Jo-Town Kanokodai).



Figure 1.11 Jo-Town Kanokodai (MSK corporation, IEA PVPS-Task 10: Japan: Jo-Town Kanokodai).

Table 1.1, Summary of case studies

Name and photo or schematic	Solar design/optimization	Energy system (BIPV, CHP etc) and key stats)	Energy storage system /grid	Density and other urban issues
<p>USA-Clarum Homes – Vista Montana Houses -</p> 	<ul style="list-style-type: none"> • South orientation • Energy use reduction of 90% as compared to conventional houses. 	<ul style="list-style-type: none"> • BIPV system Total PV power: >300 kW • PV power per unit: 1.2 to 2.4 kWp 	<ul style="list-style-type: none"> • Grid connected PV system • The systems are interconnected and net metered 	<ul style="list-style-type: none"> • 177 single-family homes, 80 townhouses, and 132 apartments • The development layout is a grid (economical land use).
<p>Germany- Solarsiedlung am Schlierberg, Freiburg</p>  <p>(Breisgau)</p>	<ul style="list-style-type: none"> • South orientation • Inclination (Terrace houses): 22 ° • Gable shed roofs are used to increase the area of PV integration. • An air-gap of 16 cm between the roof and the PV plane. 	<ul style="list-style-type: none"> • PV-System size: 445 kWp , 2 million kWh primary energy savings per year • Active ventilation with heat recovery • Contribution solar electricity in total consumption: 54% 	<ul style="list-style-type: none"> • Grid connected PV 	<ul style="list-style-type: none"> • The “Sonnenschiff” is complete solar development retail, office and living two or three stories high while the commercial buildings are four to five stories high.
<p>The Netherland- The Nieuwland</p> 	<ul style="list-style-type: none"> • Orientation: between SE and SW, Tilt angles: ranging between 20° and 90°. 	<ul style="list-style-type: none"> • PV total power: 1 MGWp PV • PV power per system/house: 0,8 - 4,4 kWp • A solar/gas combination unit, 15kW capacity each, has been installed in each house 	<ul style="list-style-type: none"> • Grid connected PV. • Experiments using ground water (12m depth) for long term storage • Electric heat pumps (as part of experimental work on semi detached houses) 	<ul style="list-style-type: none"> • The urban plan optimized for solar access, (since design stage). • The land is parceled to maximize the roof surface areas that are adequate for PV integration (around 20m² /roof)
<p>Japan: Jo-Town Kanokodai</p> 	<ul style="list-style-type: none"> • Inclined roof • PV roof tiles were selected for the PV systems. 	<ul style="list-style-type: none"> • Total PV power: 285 kW • PV power per unit: 3 kW/house • Option of all –electric houses 	<ul style="list-style-type: none"> • Grid connected PV • net-metering scheme 	<ul style="list-style-type: none"> • The community has 95 houses • Customized housing design

Discussion of the Case Studies

Table 1.1 provides a summary of the main features of each of the case studies. Some of the main observations made in these cases are discussed in the following:

- **Urban planning for PV Integration.** In many of the presented case studies, the decision of integration of PV systems was taken at a late stage in the urban planning process, after the site selection and sometimes after construction of the buildings. In some projects, such as in Germany and in the Netherlands, solar access was planned before the implementation of the large scale PV systems. In the German case study, detailed shading simulations were performed on the development site, and the results were used to guide the designers. The Nieuwland case study solar optimization was taken into account in the urban planning phase with the land being parceled out to provide as many roof surfaces as possible suitable for the installation of solar panels.
- **Optimization of the design process.** A systematic approach to analyze building shape potential was not generally conducted in the presented cases. PV systems were installed on surfaces that present a good solar layout. Therefore building geometry and roof designs were not specifically designed to maximize the solar potential. For example, in Germany, the original roofs were modified and additional separate structures were built to support the PV systems, in order to obtain a large surface of roof at an acceptable tilt angle. In the Netherlands different ranges of orientation and tilt of the PV systems were attempted, resulting in some reduction in the generation potential of the systems.

- **Consumption vs. generation.** Most of the projects were concerned mainly with maximizing electricity generation. In general, there is no procedure for energy balance between consumption and generation.
- **Role of government and utilities.** Governments together with utility companies played an important role in all the case studies. In some cases the utility companies own the PV systems, such as in the Netherlands, and therefore the cost of the PV systems was provided by these companies, while the electricity generation was fed directly to the grid. In most of the other cases the government paid a subsidy to install the PV systems. The excess of the electricity was in most cases sold to the grid with a price at least equal to the tariff of use.

1.3. Tools

1.3.1. Modeling of Net-Zero Energy Solar Houses

Modeling net-zero energy solar houses (NZESH) requires a systematic approach to predict the dynamic response of buildings and their systems and the interaction with on-site renewable energy generation (Athienitis et al, 2010). It is recommended to employ simulation programs at early design stages of NZSEH in order to attain the pre-established performance goals (IEA- SHC Task 40/ECBCS Annex 52). More advanced models may be needed in later stages to enable detailed analysis.

For the early design stage, when the shape of building is almost determined, simulations can assist in determining basic parameters such as optimal window size, thermal mass, PV size and its optimal location. Existing simple tools are limited in their capability to model basic NZESH design characteristics, including daylighting, natural

ventilation and location of thermal mass. For instance, tools like RETScreen (RETScreen International, 2005), can be employed to size BIPV systems; however it cannot model complex roof shapes or predict the effect of shading on electricity production. At more advanced stages, simulation tools that offer possibilities to combine actual climate data, various geometries, passive solar gain, HVAC-systems, energy-generation systems, natural ventilation, together with user behavior (occupancy, internal gains, manual shading) are required.

A number of simulation tools, with varying capabilities, are currently available (Hong et al., 2000; Al-Homoud, 2001; Crawley et al., 2001 and 2008). Programs that are commonly encountered in the literature and can simulate different technologies include TRNSYS (TRNSYS, 2004; Klein et al. 1976), ESP-r (Clarke et al., 2002) and Energy Plus (Crawley et al., 2000; Crawley, 2001).

TRNSYS is a powerful program with large capabilities in the modeling of active solar systems, but has some weaknesses in whole building energy modeling (Beccali et al., 2005).

ESP-r (Energy System Performance – research) is an integrated building and plant energy simulation environment. It supports early-through-detailed design stage applications and enables integrated performance assessments. It offers climatic data, construction, profiles database management, and incorporates shading, solar beam tracking, condensation analysis; air flow modelling, etc. (Clarke, 2002).

EnergyPlus has a large potential, given the fact that it is well-funded, free of charge, and has many commercial front-ends. The user can select the method of heat

transfer, whether the transfer function method, which is based on linearization of non-linear phenomena, or the finite difference method.

Several tools provide explicit models for technologies such as solar thermal collectors and geothermal heat pumps. For instance EnergyPlus and TRNSYS were employed to perform a feasibility analysis of zero-energy houses with renewable electricity, solar hot-water system and energy-efficient heating systems (Wang et al., 2009). However, the capability of modeling innovative technologies or interactions between multiple pieces of equipment is still restricted (Athienitis et al., 2010).

Despite the availability of powerful simulation programs, such as mentioned above, those that may be used for NZESH design usually lack the ability to model some passive and active solar potential in conjunction with some specific building system (e.g. HVAC systems, heat pump systems, etc., (Athienitis et al., 2010)). Two major categories of potential improvements to NZESH design tools are identified: improving the interfacing between various tools to complement each other's capability, and enhancing the potential of models to represent various technologies (e.g. PV and PV/T systems, heat pumps, etc. (subtask B of IEA task 40)).

1.3.2. Tools for Simulation of Urban Areas

The research into simulating the performance of the built environment at urban scale level started only in the late 1990s. Initial work had the objective of aiding city planners to improve energy conservation and encourage the application of solar thermal and photovoltaic panels in existing residential buildings. Simplified energy modeling tools were linked to Geographical Information System (GIS) software to achieve this purpose (Jones, 1999; Gadsden et al., 2000).

Some of the simulation programs employed for the investigation of solar access of buildings within urban context include the ray tracing program RADIANCE, which simulates the irradiation on façades (Compagnon, 2004; Mardaljevic and Rylatt, 2000; Montavon et al, 2004). Those studies that employed it, however, did not consider building energy demands.

Digital elevation models (DEMs) (see section 1.2.2) were also employed in some cases to find the effect of urban texture on building energy consumption. These models are based on image processing and were employed in lieu of detailed numerical simulation of radiation exchange (Ratti et al, 2005).

Thermal building models in urban areas range from the highly simplified heat loss calculation over the building envelope (e.g. Morello et al., 2009) to commercial or self-developed transient building energy performance simulation tools. However, these studies often ignore some aspects of energy needs (cooling, electricity needs for artificial lighting, etc).

Some simplified energy models were used to establish relationships between urban form and non-domestic energy use (Ratti et al., 2000). However, these models were basic in their calculation of solar radiation transmission and heat flows in buildings. Modeling of renewable energy technologies was either incomplete or absent.

A relatively new design tool - SUNtool, is developed to be employed for the early decision stage of sustainable urban design. SUNtool contains occupant's behavior, daylight, heat flow, micro climate and plant & equipment models. This tool has however a few disadvantages. At present it is restricted to some European countries, and to the

analysis of simple rectangular shapes. In addition, a certain expertise is required to perform the simulations and to interpret the results (Vreenegoor et al, 2008).

An additional tool – CitySim, is still under development. This tool can estimate on-site energy consumption for heating, cooling and lighting. To accomplish this analysis, the tool needs complete physical description of the buildings in the form of an Excel input file (Perez et al, 2011).

CHAPTER II: DESIGN AND METHODOLOGY OF THE INVESTIGATION

This Chapter summarizes the framework of the research, its objectives and the methodology employed at each stage. The investigation of the effects of design parameters on energy performance of dwellings and neighborhoods consists of three main stages – 1) Effects of shape of individual housing units; 2) Neighborhood patterns 3) Roof design. At each stage the object of the investigation (residential units, neighborhoods, and roofs) is first designed with different values of the design parameters, followed by performing simulations and analyzing the results to assess the effects and their significance. The employed simulation tools and modeling procedures are introduced as well.

2.1. Outline of the Investigation

2.1.1 Background

Designing the shape of a building to optimize solar capture is an essential step in achieving net zero energy status. In the design of a neighborhood, ensuring that the majority of buildings have good solar access is a major objective. Poor solar access not only reduces the efficiency of solar collectors, but also restricts the implementation of passive solar design strategies for space heating, daylighting and solar water heating.

In general, key parameters of building geometry and urban patterns affecting solar availability and utilization are not well defined. Moreover, existing guidelines do not

provide quantitative data on the effects of design parameters on energy performance – energy consumption for heating/cooling and solar energy potential. *Solar potential* refers to the potential of building and neighbourhoods to capture and utilize solar radiation. Solar potential includes radiation incident on near equatorial-facing facades and transmitted by the fenestrations of these façades, total solar heat gain by the windows, and the energy generation potential by building-integrated photovoltaic and/or photovoltaic/thermal system (BIPV/T), integrated in the near equatorial facing roof surfaces of these units.

The successful design of energy efficient dwellings and neighborhoods that aspire to achieve net zero energy status, while maintaining quality of life, needs the understanding and collaboration between architects and engineers. This work attempts to interface between engineering and architecture by providing a holistic approach to the design of solar optimized neighborhood.

The successful design of energy efficient dwellings and neighborhoods that aspire to achieve net zero energy status, while maintaining quality of life, needs the understanding and collaboration between architects and engineers. This work attempts to interface between engineering and architecture by providing a holistic approach to the design of solar optimized neighborhood.

Specific issues in the design of dwellings and neighborhoods for optimized solar potential are listed below.

1) Dwelling shape:

- Existing guidelines for the design of passive solar energy efficient houses are limited mostly to rectangular shapes. Rectangular shape is generally considered

as the optimal building shape for passive solar design and the most energy efficient (Chiras, 2002). However, under certain design conditions in urban context, this shape may not be optimal. For instance, rectangular plan does not allow uniform penetration of daylight, especially to the north part, which is usually, kept window free in energy efficient houses. In addition, it should be born in mind that shape design is governed by many constraints other than energy efficiency, such as functional demands and quality of life of inhabitants. For these reasons it is important to explore the penalties, as well as the benefits associated with plan layouts other than rectangular, and with different roof forms.

- Integrated solar design approach that applies passive solar design principles together with the architectural integration of solar technologies, should be implemented at early design stages. Dwellings should be designed to provide optimized façade potential for solar capture, that can be utilized passively in daylighting and heating, in conjunction with optimized roof shapes for increased thermal/electrical generation.

2) Neighborhoods:

- Despite the interest in the effect of urban development on the availability and utilization of solar energy, there is still no systematic approach for passive solar design on the level of neighborhoods/urban areas. Such approach should define the main parameters that affect the solar potential of the neighborhood, ranging from the building level to the neighborhood level, and present a methodology of application of such parameters in the design process. This integrated approach should encompass passive solar design of buildings, roof shape for integration of

solar technologies, and finally the placement of units on a site and with respect to each other.

- Most of the existing studies explore existing urban areas, to study their energy consumption and/or their availability for solar access. No study addresses the design methodology of new residential neighborhoods/ communities for increased solar potential. This is an important issue, especially in Canada, where new neighborhoods and communities are continuously planned and built.

2.1.2. Objectives and Scope

Objectives

The main objectives of this research are summarized as follows:

- Identifying key design parameters of housing units' shapes and neighbourhood patterns to increase their solar potential.
- Quantifying the effect of these design parameters on a set of energy performance criteria such as solar potential of dwellings and neighborhoods and their energy demand/consumption for heating and cooling.
- Based on results of the parametric study, developing design methodology of houses and neighbourhoods for improved solar performance aimed at optimising energy generation/consumption balance, subject to multidisciplinary design constraints.

The first two objectives of this research enable an in-depth understanding of the effects of design parameters on performance. This understanding can form a basis for future development of advanced design tools for net-zero energy neighborhoods.

Scope

This study investigates key parameters for solar optimized neighborhoods aiming at developing a methodology that assist in the design of net-zero energy and energy positive communities. The scope of this investigation is as follows:

- The study is restricted to two-storey dwellings for single families averaging four persons. A fixed floor area of 60 m² per storey (total area of 120 m²) is adopted, for all dwelling shapes. The two-storey house option is selected since it represents the most common option of a single family detached home in Canada (Charron and Athienitis, 2006).
- The pilot location of the project is Montreal, Canada (latitude of 45 °N).
- Only the effect of south facing windows is studied. The area of all other windows is assumed constant based on the minimum requirements for houses in cold climate (Chiras, 2002). Since the study is conducted for the northern hemisphere, the term “south facing” is employed hereunder to refer to “equatorial facing” in the more general context.
- All electrical loads, including energy required for domestic hot water, lighting and appliances, are estimated based on existing literature for energy efficient and near or net zero energy houses.
- Heating energy consumption is computed assuming a heat pump with coefficient of performance (COP) of 4 – a reasonable COP rating of commercially available heat pumps (about 3.5 to 4) (The Canadian Renewable Energy Network, 2011).
- Daylighting is not considered as a performance criterion in this investigation, although daylight considerations can affect the design of a building shape for

increased potential of solar utilization. Daylighting is, nevertheless, taken into account in the design of the interior space (e.g. the location of living area, the depth of building when it is possible and the height of the ceiling – Chapter III).

- Photovoltaic panels are assumed to cover the total south/near-south facing area of roofs. Covering a complete roof surface with a BIPV system has an advantage of forming an outer layer which acts as the weather barrier in addition to producing useful heat and electricity.
- Neighborhood characteristics, such as street widths and minimum distances between units are based on various sources in the literature (see below and Chapter IV for details).
- Selection of parameters is based on their anticipated effect on solar potential and energy efficiency of buildings and neighborhoods, as indicated by the pertinent literature (Chapter I).

2.2 Methodology

This section outlines the design principles and the selection of design parameters for the three stages of the investigation.

Shape parameters in this research are mostly selected for their effect on shading, especially non-convex shapes. These parameters are detailed below. In addition to shape parameters, roofs are affected by tilt and orientation angles, which govern the BIPV and BIPV/T potential for electrical and thermal energy generation.

On the level of neighborhood, the literature emphasizes the role of road layout and density on solar access and energy performance. For instance, site layout and roads

influence the position of buildings and their orientation. Density is known for its influence on solar access, as well as on energy demand. However, these two parameters have not been systematically investigated, separately or/and in combination, nor is their interaction with building shape.

Details of values of the design parameters and results of the analysis of their effects on energy performance are provided in the relevant chapters: Chapter III – shape study, Chapter IV – neighborhood study and Chapter V – roof study.

2.2.1 Shape Study

This stage, which is presented in Chapter III, investigates the effects of housing units' shapes on their energy performance (in terms of electricity generation and demand/consumption). Details of the simulation procedure employed in the analysis are given in section 2.3.

Plan Shape

The first step in the shape investigation is the design of various plan layouts of dwellings, focusing on south façades and the position of windows in these façades. This is followed by roof design of each shape and the integrated photovoltaic portion of the roof. The selected configurations are then subjected to simulations to determine the solar potential and energy demand for heating and cooling of each shape. The plan layouts designed at this stage are divided into two main categories, convex and non-convex.

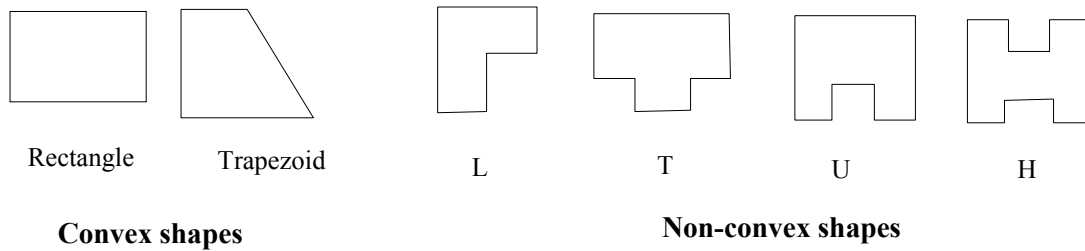


Figure 2.1, Basic shapes.

Convex layouts include rectangle, square and trapezoid. Non-convex layouts are inherently self-shading. They consist of two or more wings that at certain orientations relative to solar position may mutually shade. Non-convex shapes considered in this investigation include: L, U, H and T shapes (Fig. 2.1).

Dwellings are designed as two-storey single family units. The two-storey option is adopted in this study as representing one of the most common options of a single family detached home in Canada (Charron and Athienitis, 2006). This option requires less land compared to a single-storey house (Athienitis, 2007). The design of units incorporates energy efficiency measures and some of the basic principles of passive solar design.

Variations of some parameters governing certain shapes such as rectangular and L shapes are explored, to identify design possibilities that enhance solar radiation capture potential on near-south facing roofs and façades. The effect of these parameters on heating and cooling load/consumption is also determined.

Design parameters of rectangular shape include orientation and the aspect ratio – AR (W/L in Fig. 2.2). Design parameters of non-convex shapes include the ratio of shading to shaded façade lengths, termed *depth ratio* – DR (a/b in Figure 2.2) and variations of the angles between the wings. Figure 2.2 displays some of the shapes studied, and the dimensions governing their design. The detailed presentation of all shapes (30 different shapes), is provided in Chapter III.

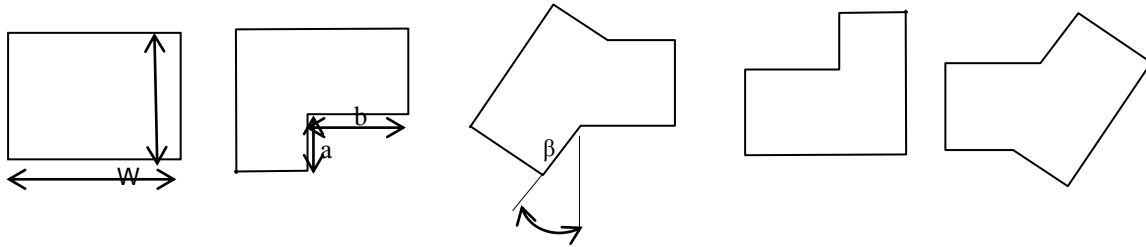


Figure 2.2, Shape parameters.

Roof Geometry

A simple roof shape is considered for this stage of the research. The effects of roof shape variations are investigated in the third stage. The adopted basic roof is a hip roof with 45° tilt and side angles, as shown in Figure 2.3 for the rectangular plan layout. Figure 2.4 shows the application of this roof shape to the non-convex shapes. The shape denoted *obtuse angle* is a variation of L shape with a large angle between the wings (see neighborhood design below).

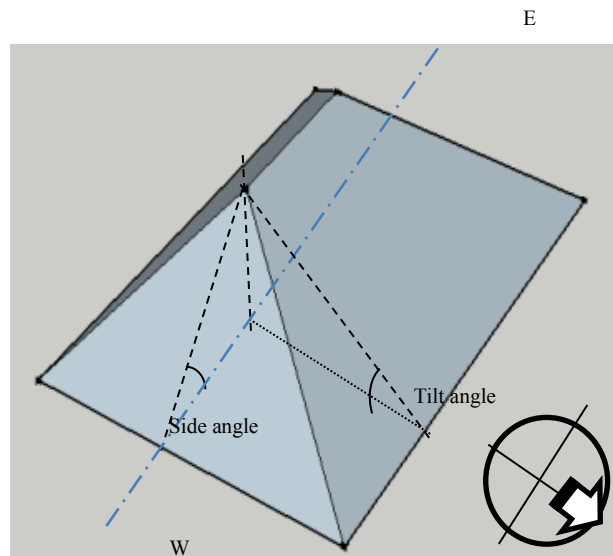


Figure 2.3, Hip roof of a rectangular plan layout.

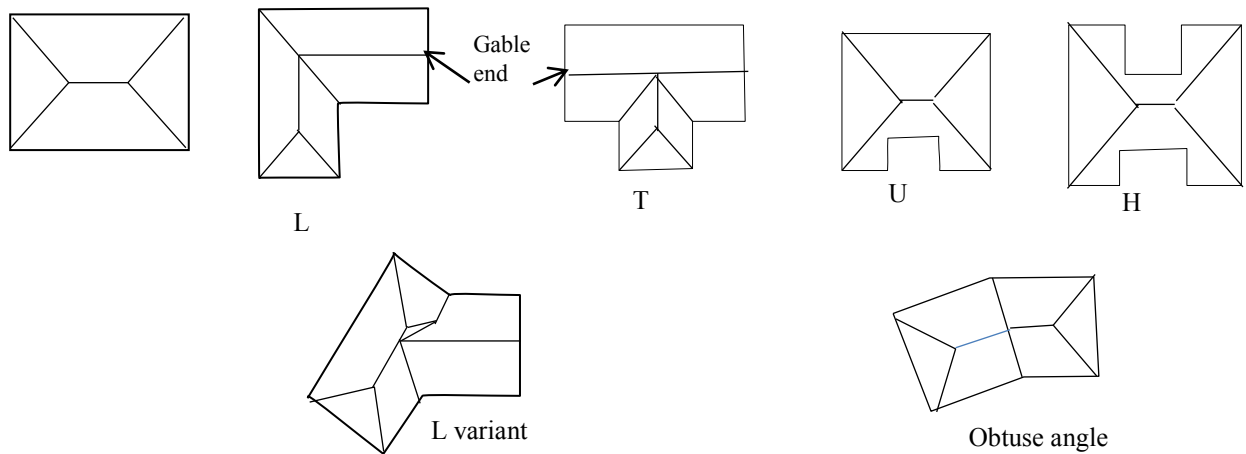


Figure 2.4, Roof shapes.

2.2.2 Neighborhood Study

The main parameters investigated in this stage are housing density and site layout. Interactions between dwellings' shapes, their density and the site layout are also investigated. The response variables are the solar potential of individual units and of the neighborhood as a whole, as well as energy load/consumption for heating and cooling.

In the design of neighborhoods, the position of trees with respect to dwellings, their heights and type may influence the shade cast on the facades and roofs of these dwellings (Nikoofard et al, 2011). This effect however is not considered in this research.

The design methodology consists of first determining the site layout, selecting unit shapes to conform to the site layout, and then combining the shapes in different configurations to fit different levels of density. All configurations are subjected to simulations, followed by a comparative analysis to assess the effect of density and of site layout on solar potential and energy performance, relative to a reference case. The reference neighborhood pattern for the comparative analysis is a site with detached rectangular units, with aspect ratio of 1.3, arranged along a straight road running east-

west. The studied parameters are outlined below. Full details of neighborhood patterns, simulation results and effects analysis are presented in Chapter IV.

Site Layout

Three main site layouts are studied. These layouts are based on the CMHC fused grid (CMHC, 2011) (Fig. 2.5). The fused grid can be a good basis for the design of a new solar neighborhood because it is designed to allow mixed use, densification, and efficient public transportation. All these factors are beneficial for a design of a new neighborhood in two ways: a) they have various energy implications (use for transportation, energy consumption in building); b) they affect affordability since all the factors mentioned above have impact on the cost of houses.

Site layout I is characterized by a straight road. The other two layouts incorporate semi-circular roads. In site II the curved road is south facing (i.e. the center lies south of the arc), while in site III it is north facing.

Straight road scenarios include an east-west running road (site I), acting as reference case, and variations, where the road is rotated relative to the east-west direction by certain angles, in both senses ($\pm 30^\circ$, $\pm 45^\circ$, and $\pm 60^\circ$, with + sign implying clockwise rotation). These variations of site I aim at studying the effect of orientation of the street on the response variables (Chapter IV).

The circular road is selected to represent an extreme case of a curved road as, for instance, in a cul-de-sac street design. Figure 2.5 illustrates the three site layouts, where they represent typical segments of a large residential complex.

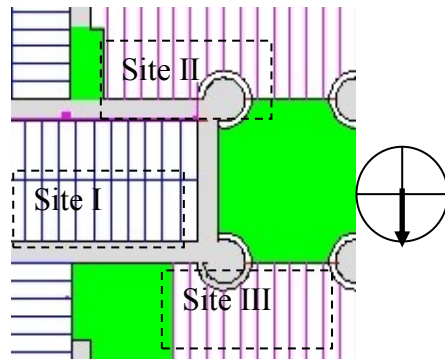


Figure 2.5, Overall site designs.

The housing units are positioned with respect to the shape of the roads in all configurations of neighborhoods. In site I only units on the north side of the road are considered. The shapes of units on the south side are assumed to be a mirror image of the units on the north side. However, the main solar façade remains the south façade, which is facing away from the road. This has architectural implications regarding the interior design and the fenestration allocated on different facades. These architectural implications may give some advantage to non-convex shapes, such as L and its variants, where the wing facing the road may remain essentially unchanged. Detailed presentation of the site layouts is provided in Chapter IV.

Density and Shapes

The main effect of increasing density of housing units is mutual shading by units and their wings (of non-convex shapes) and reduction in the effective surface area for insolation. Two density effects are analyzed. Spacing effect (s , in Fig. 2.6) is assessed by comparing attached units in triplex, quadruplex or pentuplex configurations with detached units. In addition, an effect, termed hereunder *row effect*, is assessed, whereby the south façades of selected configurations of site I is obstructed by a row of similar housing configurations (r in Fig. 2.6). Selected configurations of unit shapes (rectangle, L shapes, and L variants) are studied with varying row spaces. The minimal distance

required between rows to avoid shading on the façade of the obstructed row is first computed, and the distance is then incrementally reduced to assess its effect on energy performance.

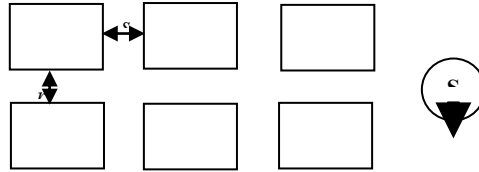


Figure 2.6, Illustration of the density parameters.

Representative shapes of dwelling units, analyzed in the previous stage (shape study) are adopted in the neighborhood study. Shapes found to have good performance, such as rectangular and L shapes with depth ratio of 1/2, are implemented in various site layouts. L shapes faced south or north are employed according to the road layout (i.e. the

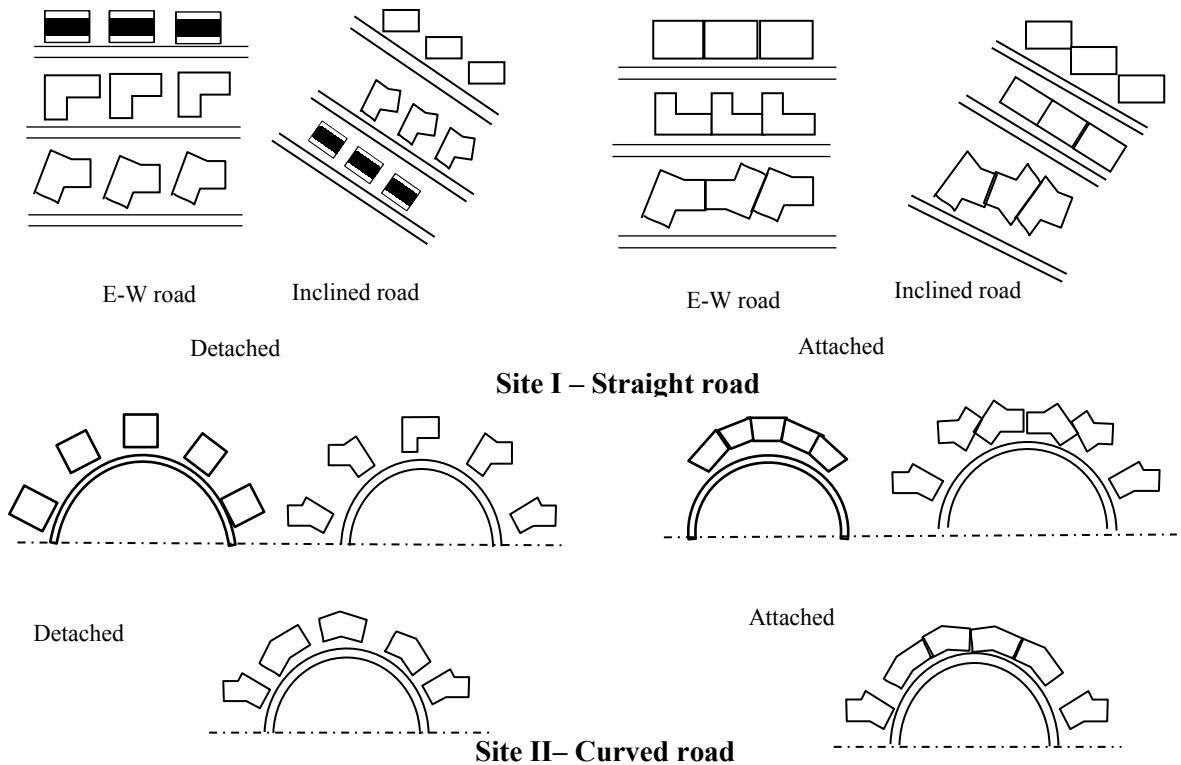


Figure 2.7, Sample neighborhood configurations.

curve south or north facing). Figure 2.7 illustrates some of the site/density/shape configurations investigated.

2.2.3 Roof Study

The objective of this part of the research is to design roof concepts that maximize the combined potential of annual electricity generation and heat production of their integrated photovoltaic/ thermal collectors. An open loop air-based BIPV/T system is assumed in this study. BIPV/T, with specially developed PV products, has the potential to meet all the building envelope requirements in addition to producing heat and electricity. This multiple functionality of BIPV/T system may improve the cost effectiveness of residential construction as compared to add - on PV/T systems which are usually attached to the outer layer of the construction, requiring thus additional mounting systems. This principle of using the PV panels as outer layer of the roof, instead of being attached to an outer layer (such as shingles) can increase the life time of the system especially if the roof shingles need to be replaced. On the other hand, the implementation of complete homogenous surfaces of BIPV/T (or BIPV) enables to avoid joints and connections, and therefore exposed screws/ nails that can lead to rain penetration. This assists in enhancing the overall durability and performance of the system. A similar principle of covering a complete roof surface by PV/T panels has been applied to the EcoTerra demonstration house (a hybrid BIPV/T system is used in the EcoTerra case, Chen at al., 2010).

The air-based BIPV/T concept utilizes circulating outdoor air behind the PV panels with the aid of a variable speed fan. The circulated air assists in cooling the panel and recovering heat that can be used for space or/and water heating. It should be noted however that not all heat generation of the BIPV/T system is useable heat. The usefulness

of BIPV/T systems is largely dependent on the end uses and demand profile, as well as the thermal storage temperature. This issue is not directly considered in this thesis.

An approximate numerical model of an open loop air-based BIPV/T system is employed to determine a correlation between potential thermal and electrical energy generation, based on the literature. The objective is to provide a simple tool for estimating thermal energy potential as a ratio of electricity generation. The investigation of roof parameters is outlined below. Details of the investigation, simulations and analysis of the results are presented in Chapter V.

The roof study investigates the effects of variations to the basic hip roof design of Figure 2.3 on thermal and electrical energy production and performance. The study is conducted in three main parts.

The first part evaluates the effect of varying tilt and orientation on BIPV/T potential per m² of roof surface. The objective is to determine the range of optimal combinations of tilt and orientation angles for annual electricity and heat generation over an assumed heating period.

The second part investigates increasingly complex roof designs. First, a hip roof design for the basic units is studied, with different combinations of tilt and side angles. Multi-faceted roof surfaces, involving varying tilt and orientation angles, are then designed for the rectangular layout plan- Figure 2.8. The south facing surface of a hip roof (with 45° side angle) is adopted as reference for comparative evaluation of the BIPV/T potential of all other roof designs. The possibility of extending complex roof design to non-convex shapes is explored (Appendix B).

The third part consists of redesigning the unit plan shapes to fit the shape of the roofs. The design of the residential unit follows the sequence: unit shape design→ roof design→ unit shape re-design.

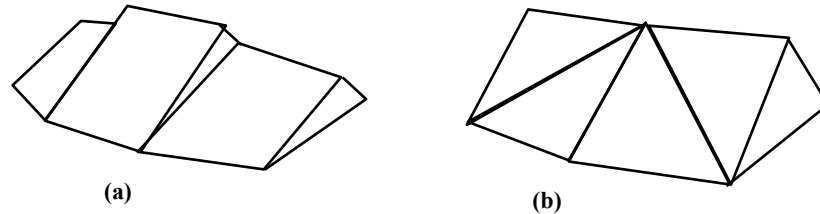


Figure 2.8, Sample modified roof shapes for rectangular housing unit: a) split surface; b) folded plate.

2.2.4. Design Methodology for Solar Neighborhoods

Chapter VI concentrates on the implications and applications of parameters studied in previous chapters for housing units and neighborhood design. It starts with a concise summary of the main design parameters and their effects on solar performance. Effects of design parameters are presented in matrices that relate design parameters to performance criteria. A listing of design considerations for high energy performance of dwellings and neighborhoods is then proposed in a concise, tabular form.

A heuristic methodology is developed for the design of near optimal solar neighborhoods. The methodology details each stage of the process and highlights neighborhood design alternatives with good solar potential and energy performance. The design methodology involves the evaluation, selection and upgrading of initial design alternatives. An evaluation system is proposed as a tool for the evaluation and selection of design alternatives.

The evaluation system is based on assigning weights to energy performance criteria (such as energy consumption and generation) associated with the effects of design parameters. The application of the evaluation system is illustrated by means of examples for housing units and neighborhoods configurations featuring in the parameter effect matrices. The sensitivity of the system to performance criteria weight assignment is also investigated.

2.3. Tools, Modeling and Simulations

2.3.1 Selection of Simulation Software

As mentioned in Chapter I (Section 1.3) various existing simulation tools deal with various aspects of energy performance of buildings and urban neighborhoods but an integrated package that handles all aspects is lacking. EnergyPlus (EnergyPlus. 2011), employed usually for single building design and energy performance, is adopted as simulation tool in this research based on the following features:

- It has extensive capabilities of integration of passive design components, together with active solar technologies, HVAC systems and control strategies.
- It enables the user to select the method of heat transfer – either the transfer function method, which models the building as a linear system, or finite difference techniques, in which the energy balance equations of the building are discretized in space and time.
- It offers a high degree of flexibility, a high level of details, and extensive documentation that enhances its accessibility. Elaborate output reports can be produced by the program following the simulations, including visual output

(DXF outputs and CSV files), which greatly facilitate the interpretation and analysis of results.

- An additional feature of EnergyPlus that makes it especially suitable for this research is the availability of Google Sketchup plug-in (Google Scketchup, 2011) that greatly facilitates the generation of geometric data of complex shapes.

Testing and Validation of EnergyPlus

The testing and validation is still an ongoing part of EnergyPlus development. For instance, numerous empirical validations were carried out to evaluate the capabilities of this software, as compared to other programs and to experimental measurements. These validations include modeling solar radiation on external façades, and predicting heat flow through windows (i.e. glazing unit and window frame). The results and analysis of these validation tests show that the simulation codes used by EnergyPlus (in addition to other simulation programs such as ESP-r) are capable of computing total irradiated solar energy on building façades with a high precision over extended time periods (months) (Loutzenhisera et al, 2009). The heat flow through windows was also predicted by EnergyPlus with a good precision, where the difference with the experiment was in the order of 5.8% (Loutzenhisera et al, 2007).

EnergyPlus implementation of PV models is preliminarily validated by comparing results from the three models of PV available in EnergyPlus, as well as to results from an independent program (DesignPro-G v5.0) (e.g. Griffith and Ellis, 2004). The results agree within 5%. The effects of coupling PV models with shading and surface heat transfer models were verified by carefully evaluating results against engineering expectations as well.

Some limitations of PV models in EnergyPlus include:

- Models for inverters, charge controllers, or batteries are not included.
- The operation of the entire electrical system is assumed to operate under ideal conditions.
- Modules are assumed to be always operating at the maximum power point.

The current research is a comparative study. Effects are measured by comparison of the values response variables to reference configurations. The true absolute values of response variables are not a major concern and therefore these limitations are not considered crucial.

2.3.2. Modeling and Simulations

The study is performed to Montreal, Canada (45° N Latitude). The heating degree days (HDD) for Montreal are about 4519 DD (the Weather Network, 2011).

SketchUp/OpenStudio is employed to generate geometric data for EnergyPlus. Each housing unit is modeled as a single conditioned zone. The Conduction Finite Difference algorithm is selected as the heat balance algorithm. This solution technique employs a one-dimension finite difference method to represent the construction elements. A short time step of 10 minutes is selected in the simulations.

Weather Data

Two design days – a sunny cold winter day (WDD) (in January), and a sunny hot summer design day (SDD) (in June) –are selected. The daily average dry bulb temperature and total solar insolation serve as basis for the selection of these design days (Hong et al, 1999). The main purpose of these design days is to explore the solar

potential of all studied configurations, thus the WDD and SDD are selected to represent two extreme sunny days. Additionally, a whole year weather data set serves as basis for estimating the annual electricity production potential of the PV system installed on south-facing roof surfaces (details are given below), as well as for the computations of heating and cooling loads.

The weather files of EnergyPlus are employed in the simulations (EnergyPlus: Weather files). The weather data file, which is based on CWEC – Canadian Weather for Energy Calculations, provides hourly weather observations. These observations simulate a one-year period, specifically intended for building energy calculations. The data collected for this typical year includes hourly values of solar radiation, ambient temperature, wind speed, wet bulb temperature, wind direction and cloud cover.

Solar Radiation Computations

The first step in the analysis is to compute solar irradiance (solar modeling). The instantaneous solar radiation accounts for the direct beam and diffuse radiation, as well as for radiation reflected from the ground and adjacent surfaces. The solar model adopted for this study is the ASHRAE Clear Sky model (ASHRAE, 2005). This model is the default model employed by EnergyPlus to estimate the hourly clear-day solar radiation for any month of the year. Sky radiation is calculated using the Perez anisotropic sky model (Perez et al, 1990).

The clear sky model yields values that are representative of conditions on cloudless days for a relatively dry and clear atmosphere. The clearness numbers usually serve as correction factors to apply this model to locations with clear, dry skies or locations with hazy and humid conditions (Threlkeld and Jordan, 1958).

Shading Calculations

To study the solar radiation incident on different shapes it is necessary to determine the shaded surfaces of a building, as well as surfaces that are directly reached by solar irradiation. The shading algorithm accounts for self-shading geometries, such as L shapes. This algorithm is based on coordinate transformation methods (Groth and Lokmanhekim, 1969) and the shadow overlap method (Walton, 1983).

Slab on Grade Model

Slab on grade foundation is assumed in this research, for the sake of simplicity. The concrete slab is 200 mm thick, and it is insulated both underneath and along the perimeter. Characteristics of the slab are provided in Chapter III (Table (3.1)). The *slab program* (EnergyPlus, 2011), is employed to compute the temperature of the under-surface of the slab (in contact with the ground). Taking into account the slab and ground properties, the slab program produces average monthly temperature of the slab, which is input in EnergyPlus to carry out the simulations.

BIPV and BIPV/T Models and Computations

BIPV Model

The Equivalent One-Diode Model (or “TRNSYS PV” model, Eckstein, 1990) employed in EnergyPlus is selected to perform electricity generation simulations of the BIPV/T systems. The TRNSYS model employs a four-parameter empirical model to predict the electrical performance of PV modules (Duffie and Beckman, 2006).

The current-voltage characteristics of the diode depend on the PV cell’s temperature. The model automatically calculates parameter values from input data,

including short-circuit current, open-circuit voltage and current at maximum power (Griffith and Ellis, 2004). For this study, the PV array is selected from EnergyPlus database to provide approximately 12.5% efficiency, under standard conditions (Athienitis et al., 2011). The electrical conversion efficiency decreases by some 0.45% for each °C increase of cell temperature from the temperature under standard conditions. For Montreal, the annual potential of PV electricity generation of south facing surfaces at latitude tilt angle is about 1200 kWh per kW_{peak} of installed PV (NRCan, 2011).

BIPV/T Simple Model

A transient quasi-two-dimensional finite difference model is utilized to determine the thermal energy generation potential of the BIPV/T system, and to establish a correlation between electricity and useful heat generation. A gable roof, associated with a rectangular plan layout with a tilt angle of 45° serves as basis for deriving the correlation model. Details of the model are presented in chapter V. The model is applied as well to roofs with different tilt angles, for the winter design day.

The approximate correlation serves as a simple tool to explore the thermal potential of BIPV/T system. For actual design applications a more detailed model would be required.

CHAPTER III: DWELLING SHAPE¹

This chapter investigates in depth the solar potential and energy demand of dwellings of various geometrical shapes. A large number of geometries (ca. 30 geometrical shapes) are explored, ranging from basic shapes commonly employed in dwellings to more complex configurations. The study investigates the effect of these shapes on two major response variables – solar potential and energy load/consumption for heating and cooling. The parameters, whose effects on the response variables are investigated, include, in addition to the basic shapes, variations to the geometry of L and U shapes. Shape variations include varying values of the relative dimensions of the wings and variations to the angle enclosed by the wings of these shapes. The balance between energy supply and total energy consumption is evaluated as well.

3.1. Shape Design and Investigation

In this section the design assumptions of the dwelling units are first detailed. This is followed by the design of basic shapes, and detailing the criteria that govern the design. Next, the parametric investigation is outlined, detailing the parameters whose effects on the energy performance of dwelling units are studied, the values of these parameters and the combination of parameter values that are analyzed.

¹ The study and some of the results presented in this chapter are published in:
Hachem C., A. Athienitis, P. Fazio, (2012a). Evaluation of energy supply and demand in solar neighbourhoods, *Journal of Energy and Buildings*, DOI: 10.1016/j.enbuild.2012.02.021.
Hachem C., A. Athienitis, P. Fazio, (2011a), Parametric investigation of geometric form effects on solar potential of housing units, *Journal of Solar Energy*, Volume 85, Issue 9, Pages 1864-1877.

3.1.1 Basic Design Assumptions

Energy efficiency measures are adopted in the design of dwellings. Building envelope design aims at ensuring high energy efficiency. The level of wall insulation and window characteristics are selected based on a sensitivity analysis of the effect of these factors on the energy performance of the rectangular shape. The results of this analysis are presented in Figures A-1, A-2 and A-3 of Appendix A. The characteristics of the building envelope together with the energy efficiency measures that are implemented in all dwelling units are detailed in Table 3.1.

A heat pump with a coefficient of performance (COP) of 4 is assumed to supplement passive and active solar heating. An intelligent shading control is considered: Interior blinds are assumed to be shut when the indoor air temperature exceeds 22°C, throughout the cooling season. A ventilation rate of 0.35 air changes per hour (ACH) is assumed. This value conforms to ASHRAE standard 62.2 requirements for air change rate associated with a given house size and occupancy (ANSI/ASHRAE Standard 62.2; 2010).

Electrical loads for major and minor appliances, for lighting and for domestic hot water (DHW) are assumed based on a variety of sources dealing with the electrical load in energy efficient and net zero energy solar houses (NZESH) (e.g. Armstrong et al, 2009, Sartori et al, 2010, Pohgarian, 2008) and on an assumed energy conscious behaviour of occupants (Brandemuehl and Field, 2011).

Loads for major appliances including refrigeration, washing and cooking appliances, and minor loads for kitchen and entertainment devices are summarized in Table 3.1. Lighting consumption can be limited to 3kWh/m²/yr for a NZESH in mid-

latitude locations, based on the assumption that a NZESH is expected to optimize daylight utilization (Sartori et al, 2010).

Hot water energy consumption can be limited to a daily average of 2.75 kWh per occupant (Sartori et al, 2010), based on the assumption of hot water usage of 50L/day/person.

Table 3.1, Main Characteristics and Electric Loads of Housing Units

Thermal resistance values:	Exterior wall: 7 RSI Roof: 10 RSI Slab on grade: 1.2 RSI Slab perimeter: 7 RSI
Thermal mass	20cm concrete slab
Window type	Triple glazed, low-e, argon filled (SHGC=0.57), 1.08 RSI
Area of south glazing	Analysed below
Shading Strategy Shading control	Interior blinds Blinds shut at indoor air temperature of 22 °C
Occupants	2 adults and 2 children, occupied from 17:00 - 8:00
Setpoint temperatures	Heating set point 21°C, cooling set point 25°C
Infiltration rate	0.8ACH @50Pa
Ventilation rate	0.35ACH
Assumptions for electrical loads	
Lighting	3kWh/m ² /yr (Sartori et al., 2010)
DHW	2.75kWh/day/person (Sartori et al., 2010)
Major appliances	1600kWh/yr (Pohgarian et al., 2008)
Minor appliances	1100kWh/yr (Charon, 2007)

3.1.2 Shapes of Dwelling Units

Basic Shapes

Seven basic plans of single family two-storey dwelling units are studied. Dwelling shapes include the convex shapes rectangle, square, trapezoid, and the non-convex shapes L, U, H and T. A constant area of ca. 60m² per floor is adopted for all shapes.

The basic design of dwelling shapes relies on passive solar design principles (Chiras, 2002) and rules of thumb (CMHC, 1998). The design ensures that the overall width of the south (equatorial) façade, when applicable, is larger than the width of the

lateral (east and west) façades to maximize passive solar gains in winter. The layout of the interior space ensures that the living area and the kitchen, in the ground floor, are adjacent to the south wall. The interior spaces of all units are partitioned to fit a family of four persons. The floor area is based on the need to reduce costs by maintaining a compact design.

An important parameter characterizing non-convex shapes, which are self-shading, is the relative dimensions of the shading and shaded façades (depth ratio (DR) – a/b , in Fig. 3.1). The shaded façade's width and the depth ratio are determined so as to maintain a functional interior space. Decisions on the dimensions and configuration of non-convex shapes are based on functional partitioning of the interior space, so as to avoid wasted space, or long corridors. The main considerations governing the design of shapes in this study are as follows:

- An aspect ratio of 1.3 should be applied, when possible. This ratio is within the optimal range for passive solar design in northern climate (Athienitis and Santamouris, 2002).
- The basic L shape has a depth ratio of 1 and an overall aspect ratio of 1. An aspect ratio of 1.3 is adopted for L shape with depth ratio (a/b) of $\frac{1}{2}$.
- A symmetric design is adopted for U, H and T shapes, in order to simplify the analysis.
- Interior dimensions should allow a functional distance of not less than 3m.
- For the trapezoid, an additional parameter is the angle between the south (or north) façade and the inclined façade. An acute angle (θ , in Figure 3.1) of less

than 60° is avoided. The dimension of the narrow façade is determined by the aspect ratio and the angle θ .

- Design for daylight penetration is taken into consideration when it is applicable. It is generally recommended that the depth – the dimension perpendicular to the south façade – should not exceed 1.5 to 2 times the head height of the window, for proper daylight penetration (corresponding to 4-5 m for the current plans) (Lechner, 2001). Non-convex shapes allow the implementation of such lateral dimension in some parts of the plans (i.e. the main wing), which make them particularly suitable for daylight penetration.

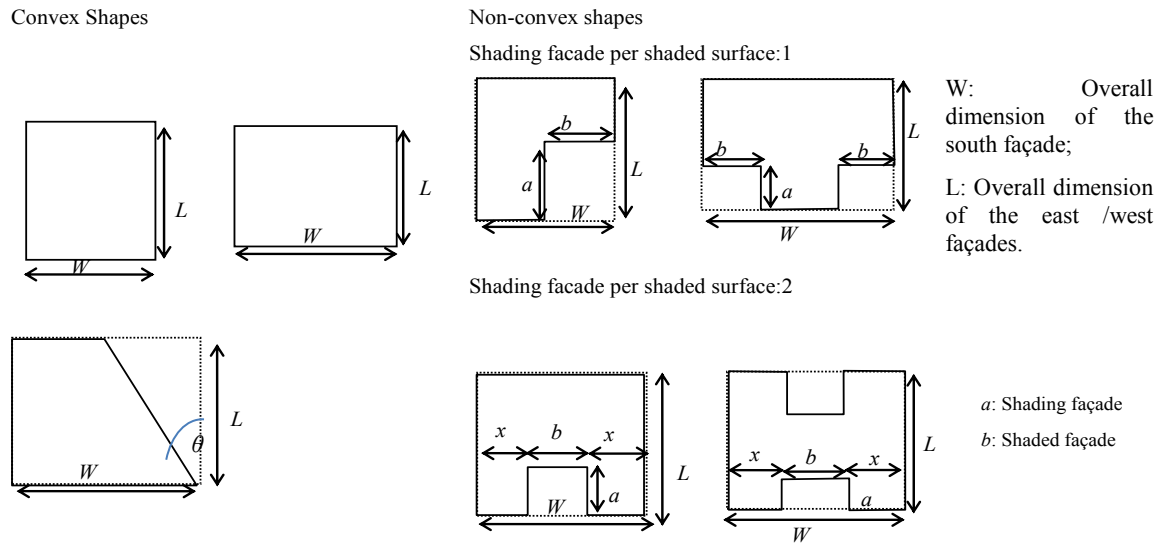
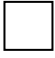
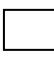



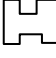



Figure 3.1, Basic shapes.

The shapes shown in Figure 3.1 are characterized by the parameters presented in Table 3.2.

Table 3.2, shape design parameters for basic cases (south windows are designed as percentage of floor area- see below)

	 square	 Rectangle	 Trapezoid ($\theta=60^\circ$)	 L shape	 U shape	 H shape	 T shape
Aspect ratio (W/L)	1	1.3	1.3	1	1.3	1.4	1.6
Number of shading façades	n/a	n/a	n/a	1	2	2	1
Depth ratio a/b –				1	1	1/4	2/3
Ground floor south window as percentage of ground floor south-facing wall area	26%	23%	20%	23%	20%	19%	19%

Façades and Windows

The ceiling height of the ground floor is set at 3 m, to enhance daylight penetration (Athienitis, 2007). The first floor ceiling height is about 2.7 m. Triple glazed, low-e, argon filled (SHGC=0.57, Visible transmittance =0.65) are selected for the south facing windows. Various sizes of these windows are explored, for the basic cases (see below). The east and west windows are 4% of the total heated floor area. This is based on recommendations to minimize non-south glazing area to 4% or less of the total heated floor area, under northern climate conditions (Chiras, 2002), while maintaining functional considerations.

The south window area in the basic cases constitutes 10% of the total floor area (120m²). The size of south-facing windows of the ground floor constitutes 12 % of the ground floor area, to enable the living area to benefit from daylight and heat gain during the day. The first floor south façade windows are 8% of first floor area. Due to the different areas of south facing façades of different shapes, south windows' areas, when computed as percentage of floor area, constitute differing percentages of these façades (Table 3.2).

For non-convex shapes, the south façades are not co-planar, and therefore the total window area is distributed over the different portions of the facade. This is to

accommodate both the predetermined area of window and functional requirements, such as providing daylight for different zones of the plan.

Roofs

The basic roof design in this study is a hip roof with tilt and side angles of 45° (Fig. 3.2a). The effect of varying tilt and side angles of the roofs of the basic shapes is studied in Chapter V (Roof Study).

The height of the lowest edge of the roof is kept constant at seven meters above ground level. The roofs are designed with their ridge running east-west at the center of the plan area for all shapes, except L and T (Fig. 3.2b). L and T shapes consist of a main wing running east-west and a branch facing south. In these shapes the ridge of each wing runs along its center, with a triangular south facing hip at the end of the branch. The main wing roof ends with gables (Fig. 3.2b).

The ridge height varies depending on the width perpendicular to the ridge, and the tilt angle. For a tilt angle of 45° , the ridge can reach a height of 3.5 m from the lower plane of the roof, in the rectangular shape. U and H shape roofs are designed with a single ridge, in a similar way to the rectangular shape roof, with the central recess cut out (Fig. 3.2c).

PV modules are assumed to be integrated within the total area of all south-facing and near-south-facing roof surfaces as shown in Figure 3.2. This includes the triangular portions of hip roofs in L and T shapes.

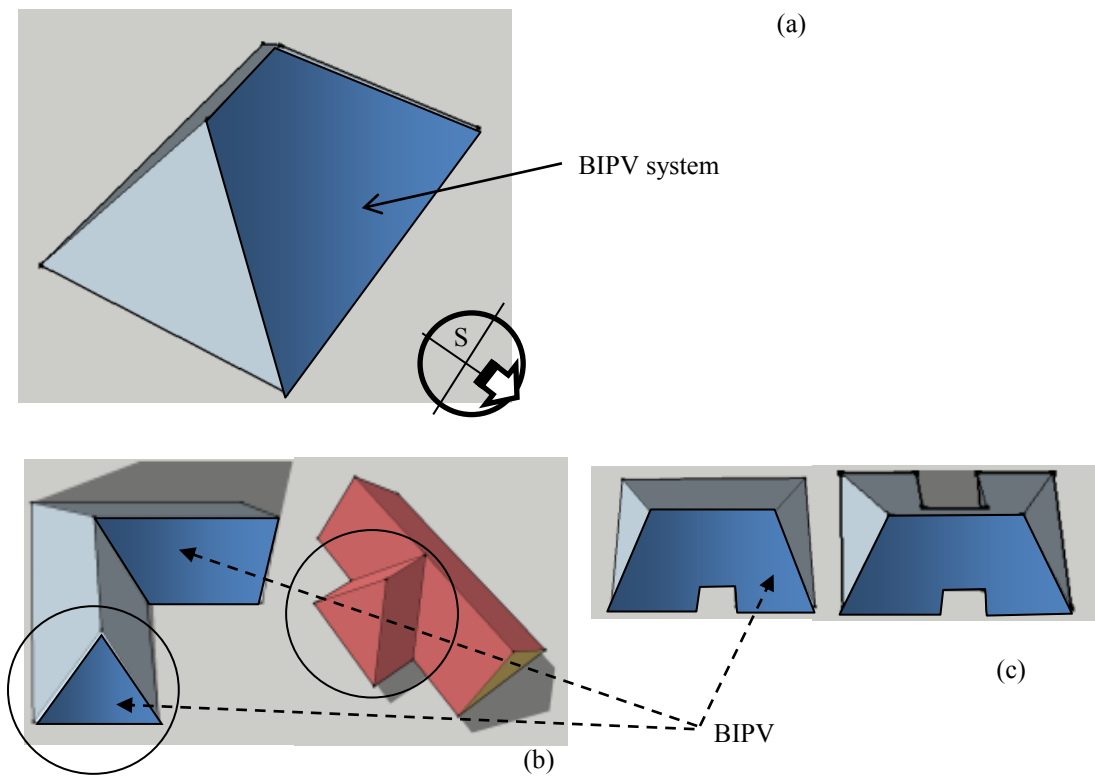


Figure 3.2, Roof layouts of basic designs: a) Single ridge design for convex shapes; b) Double ridge designs in L, T; c) Roofs of U and H shapes.

3.1.3 Parametric Investigation

The study investigates the effects of a number of parameters on the two major response variables – solar potential and energy demand for heating and cooling. Solar potential includes in this chapter, radiation incident on south façades and transmitted by their windows, total heat gain from windows, and PV electricity production potential. The thermal potential of the BIPV system (i.e. hybrid BIPV/T system) is studied in detail in chapter V.

The parameters, whose effects on the response variable are investigated, include, in addition to the basic shapes and south window areas, several variations to some of the basic design configurations. These additional parameters are: variations to the geometry

of the rectangular and L shapes and variations to the orientation of the rectangular unit. Variation of the rectangular shape, representing convex shapes, consists of changing the aspect ratio (AR). L shape variations include varying values of the depth ratios (DR) and variations to the angle enclosed by the wings, which in the basic design are at right angle. The effect of an increased number of shading façades is explored by studying U shape with various depth ratios. Combinations of parameter values analyzed in this study are summarized in Table 3.4.

South Window Size

The size of the south facing window for the basic cases is as detailed in Table 3.2, based on percentage of floor area. Two south facing window sizes are explored, in addition to the basic value. In the second and third options, the south facing windows constitutes 35% and 50%, respectively, of the south façades of all shapes.

Variations on Basic Shapes

Rectangular Shape

The effect of two parameters on the solar potential and energy performance of the rectangular shape are studied: aspect ratio (AR) and orientation relative to due south. AR values range from a ratio of 0.6, resulting in a south façade that is narrower than the perpendicular façade, up to the value of 2. An AR of 1 is associated with a square plan.

The angle of orientation, relative to south, ranges from -60° (rotation east) to $+60^{\circ}$ (rotation west). These two parameters are detailed in Table 3.4.

L shape Variations

L shape consists of a main wing and an attached branch. The main wing is assumed to be oriented east-west, so as to have the long façade facing south. The branch can be attached at either the west end, W configuration, or at the east end, E configuration. It can also be facing south (S) or north (N). Thus the configuration L-WS, for instance, denotes L shape with the branch attached to the west end of the main wing towards the south (Table 3.3).

Depth Ratio

The depth of the shadow receiving facade and the number of shadow projecting façades play an important role in determining the amount of solar radiation incident on the shaded façade and transmitted by its windows. Two values of the depth ratio – $\frac{1}{2}$ and $\frac{3}{2}$ – are adopted for L shape, and U shape (to study the effect of two shading facades), in addition to the basic value of 1. In the design of units with varying depth ratios, the floor area is kept constant (ca. 60 m^2). An aspect ratio of 1.3 is applied in L shape with depth ratio of $\frac{1}{2}$.

Wing Rotation

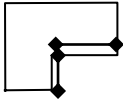
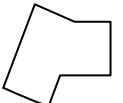
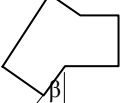
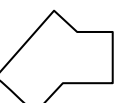
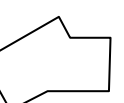

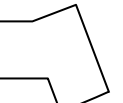
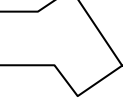
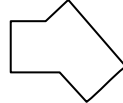
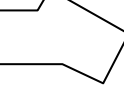
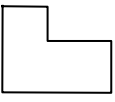


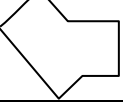
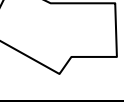

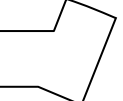
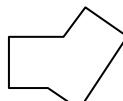
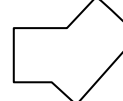
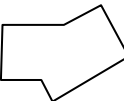
The L shape used for the study of the effect of wing rotation is characterized by a depth ratio of $\frac{1}{2}$. This ratio is selected, based on practical, functional considerations.

L variants are characterized, in addition to the depth ratio, by the angle β – the deviation from 90° of the angle enclosed by the wings of the L (Table 3.3). Four values of β are considered in this study – 15° , 30° , 45° and 60° . L variants are identified by the letter V followed by a series of characters specifying the position and angle of the branch

(Table 3.3). For instance V-WS30 is a variant with a branch attached to the west end of the main wing, facing south and having an angle $\beta=30^\circ$.

An additional shape, termed hereunder *Obtuse-angle* (O) can be considered a special L variant with larger values of the angle β ($\beta=70^\circ$ is adopted). For obtuse-angle shape, the depth ratio has no significant effect as the wings, generally, do not mutually shade. The obtuse shape may be facing in a generally south direction – O-S or north direction – O-N.

Table 3.3. Variations of L shapes

Direction of Branch	Shape					Obtuse angle
	L shape	Variations of L shape				
		L variant (V)				
South	(L-WS*) 	$\beta=15^\circ$ – West (V-WS15) 	$\beta=30^\circ$ – West (V-WS30) 	$\beta=45^\circ$ – West (V-WS45) 	$\beta=60^\circ$ – West (V-WS60) 	(O-S) 
		$\beta=15^\circ$ – West (V-WS15) 	$\beta=30^\circ$ – East (V-ES30) 	$\beta=45^\circ$ – East (V-ES45) 	$\beta=60^\circ$ – East (V-ES60) 	
North	(L-WN) 	$\beta=15^\circ$ – West (V-WN15) 	$\beta=30^\circ$ – West (V-WN30) 	$\beta=45^\circ$ – West (V-WN45) 	$\beta=60^\circ$ – West (V-WN60) 	(O-N) 
		$\beta=15^\circ$ – West (V-EN15) 	$\beta=30^\circ$ – East (V-EN30) 	$\beta=45^\circ$ – East (V-EN45) 	$\beta=60^\circ$ – East (V-EN60) 	

*Solar potential and energy demands of L-E and L-W are not significantly different (with L-W performing slightly better than L-E)

Obtuse angle and trapezoid shapes typically feature in sites of curved layout, covered in Chapter IV. Trapezoid is analyzed in this chapter as a basic shape (angle $\theta=60^\circ$, Fig. 3.1). In chapter IV it features (with a different geometry) in attached configurations in sites of curved layout. Obtuse angle is studied in this chapter for south and north orientations, as shown in Table 3.3.

A photovoltaic system is assumed to cover all south and near-south facing roof surfaces, including the triangular portions of hip roofs in L shape and its variants, and the two near south facing surfaces in obtuse-angle roofs. Figure 3.3 presents roofs of selected L variants and the BIPV portion of the roofs.

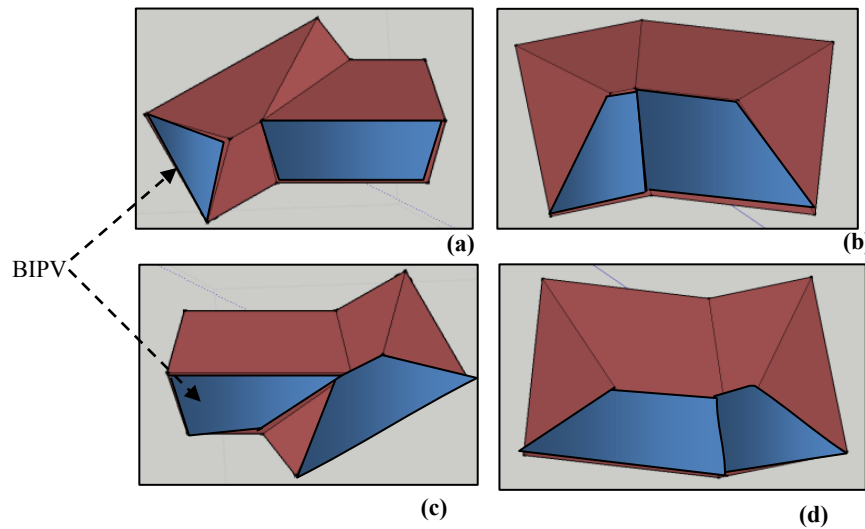


Figure 3.3, Irregular roof shapes and PV integration. PV integrated surfaces are shown hatched. a) and b) represent roofs of V-WS60- variant and obtuse angle O-S, c) and d) represent V-EN60 and O-N.

Summary of Parametric Investigation

Values of the parameters investigated in the study of dwelling shapes are summarized in Table 3.4. These parameters consist mainly of the basic shapes and variations on the rectangular, L and U shapes. A total of 30 configurations of parameter

combinations are designed and investigated. This is in addition to a large number of scenarios designed to identify the effect of single independent design parameters that are decoupled from others (e.g orientation, aspect ratio, south window area (as fixed area or as percentage of the south façades), etc.).

Table 3.4, Parameter combinations

Shape		Aspect ratio (AR)	Orientation	Depth ratio (DR)	Rotation of branch (L shape)	South facing window area	
Basic shapes (Fig.2)		Basic	South	Basic design	n/a	10% of total floor area 35% of south façade 50% of south facade	
Variations of shapes	Rectangle	1-2 (step of 0.1)	South	n/a	n/a	35% of south façade	
		1.3	-60° to +60°	n/a	n/a		
	L shape	L	Basic	South and North (see Table 3.3)	1/2- 3/2		n/a
		L variants	1.3	South and North (see Table 3.3)	1/2		$\beta=15^{\circ}-60^{\circ}$ (15 ° step)
		Obtuse Angle	1.2	South and North (see Table 3.3)	1/2		$\beta=70^{\circ}$

3.2 Presentation and Analysis of Results

Simulations are performed to analyze the effect of the design parameters detailed above on solar potential and heating and cooling loads and consumption (assuming a heat pump of COP 4). Assumptions employed in the simulations are detailed in Chapter II. The effects of basic shape design are first presented, followed by the analysis of variations to the basic designs.

3.2.1. Effects of Basic Shape Design

Solar Potential

Solar Radiation and Heat Gain

The mean daily global insolation for the south facing non-shaded façade obtained from EnergyPlus simulations is about 3.23kWh/m². This value falls within the range estimated by Natural Resources Canada (NRCan) (2.5-3.3 kWh/m²) for the studied location (NRCcan, 2011).

The results include allowance for shading in non-convex shapes such as L, U, H and T. The total radiation is compared with radiation on the rectangular shape, which serves as reference. Figure 3.4 displays the total transmitted radiation (in kWh) for a single south facing window unit (2 m²), for both shaded and non-shaded façades, for the winter and summer design days. It should be noted that for the basic cases, where the south facing windows are considered as percentage of the floor area, the total area of south-facing windows is the same for all shapes. Following are some comments on the more significant results.

- In the absence of shading in convex shapes, the amount of radiation incident and transmitted by windows depends solely on the size of the south façade and windows.
- For non-convex shapes, an additional factor that influences solar radiation is the shade cast by adjacent façades. The reduction of incident radiation on the south shaded façade of the basic non-convex shapes as compared to the rectangle amounts to 22% for the L shape and 43% for the U shape (DR=1) (Fig. 3.4). A

similar effect is observed for the transmitted radiation by windows of the south façades of L and U shapes. This effect is studied below in more detail.

- Heat gain through windows in convex shapes is affected only by the size of the windows. In non-convex shapes, solar heat gain is affected by shading parameters in addition to window size. Figure 3.5 presents the annual solar heat gain associated with different window size options for each of the shapes. It can be observed that while for the basic window size (10% of the floor area) shape effect is not significant, heat gain for windows of 35% and 50% of façade area is strongly affected by shape.

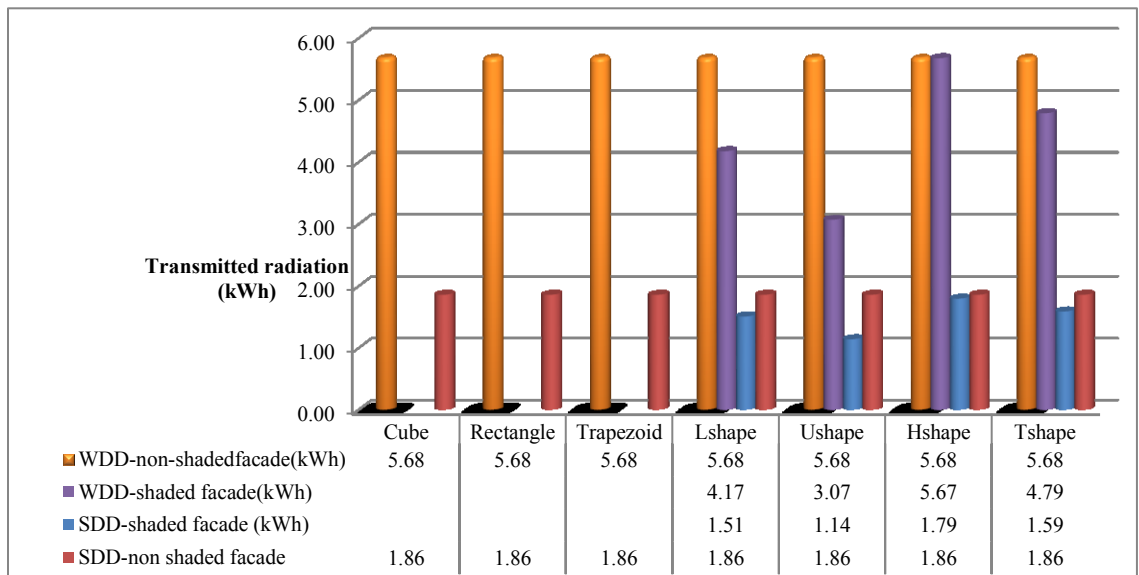


Figure 3.4, Transmitted radiations by windows in south façades for a WDD and for a SDD.

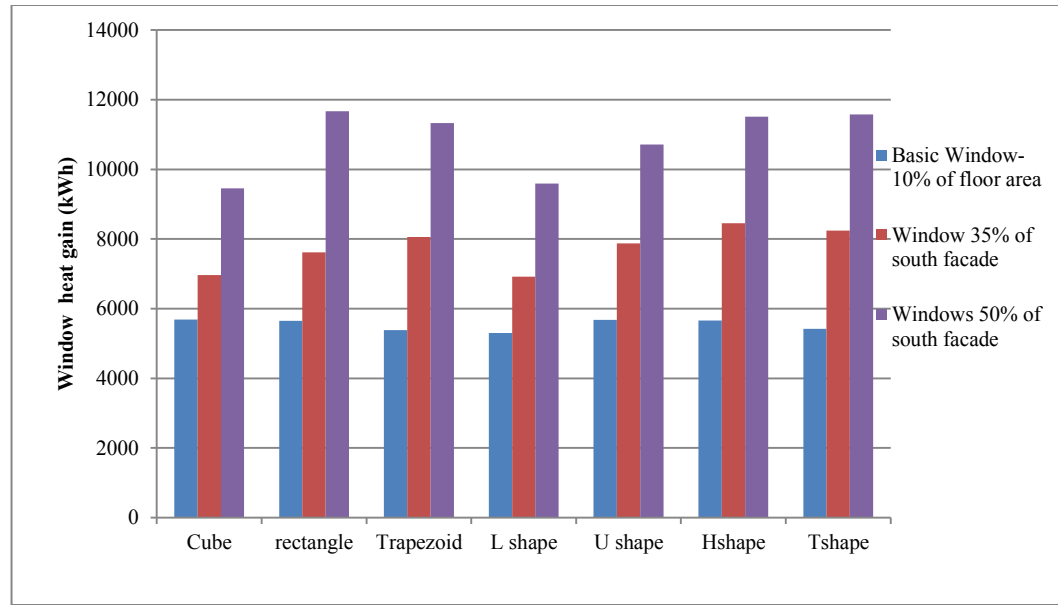


Figure 3.5, Window annual heat gain of all shapes associated with different south window areas.

Electricity Generation by the BIPV System

The roofs of the basic shapes are all designed with the same tilt angle and orientation (south facing). Therefore the electricity generation of the BIPV systems integrated in the south facing roof surfaces is affected only by the total area of these surfaces and by shading from adjacent surfaces. The main observations of the analysis of results are highlighted as follows:

- The annual electricity generation of shapes with basic roof design (45° tilt and side angles) shows that the T shape has the maximum generation. The trapezoid and H shapes have larger electricity production than the rectangular shape, while U and L generation approximates the generation of the rectangular shape (difference of 5% or less). Square shape has the lowest production of all shapes.
- Effect of shade from adjacent surfaces on energy generation is not as significant as for the façades, due to the inclination of the roof. The reduction in electricity

generation reaches a maximum of 6% per m², averaged over the roof area, for the basic L shape.

- U and H shape roofs are not affected by the number of shading façades and the DR in the studied cases, due to the roof design adopted in these cases (Fig. 3.2c).

Figure 3.6 presents the winter design day (WDD) peak electricity generation and the annual energy generation associated with all basic shapes. A comparison of the annual electricity generation of the BIPV system of each shape to the reference case (rectangle) is presented in Table 3.5, which gives a summary of energy performance of all basic shapes.

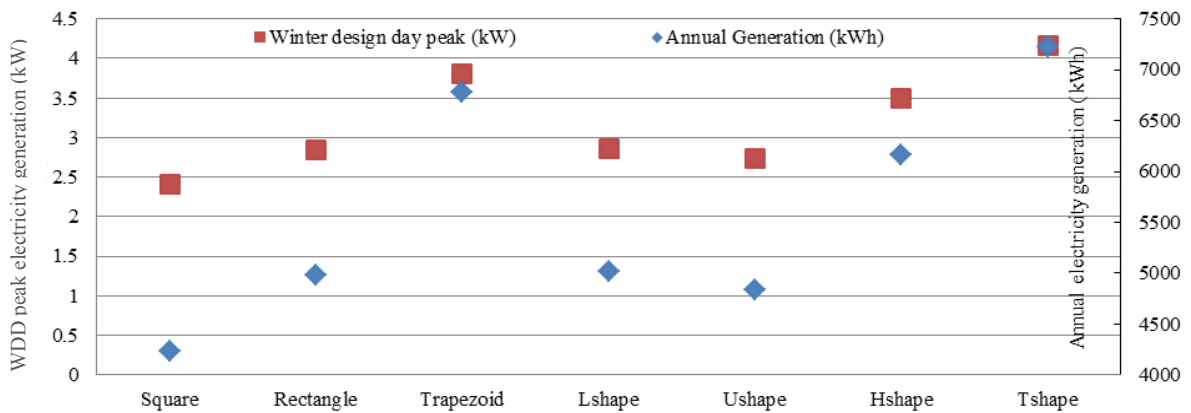


Figure 3.6, WDD peak electricity generation and annual electricity generation for all basic shapes.

Energy Demand

The effect of basic shape of units on the energy demand is first determined by analyzing the effect of the building envelope. The results indicate a correlation between heating energy demand and the total building envelope area – Fig. 3.7. The correlation between heating load and the building envelope area is inversely proportional to window area. Heating and cooling loads of all basic shapes and the comparison of heating load of

these shapes to the reference are presented in Table 3.5. Energy balance between production and total energy consumption is discussed in section 3.2.3.

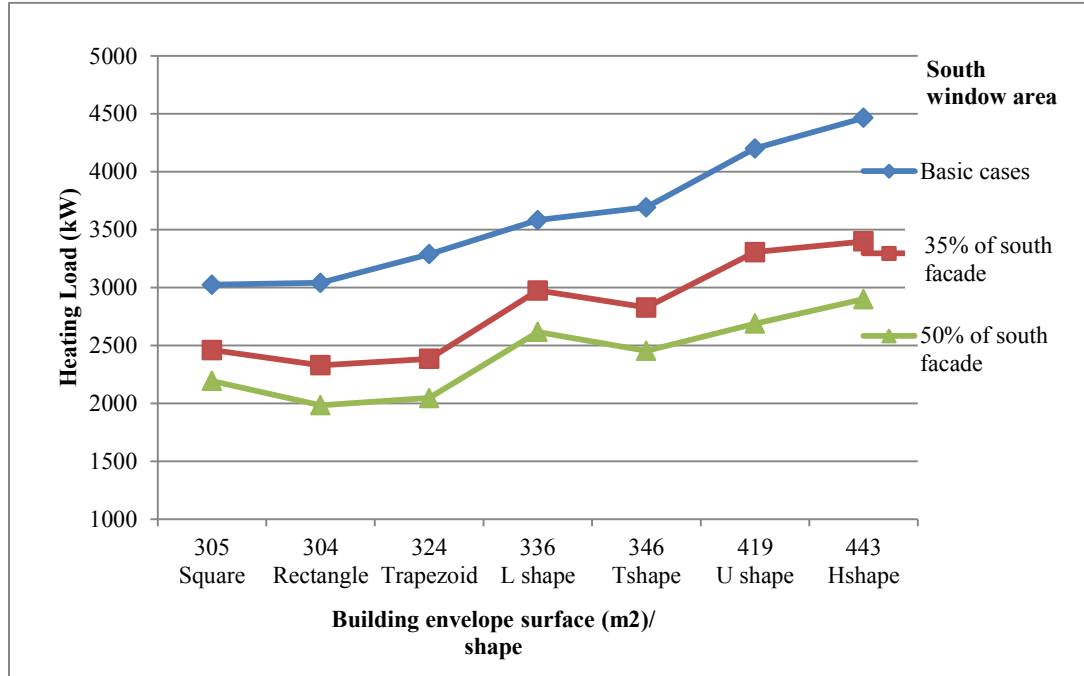


Figure 3.7, Correlation between building envelope area and heating load for varying ratios of south facing window areas.

Table 3.5, Energy performance of basic shapes

	Total envelope area (m ²)	South facing roof area (m ²)	Yearly window heat gain (kWh)	Yearly Heating load (kW)	Yearly Cooling load (kW)	Yearly Energy generation (kWh)	Ratio of heating load to reference	Ratio of energy generation to reference
Square	305	21.8	5685	3024	110	4233	0.99	0.87
Rectangle	304	25.6	5652	3041	107	4867	1	1
Trapezoid	325	34	5383	3287	90	6777	1.08	1.37
L shape	336	27.4	5304	3581	106	4948	1.20	1.014
U shape	390	24.7	5682	3780	106	4835	1.24	0.99
H shape	443	31.5	5656	4460	74	6168	1.47	1.26
T shape	346	37	5424	3693	79	7228	1.21	1.48

The annual heating and cooling loads associated with various south window areas are presented in Table 3.6 and in Figure 3.8. Heating load is reduced dramatically for shapes like U and H (about 35%) when the south window constitutes 50% of the façade, as compared with the basic cases.

Increasing the south window area to 50% of the total south façade leads to an increase in the cooling load. This increase is particularly significant for the rectangular and trapezoid shapes. Cooling load constitutes 31% and 24% of their heating load, respectively. It should be noted however that cooling load for the basic cases is lower by over an order of magnitude than the heating load, and the design should therefore aim at minimizing heating load, in climatic conditions similar to those employed in this research.

Table 3.6, Effect of window size on annual heating and cooling loads of basic shapes

Shapes	Basic south window (10% of floor area)			Window 35% of south facade			Window 50% of south facade		
	Heating load (kW)	Cooling load (kW)	Ratio of cooling to heating load	Heating load (kW)	Cooling load (kW)	Ratio of cooling to heating load	Heating load (kW)	Cooling load (kW)	Ratio of cooling to heating load
Square	3024	110	0.04	2662	173	0.07	2193	371	0.17
Rectangle	3041	107	0.04	2511	212	0.08	1983	624	0.31
Trapezoid	3287	90	0.03	2536	211	0.08	2045	499	0.24
L shape	3581	106	0.05	3062	162	0.05	2616	379	0.15
U shape	4200	106	0.03	3473	170	0.05	2688	454	0.17
H shape	4464	74	0.02	3566	182	0.05	2899	392	0.14
T shape	3693	79	0.02	2919	233	0.08	2453	542	0.22

Heating energy consumption is computed assuming a heat pump of coefficient of performance (COP) of 4. Figure 3.8 displays the heating energy consumption of all shapes, associated with each window area option.

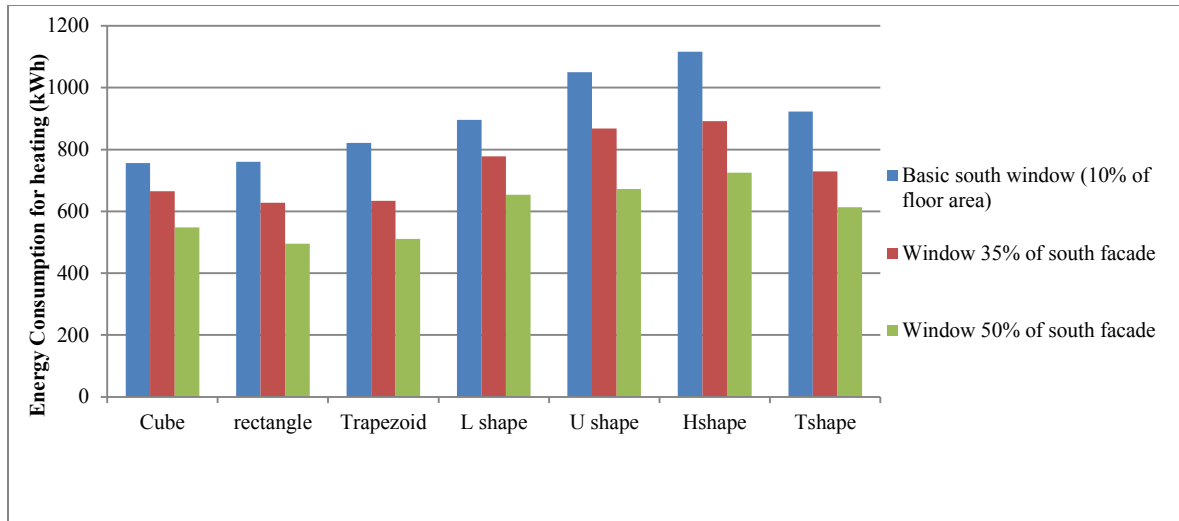


Figure 3.8, Effect of window size on annual energy consumption for heating of basic shapes.

3.2.2. Variations of Basic Shapes

In the following analysis, all variations of the basic shapes are studied for a south window area of 35% of the facade, since this option enables a significant reduction of the heating load without significantly compromising the cooling load.

Rectangular Shape

Variations on the rectangular shape consist of changing the aspect ratio and the orientation from due south. The effects of these design parameters on the energy performance are detailed below.

Aspect Ratio

Radiation on façades, solar heat gain and BIPV electricity generation are all affected by the aspect ratio. They increase with a larger aspect ratio and vice versa.

The effect of various aspect ratios of the rectangular shape on heating and cooling loads is plotted in Figure 3.9. The results show that heating increases sharply for an aspect ratio smaller than 1.3. For an AR that ranges between 1.3 and 1.6, heating load is

decreased by a maximum of 2% while cooling load is increased by a maximum of 10%. For Northern climate, a ratio of up to 1.6 -1.7 can be achieved without large increase in cooling load, especially since cooling load constitute about 10% or less of the heating load.

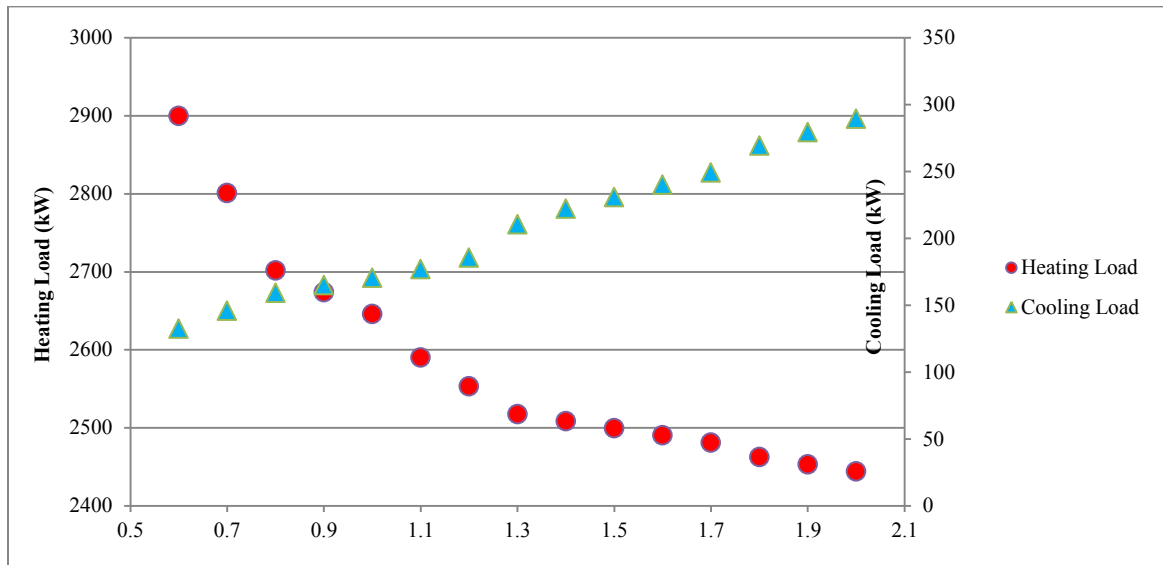


Figure 3.9, Relation between heating and cooling loads and aspect ratio of rectangular shape

Orientation

Solar Potential

In the absence of shading, solar irradiation on a surface depends primarily on the orientation of this surface relative to the south, independently of shape. The effect of surface orientation is analyzed by computing the ratio of transmitted radiation by windows of a surface at a given orientation angle to that transmitted by south facing windows. Results for incident radiation are expected to be similar.

The ratio of radiation transmitted by the façade rotated in respect to the south façade, to that of south façade is plotted against the angle of rotation towards the east (-) or west (+), for the two design days (Fig. 3.10). In WDD the best performance is

associated with the south orientation and it is reduced by 50% when the orientation angle approaches 60° west or east from south. By contrast, for the SDD, the transmitted radiation increases with increasing rotation angles (up to 60%) (Fig. 3.10).

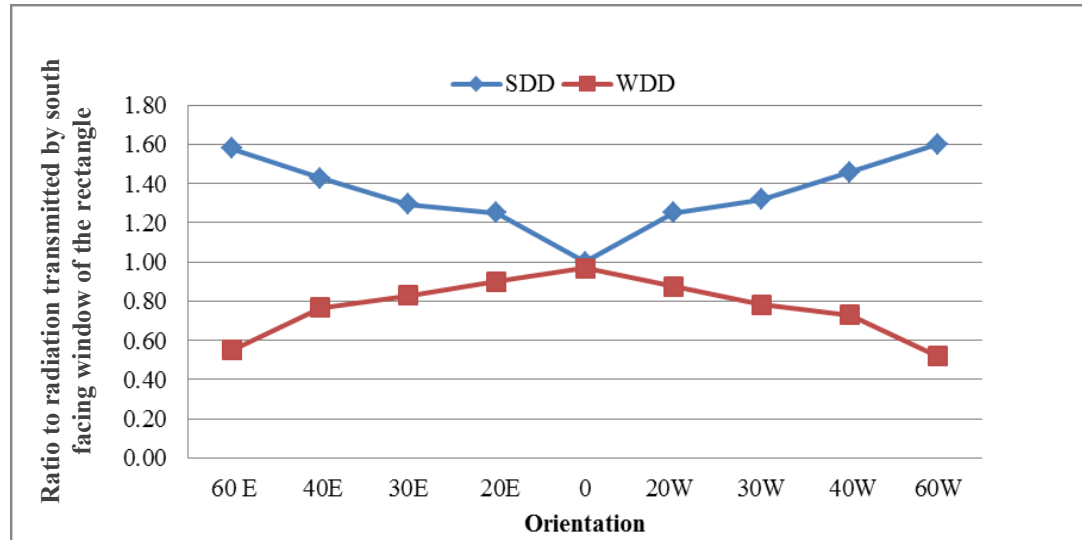


Figure 3.10, Effect of orientation on transmitted radiation over a summer and winter design day (SDD and WDD).

The effect of the orientation of roof surfaces on electricity generation, in the absence of shading, is independent of shape. This effect is studied in detail in Chapter V (Roof study). Following is a summary of the main effect of the orientation on the basic hip roof (with 45° tilt angle) of the rectangular shape.

- For the WDD, the best performance of the BIPV is associated with the south orientation and it declines sharply, when the orientation exceeds 30° of true south.
- For the SDD, an increase of about 25% of electricity generation can be achieved with an orientation of 60° towards the west. This is due to the long daylight period, with high solar intensity in the afternoon.

- Annually, the highest energy yield is associated with a south facing BIPV system. Deviation of the orientation of the system from the south by up to 45° west or east leads to an approximate reduction of 5% of the annual generation of electricity. A rotation of the system by 60°, west or east of south, results in a reduction of some 12% of the total annual electricity generation.
- Orientation of the PV system towards the east or west results in shifting the time of peak electricity generation. Shift of peak generation enables more overlap with the utility grid. Detailed discussion of this issue is provided in Chapter V.

Energy Demand

The annual heating load for rectangular units is determined as function of their orientation from due south (Fig 3.11). The results indicate that both heating and cooling loads increase with increased angles of rotation. The heating load is increased by up to 30% with a rotation angle of 60° east or west from south, as compared to the south facing rectangular shape. Cooling load increases significantly with the orientation toward east or west. An increase of 65% is associated with an orientation of 60° from due south. This increase in cooling load is mainly due to the large window area on the south-east or south- west facade, which was originally intended to be south facing.

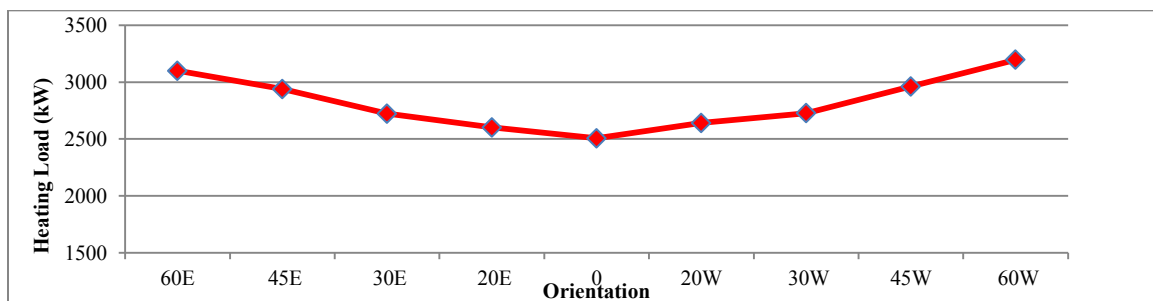


Figure 3.11, Heating load of rectangular units with various orientations.

Non- Convex Shapes

Variations of non-convex shapes are studied for L shape, where the effect of changing the depth ratio and the angle between the wings is investigated. L shape can be considered as the basic non-convex shape and other non-convex shapes can be derived by combinations/variations of this shape.

In addition, U shape is briefly analyzed to study the effect of increasing the number of shading façades associated with different depth ratios on the solar radiation incident on the façades and transmitted by their windows. Other aspects of energy performance of U shape variations are not explored, due to the difficulty to realize a functional plan design for U shape with other depth ratios, under the design conditions and the floor area limitations employed in this research.

Depth Ratio

Solar Potential

Solar radiation incident on the shaded façade of a non-convex shape is significantly dependent on the depth ratio. Another important effect is the number of shading façades.

The effect of depth ratio on incident and transmitted solar radiation of U and L shapes for a winter design day is shown in Table 3.7. Following are the main observations:

- The results indicate that the average radiation, per m^2 , incident on the shaded south façade of L shape is reduced by 12%, 22% and 26%, for depth ratio values

of 1/2, 1 and 3/2, respectively, as compared to the radiation on the exposed south façade.

- The reduction of the average incident radiation on the south facing shaded façade of U shape, and transmitted by its window is approximately double that of the corresponding L shape (with similar depth ratios) (Table 3.7).

Table 3.7, Effect of depth ratio on incident and transmitted radiation of L and U shapes

shape	Number of shade projecting façades		$a/b=1/2$	$a/b=1$	$a/b=3/2$
L shape	1	Reduction of average radiation on shaded façade	12%	22%	26%
		Reduction of average transmitted radiation	7%	27%	34%
U shape	2	Reduction of average radiation on shaded façade	23%	43%	53%
		Reduction of average transmitted radiation	14%	46%	60%

The effect of depth ratio on electricity generation is analyzed only for L shape since U shape is designed with a roof similar to the rectangular shape, with no shading effect.

Electricity generation is affected only slightly by the depth ratio, due to the inclination of the roof which reduces the shading effect. For instance, the electricity generation of the basic L shape (with depth ratio =1) is reduced annually by a maximum of 6% when averaged per unit area, as compared with the electricity generated per unit area of a non-shaded south facing roof. The maximum difference in annual electricity generation per unit area of L shape for the different depth- ratios studied is 3% or less.

Energy Demand

The depth ratio effect on energy demand is coupled with other effects such as the aspect ratio, which changes with different depth ratios in order to maintain the same plan

area, and south facing window area, which changes as percentage of the facade. Therefore it is difficult to isolate the effect of depth ratio on energy demand for heating and cooling.

The effect of depth ratio (including the design issues mentioned above) are shown in Table 3.8. L shape with DR of $\frac{1}{2}$ requires 9% less heating than L shape with DR of 1 (and about 7% more than the rectangle). The effect of DR on incident radiation on the shaded south façade as compared to the rectangular shape is presented in Table 3.8 as well.

Table 3.8, effect of DR on solar potential and energy performance

DR	Window heat gain (10^3 .kW)	Percentage of reduced incident radiation (WDD)	Heating load (kW)	Cooling load (kW)	Electricity generation (kWh)
1/2	8244	12%	2686	259	5840
1	7904	22%	3062	162	4958
3/2	7328	26%	3165	155	4111

Wing Rotation in L Variants (V)

Solar Potential

L variants (V) are designed with a DR of $\frac{1}{2}$. The effect of wing rotation on solar potential is assessed by comparison to the rectangle.

Two main observations are highlighted in the analysis of the incident and transmitted solar radiation of L variants:

- A larger angle between the wings of L shape allows reducing the shade on the main wing (shaded façade), and therefore increasing transmitted radiation and windows heat gain. The reduction of solar radiation on the shaded façade is not significant when the angle β is larger than 30° ($\leq 1\%$) for the depth ratio of $\frac{1}{2}$.

- Rotation of the south facing façade of the branch of L shape causes an increase of the incident radiation on this facade, for the SDD and decrease of this radiation for the WDD. This effect of rotation of the wing on incident/transmitted radiation follows the same principles detailed in the analysis of the effect of orientation on the solar potential of the rectangular shape presented above and depicted in Figure 3.10.

The annual electricity generation of selected south facing L variants (V-ES and V-WS) and north facing L variants (V-EN and V-WN), with a depth ratio of $\frac{1}{2}$, is compared to the rectangle in Table 3.9. Figure 3.12 displays the annual electricity generation of these selected shapes. The main observations of L variations effect on electricity generation are as follows:

- The shade on the south facing roof in all non-convex shapes is mitigated by a small depth ratio as well as by increased angle between the wings. Consequently the electricity generation potential in such units is not significantly affected by shading.
- The L and L variant shapes provide larger roof area, than the reference case (rectangle with a hip roof) and therefore an increase in annual electricity generation.
- The comparison of the annual electricity production of south facing L variants indicates an increase of the annual generation ranging from 20% to 35% relative to the reference case. This effect is attributed to the larger south facing roof area (31m^2 for the L variant, in comparison with 25.6m^2 for the rectangular shape).

- The increase in total annual generation of the north facing L variant (V-WN60), relative to the reference, can reach 53%. North facing obtuse-angle shape generates up to 30% more electricity annually than the reference.

Table 3.9, Comparison of annual electricity generation of selected L variants to the reference case

South facing	Rectangle	V-ES60	V-ES30	L-WS/L-ES	V-WS30	V-WS60	O-S
Comparison to reference	1	1.35	1.26	1.22	1.26	1.38	1.10
North facing	Rectangle	V-EN60	V-EN30	L-WN/L-EN	V-WN30	V-WN60	O-N
Comparison to reference	1	1.50	1.18	1.32	1.18	1.53	1.30

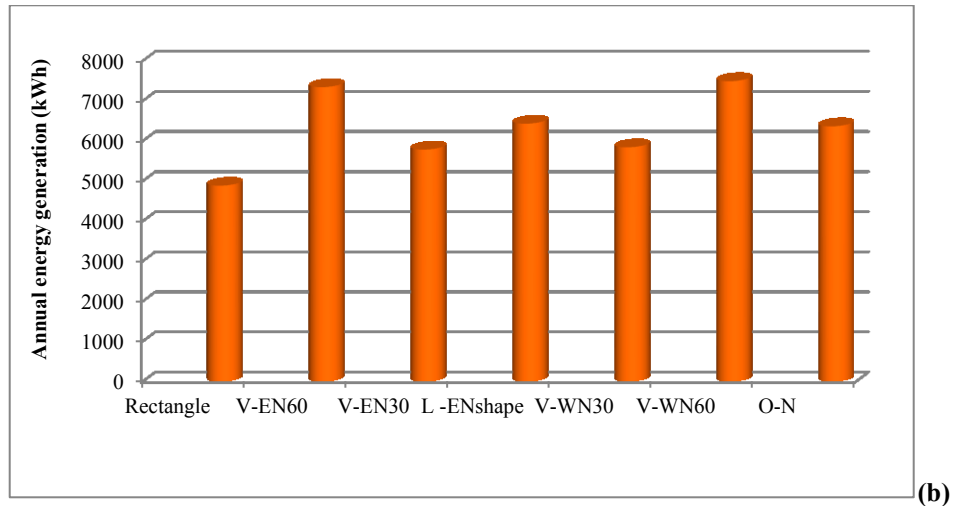
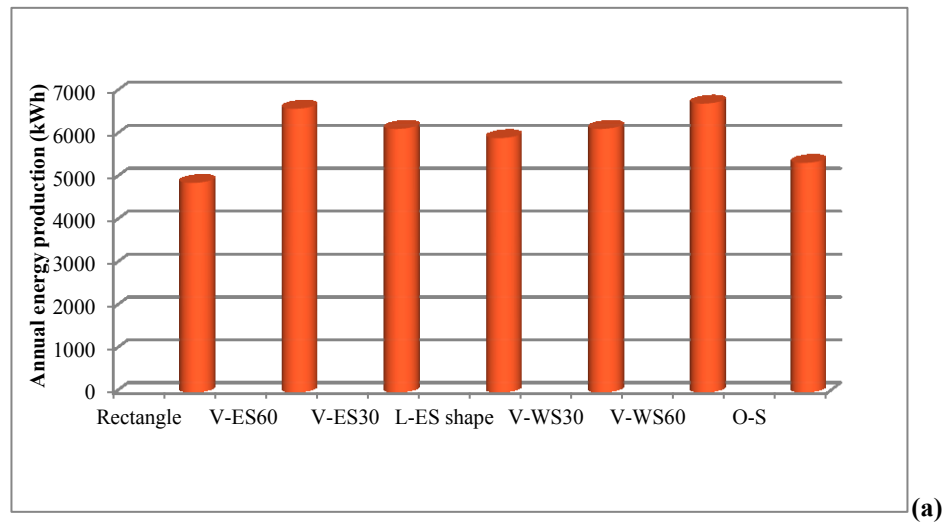
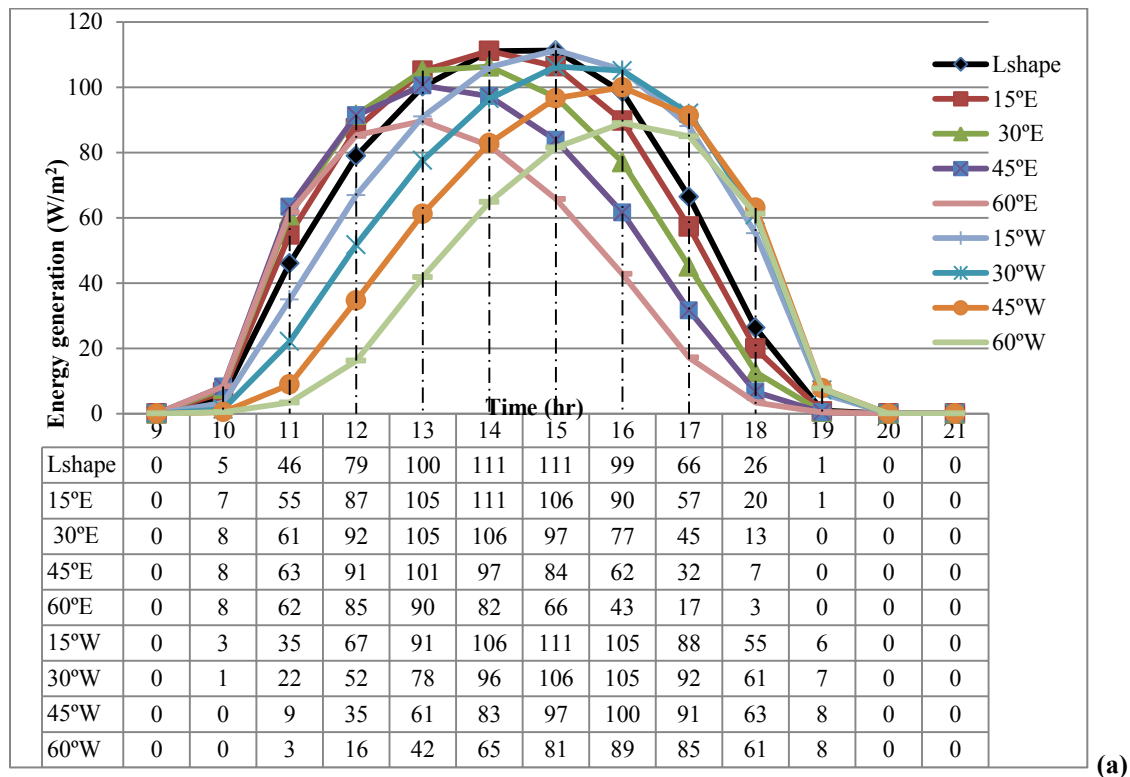


Figure 3.12, Annual energy production of selected L variants, (a) South Facing (V-ES and V-WS), (b) North Facing (V-EN and V-WN).

Peak Generation Timing

The hourly electricity generation during the WDD indicates that the different variations of L shape allow reaching the peak at different times, as shown in Figures 3.13a and 3.13b for L variants with south facing wings. The peak generation is reached earlier than solar noon for V-ES variants and later for V-WS variants. Figures 3.13a and 3.13b show the normalized peak generation per unit area of different variations of L shape on a WDD and SDD respectively. A difference of peak of about 3 hours is observed between L variation with $\beta=30^\circ$ east (peak between 11 – 12 hours) and the variation with $\beta=30^\circ$ west (peak between 13 – 14 hours).

A maximum shift of 3 hours relative to solar noon can be obtained by the BIPV system of L variants with 60° - 70° wing rotation. This is discussed in detail in chapter V.



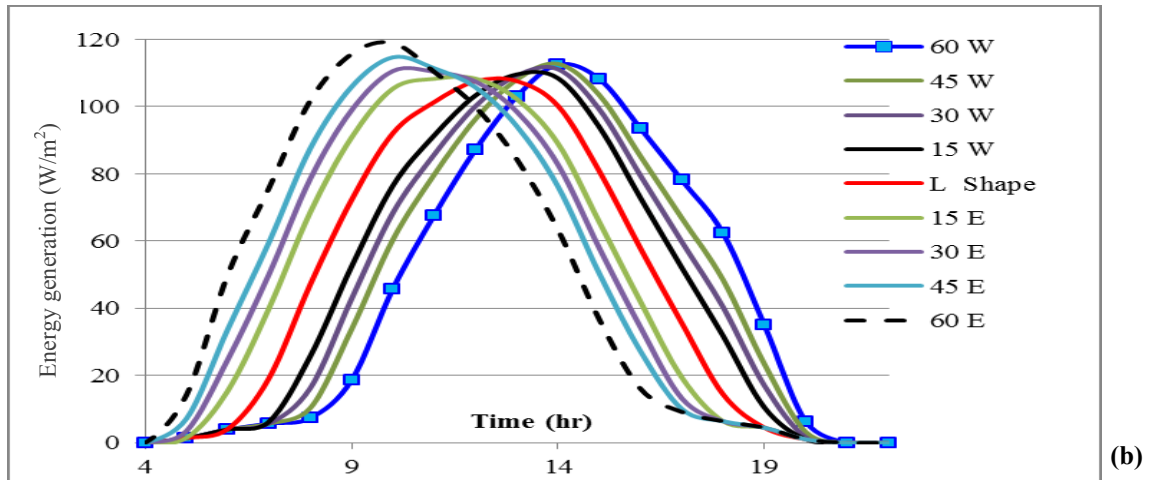


Figure 3.13, Electricity generation for L shape with wing rotation (kW/m^2), (a) WDD, (b) SDD.

Energy Demand

Heating load (and heating consumption determined assuming a heat pump of COP 4) is not significantly affected by wing rotation of L variants. L shape, south facing L variants with angle $\beta = 60^\circ$ (V-ES60 and V-WS60), and obtuse angle shape (OS) require 7%, 6% and 2% respectively, more heating energy than the reference case (rectangle). The cooling load of L variants exceeds that of the reference case by up to 30% (associated with an angle β of 60°). This is caused by increased transmitted radiation in the morning and evening during the summer period, by windows that are originally designed as south facing. This effect can be mitigated by modifying the window area, on the rotated façade. This is not investigated however in this research in order to avoid introducing additional design parameters.

North facing L variants (V-EN, V-WN) require more energy for heating than the corresponding south facing (V-ES, V-WS). For instance the increase of heating load of

V-EN60 is about 15% as compared to the reference case, and 9% compared to V-ES60°. This is mainly due to the reduced total south projection of façades.

Figures 3.14a and b presents cooling and heating consumption, of some selected L variants, south facing (V-ES and V-WS) and north facing (V-EN and V-WN), respectively, assuming that a heat pump is employed to convert heating and cooling loads into consumptions.

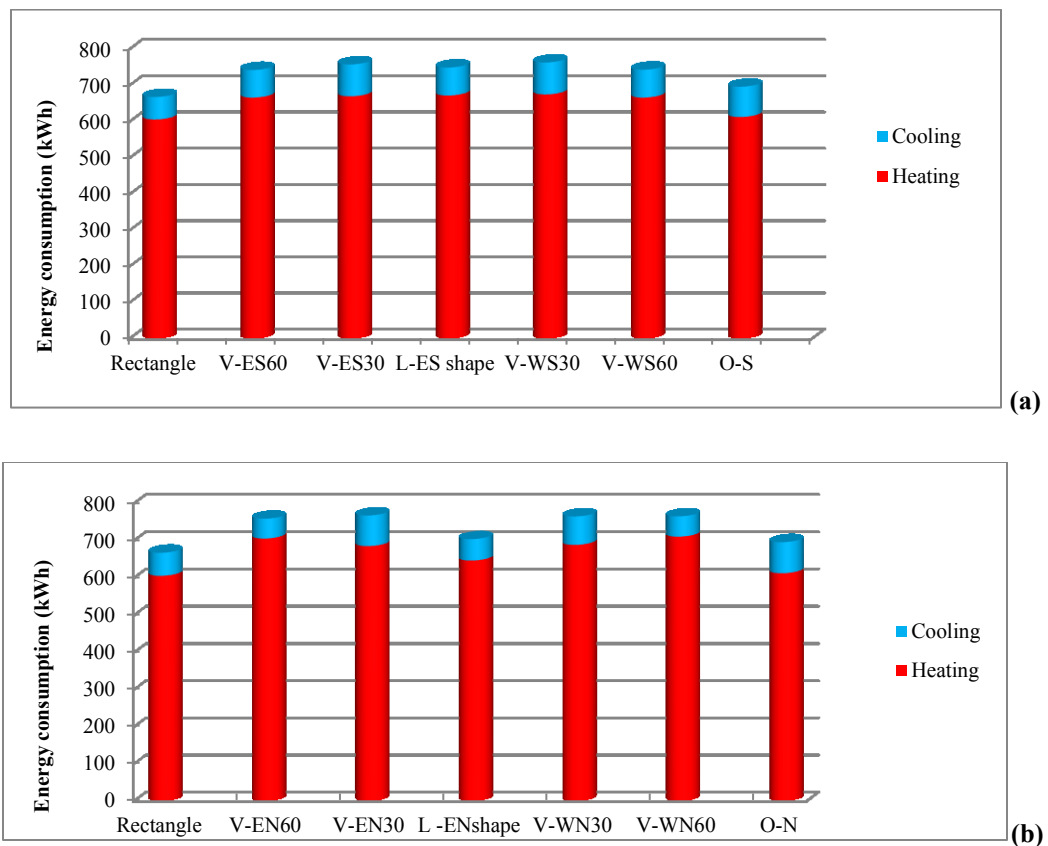


Figure 3.14, Annual heating and cooling consumption of selected L and L variant shapes (a) South facing, (b) North facing

3.2.3. Energy Balance of Basic Shapes

This section analyses the balance between energy supply and total energy consumption of the basic shapes. The basic L shape with DR of 1 is presented in this section. The energy performance of L shape with DR of ½ and the variations of this

shape (studied in section 3.2.2), are presented in Chapter IV together with the energy balance of the studied neighborhood patterns.

The total consumption of electricity for lighting, DHW and appliances, in addition to the computed heating and cooling energy consumption, for each basic shape is detailed in Table 3.10 and depicted in Figure 3.15 alongside the energy production of the corresponding units. The results, in terms of percentage of energy production to energy consumption of all shapes, are also presented in Table 3.10.

The results indicate that the electricity production of the reference rectangular layout with hip roof falls short by some 35% of its energy consumption. T shape produces up to 95% of total consumption, meaning that this shape is very close to achieving a net zero energy status, even though it consumes about 9% more heating energy than the rectangular shape.

It should be noted that energy consumption for lighting in this research is considered as the same for all shapes. However lighting in some non-convex shapes, particularly in L and T shapes can be further reduced if additional daylight considerations are accounted for, due the benefit of the shallow depth of these shapes. This is to be investigated in future research. Thermal potential of a hybrid photovoltaic thermal system, which is investigated in detail in Chapter V, is expected to further reduce energy consumption for space and water heating and for some appliances (clothes drier, for instance).

Table 3.10, Energy consumption for all basic units

	Square	Rectangle	Trapezoid	L shape	U shape	H shape	T shape
Heating energy consumption (kWh)	665	627.6	634	765	868	891	730
Cooling energy consumption (kWh)	43	53	53	40	42	45	58
DHW (kWh)	3786	3786	3786	3786	3786	3786	3786
Appliances (kWh)	2700	2700	2700	2700	2700	2700	2700
Lighting (kWh)	360	360	360	360	360	360	360
Total Energy use (kWh)	7554	7526	7532	7664	7756	7782	7633
Annual electricity generation (kWh)	4233	4887	6777	4958	4835	6168	7228
Ratio Energy supply/energy use	0.56	0.66	0.90	0.65	0.62	0.79	0.95

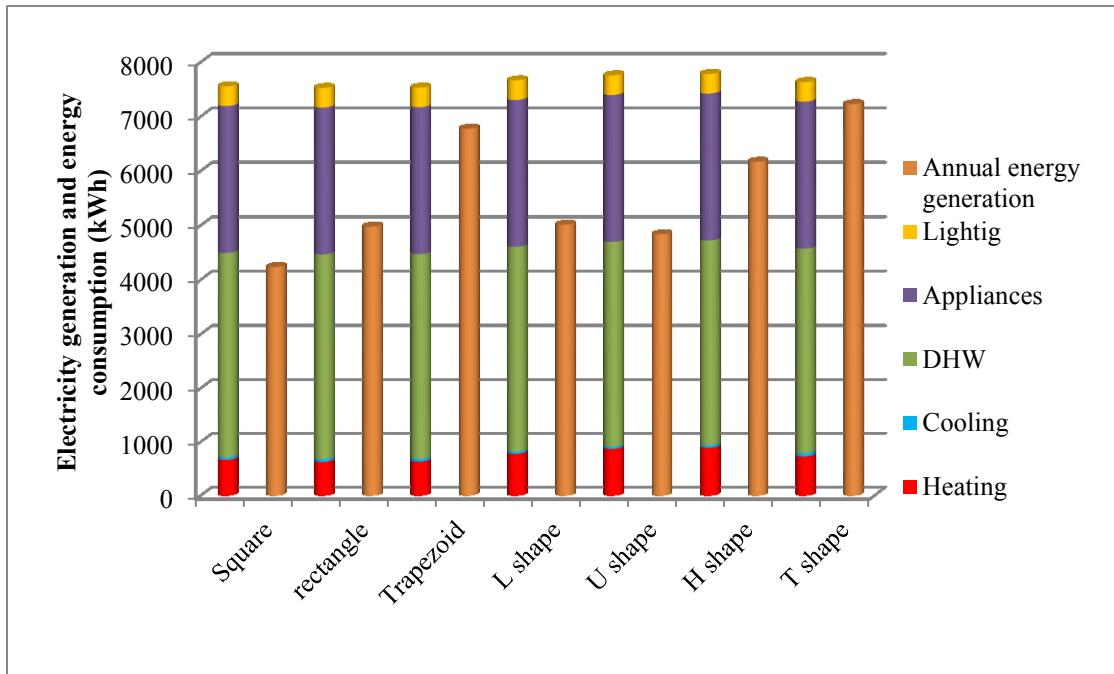


Figure 3.15, Energy use and energy supply of all basic shapes.

CHAPTER IV: NEIGHBORHOOD DESIGN²

The objective of this chapter is to assess the effects of a variety of parameters associated with residential neighborhood design on the solar performance and energy balance of a neighborhood and of the individual housing units composing it. The two main parameters affecting neighborhood solar performance are the site layout and the density of housing units. Each of these parameters is associated and interacts with several secondary parameters, such as units' shapes, their orientation, their relative position etc. The selection of housing shapes for the neighborhood investigation is based on results obtained in the investigation of shape effects (Chapter III).

The chapter includes two main sections. Section 4.1 presents the design parameters selected in this study and the values assigned to them. Section 4.2 presents results and evaluation of the simulation analysis, in terms of the effects of the design parameters on solar potential and energy consumption of units in a neighborhood and the energy performance of the neighborhood as a whole.

4.1 Design Parameters

This section details the parameters considered in the neighborhood investigation, their values and the various combinations studied. It comprises four main subsections. The general neighborhood characteristics and site layouts are presented in section 4.1.1.

² The study and some of the results presented in this chapter are published in:

Hachem C., A. Athienitis, P. Fazio, (2012a). Evaluation of energy supply and demand in solar neighbourhoods, *Journal of Energy and Buildings*, DOI: 10.1016/j.enbuild.2012.02.021.

Hachem C., A. Athienitis, P. Fazio, (2011b), Investigation of Solar Potential of Housing Units in Different Neighborhood Designs, *Journal of Energy and Buildings*, Volume 43, Issue 9, Pages 2262-2273.

Section 4.1.2 introduces the main parameters associated with mutual shading by adjacent housing units in a neighborhood. Values of neighborhood design parameters are detailed in section 4.1.3, under three main headings, representing the three categories of design parameters: unit shapes; density and site layout. Section 4.1.4 presents a summary of the parametric investigation, including the combinations of parameter values analyzed.

4.1.1. Neighborhood Characteristics

The general characteristics of the neighborhood are based on various sources, including guidelines of urban design and by-law zoning (e.g. CWP, 1998; Cohen, 2000; Burden et al, 1999). Table 4.1 summarizes the neighborhood design guidelines adopted in this study. The design methodology consists of first determining the site layout, then designing the unit shapes to conform to this layout, and combining the shapes in different configurations.

Table 4.1, Characteristics of the studied neighborhoods

Land use designed	Building total floor area		120 m ² (designed)	
	Lot Coverage Ratio ($LCR = \frac{Ground\ floor\ area}{Lot\ area}$)		37% (calculated)	
	Distance from sides	Front		4m
		Back		6m
		Sides	Units positioned with respect to a straight road	2m
Units positioned with respect to curved road			2 - 3.5m	
Roads based on (CWP, 1998, Cohen, 2000, Burden et al, 1999)	Road width	Neighborhood streets ^a	12 -15m	
		Gravel alley ^b	4m	
	Cul de sac	Diameter see Table 4.3	D1=42 m D2=52m	
Density (based on Teed et al., 2009)	Low/ medium -Low - outer suburban area (detached units-see Table 4.3)		5-9 u/a	
	Medium- high -outer suburban area (attached units see Table 4.3)		16 u/a	
	Medium- inner suburban (row townhouse see Table 4.3)		up to 35 u/a	
^a Access to residential, includes street width with parking on one or two sides, planting strip, sidewalks on both side.				
^b Access to sanitation and utilities, garages, backyard and secondary units.				

Three basic site layouts are considered in this study (see Fig. 2.5, Chapter II). Site I is characterized by a straight road, while sites II and III feature curved roads facing south and north, respectively. Variations on site I are also designed to find the effect of varying straight road orientations.

For each site, several configurations consisting of combinations of groups of three to six units of a given shape are studied. For each site/shape combination, three densities are considered: low density (around 5 units per acre (u/a)), medium -low density (around 9 units per acre (u/a)) of detached units (Teed et al, 2009) and medium- high density (around 16 (u/a)) consisting of attached units (Table 4.1). In site I, the effect of mutually shading rows of dwelling units, in what is termed *row effect*, is also studied. A higher density of up to 35 u/a can be achieved employing row configurations.

4.1.2 Shading Effects

A major effect on solar potential of neighborhoods is mutual shading by adjacent dwelling units. Two parameters define the relative position of the shaded and shading units: the angle of obstruction and the distance between the units.

Planar Obstruction Angle (POA) is a new concept introduced in this research representing the angle between the center of the south façade of the shaded unit and the closest corner of the shading unit (Figs. 4.1 and 4.2). In the analysis of POA effects, POA values of 15°, 30°, 45°, 60°, 75° and 90° are studied, in addition to the effect of aligning the units, as shown in Figure 4.1.

The second parameter is the distance (d) from the center of the south façade of the shaded unit to the closest corner of the obstructing unit. Four values of d are adopted in

the analysis: 20m, 15m, 10m, and 5m. A distance of 5m is unlikely to be applied in practice but it is studied in order to assess the trend. The effects are studied for a single shading unit (Fig. 4.1 a, b) and two shading units (Fig.4.1 c, d). The two shading units are positioned symmetrically with respect to the shaded unit. In total, 44 combinations of POA and distance (d) are simulated.

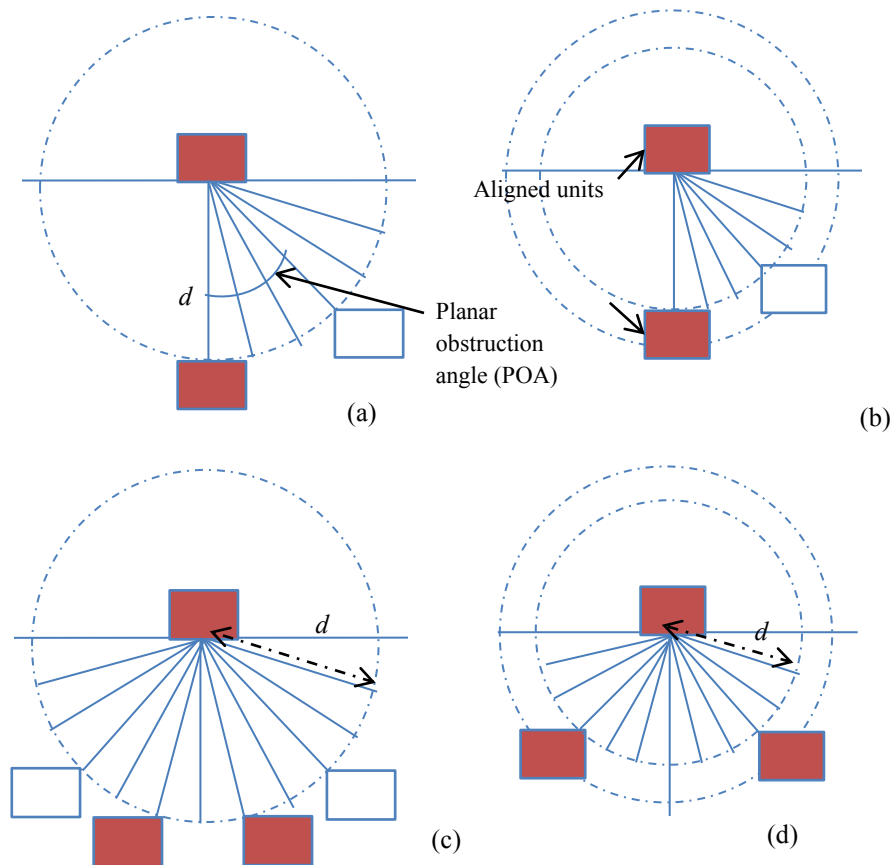


Figure 4.1, POA concept, shading and shaded units are represented by solid colour; shaded unit is in the centre of the circle; (a) and (b) single shading unit with different , (c) and (d) two shading units.

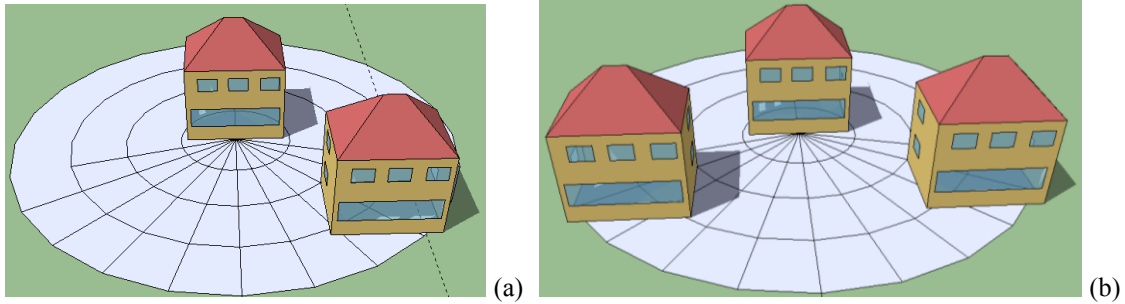


Figure 4.2, 3-D view of the POA concept, (a) one shaded unit, (b) 2 shaded units.

4.1.3 Neighborhood Design Parameters and their Values

Housing Units' Shapes

Rectangle and L shape and its variations are selected for the neighborhood study, since they can be considered as prototypes of convex and non-convex shapes for passive solar design. Other basic shapes can be derived from combination / variation of these shapes. Non-convex dwelling units employed in the neighborhood study are shown in Table 3.3 (Chapter III). Details of the design and analysis of all shapes considered in this research are provided in sections 3.1.1 and 3.1.3 of Chapter III.

Site Layout

Site layout is mainly characterized by the layout of streets. Two main street layouts are studied: straight, and semi- circular.

Straight Road – Site I

Six directions of the straight road are studied, in addition to the reference case – an east-west running road (Fig. 4.4.a), with the E-W road rotated by 30°, 45° and 60° in each of clockwise (+) and anticlockwise (-) senses. Only detached configurations are

studied in these inclined configurations, since the purpose is to study the effect of mutual shading, which is not relevant to attached units.

For each of the inclined layouts of site I, 3 housing units' configurations are studied: south facing rectangle, rectangle oriented toward the street, and L variants (V), with the angle between the wings to conform to road direction. Figure 4.3 shows sites with $+45^\circ$ orientation (rotation towards the west) of the three configurations mentioned above.

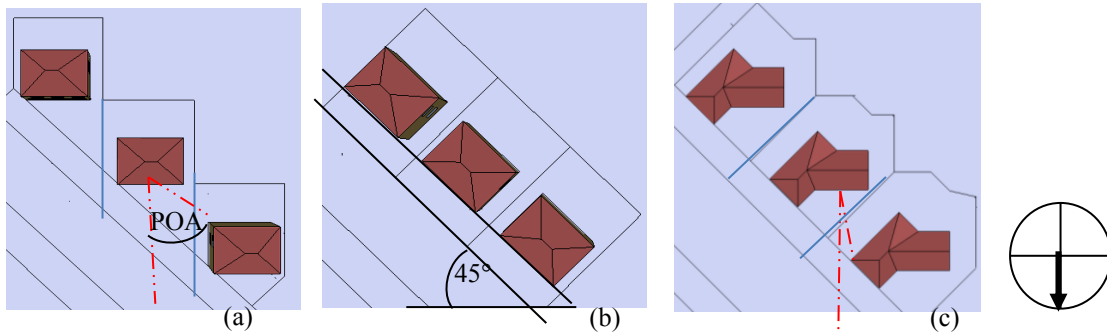


Figure 4.3, variation of site I, (a) south facing rectangle, (b) rectangles oriented to the street, (c) L-variants (V).

Curved road – Sites II and III

Site layout II and III incorporate semi-circular roads, facing south and north, respectively. The housing units are positioned with respect to the shape of the roads, in both curved sites. Configurations of site II include rectangular shape (R), combination of L shape and its variants and a configuration of obtuse-angle shapes (Fig. 4.4b). In the last configuration (Obtuse angle) the two extreme units – U1 and U5 in Fig. 4.4b – are L variants (V-ES60 and V-WS60), in an attempt to optimize façade orientation for insolation. Configurations of site III are mirror images of those of site II, relative to an east-west axis (Fig. 4.4c).



Figure 4.4, Configurations of shapes in different site layouts: a) site I; b) Site II; c) Site III.

Additional Information

In site I with inclined road and in site II, the positioning of some units results in mutual shading – for instance rectangle south facing (Fig. 4.3a) and L variants (Fig. 4.3c) in site I variations, and L variants in site II (Fig. 4.5). In these cases the planar obstruction angle (POA) discussed above has an important effect on energy performance.

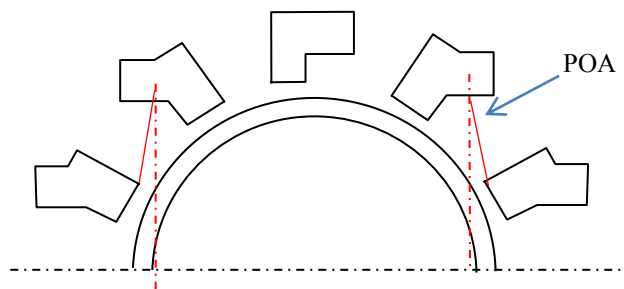


Figure 4.5, Illustration of the POA concept for L variant in site II.

The land partitioning is based on the details given in Table 4.1, where the minimum required distance from the house is applied in the back, front and sides. The total area use per unit changes therefore according to the configuration. Land use area can

be critical in certain situations where the land is quite limited or costly (in crowded cities for instance). In these cases the tradeoff between reducing land use and achieving more energy efficient design should be considered. Table 4.2 presents the land use area per unit, the POA and distance (d) for all configurations. It should be noted that land use areas of corresponding configurations in sites II and III are identical.

Table 4.2, Some design characteristics of the site layouts

Road	Site I												Site II		
	E-W			$\pm 30^\circ$			$\pm 45^\circ$			$\pm 60^\circ$					
	R	L	L-V	R-0	R-30	V-30	R-0	R-45	V-45	R-0	R-60	V-60	R	V	O
Land use (m ²)	220	230	240	270	230	240	285	230	245	270	230	250	250	290	260
POA (°)	-	-	-	45	-	30	60	-	10	30	-	Aligned	-	10	-
Distance (d) (m)	-	-	-	10	-	10	10	-	8	10	-	7	-	10	-

Density

Density is influenced by the spacing between units in a row (s) and by the spacing between rows of units (r). The design of various levels of density is presented below.

Spacing of Units

Three values of spacing are adopted for each site: s_1 , the basic spacing of detached units, is assumed as 4 m in site I. The spacing between detached units in a curved site varies, depending on the curvature of the road and the shape of the units (Fig. 4.4b, c). In a site with a curved road of 42 m diameter the basic spacing s_1 between rectangular units is assumed as 4 m. For L variant units, it varies between 4 and 7 m. In order to assess the influence of increased spacing on energy demand, a second spacing $s_2=2s_1$ is adopted. In a curved site this spacing corresponds to a road diameter of 52 m.

At the other extreme, the highest density is obtained by attaching units in triplex, quadruplex or pentuplex configurations, with $s_0=0$. Attached configurations for sites I, II and III are shown in Figure 4.6.

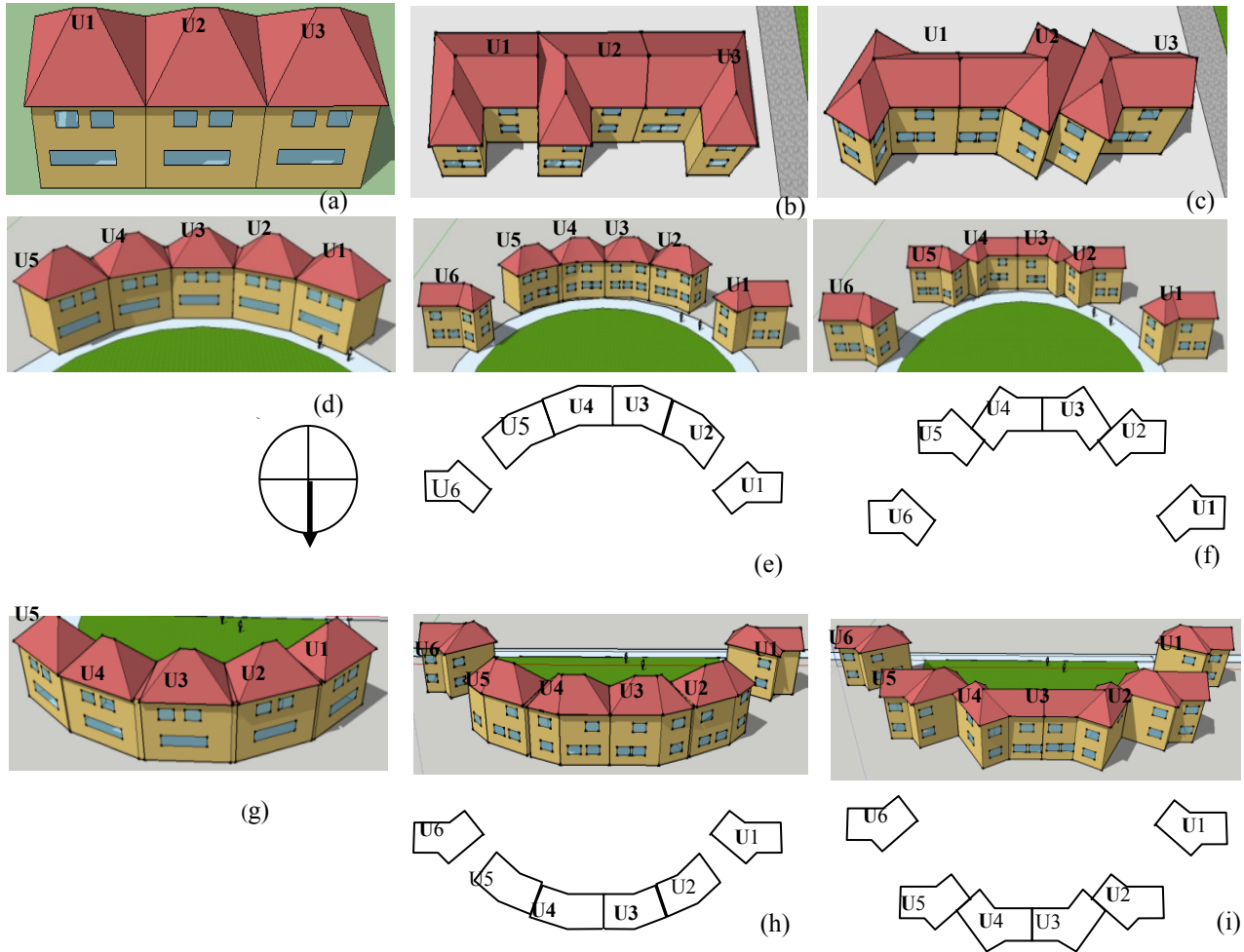


Figure 4.6, Attached units in sites I, II and III. Site I: a) rectangular, b) L shape, c) L variants; Site II: d) trapezoid; e) obtuse-angle; f) L variants. Site III: g) trapezoid; h) obtuse-angle; i) L variants.

Three shapes are employed in attached configurations of each site. In site I these shapes are rectangle, L and L variant (Fig. 4.6 a, b, c). In sites II and III the rectangle is replaced with trapezoid, to allow attachment of units along the curve. The south facing curve of site II implies that the narrower side of the trapezoid is south or near-south

facing (see figure 4.6d), whereas for site III the wider side faces south (Fig. 4.6g). The other two shapes are L variants and obtuse-angle (Fig. 4.6 d-i).

Layouts of attached non-convex shapes include in addition to the four central attached units two detached units at the extremes of the curve for improved site design. These detached units are not included in the analysis for density effect.

Rows

The effect of obstructing the south façades of selected configurations by a row of similar housing configurations – the *row effect* (Chapter II) – is investigated for site I. The minimum distance between the two rows (x), to avoid shading, can be estimated based on the shadow length equation (NRC-IRC, 2005):

$$SL = \frac{H \cdot \cos(\phi - \psi)}{\tan \alpha} - \frac{w}{2} \quad (eq.4.1)$$

where, SL is the shadow length, H is the total height of the shading building, ϕ is the solar azimuth, ψ is the azimuth of the surface, α is the solar altitude, w is the width of the shading building.

Using the shadow length equation for the 21st of December, associated with the lowest sun altitude at solar noon, the minimum spacing (x) to avoid row shading for the units studied is ca. 25m. To assess the effect of shading, four values of row spacing (r) are simulated (Table 4.3): 5m, 10 m, 15 m and 20m, corresponding to 20%, 40%, 60% and 80%, respectively, of the minimum spacing between rows to avoid shading. The studied configurations are the detached and attached rectangular units, the detached and attached L units and the detached and attached configurations of L variant (V-WS30)

(Fig. 4.7). Two configurations of L units are studied, with the branch facing south L-S and the branch facing north L-N.

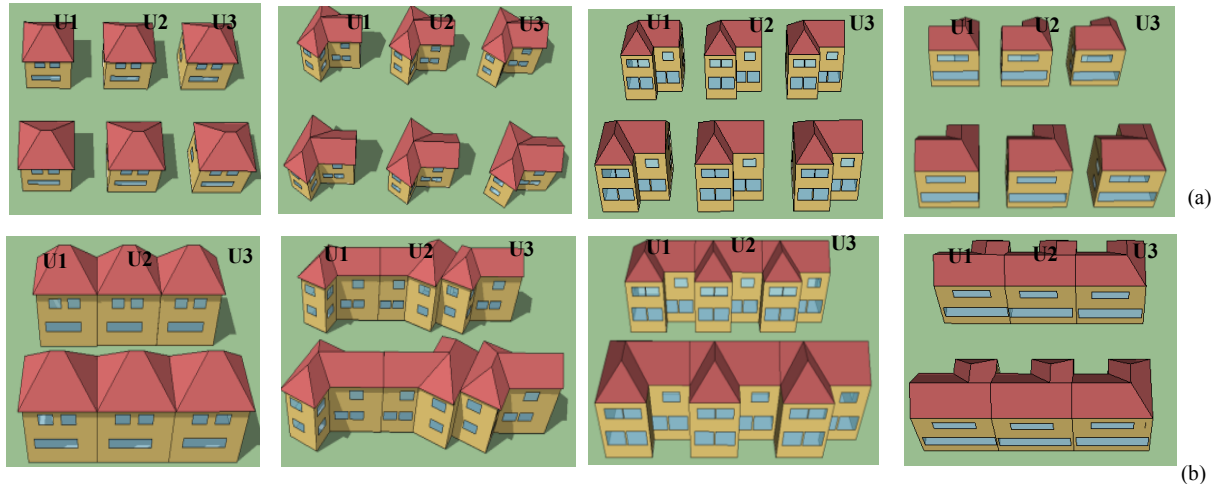


Figure 4.7, row configurations of all studied shapes; (a) detached configurations; (b) attached configurations.

It should be noted that 5m is unlikely to be employed when the south facing façade is the principal façade and its inclusion in the study is aimed at providing an extreme case in order to assess the trend.

4.1.4 Summary of Parametric Investigation

In total, 77 neighborhood patterns employing various combinations of parameters are simulated (Table 4.3). In addition, 44 simulations of different combinations of distance and POA values were performed to investigate the shading effect. Values of the design parameters whose effects on energy performance of neighborhoods are studied in this stage are summarized in Table 4.4. The parameters are: housing units shape, site layout and density (spacing and rows).

Table 4.3, Configurations simulated – Parameter combinations

No.	Site	Shape	Spacing	Row	Orientation	No.	Site	Shape	Density	Row	Orientation
1	I	R	<i>sl</i>	<i>r0</i>	S	40	I	V	<i>sl</i>	<i>r1</i>	S
2	I	L	<i>sl</i>	<i>r0</i>	S	41	I	V	<i>sl</i>	<i>r2</i>	S
3	I	V	<i>sl</i>	<i>r0</i>	S	42	I	V	<i>sl</i>	<i>r3</i>	S
4	II	R	<i>sl</i>	<i>r0</i>	S	43	I	V	<i>sl</i>	<i>r4</i>	S
5	II	L/V	<i>sl</i>	<i>r0</i>	S	44	I	R	<i>s0</i>	<i>r1</i>	S
6	II	O	<i>sl</i>	<i>r0</i>	S	45	I	R	<i>s0</i>	<i>r2</i>	S
7	III	R	<i>sl</i>	<i>r0</i>	N	46	I	R	<i>s0</i>	<i>r3</i>	S
8	III	L/V	<i>sl</i>	<i>r0</i>	N	47	I	R	<i>s0</i>	<i>r4</i>	S
9	III	O	<i>sl</i>	<i>r0</i>	N	48	I	L(S)	<i>s0</i>	<i>r1</i>	S
10	I	R	<i>s2</i>	<i>r0</i>	S	49	I	L(S)	<i>s0</i>	<i>r2</i>	S
11	I	L	<i>s2</i>	<i>r0</i>	S	50	I	L(S)	<i>s0</i>	<i>r3</i>	S
12	I	V	<i>s2</i>	<i>r0</i>	S	51	I	L(S)	<i>s0</i>	<i>r4</i>	S
13	II	R	<i>s2</i>	<i>r0</i>	S	52	I	L(N)	<i>s0</i>	<i>r1</i>	S
14	II	L/V	<i>s2</i>	<i>r0</i>	S	53	I	L(N)	<i>s0</i>	<i>r2</i>	S
15	II	O	<i>s2</i>	<i>r0</i>	S	54	I	L(N)	<i>s0</i>	<i>r3</i>	S
16	III	R	<i>s2</i>	<i>r0</i>	N	55	I	L(N)	<i>s0</i>	<i>r4</i>	S
17	III	L/V	<i>s2</i>	<i>r0</i>	N	56	I	V	<i>s0</i>	<i>r1</i>	S
18	III	O	<i>s2</i>	<i>r0</i>	N	57	I	V	<i>s0</i>	<i>r2</i>	S
19	II	R	<i>s0</i>	<i>r0</i>	S	58	I	V	<i>s0</i>	<i>r3</i>	S
20	I	L	<i>s0</i>	<i>r0</i>	S	59	I	V	<i>s0</i>	<i>r4</i>	S
21	I	V	<i>s0</i>	<i>r0</i>	S	60	I	R	<i>sl</i>	<i>r0</i>	+30°
22	II	R	<i>s0</i>	<i>r0</i>	S	61	I	R	<i>sl</i>	<i>r0</i>	+30°
23	II	L/V	<i>s0</i>	<i>r0</i>	S	62	I	V	<i>sl</i>	<i>r0</i>	+30°
24	II	O	<i>s0</i>	<i>r0</i>	S	63	I	R	<i>sl</i>	<i>r0</i>	+45°
25	III	R	<i>s0</i>	<i>r0</i>	S	64	I	R	<i>sl</i>	<i>r0</i>	+45°
26	III	L/V	<i>s0</i>	<i>r0</i>	N	65	I	V	<i>sl</i>	<i>r0</i>	+45°
27	III	O	<i>s0</i>	<i>r0</i>	N	66	I	R	<i>sl</i>	<i>r0</i>	+60°
28	I	R	<i>sl</i>	<i>r1</i>	S	67	I	R	<i>sl</i>	<i>r0</i>	+60°
29	I	R	<i>sl</i>	<i>r2</i>	S	68	I	V	<i>sl</i>	<i>r0</i>	+60°
30	I	R	<i>sl</i>	<i>r3</i>	S	69	I	R	<i>sl</i>	<i>r0</i>	-30°
31	I	R	<i>sl</i>	<i>r4</i>	S	70	I	R	<i>sl</i>	<i>r0</i>	-30°
32	I	L(S)	<i>sl</i>	<i>r1</i>	S	71	I	V	<i>sl</i>	<i>r0</i>	-30°
33	I	L(S)	<i>sl</i>	<i>r2</i>	S	72	I	R	<i>sl</i>	<i>r0</i>	-45°
34	I	L(S)	<i>sl</i>	<i>r3</i>	S	73	I	R	<i>sl</i>	<i>r0</i>	-45°
35	I	L(S)	<i>sl</i>	<i>r4</i>	S	74	I	V	<i>sl</i>	<i>r0</i>	-45°
36	I	L(N)	<i>sl</i>	<i>r1</i>	S	75	I	R	<i>sl</i>	<i>r0</i>	-60°
37	I	L(N)	<i>sl</i>	<i>r2</i>	S	76	I	R	<i>sl</i>	<i>r0</i>	-60°
38	I	L(N)	<i>sl</i>	<i>r3</i>	S	77	I	V	<i>sl</i>	<i>r0</i>	-60°
39	I	L(N)	<i>sl</i>	<i>r4</i>	S						

Table 4.4, Design parameters of the neighborhood study

Parameters and values			
Shape	Site layout	Density	
		Spacing effect (s)	Row effect (r)
R* – Rectangle/ Trapezoid L – L V – L variant O – Obtuse-angle	I* – Straight East west (reference case); Inclined ($\pm 30^\circ$, $\pm 45^\circ$, $\pm 60^\circ$) II – Curved south, with diameter: $D1=42\text{m}$ (associated with $s1$) $D2=52\text{m}$ (associated with $s2$) III – Curved north ($D1, D2$)	$s_0 = 0$ (attached) $s_1^* = \left\{ \begin{array}{l} 4\text{m} - \text{site I, detached} \\ \text{rectangles in sites II, III;} \\ 4\text{m}-7\text{m detached L} \\ \text{variants in sites II, III} \end{array} \right.$ $s_2 = 2 \cdot s_1$	r_0^* – no 2 nd row $r_1 - 5\text{m}$ $r_2 - 10\text{m}$ $r_3 - 15\text{m}$ $r_4 - 20\text{m}$

Parameters marked * serve as reference for computing effects

4.2 Presentation and Analysis of Results

Three response variables represent the effects of the design parameters considered in this study. The effects on units in the neighborhood are measured by solar potential, on the one hand, and by energy demand, on the other. Potential heat gain for dwelling units from windows is studied in Chapter III. The third response parameter is energy performance of the neighborhood as a whole, measured as energy balance between production and consumption.

The following sections present the results in terms of the above-mentioned effects. Section 4.2.1 examines the effects of shading of a housing unit in a neighborhood by an adjacent unit or two units, as function of the relative position of the units. Housing units' density effects are presented in section 4.2.2, including the effect of units arranged in rows in site I (straight E-W road). Section 4.2.3 presents the effect of site layout, including straight road of different orientations and curved road sites. Section 4.2.4 analyses energy performance of the neighborhood as a whole, in terms of energy production versus consumption.

4.2.1. Shading Effect

Shading effect is assessed by analyzing the effect of different combinations of planar obstruction angles (POA) and distance (d) between shaded and shading units.

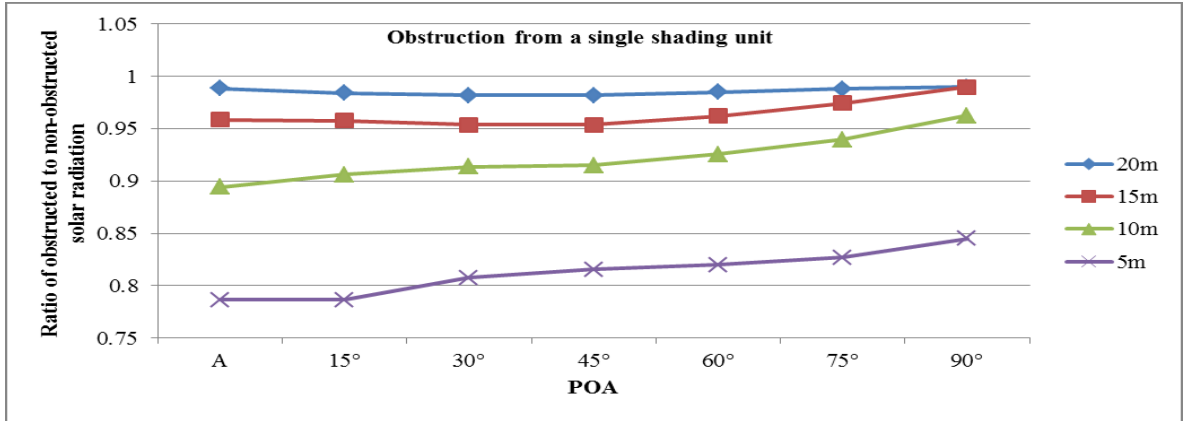
Solar Potential

Solar Irradiation

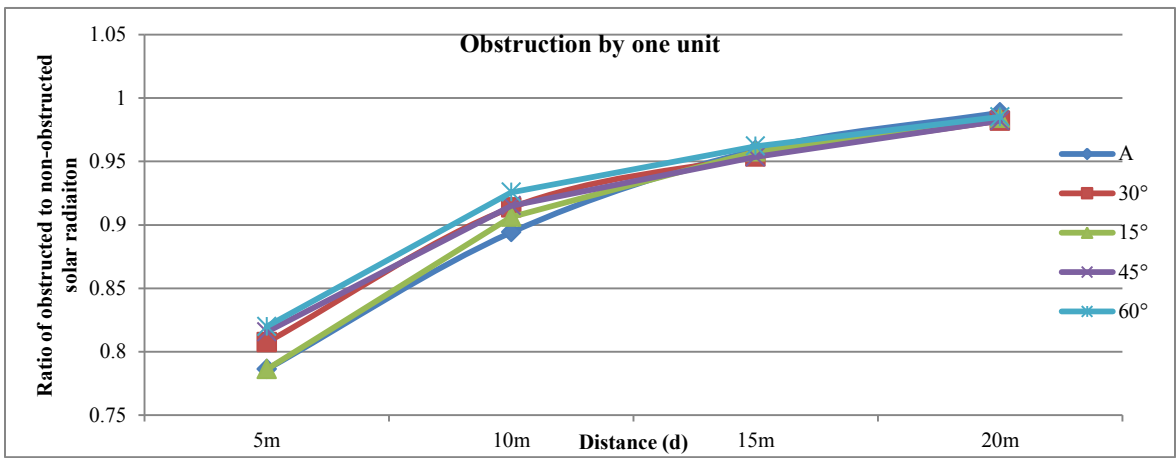
The effect of obstructing a rectangular dwelling unit by an identical unit, at different angles of obstruction and different distances is analyzed. The largest yearly incident radiation reduction occurs when the shading unit is aligned with the shaded unit (denoted A). Figures 4.8a and 4.8b illustrate this effect in terms of the ratio of annual solar radiation incident on the south façade of the obstructed unit, to the radiation incident on the south façade of the non-obstructed unit. Figure 4.8b indicates an exponential relationship between solar radiation reduction (shading effect) and distance. The exponential function representing the relation is shown in the figure. It should be noted, however, that the curve fitting is based only on four points. At a distance of 5m a reduction of 20% of the total annual irradiation is observed. For a distance of 15m or more, the reduction of solar radiation incident on the south facing façade and transmitted by the windows is 5% or less. For the WDD, a reduction of 40% in incident solar radiation is associated with 5m distance.

The effect of obstructing a dwelling unit by two identical units placed symmetrically with respect to the shaded unit, is almost double the effect of a single shading unit (Fig. 4.8 c,d). The major effect occurs when the units are placed on a small POA (15°). For 5 m distance the annual reduction in incident and transmitted radiation is

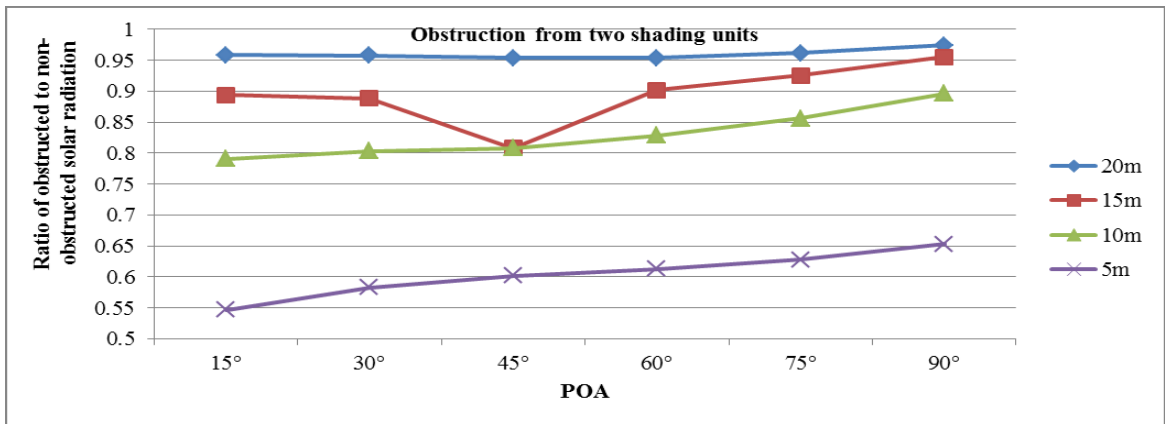
about 45%, while for a 15m distance the reduction is about 10%. For WDD at 5m the reduction in incident radiation reaches 80% as compared to the unobstructed unit.



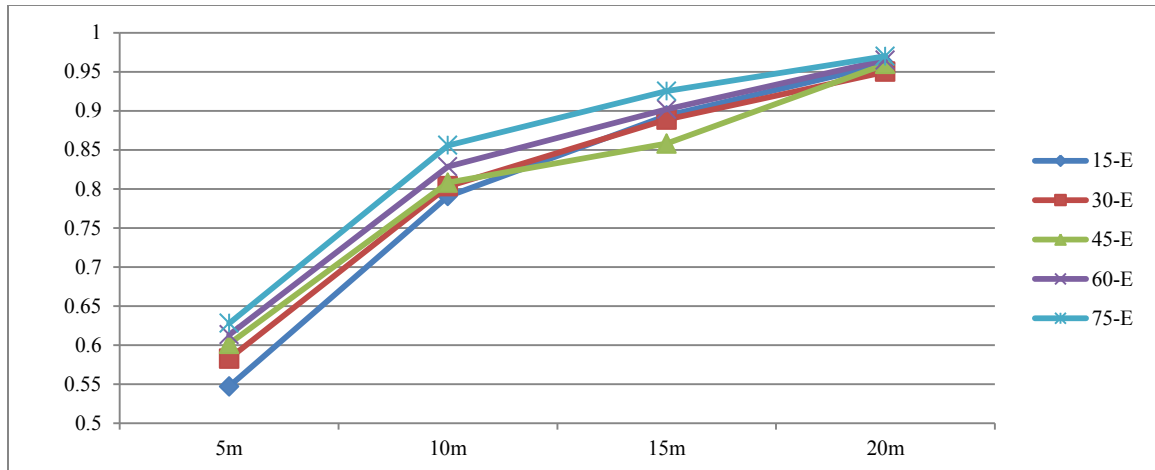
(a)



(b)



(c)



(d)

Figure 4.8, Shading effect on annual solar radiation of a rectangular shape, (a) single shading unit- radiation as function of POA, (b) single shading unit- radiation as function of distance (d), (c) two shading units- radiation as function of POA, (d) two shading unit- radiation as function of distance (d)

Energy Generation

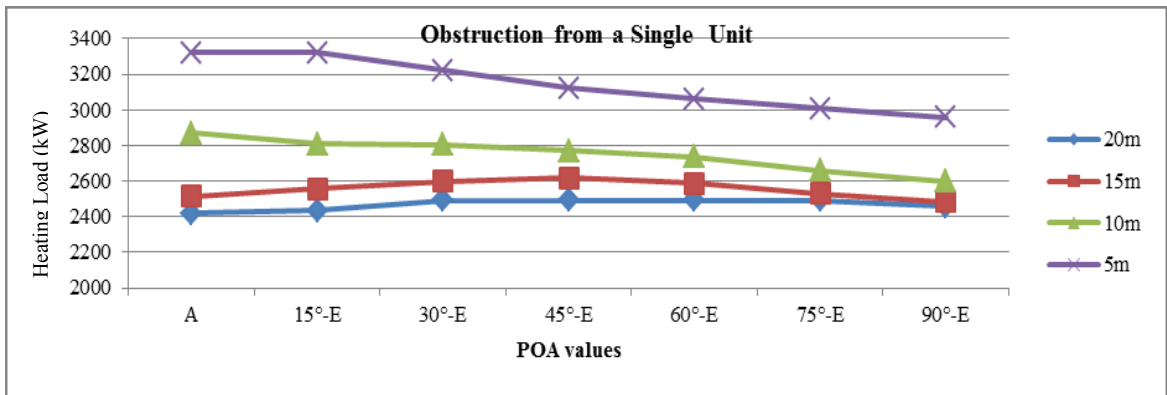
The results show that for aligned units with a distance of 5 m, the yearly electricity generation of the rectangular unit is reduced by about 4%. No shadowing effect on electricity generation is observed for a distance larger than 5 m. Electricity generation of non- aligned units is not significantly affected by the POA and distance between the units ($\leq 3\%$).

Energy Demand

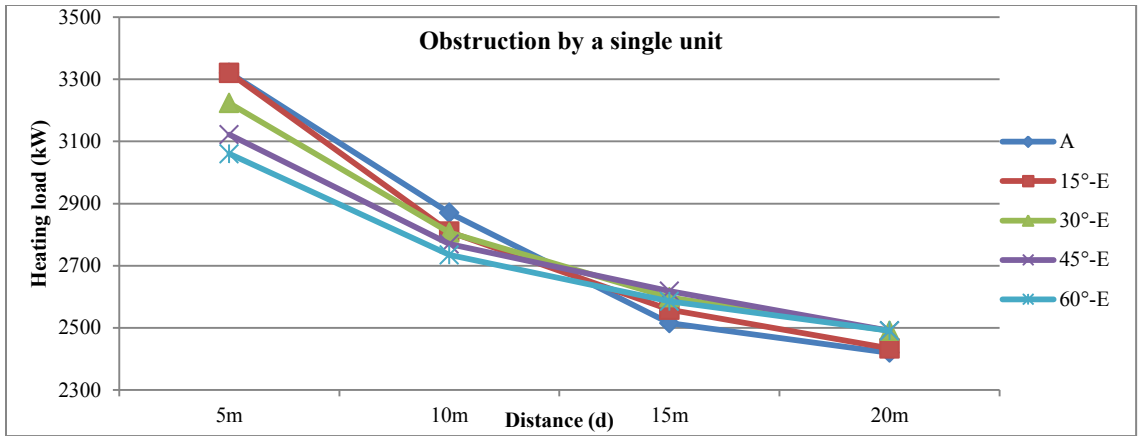
The effect of obstruction of a dwelling unit by one and two identical units on the energy use for heating is presented in Figures 4.9a-d. The results are presented as function of the POA angle and the distance from the center of the south façade of the shaded unit. Figures 4.9b and 4.9d indicate that the heating load decreases with increasing distance (d) between the units, and vice versa. The exponential curves based on four points are indicated in the figures.

It can be observed that at larger distance, the heating load initially increases with an increase of a POA. This is a result of the shortening of the vertical (north-south distance) as the angle increases. For shorter distance between the units the effect of reduction in shading with increased POA dominates, resulting in decreasing demand. The increase in heating load as compared to unobstructed unit, can reach 35% for a POA of 15° or less, at a distance of 5 m.

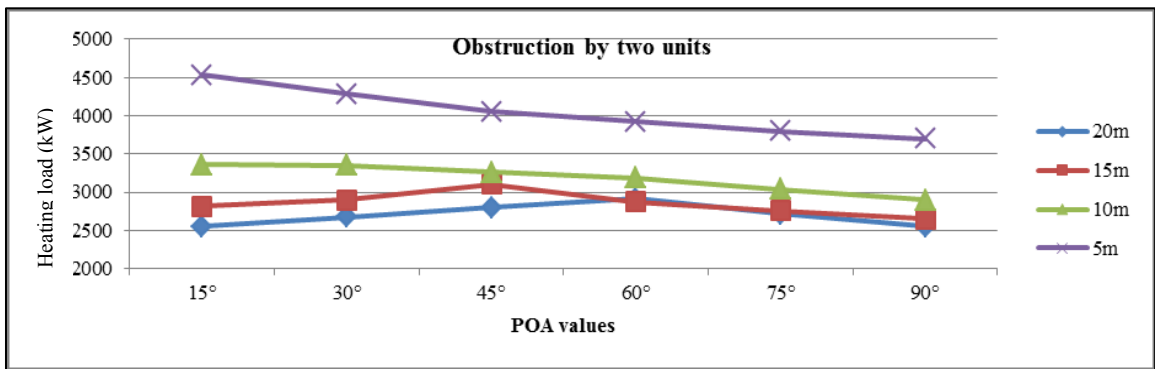
In scenarios where the dwelling unit is shaded by two obstructing units, the increase in heating load, relative to the unobstructed unit, is significantly higher. The increase in heating can reach 70% for a POA of 15°, at a distance of 5m. For a distance of 15 m, the larger heating load is associated with a POA of 45° and it reaches 35%, as compared to the non-obstructed unit.



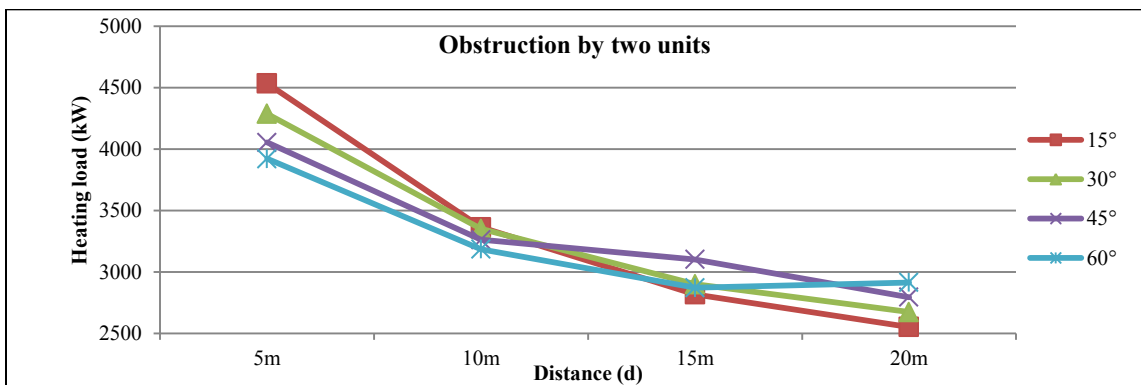
(a)



(b)



(c)



(d)

Figure 4.9, Shading effect on heating load of rectangular shape, a) single shading unit- heating load as function of POA, (b) single shading unit- heating load as function of distance (d), (c) two shading units- heating load as function of POA, (d) two shading unit- heating load as function of distance (d)

4.2.2 Density Effect

This section investigates the effects of spacing of units (s) in the three sites and the effect of row spacing (r) in site I.

Effect of Spacing

Solar Potential

Solar Irradiation

The effect of density on solar irradiation is assessed for site I (E-W road) by comparison of the response of attached configuration (A- $s0$) to the corresponding basic detached units (D, at a distance of $s1$) of the same configuration. In addition, the effect of units in detached configurations is evaluated by comparison with the corresponding isolated units. This effect is directly related to the shading effect discussed in section 4.2.1, with results presented here on a whole neighborhood scale.

In sites II and III, and variations of site I (inclined road variations), density effect is strongly coupled with site effect and some aspects are considered under site effects. Following are the main observations, relating to site I:

- For detached configurations of spacing – D- $s1$ (4m) the annual incident and transmitted radiation are reduced by about 15% for some L variant units, as compared to the corresponding isolated units. This reduction is due to the shading effect studied above. For increased spacing between the units ($s2=2s1$) the reduction of incident and transmitted radiation is about 10%. The WDD values of radiation reduction are double the annual – 30% for D- $s1$, and 20% for D- $s2$.

- For attached L units in site I (Fig. 4.6b), the maximum WDD reduction of incident radiation (about 13%), as compared to the detached L shape configuration, occurs on the main wing due to shading by the two wings of the adjoining units.
- A maximum of 20% reduction of the SDD incident radiation on rotated façade of the V-WS30 variant (unit U3 in Fig. 4.6c) is observed for attached as compared to detached units. This effect is due to the shade from the adjacent unit. For WDD, no significant effect is found (less than 3% reduction).

Energy Generation

The results for site I indicate that there is no significant difference in electricity generation between attached and detached configurations of a given shape. A maximum reduction of 3% or less of the average annual generation is observed in the attached units of L shape due to mutual shadings between units. For sites II and III, the results of the comparison of attached to detached configurations are presented in in Table 4.5. The main results are summarized as follows:

- The reduced south-facing roof area of the trapezoid roof of attached units in site II (Fig. 4.6d), as compared to the rectangular shape of detached units, results in reduction of the average annual electricity generation by up to 10%. In site III there is an increase of similar magnitude, due to the increased south facing roof surface area.
- No significant difference is observed for site II between the annual electricity production of the detached and attached configurations of L variants and obtuse-angle shapes.

- In site III, the attached configurations of both L variants and obtuse-angle perform better than the corresponding detached configuration (10% difference for L variants, and 3% for obtuse-angle). This is mainly due to the larger roof surface area obtained by replacing L shape and some L variants in the detached configurations by other L variant (with different angle β , compare Figs. 4.4 and 4.6) , in order to facilitate the assemblage of multiplex configurations.

Table 4.5, Density effect on electricity generation in sites II and III for summer and winter design days (SDD and WDD), and annually

Attached/detached	Site II			Site III		
	SDD	WDD	Annual	SDD	WDD	Annual
Trapezoid/rectangle	0.90	0.91	0.90	1.09	1.11	1.10
L variant	1.06	0.98	1.00	1.12	1.08	1.10
Obtuse-angle	0.99	0.96	0.99	1.00	1.11	1.03

It should be noted that in many cases attaching units enables larger roof area. Roofs can be redesigned to obtain a continuous roof (as compared to individual hip roofs in the present neighborhoods) which enables the design of larger PV system. Redesigning roofs for individual units is discussed in Chapter V (roof design).

Energy Demand

Comparison between Detached and Isolated Units

The arrangement of units with respect to each other in a site can result in mutual shading. An additional effect is the orientation of individual units. In order to uncouple the adjacency effect from the effect of orientation in curved site layouts, only the central due south unit in such a site is compared to the corresponding isolated unit. The results indicate that in general, heating load increases for detached units in a neighborhood while cooling load decreases (Fig.4.10). The increase in heating load reaches 12 % and 22% for

the rectangular shape in site I and site II, respectively. L shape heating load increases by 15% in site II as compared to 12% in site I. One reason for this effect is the shade cast on the east and west façades, in all configurations, and partially on south facing façades in sites II and III. The shade on south facing façade depends on the POA effect described above.

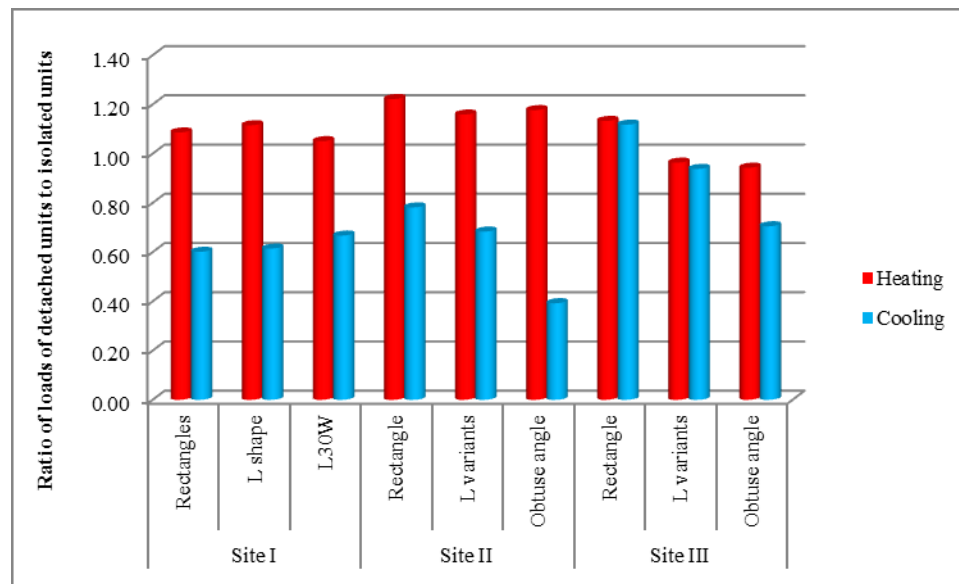


Figure 4.10, Comparison of heating and cooling demand between isolated units and detached units in a neighborhood.

Comparison between Attached and Detached Units.

Energy demand for heating and cooling of attached units is lower than for the corresponding detached configurations. For instance, heating demand of the attached rectangles and attached obtuse angle configurations in site II is reduced by 35% and 20%, respectively, relative to the detached units.

The average heating consumption is computed assuming a heat pump of COP of 4. The average values of heating consumption for units of each site, corresponding to the spacing values (attached – s_0 , detached – s_1 , and $s_2=2s_1$) are shown in Figure 4.11. For

site I, only configurations of the rectangular shapes and of L variants are shown in Figure 4.11, since obtuse angle is not applicable to this site.

Doubling the spacing of units (from s_1 to $s_2=2s_1$), does not affect significantly the heating energy consumption. While cooling energy consumption increases with larger spacing between units, it should be noted that it is negligible compared to heating energy consumption (ca. 10%).

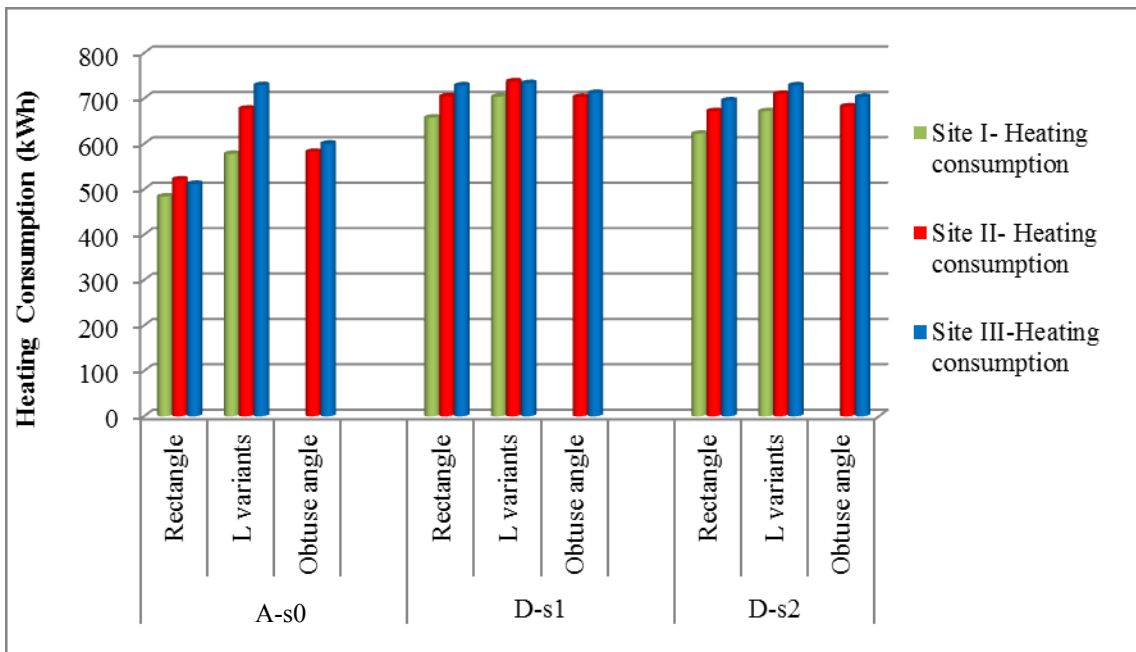


Figure 4.11, Heating consumption at different spacing between units.

Row Effect

Solar potential

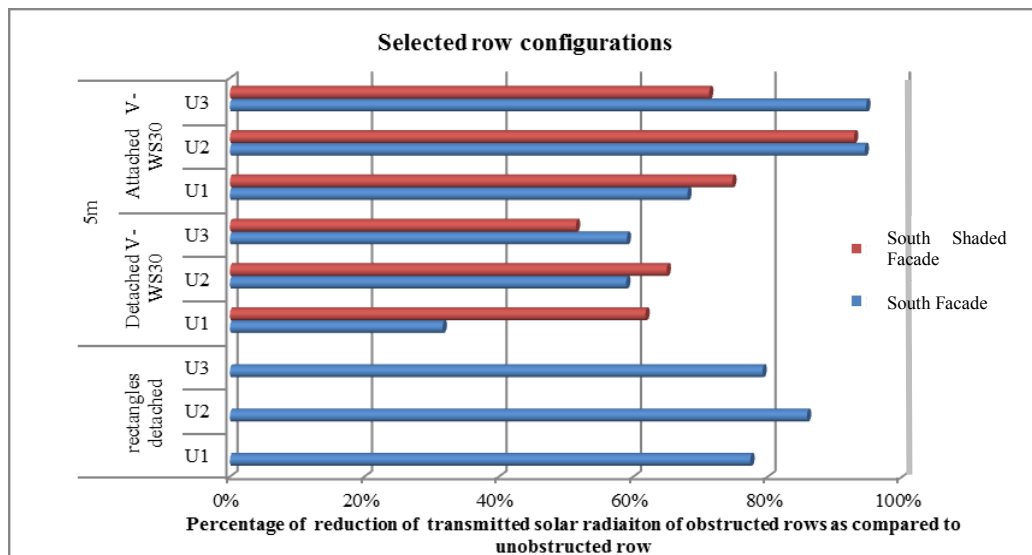
Solar Irradiation

The row effect on incident and transmitted radiation in site I is assessed by comparison of the corresponding radiation levels on south façades of the obstructed row with those of the unobstructed row. The results indicate that the distance between rows

has a significant effect on solar radiation incident on the façades of the obstructed row. For instance, for the smallest row spacing ($r=5m$) the transmitted radiation by the south façade windows may be reduced by as much as 95% on the exposed branch façade of attached L variant configuration (Fig. 4.12a), by 60% for the detached L variants and by some 85% for the detached rectangular shapes. A similar effect is found for the incident radiation.

At 20m, corresponding to a density of about 8 -10 u/a , the maximum effect is about 13% reduction of incident and transmitted radiation on the attached L variant configuration and 9% on the detached rectangle. At 20m, the row effect on the shaded façades of L variant configurations is small, reaching a maximum reduction of about 6% for WDD.

Figures 4.12a and 4.12b represent the results in term of the reduction of solar radiation transmitted by the windows of the obstructed row as compared to the corresponding unobstructed row, for some selected configurations. For non-convex shapes (VWS30) the effect is given for the shaded and for the exposed façades.



(a)

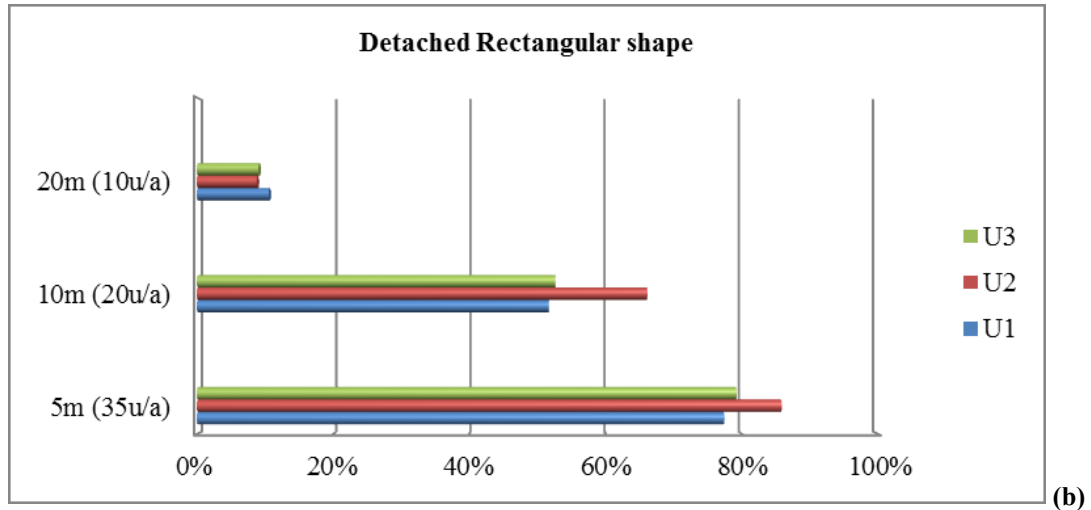


Figure 4.12, Reduction in transmitted radiation due to row effect for WDD. U1, U2 and U3 are the units of the shaded row (U2 is the middle unit): a) Effect on selected configurations at 5m row separation; b) Effect on detached rectangular units, at separations of 5, 10 and 20 m.

Energy Generation

The row effect on electricity generation is measured by comparing the electricity generation of the roofs of the obstructed rows to that of the exposed row. The results show that for a row separation of 5 m the electricity generation of the rectangular unit is reduced by a maximum (for the middle units) of 3% for the SDD and 7% for the WDD. The row configuration has no significant effect on the south facing L shape (L-SW) and L variant V-WS30 ($\beta=30^\circ$), both attached and detached. North facing L shape (L-N) performs in similar way to the rectangular shape. No shadowing effect on electricity generation is observed for row separation larger than 5 m. The yearly generation of all configurations is not significantly affected by the distance (<4%).

Energy Demand

The row effect on heating and cooling loads is assessed for site I by comparing the loads of obstructed and obstructing rows to the corresponding isolated row. The results for heating loads are presented in Fig. 4.13 for detached configurations and in Fig.

4.14 for attached configurations. Figures 4.13a and 4.14a show the heating loads of the obstructing and obstructed row relative to the isolated row. Figs 4.13b and 4.14b present the actual average heating loads. Results indicate that, generally, the average heating load increases significantly for the units of the obstructed row (R2), while the cooling load decreases. For the exposed row (R1), heating and cooling load are affected for a row spacing of 10m or less. Following are the main observations:

- The heating load of the obstructed row of detached rectangular units (Fig. 4.13) increases by ca. 50% at 5m row spacing and by 25 % at 10m spacing. The corresponding values for the exposed row are 15% and 5%, respectively.
- For attached rectangular units (Fig. 4.14), the increase in the heating load of the obstructed row is about 70% at 5m row spacing and 30% at 10m spacing. At 20 m there is no significant effect.
- For detached L-S and L-N configurations, at 5m distance the obstructed row requires around 40% more energy for heating than the isolated row (Fig. 4.13). The effect on the obstructed row is not significant for a distance of 15m or more. For the attached configurations, an effect of 50% is observed for a distance of 5m. For a distance of 10m and more, heating load of the obstructed row is not significantly affected by the obstructing row.
- For L variant, the exposed row is not affected, while the obstructed row of detached units requires 25% more heating at 5m spacing, and 10% at 10m. The attached units of L variant in the obstructed row require 35% more heating at 5m, and 15% at 10m spacing.

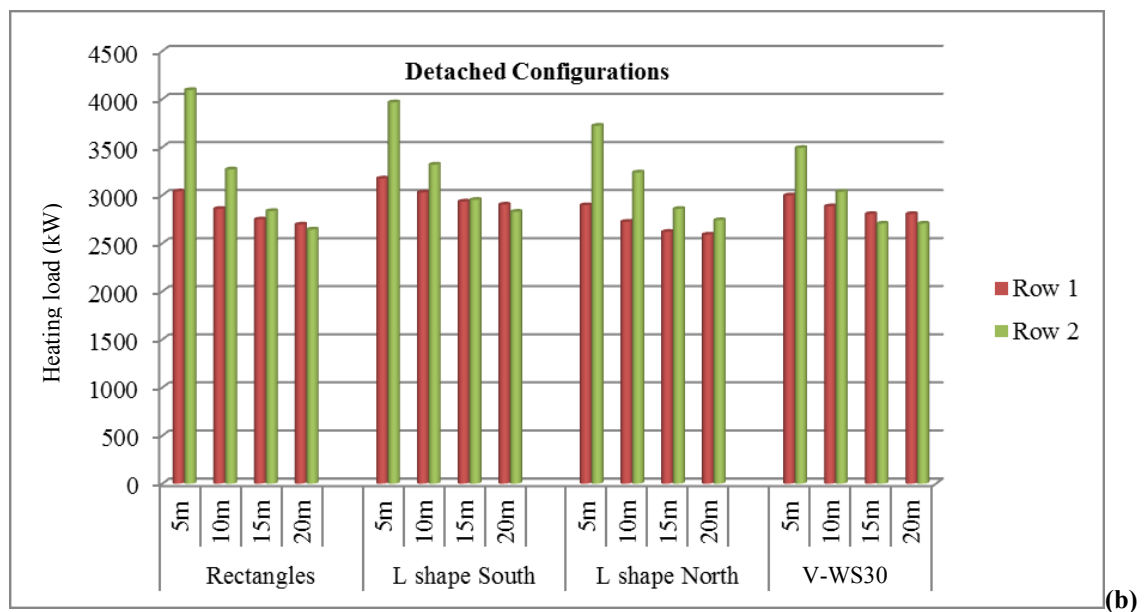
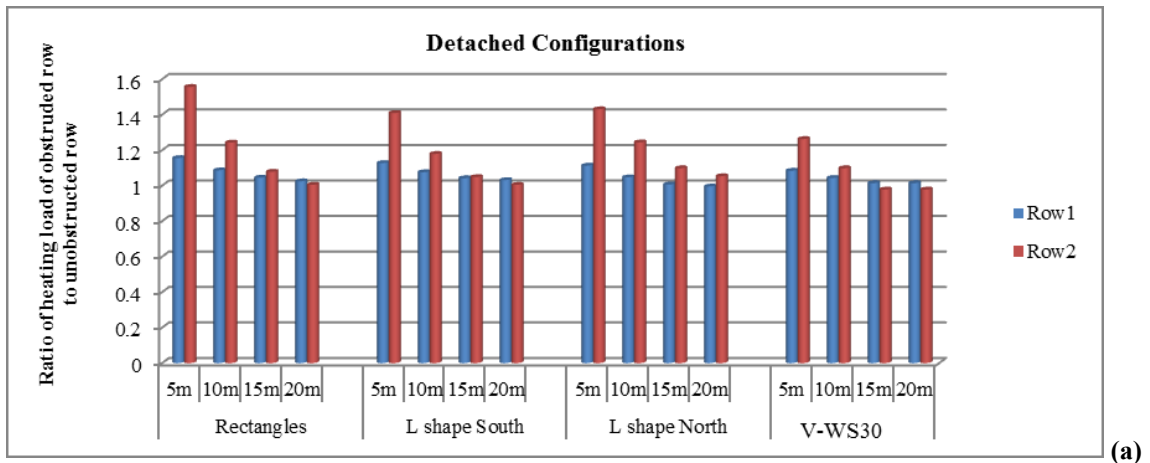


Figure 4.13, Detached units (a) Heating load of two rows relative to isolated rows, (b) Heating load of the two rows of detached units.

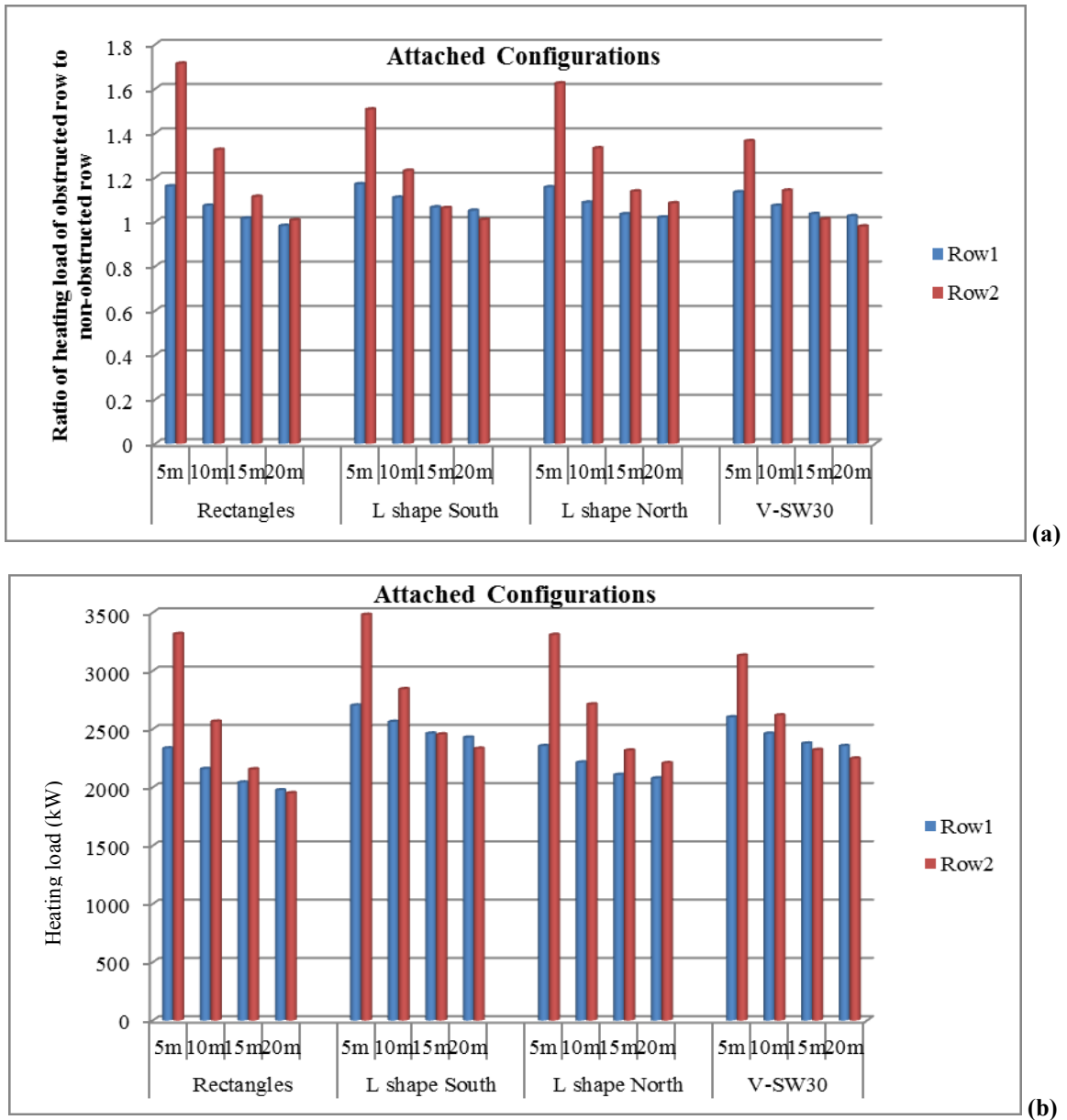


Figure 4.14, Comparison of the row effect in site I – R1 exposed row, R2 obstructed row: (a) Comparison to isolated row, (b) Heating loads of the two rows.

Fig. 4.15 presents the ratio of heating load of the obstructed to isolated row, for detached rectangular shape, expressed as function of the distance between rows. This distance is presented as percentage of the minimum distance between rows to avoid shading ($x = 25$ m, see above). The decrease in heating load has a quadratic correlation with the distance between the rows, as shown in Figure 4.15.

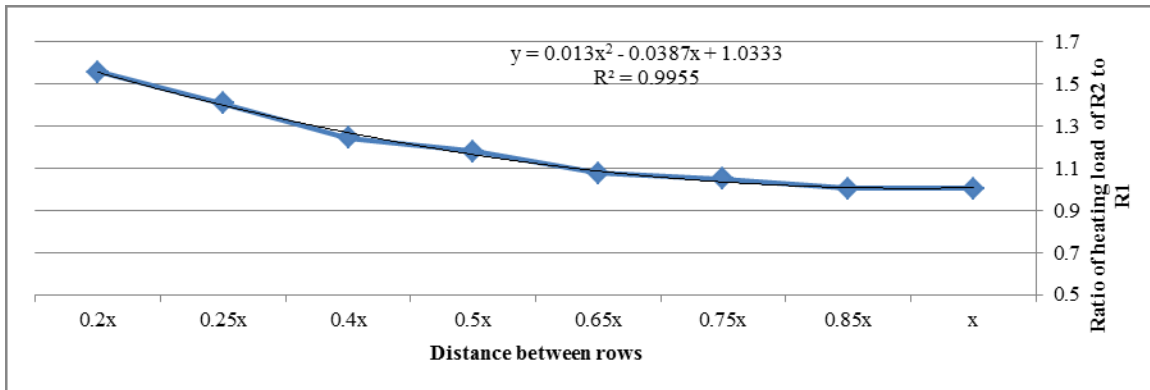


Figure 4.15, Ratio of heating load of the obstructed row to the unobstructed row as function of the minimal distance required to avoid shading

4.2.3. Effect of Site Layout

This section investigates the effects of site layout on the solar potential and energy performance of neighborhoods. Site I with east-west (E-W) oriented road serves as reference for assessing the effects of different site layouts on the response variables of housing unit configurations that are common to these layouts. Additional effects are studied for site specific configurations that are not shared by the reference site. The detailed analysis is presented below.

Straight Road - Effect of Road Orientation

The effect is studied only for detached units (Fig. 4.3). The main site effect comparison is between inclined roads and the E-W road which is the reference. Effects on individual units are assessed by comparison is to isolated units of the same shape and orientation.

Solar Potential

Solar Radiation

The effect of road orientation on solar radiation on façades of units along the road is influenced by the orientation of the units and their façades, as well as by shading due to POA and the distance between the units. To assess the effect of variations of road orientation on the incident solar radiation, units in different configurations are compared to the corresponding isolated units, of the same orientation. The effect of orientation on solar radiation is studied in Chapter III (section 3.2.3).

The effect on L variant configurations is as follows: The yearly solar radiation on the shaded façade of LVW60 (+60° road) is reduced by up to 15%, and by about 30% for the WDD, as compared to the isolated unit. For LVW45 (+45° road) the yearly reduction is about 10%.

The solar radiation incident on the south facing rectangular shape is reduced by a maximum of 9%, due shade cast by adjacent units. For the configurations where the whole rectangular unit is oriented toward the street, there is no shading effect and the radiation on the façade changes according to the orientation of the isolated unit, as indicated in Chapter III (a reduction of about 20% for 30° and up to 60% for an orientation of 60° on a WDD).

Energy Generation

The effect of road orientation on the average electricity generation is evaluated by comparing the annual energy yield of each of the studied configuration with its counterpart in the E-W road layout. Thus, the rectangular configurations in each inclined

road configuration are compared to the rectangular configuration of E-W road. Since the only L variant studied in the E-W road of site I is LVW30, the corresponding L variations configuration in the inclined road (+30°) is analyzed (Fig. 4.3).

No significant effect is found in the case of the south facing rectangles or L variants. In configurations where rectangular units are oriented to face the road, electricity generation is only affected by the orientation, since mutual shading has no effect. Detailed study of the effect of orientation on electricity generation is presented in Chapter V.

Energy Demand

The effect of road orientation on the energy demand for heating and cooling of units is found by comparing the heating and cooling load of the units of rectangular and V-WS30 configuration to the corresponding configuration in the E-W reference road. Comparison to the isolated units is also given to allow for those configurations that are not shared by the E-W road layout (such as non-south-facing rectangles and L variants with wing rotation other than 30°). The main observations are summarized in the following:

- The energy demand for heating of the rectangular south facing configurations (R) is not significantly affected by the road inclination (maximum of 9% increase). However the use of land is increased significantly (by up to 29%) as compared to the south facing rectangles of E-W road.
- Rectangular configurations that are oriented (R (O)) towards the road use less land than all other configurations. However, they require significantly larger

heating energy (up to 36%) as compared to the south facing rectangular E-W road configuration.

- V-WS60 requires up to 29 % more energy than the isolated units. V-WS60 has an increased energy demand primarily because of the relative position of the units, where a large portion of the south facing façade is shaded. This effect can be reduced by increasing the distance between units. However, increasing the distance can lead to an increase of land use area.

Figure 4.16 and Table 4.6 present results for positive rotations of road orientations (General SE-NW orientation). Configurations with negative rotation show similar results with a difference of 2-3% in loads (requiring less energy).

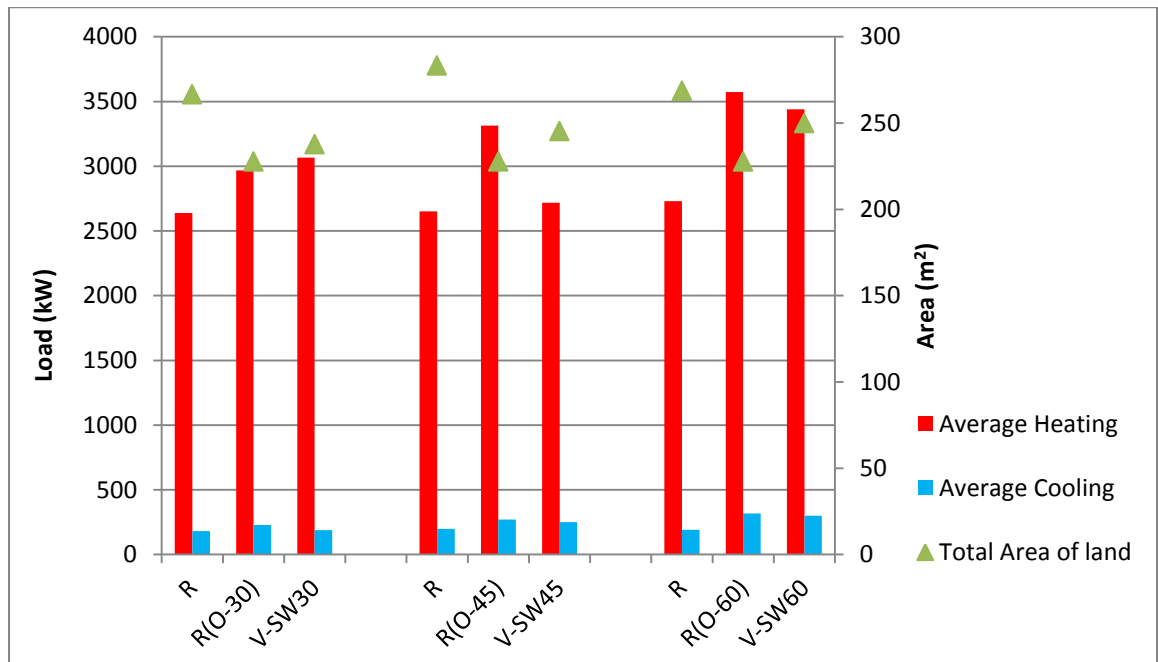


Figure 4.16, Comparisons of heating/ cooling loads and land use area of all configurations (R-south facing rectangles; (R-O) rotated rectangles and V shapes), of the inclined road sites.

Table 4.6, Summary of the results analysis of the inclined road configurations

Configurations	Average Heating load (kW)	Average Cooling load (kW)	Land area per house (m ²)	Comparison of heating load to configuration of E-W	Comparison to isolated units	Ratio of land area to reference case (E-W)
Road +30°						
R	2638.20	180.72	266.67	1.00	1.05	1.21
R(O-30)	2967.01	229.21	227.67	1.13	1.18	1.03
V-WS30	3065.69	189.56	237.67	1.15	1.14	1.08
Road +45°						
R	2650.72	198.50	283.33	1.01	1.06	1.29
R(O-45)	3312.84	269.76	227.67	1.26	1.32	1.03
V-WS45	3052.00	249.81	245.33	-	1.13	1.12
Road +60°						
R	2730.73	190.08	268.67	1.04	1.09	1.22
R(O-60)	3573.96	318.18	227.67	1.36	1.42	1.03
V-WS60	3439.43	300.80	250.00	-	1.29	1.14

Curved Road

As mentioned above, the effects of density and site layout are strongly coupled for curved layouts. The main comparison for overall site effect is between sites with curved road (II and III) and site I (with E-W road). This comparison can only be applied to configurations of similar unit shapes and density. The effect of curvature on solar performance of individual (detached) units of a given shape in the neighborhood can be assessed by reference to the isolated, south oriented unit of the same shape.

Solar Potential

Solar Radiation

The incident radiation on the near south façades of individual units and transmitted by their windows, in each detached assemblage is compared to isolated south facing units to assess the effect of shade from adjacent units. In attached configurations comparison is carried out with respect to the corresponding detached units of the same configuration, to assess the effect of density.

The rectangular units of site I are positioned in straight layout facing south and therefore the south facing façades of detached units are not affected by adjacent units. For detached L and L variants in site II and III, the main effect, as compared with site I, is due to the rotation of units relative to the south, along the curved layout. In addition, some units in these configurations cast shadows on façades of adjacent units. The WDD reduction of incident radiation on the south facing façades ranges from about 4% on the central units, to up to 30% for some adjacent units (e.g. U2 and U4 in L variants, Fig.4.4b), in comparison to the isolated south facing units. This depends on the distance between the units, and on the POA value which determine the extent of shading.

For the attached configurations, the method of assemblage of L variant (Fig. 4.6) results in self- shading geometries (non-convex configurations). In these cases the ratio of the dimensions of mutually shading façades of adjoined units is of importance, and should be taken into consideration in the design. The decrease of solar radiation, relative to the corresponding detached unit, can reach up to 30%, in some of the studied cases, depending on the ratio of the dimensions of mutually shading façades (similar to the depth ratio effect of a non-convex shape, Chapter III).

Energy Generation

The site layouts are compared for the three configurations that are common to the three sites. These configurations are detached rectangles, detached L variants, and attached L variants. The performance of these configurations of sites II and III, is compared to the performance of site I. The response variable for the comparison is electricity generation per unit area averaged over all units in a neighborhood.

No significant effect of the site layout is indicated on overall electricity generation per unit area. A maximum reduction of about 3% is observed in the generation of the detached rectangle configuration in sites II and III as compared with the similar configuration in site I. Comparing the annual energy generation of the total roof area, an increase of 6% and 9% is observed, for the attached L variant configuration in site II and site III respectively, as compared to the corresponding configuration in site I. The results are presented in Table 4.7.

Table 4.7. Site layout effect on average electricity generation for summer and winter design days (SDD and WDD), and annually

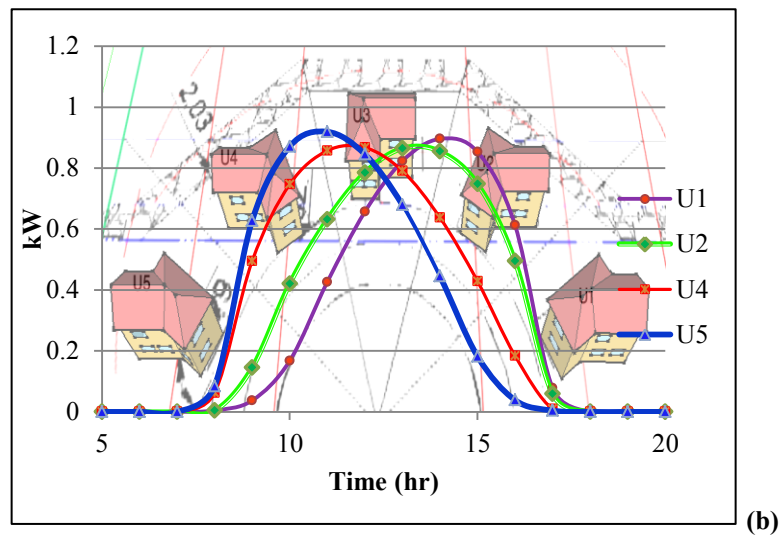
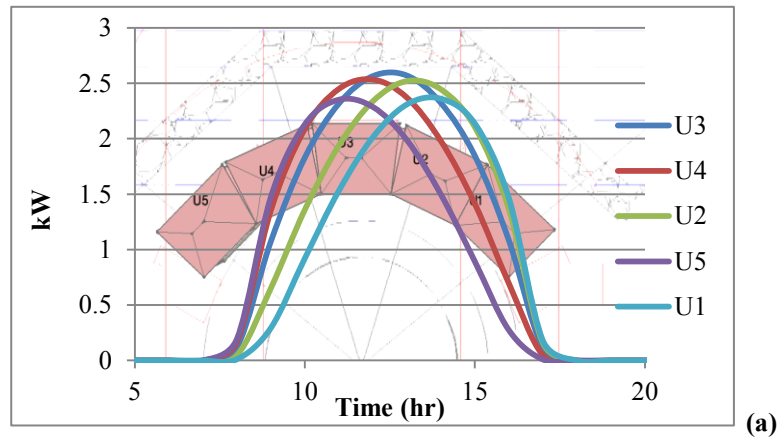
Site	Site II/site I				Site III/site I			
	SDD	WDD	Annual	Annual per total area	SDD	WDD	Annual	Annual per total area
Detached Rectangles	1.02	0.91	0.97	0.97	1.02	0.90	0.97	0.97
Detached variant L	0.98	0.97	0.99	1.04	0.88	0.99	1.00	1.05
Attached variant L	1.04	0.99	1.01	1.06	0.99	1.00	1.01	1.09

Shift of Peak Electricity Generation

An important result of the interaction of site layout and configurations is the shift of peak electricity generation. This effect is mainly found in sites II and III, where different shape orientations are dictated by the layout of the road.

A significant shift of the profile of the electricity generation is obtained by the BIPV of different units. In site I the difference in timing of peak electricity is due, to the rotation of the south wing of V shape. A maximum shift of 3 hours is obtained in site I. In sites II and III an additional source is the rotation of whole units. A difference of peak time of up to 6 hours is observed in the configurations of site II and site III.

Figure 4.17 presents the daily variation of electricity generation of configurations of site II for the winter design day. Electricity generation profiles for attached rectangular (trapezoid) units are presented in Figure 4.17a. The graphs of Figure 4.17 b, c show the electricity generation profiles of the hip roof of wings of units of detached and attached L variant configurations of site II. It should be noted, however, that the hip constitutes a small portion of the electricity generating roof surface and the overall effect on total generation would be reduced.



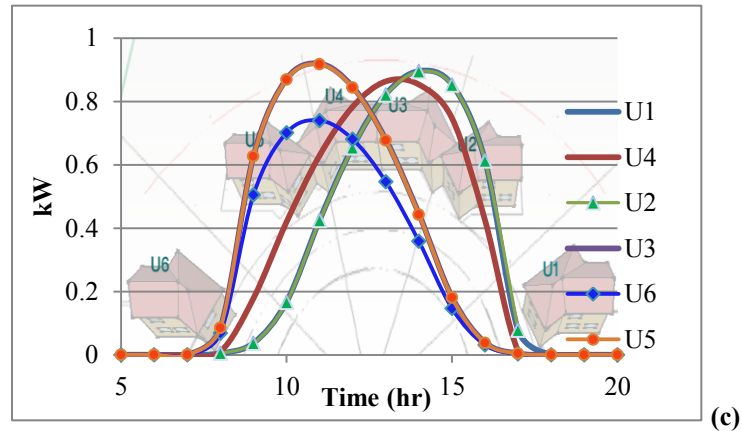


Figure 4.17, Hourly electricity generation (from 4-6 AM to 6-8 PM) (kW) for site II, on a WDD: a) on the total south roof of attached rectangular (trapezoid); b) on the hip of L variants of detached L variants; c) on the hip of L variants of attached L variants.

Energy Demand

The effect of site layout on energy demand is analyzed by comparing configurations of rectangular and L variant shapes in site II and site III to the corresponding configurations in site I. The results are presented in Figure 4.18. For detached configurations, only the cooling load increases in site II and III. For instance, the cooling load of the rectangular configurations is increased by approximately 45% and 48% for site II and site III, respectively. However, the energy demand for cooling is low relative to heating (<10%, for the rectangular configuration in site II). One important reason for the increase of cooling load in sites II and III, particularly for rectangular units, is the rotation of units around the curve towards east or west, resulting in increased transmitted radiation in the morning and the evening, when the sun is at low altitude during the summer period. This can be resolved by modifying the window area, for the rotated units.

In attached configurations, the heating load of L variants in site III is 25% higher than in site I. This can be explained by the shade cast on several south façades of this

configuration. The attached trapezoid configuration requires 8% and 6% more heating for site II and III, respectively, than the attached rectangles of site I.

For all shapes, heating demand is lower in site I than in the two other sites. Heating load of attached L variant is up to 25% higher in site III and 18% in site II, as compared to site I. For the rectangular configuration the increase of heating load is some 8% for attached units (trapezoids) and 11% for detached units.

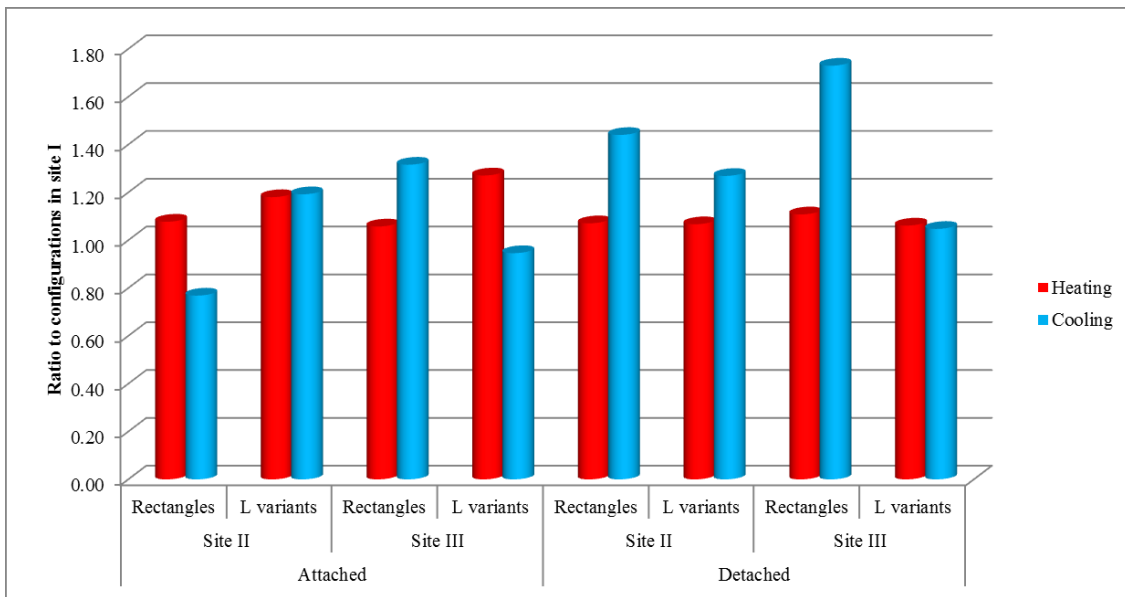


Figure 4.18, Heating and cooling loads of sites II and III relative to site I.

4.2.4. Evaluation of Energy Balance of Neighborhoods

In this section energy consumption and supply are compared for the different configurations studied.

Isolated Units

The total consumption of electricity for lighting, DHW and appliances, in addition to the computed heating and cooling energy consumptions, for isolated south-facing units of each shape is presented in Figure 4.19 alongside the energy production of the

corresponding units. The electricity production of the reference rectangular layout with hip roof is some 35% less than consumption. Some L variants, such as V-EN30W, produce up to 96% of total consumption. The results in terms of percentage of energy production to energy consumption of all shapes are presented in Table 4.8.

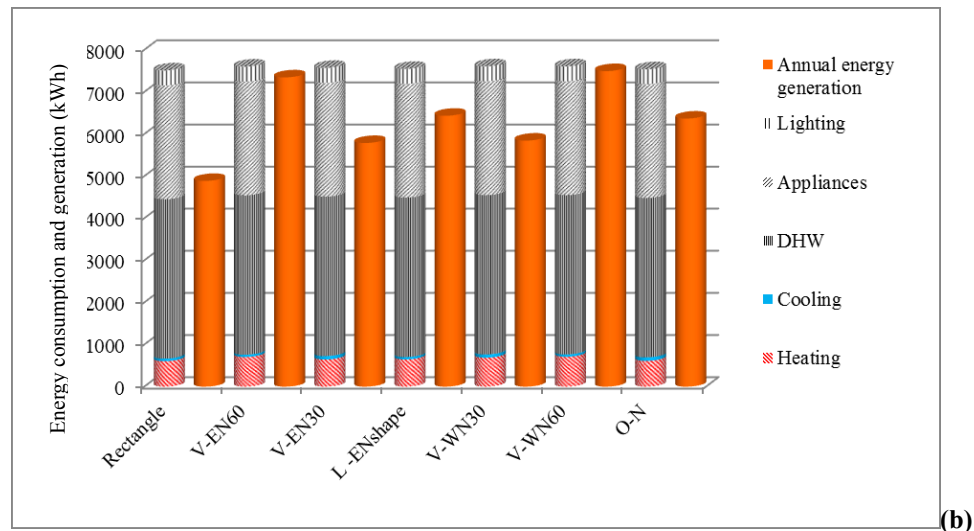
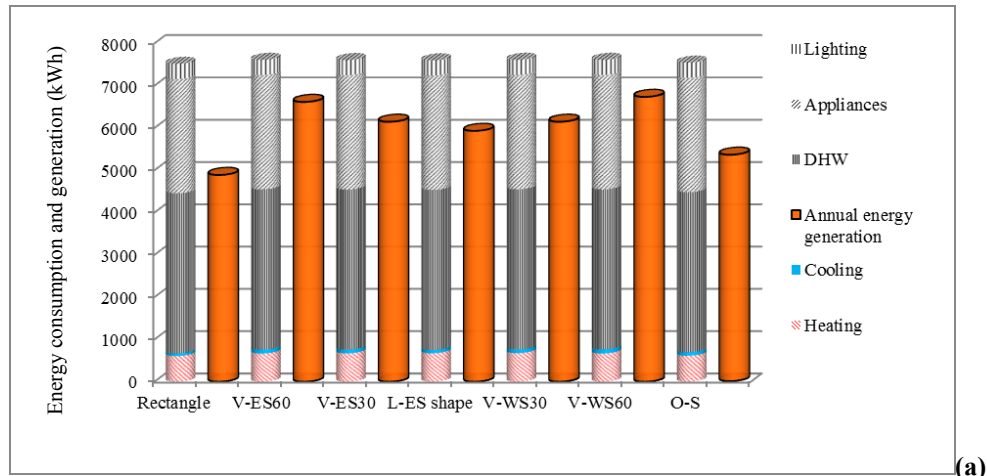


Figure 4.19, Energy consumption and production for isolated units of different shapes: a) Shapes of sites I and II; b) Shapes of site III.

Table 4.8, Ratio of energy production to consumption

Shapes – site II and site I	Rectangle - Gable roof	R	V-ES60	V-ES30	L-ES	V-WS30	V-WS60	O-S
Ratio of energy generation to energy use	1.02	0.65	0.87	0.81	0.78	0.81	0.89	0.71
Shapes – Site III		R	V-EN60	V-EN30	L-EN	V-WN30	V-WN60	O-N
Ratio of energy generation to energy use		0.65	0.94	0.74	0.83	0.74	0.96	0.81

Neighborhoods

Total energy supply/consumption balance for assemblages in all sites is presented in table 4.9. Following are the main observations:

- Configurations of L variants, in both site I and site II generate around 80% of their total energy consumption.
- In site III, L variant shape is optimal for detached configuration while the obtuse angle is optimal for the attached configuration. These configurations generate 85% of the total energy consumption (Table 4.9).
- In site I, L variants can supply 79% of the total energy need, while the rectangular configuration generates ca. 65%.

Table 4.9, Ratio of energy production to total energy consumption of all configurations

Site	Site I		Site	Site II		Site III	
Density shape	Detached	Attached	Density shape	Detached	Attached	Detached	Attached
Rectangle	0.65	0.66	rectangle	0.62	0.58	0.63	0.70
L shape	0.74	0.75	L Variants	0.81	0.81	0.85	0.82
L variants	0.79	0.79	Obtuse	0.74	0.73	0.75	0.85

CHAPTER V: ROOFS³

This chapter presents an in-depth study of roofs for increased solar potential. The basic principle is the utilization of complete near-south facing roof surfaces for solar collectors that generate both heat and electricity through the application of a building-integrated photovoltaic/thermal (BIPV/T) system. An open loop air-based BIPV/T system is assumed in this study. Following is a brief outline of the chapter's contents.

Section 5.1 presents the principles of the open loop air based BIPV/T system, as well as the numerical model employed to obtain a correlation between thermal and electrical output of the system. Section 5.2 investigates the effect of combinations of tilt and orientation angles of a roof surface on the BIPV/T output. Section 5.3 presents design alternatives for the roof of a building of rectangular layout, starting with a simple hip roof design and advancing to more complex multi-surface configurations, aimed at optimizing energy production. Values of the design parameters investigated are presented in terms of the tilt and orientation angles of the various surfaces. An option of redesigning the basic rectangular shape to follow the contour of multi-surface roof geometries is also investigated.

Simulation results and their analysis are presented in section 5.4. The analysis relates to energy production, including both electricity and useful heat collection. The effect of roof design on energy demand, in terms of heating and cooling loads, is also investigated. This analysis is performed for all roof configurations, as well as for

³ The study and some of the results presented in this chapter are published in: Hachem C., A. Athienitis, P. Fazio, (2012b). Design of roofs for increased solar potential of BIPV/T systems and their applications to housing units", ASHRAE Transactions, TRNS-00226-2011.R1.

redesigned layout to fit multi-surface roofs. A rectangular unit with hip roof (45° side and tilt angles) serves as reference for comparing design alternatives. Overall energy performance is assessed in terms of annual electricity generation versus total energy consumption for all roof variants.

5.1. BIPV/T system

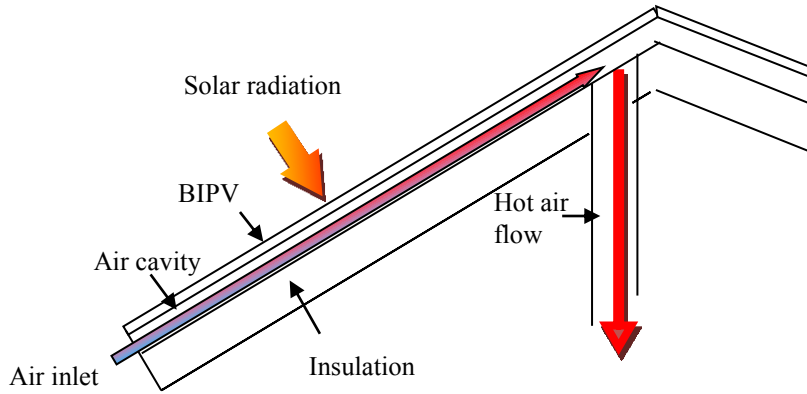
This section presents the numerical model employed to obtain a correlation between thermal and electrical efficiency of the open loop air based BIPV/T system. The air circulated behind the PV panels assists in cooling these panels, increasing thus their electrical efficiency, and in recovering heat that can be used for space or/and water heating. The useful fraction of thermal energy generation depends on the temperature of the solar heated air and on the end uses. For instance, a BIPV/T system coupled with a heat pump enables exploiting low temperature outlet air to offset heating load or for direct space heating, while higher outlet air temperature can be employed to heat domestic hot water or sent to storage.

Approximate Model

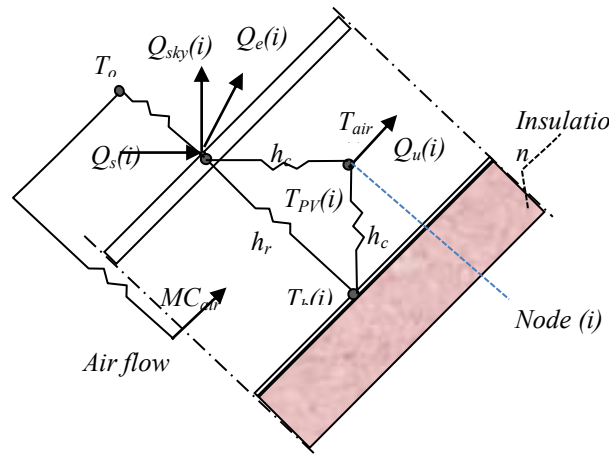
A transient quasi-two-dimensional finite difference model is employed to determine the thermal energy generation potential of the BIPV/T system, and to establish a relationship between electricity and useful heat generation. A gable roof of the rectangular unit, with a tilt angle of 45° is employed in the model. The model is applied to the design days as well as to selected sunny days representing each month of the year. The model is applied to roofs with different tilt angles, ranging from 30° to 60°, at 5 degrees increments. Environmental parameters including outside temperature, solar

radiation, wind speed and sky temperature are provided by the weather data files of EnergyPlus.

The BIPV/T system, illustrated in Fig. 5.1a, is divided into five control volumes along the direction of the ridge. Figure 5.1b depicts the thermal network of one control volume of the BIPV/T system. The various thermal conductance coefficients, including that associated with the air flow (MC_{air}), are presented in Figure 5.1b. The PV panels are assumed to have negligible thermal resistance and thermal capacity (Liao et al, 2007). The bottom surface of the air cavity is assumed to be well insulated.



(a)



(b)

Figure 5.1, a) Cross-section illustrating an open loop BIPV/T system , b) schematic illustrating the thermal network in one control volume of the BIPV/T system (refer to eqs. 5.1-5.8 for meanings of symbols).

The governing equation describing the explicit finite difference method for a thermal network, corresponding to a node i and time interval p , is expressed by Athienitis (1998):

$$T_{(i,p+1)} = \frac{q_i + \sum_j (U_{(i,j)} T_{(j,p)})}{\sum_j (U_{(i,j)})} \quad (\text{eq. 5.1})$$

where T is the temperature of a node at a specific time, q_i is the heat source at the node in question, j is an adjacent node, $U_{(i,j)}$ is the heat transfer coefficient between nodes i and j , and p indicates the present time step.

The total electrical energy is determined as function of the efficiency and the solar radiation as follows:

$$Q_e = \eta_{pv} \cdot A \cdot G \quad (\text{eq. 5.2})$$

where (η_{pv}) is the PV efficiency (Eq. 5.3), A is the surface area of the roof and G is the solar radiation (W/m^2). The electrical efficiency of the BIPV (η_{pv}) system is computed by the following linear equation (Skoplaki and Palyvos, 2009; Whitaker et al., 1991):

$$\eta_{pv} = \eta_{STC} \{1 - \beta (T_{pv} - T_{STC})\} \quad (\text{eq. 5.3})$$

where η_{STC} is the efficiency of the PV cells under standard test conditions (STC), β is the PV module temperature coefficient, and T_{STC} is the standard test condition temperature (25°C). A value of 12.5% is assumed for η_{STC} .

The total thermal energy generated by the BIPV/T (Q_u) can be expressed as follows:

$$Q_u = \eta_{thermal} \cdot A \cdot G \quad (\text{eq. 5.4})$$

Q_u is determined as function of the inlet air temperature entering the BIPV/T system, assumed as the outside air temperature (T_o), and the outlet air temperature of the system ($T_{outlet-BIPV/T}$) (outlet air of the last control volume), (Athienitis et al., 2011):

$$Q_u = M \cdot C_{air} (T_{Outlet-BIPV/T} - T_o) \quad (\text{eq. 5.5})$$

The outlet air temperature at each control volume is determined as:

$$T_{outlet}(i) = T_{in}(i) + \frac{Q_u(i)}{M \cdot C_{air}} \quad (\text{eq. 5.6})$$

where $T_{in}(i)$ is the inlet air temperature at each control volume, M is the mass flow rate of air, C_{air} is the specific heat of air, and $Q_u(i)$ is the heat carried by the air flow and is determined by the finite explicit model at each control volume as:

$$Q_u(i) = A_s \cdot [h_c \cdot (T_{pv}(i) - T_{air}(i)) + h_c \cdot (T_b(i) - T_{air}(i))] \quad (\text{eq. 5.7})$$

where A_s is the area of each BIPV/T section, h_c is the convective heat transfer coefficient in the cavity, T_{pv} is the temperature of the PV panel, T_b is the temperature at the bottom side of the cavity, and (T_{air}) is the air temperature, computed in each control volume by means of equation 5.8 (Charron and Athienitis, 2006).

$$T_{air}(i) = \frac{T_{pv}(i) + T_b(i)}{2} + \left(T_{in}(i) - \frac{T_{pv}(i) + T_b(i)}{2} \right) \cdot e^{-\frac{x \cdot a}{2}} \quad (\text{eq. 5.8})$$

where x is the length of the studied section, and

$$a = \frac{M \cdot C_{air}}{W \cdot h_c} \quad (\text{eq. 5.9})$$

where W is the cavity width.

Based on Equations 5.2 and 5.4, the thermal efficiency can be determined as:

$$\eta_{thermal} = \frac{Q_u}{Q_e} \cdot \eta_{pv} \quad (\text{eq. 5.10})$$

The ratio (Q_u/Q_e) determines the correlation between the heat and electricity generation of the BIPV/T systems. Q_u/Q_e for selected sunny days, of each month of the year for a 45° tilt angle is presented in Figure 3a. Figure 3b presents the results of the simulations of the BIPV/T systems with various tilt angles, for the (WDD). The ratio of solar thermal production to the electricity production (Q_u/Q_e) varies between 3 and 3.5 (mean value of 3.1 and standard deviation of 0.2). A value of $Q_u=3Q_e$ is adopted in this study for an air speed of 2m/s in the BIPV/T system, selected to ensure high efficiency of the BIPV/T system (Athienitis, 2011).

The correlation between thermal and electrical energy $(Q_u=3Q_e)$ is based on the assumption of a constant flow (of 2m/s) in the BIPV/T system. This approach is considered as appropriate for this research since the main goal is to explore the potential of the BIPV/T system. In practice, for design purpose, detailed models involving yearly simulations would be advisable to regulate outlet temperature according to desired applications and therefore to maximize useful heat produced by the BIPV/T system.

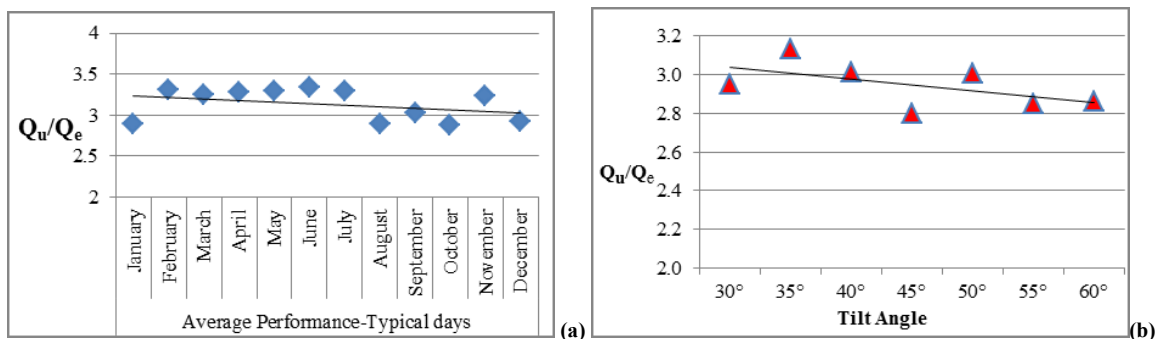


Figure 5.2, a) Q_u/Q_e for 45° tilt angle roof for one sunny day of each month, over a year; b) Q_u/Q_e for WDD of roofs with different tilt angles.

The correlation between thermal and electrical energy generation is employed to determine the thermal energy as well as the outlet air temperature of BIPV/T systems of different complex roof designs developed in this study.

Variable speed fan enables controlling the outlet air temperature, which can be used for different purposes. Figure 5.3 presents the relation between air velocity and the average air change temperature (ΔT - the difference between inlet and outlet air temperature of the BIPV/T system), over the winter design day, in the BIPV/T system. This relation is determined for the gable roof of the rectangular shape.

The inlet air temperature is the outside temperature obtained from EnergyPlus weather data. The outlet air temperature decreases exponentially with increasing flow rate, and vice versa. Flow rate and outlet air temperature should be determined to fit the intended application. For instance, for heat pump lower outlet air temperature can be used, while for space heating and hot water higher temperature is needed.

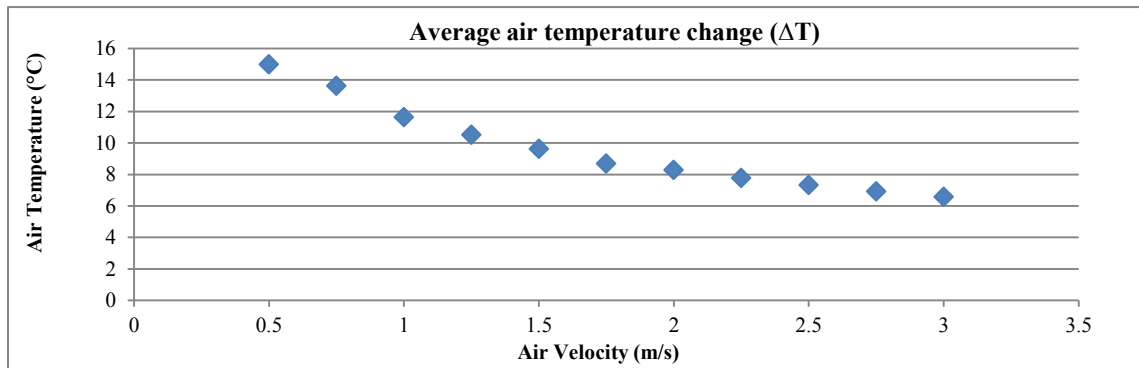


Figure 5.3, Relation between air velocity and the average air change temperature in the cavity (ΔT), on a WDD.

5.2. Basic Surface Parameters and their Effect

This section investigates the effect of roof surface parameters – tilt angle and orientation relative to south – on the energy performance of the BIPV/T system per m² of surface. The main response variables in assessing performance are the annual electricity generation, the heat production during a heating period, assumed from October 15 to April 15, and the total combined energy production.

5.2.1. Effect of Tilt Angle

The annual electricity generation of the BIPV/T system is not significantly affected by a tilt angle that ranges between 30° and 50°. For a 60° tilt angle, the annual electricity production is reduced by some 7% as compared to 45° tilt angle, while the heat generation for the assumed heating period is reduced by only 2%. This is mainly due to larger tilt angle having advantage in the winter months. For instance, the electricity generation of the BIPV/T system with 60° tilt angle is reduced by 16% in June, as compared to the system with 45° tilt angle, while the maximum monthly increase of generation in December is about 6%. Figure 5.2 presents the average monthly electricity production of various tilt angles.

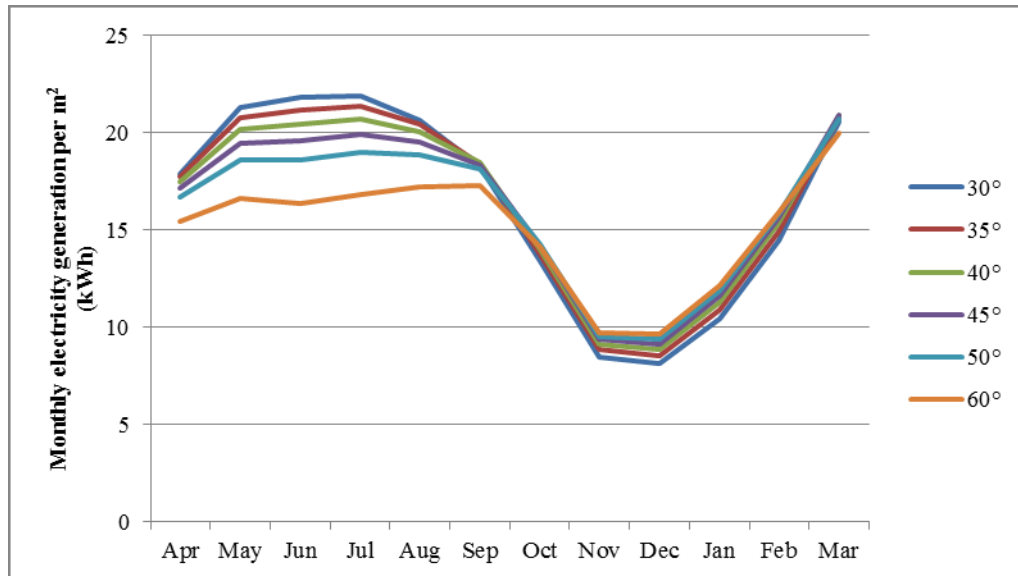


Figure 5.4, Monthly electricity generation for different tilt angles.

5.2.2. Effect of Orientation Angle

Orientation affects the solar potential in two ways: the amount of generation and the time of peak generation. Annually, the highest energy yield is associated with a south facing system. Deviation of the orientation of the system from the south by up to 40° west or east leads to an approximate reduction of up to 5% of annual electricity generation (Fig. 5.5), and reduction of the heat generation for the assumed heating period by up to 9%. A rotation of the system by 60°, west or east of south, results in a reduction of some 12% of the total annual electricity generation and of 20% of the heat generation during the heating period. Figure 5.5a presents the effect of the orientation on electricity generation, for the design days and the total year generation associated with a 45° tilt angle BIPV/T system. Figure 5.5b presents the effect on heat generation during the heating period. The effect is measured as the ratio of the electricity and heat generated by the BIPV/T at different orientation angle to the generation of a south facing BIPV/T system (orientation = 0°).

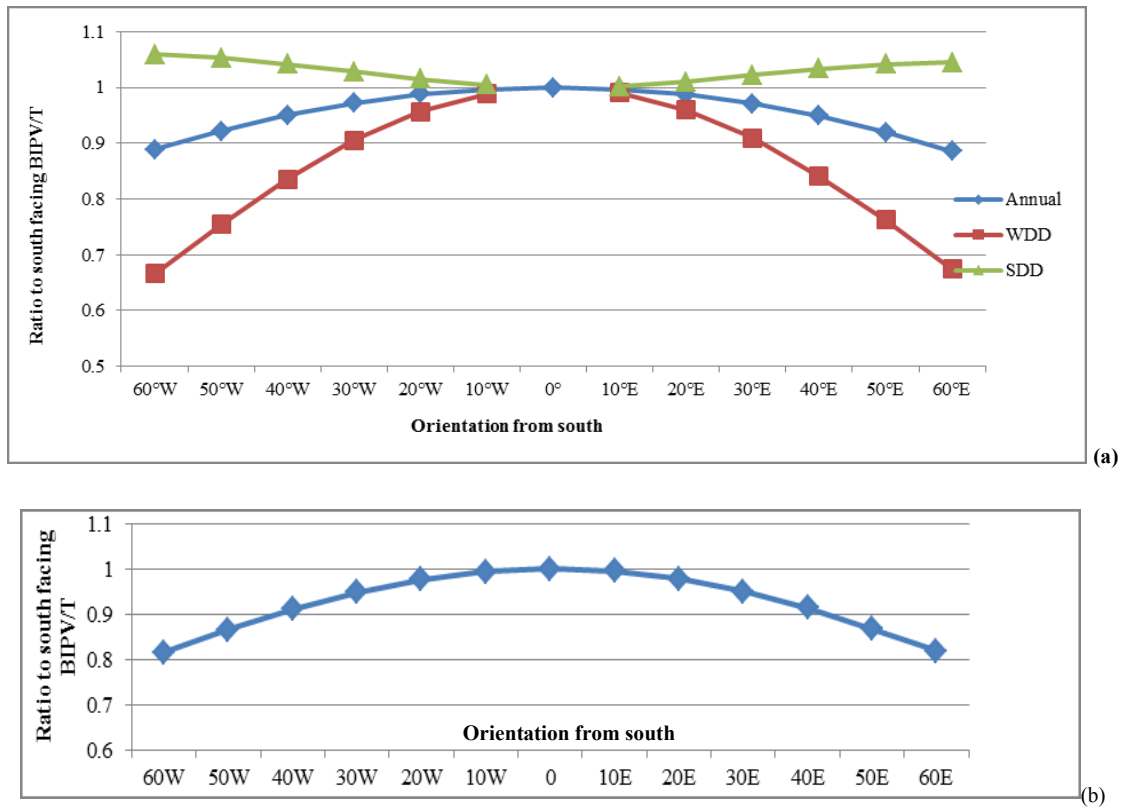


Figure 5.5, Effect of the angle of orientation on: (a) the electricity generation, (b) heat generation over the period between mid-October and mid-April.

Monthly generation indicates that in the summer months, orientation of the BIPV/T system towards west or east results in electricity generation that is close or slightly higher than south orientation. Figure 5.6 presents the effect of orientation on monthly electricity generation.

The orientation of the BIPV/T system affects not only the value of the electricity generation, but also the time of peak generation. For a south facing system, the peak generation is at solar noon. Rotation of the BIPV/T system towards the west results in shifting the peak radiation to the afternoon and vice versa for east rotation. A 30° orientation (east or west), enables a shift of peak generation time to up to 2 hours relative to solar noon. An orientation of 60°-70° enables a 3 hours shift of peak. Roofs that

combine both east and west orientations can lead to a spread of peak generation time, reaching six hours.

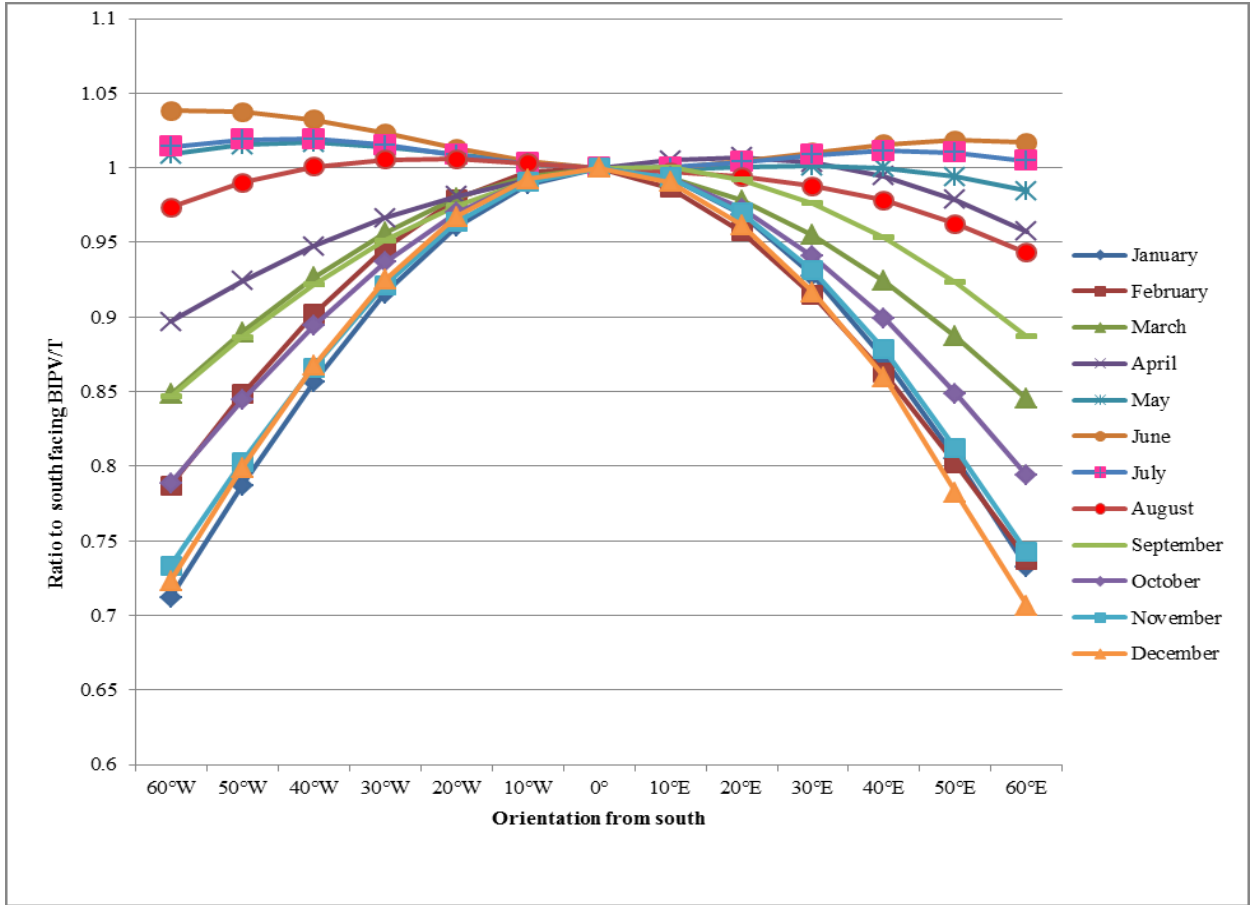


Figure 5.6, Effect of the angle of orientation on the monthly electricity generation of the BIPV/T systems.

In some cases, return on annual energy produced may be a more important object than the total energy produced, particularly in locations where prices of electricity vary with time of day. Optimizing return on electricity production involves consideration of orienting the BIPV/T systems to obtain peaks at time of high electricity demand, enabling thus larger annual income from selling the excess electricity to the grid and cost saving for consumption at high demand time.

Figure 5.7 presents electricity generation profiles for the WDD and SDD at selected orientation angles, relative to south.

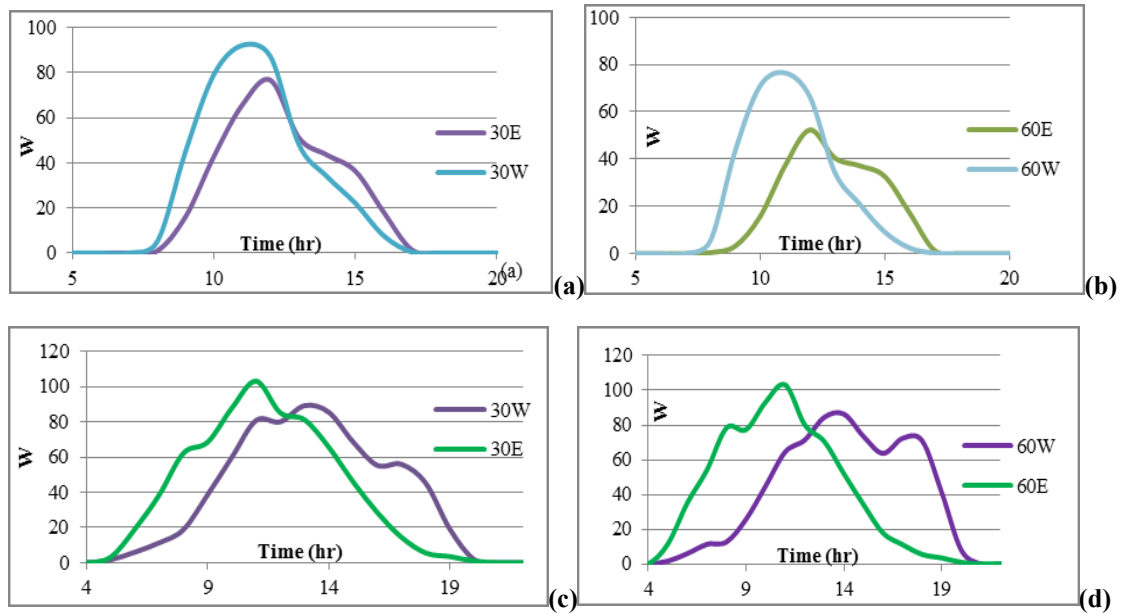


Figure 5.7, Effect of the angle of orientation on the electricity generation, (a) 30° for the WDD, (b) 60° for the WDD, (c) 30° for the SDD, (d) 60° for the SDD.

5.2.3. Combination of Tilt and Orientation Angles

The yearly study shows that for the winter months between September and March, the most effective BIPV/T systems are those that combine a tilt angle of 45° to 60° together with a south facing orientation. These configurations allow the highest yield of electricity generation as well as heating energy. In the summer months, lower tilt angles and rotation, particularly west, are advantageous.

Table 5.1 presents the annual electricity generation, the heat generation for the heating period and the combined energy generation, for different combinations of tilt and orientation angles.

Table 5.1, Electricity generation, heat generation and combined generation of various combinations

Orientation	Tilt								
	30°			45°			60°		
	Yearly electricity Generation (kWh)	Heat generation (heating Period) (kWh)	Combined generation (kWh)	Yearly electricity generation (kWh)	Heat generation (heating Period) (kWh)	Combined generation (kWh)	Yearly electricity generation (kWh)	Heat generation (heating Period) (kWh)	Combined generation (kWh)
South	197	292	490	195	303	499	176	280	456
30W	193	281	473	189	288	477	181	297	478
30E	192	281	474	189	289	478	176	279	455
60W	179	250	429	173	248	421	159	234	394
60E	178	251	430	173	248	421	159	236	395

Figure 5.8 presents the comparison of the results of all these combinations to a south facing BIPV/T system with 45° tilt angle.

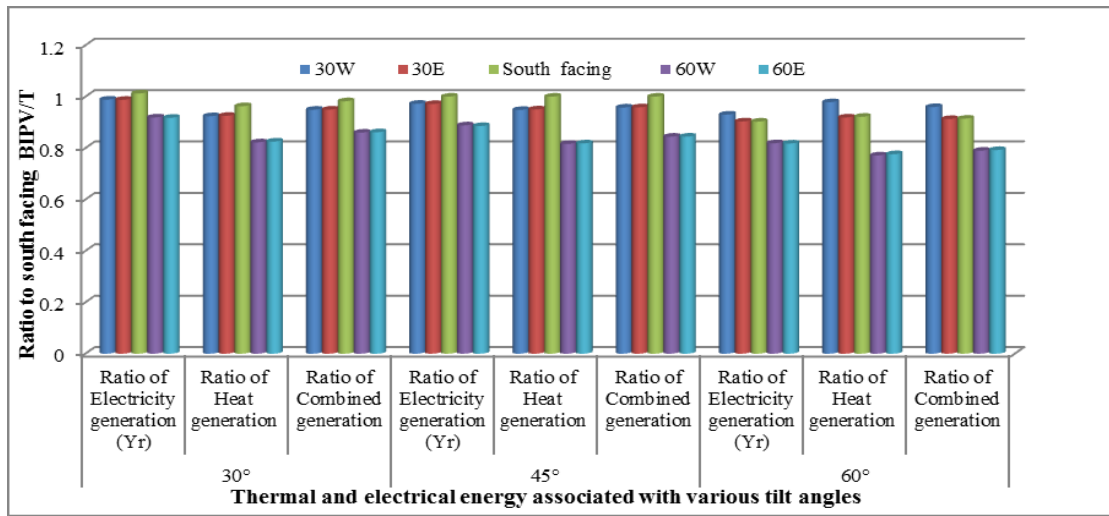


Figure 5.8, Ratio of energy generation of different configurations to south facing BIPV/T system with 45° tilt angle.

5.3. Design of Roofs

This part of the study, explores various design possibilities of roof shapes for a rectangular house, to maximize solar energy potential. The design proposed in this study is conceptual; technical considerations relating to PV technologies are not addressed. The

photovoltaic system is assumed to cover the total area of all south and near-south facing roof surfaces. In practice, a small percentage of the roof area is used for the mounting structure, for framing and for other technical considerations. It is further assumed that, given the dynamic nature of current PV technology development, any future technology will be capable of accommodating any specific requirements raised by the proposed roof designs, such as PV modules of varying shape and size as well as inverters for different BIPV/T orientations.

Three basic geometries of roofs are studied. The first geometry is a commonly applied hip roof with varying tilt and side angles (Fig. 5.9). This Basic roof is applied to all housing shapes. The second and third types of roofs are designed relatively independently of the shape of the house, employing a multi-faceted roof surface combining a range of tilt and orientation angles.

5.3.1. Hip Roofs

The basic roof design considered in Chapters III and IV is the hip roof with tilt and side angles of 45° (see Fig. 5.9). Variations of this roof type, obtained by different tilt and side angles are explored in this section for the basic shapes (Fig. 3.1) - square, rectangle (aspect ratio 1.3), trapezoid (with aspect ratio of 1.3 and $\theta=60^\circ$), L (depth ratio 1), T, U, and H shapes. The tilt/side angle combinations studied are: $45^\circ/45^\circ$; $45^\circ/60^\circ$; $30^\circ/45^\circ$ and $30^\circ/60^\circ$. L and T shapes have gable ends for the main wings (where side angle is 90°).

An additional roof, termed hereunder the *optimum roof*, is designed to serve as reference for comparative evaluation of the electricity generation potential by the BIPV/T

systems of all other roofs. The optimum roof is a gable roof with 45° tilt angle covering the rectangular shape with aspect ratio of 1.3.

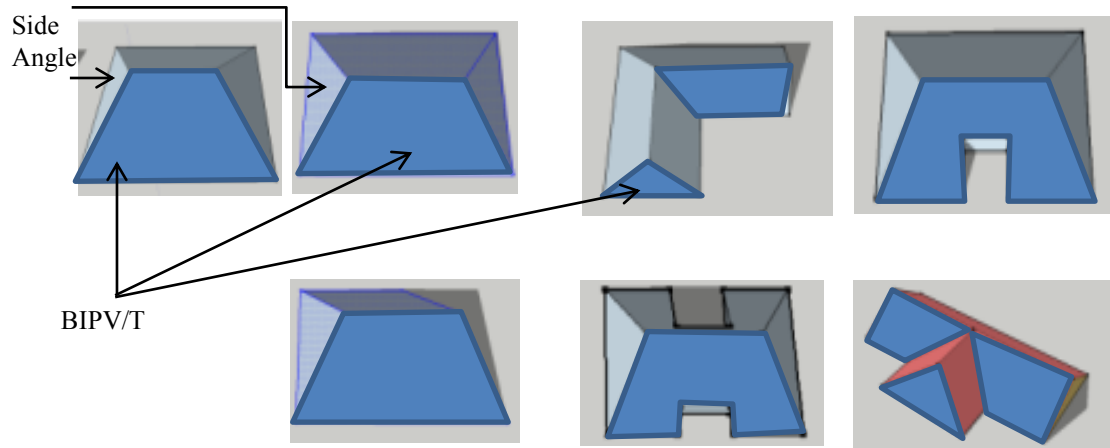


Figure 5.9, Illustration of hip roofs of basic shapes.

5.3.2. Advanced Roof Design

This section presents an advanced roof system design, which combines surfaces of various tilt and orientation angles. The main goal of these roofs is to offer design options that increase the solar potential of the BIPV/T systems. Orientation and tilt angles that are optimal for the summer and winter months are selected and combined in such roof systems. These advanced roof systems are applied to rectangular shapes. Some additional studies that apply such roof concepts to L shape and L variants are included in Appendix B. This extension of the concept, which is beyond the scope of this research, can result in a large variety of roof shapes and possibilities that can be explored in future investigation.

Split-surface Roof

The south-facing portion of the roof is divided into three plates of differing orientations and tilt angles. A BIPV/T system is assumed to cover the total area of each of these plates.

Two variants are considered, as well as some variations of these options. The mid plate is south oriented while the side plates are rotated by equal angles, the east plate towards the east and the west plate towards the west. In the first option, the orientation angle of the side plates is 15° , while in the second option this angle is 30° .

For each of the two orientations, the effect on the overall solar potential of the roof is assessed for a number of tilt angles . The two configurations of the split-surface roofs are presented in Figure 5.10 and details of the combinations are included in Table 5.2.

Although the study assumes availability of suitable technology to cover the full surface, investigation of employing PV strips of currently available systems, results in a maximum loss of 4% of the total area.

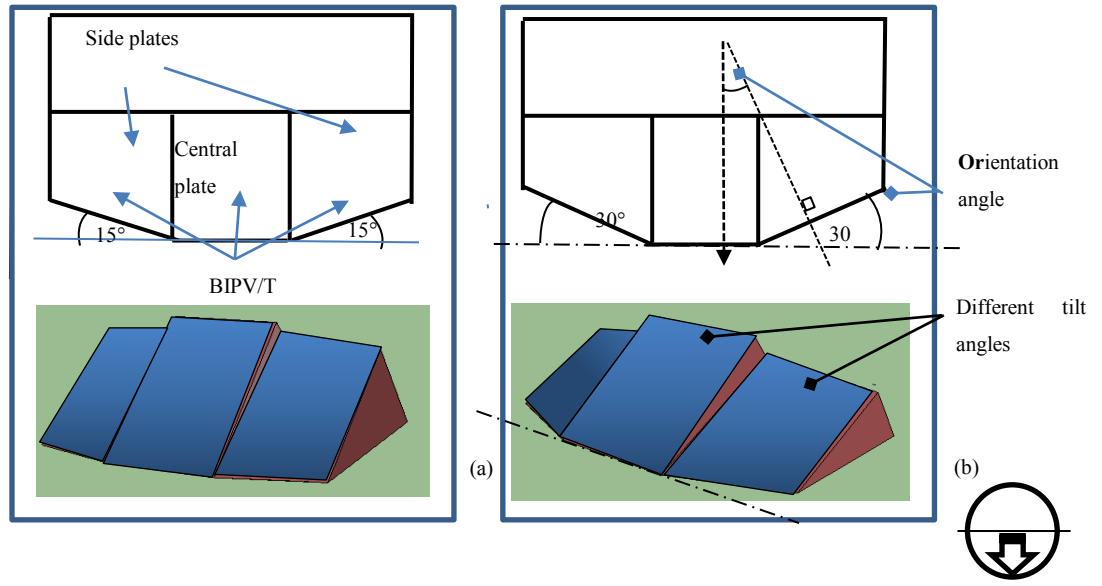


Figure 5.10, Split-surface roof designs: (a) configuration 1, side plates with 15° orientation from south; (b) configuration 2, side plates with 30° orientation from south.

Folded plate

Folded plate roof design refers in this thesis to the shape of the roof, not necessarily to the structural system. The folded plate roof geometry is composed of triangular plates with various orientations. Two basic shapes are designed. The first configuration is composed of four plates, with the two side plates facing south (Fig. 5.11a). The second basic shape consists of three plates with the central plate facing south. Figure 5.11c shows a variation of this shape composed of two basic units.

More complex designs can be derived by joining together two or more units of the basic shape. Figure 5.11 presents the three configurations analyzed in this study. The first configuration (Fig. 5.11a) is the 4-plate basic shape, with the central plates rotated 15° east and west and the side plates having 45° tilt angle. The second configuration (Fig. 5.11b) is composed of two basic 4-plate units, with central plates rotated 30° east and west. The third configuration (Fig. 5.11c) is composed of two three-plate basic shapes with side-plates rotated 30° east and west. It should be noted that the configurations of

Fig. 5.11 maintain the same geometry on the north side. In practice, there is no need to shape the roof symmetrically since it can add to the cost. Details of the folded plates' configurations are presented in Table 5.2.

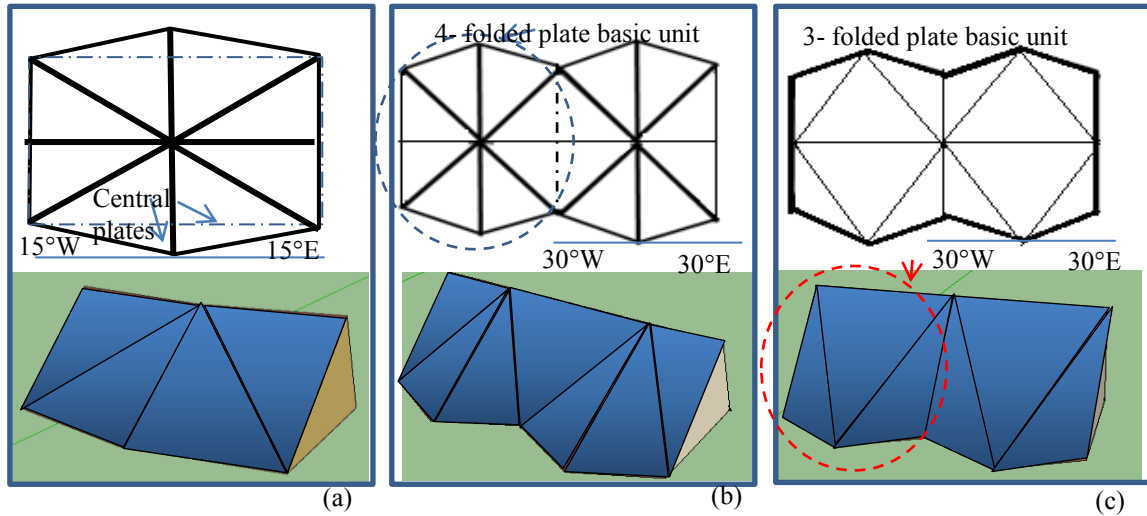


Figure 5.11, Folded plate roof designs, (a) configuration 1 – basic 4-plate with 15° orientation of the central plates; (b) Configuration 2 – two basic 4-plate units with 30° orientation, (c) Configuration 3 – two basic 3-plate roof with 30° orientation.

Table 5.2, Design Consideration Split- Roofs and Folded Plates' Roofs

Complex roof	Side angle	Number of surfaces	Combinations of orientation and tilt of the plates (The first number refers to the orientation and the second to the tilt angle)				
split-surface roofs	90°	3	Configuration 1	Center plate	0°, 45°;	0°, 50°;	0°, 45°;
				Side plates	15°(E,W), 40°	15° (E,W), 40°	15° (E,W), 30°
			Configuration 2	Center plate	0°, 45°;	0°, 50°;	0°, 45°;
				Side plates	30°(E,W), 40°	30° (E,W), 40°	30° (E,W), 30°
Folded plate	90°	4 (Basic 4-plate)	Configuration 1	Center plates	15° (E, W)		
				Side plates	0°, 45°;		
		7 (2 basic 4-plates)	Configuration 2	Center + end plates	0°, 45°;		
				Side plates	30° (E, W)		
		6 (two 3-plate basic shapes)	Configuration 2	Center plates	0°, 45°;		
				Side plates	30° (E, W)		

5. 3.3 Redesign of Units

Configurations that involve surfaces of varying orientations (such as split-surface and folded plates) may result in large overhangs. Modification of the south façade to follow the roof outline can be applied to avoid such overhangs. In this section the rectangular shape of the housing unit is re-designed to fit the outline of the multi-faceted roof. The floor area is maintained fixed. The objective of this section is to assess the effect of the design change on energy demand for heating and cooling.

In the split-surface option the south façade is split into three surfaces that are oriented according to the associated roof portions. Figure 5.12 shows the rectangular shape in its original form and the redesign associated with the split-surface option of configuration 1 (Table 5.2. Configuration 2 is similar in shape).

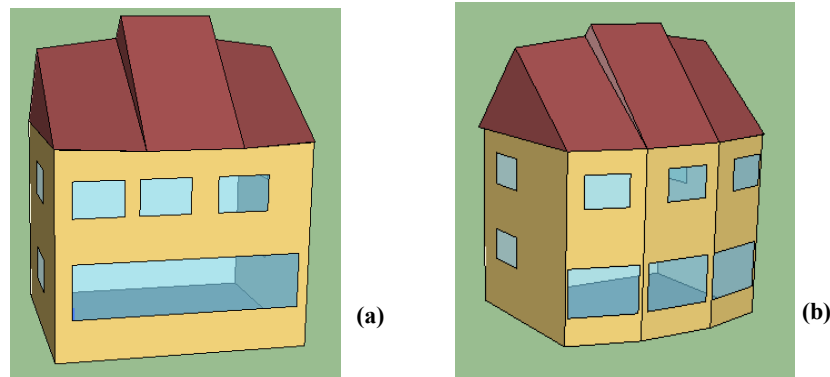


Figure 5.12, Split- roof option with: (a) rectangular shape, (b) redesigned south facing façade.

Redesign of the south façade of the folded plate roof options follows the same principle. In configuration 1 (basic 4 folded plates, Table 5.4). The result is a two-surface façade of a convex shape (Fig. 5.13a). Redesign for the second and third configurations

(Fig. 8b and c, Table 5.4) leads to a non-convex saw-tooth shape of the south façade, in order to conform to the roof outline (Fig. 5.13b).

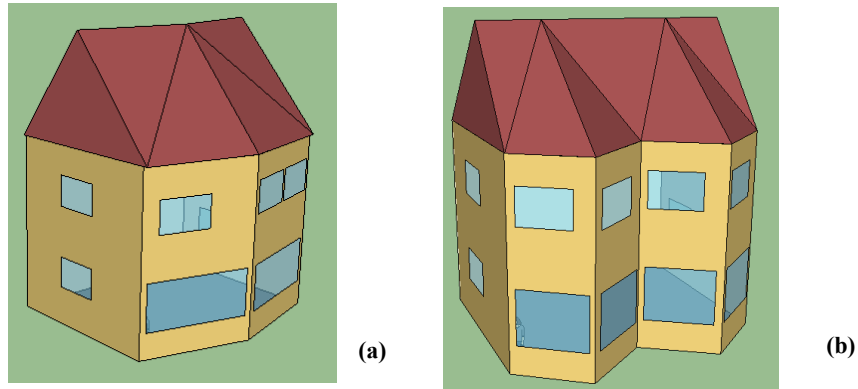


Figure 5.13, Folded plates roof option with: (a) rectangular shape, (b) redesigned south facing façade.

Complex roof surfaces with associated compatible facades such as saw-tooth may be more applicable to projects of larger size than single family housing units, such as large residential developments (for instance multiplexes) or commercial buildings, which are more conducive to increasing architectural complexity.

5.4 Presentation and Analysis of Results

5.4.1. Roof Morphology Effect

The effect of roof morphology on its thermal/electrical potential is assessed by comparing the electricity and heat generation of each roof design to those of the reference case and the optimal roof (rectangular gable roof with tilt angle of 45° , Table 5.3).

Simulations using EnergyPlus were performed to determine the energy generation potential of all roof shapes presented in section 5.3. The thermal generation of the BIPV/T system, for a constant air flow of 2m/s, is assumed to constitute 3 times the

amount of electricity generation for a given period (based on an approximate model, see section 5.1 above). Results are presented for the annual electricity generation and for the winter and summer design days. Heat generation results are over the assumed heating period (mid-October to mid-April) and for the winter design day. The combined annual electricity and winter heating energy production is also presented. The main observations drawn from the analysis of all roof designs are summarized below.

It should be noted that heat generation can be employed for water heating and for various appliances, resulting in an increase of the overall potential use of the output of the BIPV/T system year round.

Hip Roofs

Table 5.3 presents the comparison of all studied configurations to the optimum roof (rectangular layout with gable roof), expressed as the ratio of annual electricity generation of each roof to that of the optimal roof. Annual energy generation and heat generation during the heating period are presented in Table 5.4, for all hip roof options. Figures 5.14 and 5.15 illustrate the annual generation and the peak electricity generation, respectively, for the design days for all variants. The main observations are highlighted as follows.

- With a tilt angle of 30°, the peak generation on the SDD is slightly lower than on the WDD (Figure 5.15a). However, with tilt angle of 45°, the peak generation is significantly larger for a WDD (Figure 5.15b). This is mainly due to the fact that a tilt angle of 45° is more advantageous for the winter solar radiation incident angle than for the summer radiation.

- In general, electricity generation is proportional to roof surface area. Given a fixed floor area, roof surface area can be manipulated through various design strategies such as:
 - Combination of side angle and tilt angle. For instance, a rectangular layout with side angle of 45° and tilt angle of 30° possesses a larger south-facing surface area than with a tilt angle of 45°. Consequently the yearly electricity generation is larger with the 30° tilt, even though a tilt angle of 45° allows higher radiation per unit area (5.67kWh/m², as against 4.86kWh/m² for 30° tilt angle, for the WDD).
 - The largest south roof area is obtained with large side angle (60° for all shapes). The optimal roof, having a side angle of 90° corresponding to a gable roof. The electricity and heat generation of a hip roof with a 45° side angle is reduced by approximately 40% as compared to the gable roof.
 - The effect of different designs of hip roof (changing the magnitude of side angle) on the heating and cooling loads is not significant (5% or less). For instance, the heating load required for the housing unit with gable roof is approximately 5% larger than for the unit with hip roof of 45° side angle (reference case).

Table 5.3, Ratio of annual electricity generation of different variants of roofs, to the optimum roof (gable roof)

Tilt-Side angles	Ratio of annual electricity generation to gable roof for different shapes						
	Square	Rectangle	Trapezoid	L shape	U shape	H shape	T shape
1) 45-45 °	0.53	0.62	0.85	0.63	0.60	0.77	0.90
2) 45-60 °	0.75	0.81	1.10	0.58	0.76	0.97	0.86
3) 30-45 °	0.61	0.66	0.88	0.47	0.64	0.77	0.70
4) 30-60 °	0.73	0.75	0.95	0.44	0.73	0.86	0.66


Optimum roof - Gable roof		Total Area of PV covered surface (m ²)	Electricity generated per WDD (kWh)	Peak electricity generated - WDD (kW)	Electricity generated per SDD (kWh)	Peak electricity generated -SDD (kW)	Annual electricity (MWh)
		40	26.48	4.32	34.81	4.33	7.85

Table 5.4, Yearly energy and heat generation of all hip roof options

Shape	Hip roofs							
	45°-45°		45°-60°		30°-45°		30°-60°	
	Electricity generation (kWh/yr)	Heat generation (heating period) kWh/yr	Electricity generation kWh/yr	Heat generation (heating period) kWh/yr	Electricity generation (kWh/yr)	Heat generation (heating period) kWh/yr	Electricity generation (kWh/yr)	Heat generation (heating period) kWh/yr
Square	4233	5588	5671	7485	4612	6088	5520	7286
Rectangle	4867	6451	6124	8084	4990	6587	5671	7485
Trapezoid	6777	8945	8317	10979	6654	8783	7183	9481
L shape	4948	6544	4385	5789	3554	4691	3327	4391
U shape	4835	6382	5746	7585	4839	6388	5519	7286
H shape	6168	8142	7334	9681	5822	7685	6502	8583
T shape	7228	9540	6502	8583	5293	6986	4990	6587

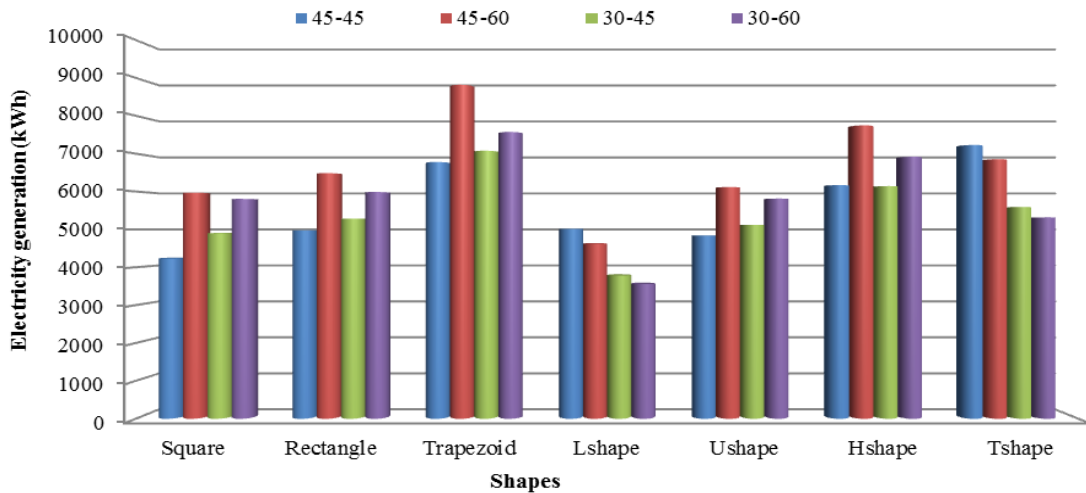
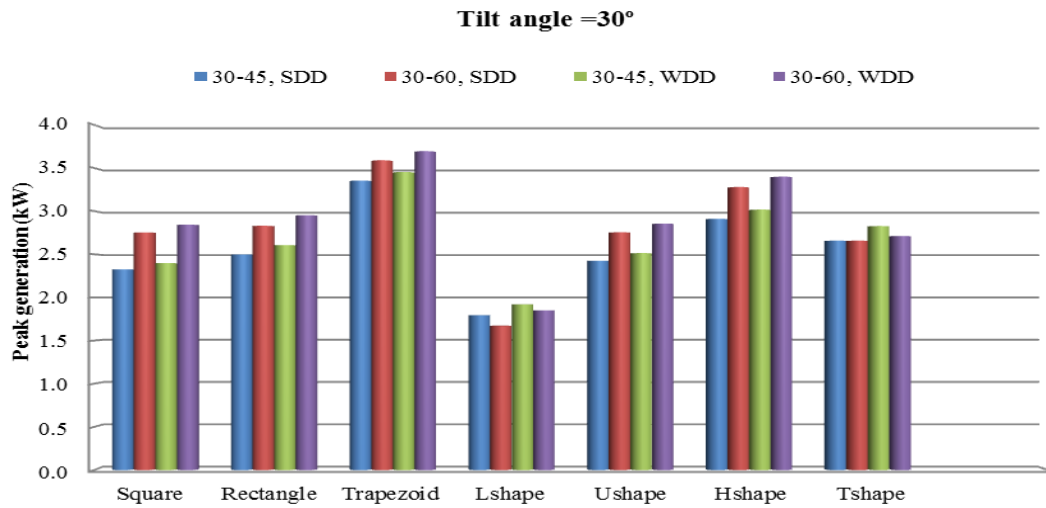


Figure 5.14, Annual electricity generation of roofs with differing tilt-side angles and shapes.



(a)

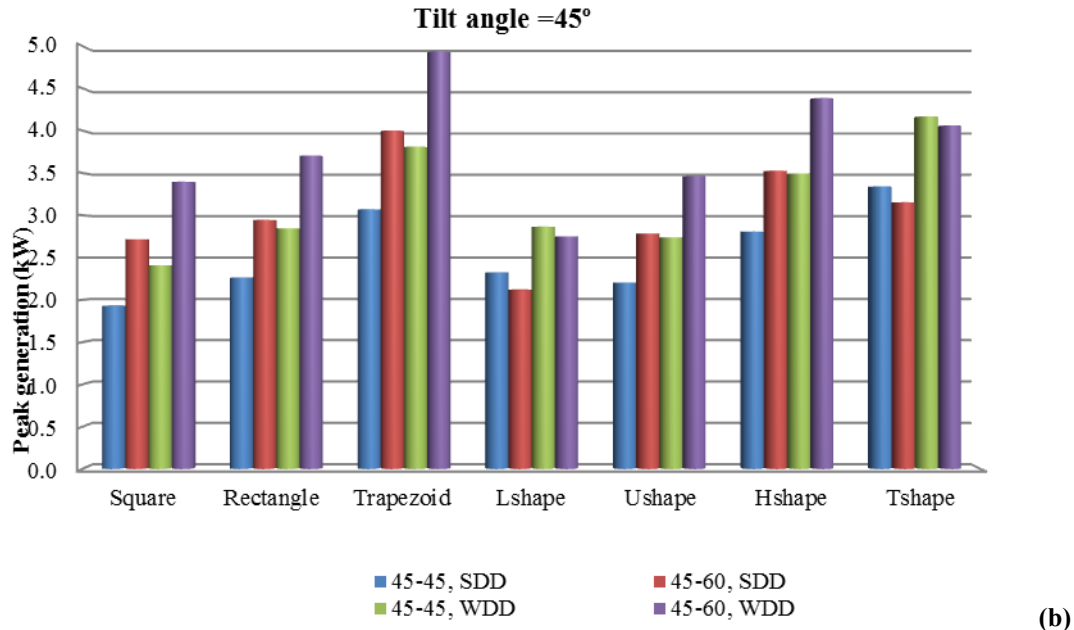


Figure 5.15, Peak electricity generations (kW): a) Tilt angle 30°; b) Tilt angle 45°.

Advanced Roof Designs

Split-surface Roofs

The split-surface roof design has two main characteristics: it enables larger south facing roof area (about 48m² as compared to 40m² for the gable roof) and it facilitates combinations of orientation and tilt angles, which allows obtaining spread of peak generation time of up to 3 hours (Fig.5.16).

The results (Table 5.6) indicate that there is no significant change of the energy potential between the different combinations, of configuration 1 and 2 (3% or less). A significant increase in the annual energy production is however obtained using this roof design, as compared to the gable roof. For instance, configuration 1 (with 15° orientation) exceeds annual electricity generation of the gable roof by 17% and heat generation for the assumed heating period by 15%. Table 5.6 presents the annual electricity generation, the heat generation for the heating period and the combined energy potential. The potential

heat generation on the WDD and the average air temperature difference (ΔT) are also presented in Table 5.6.

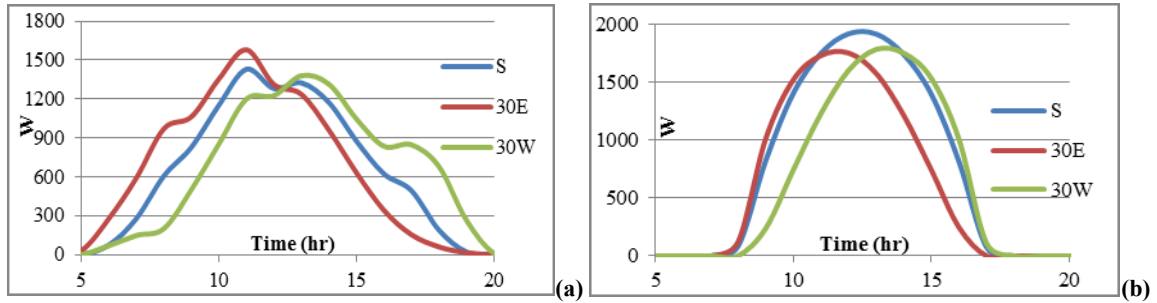


Figure 5.16, Electricity generation on design days for the plates of the 30°(E,W), 40° split-surface roof option, (a) SDD, (b) WDD.

Folded Plate Roofs

Folded plate roof design enables obtaining various orientations for the same rectangular plan roof. Furthermore, this roof shape has significantly higher south facing surface area than the gable roof (see Table 5.5). The difference in the BIPV/T potential of the different configurations analyzed is not significant (maximum difference of 4%).

The roof options with 15° orientation allows a spread of time of peak generation of approximately 2 hours while the 30° enables 3 hours difference. The electricity generation of the six-plate folded roof (Fig. 5.11c) exceeds the generation of the gable roof by approximately 30% (Table 5.6). The BIPV/T potential of these roof options are presented in Table 5.6.

Table 5.5, Comparison of Multi-Faceted Roof Design Options to the Gable Roof

	Split-surface roof (orientation, tilt of side plates)		Folded Plate roof (orientation)		
	15°(E,W),40°	30°(E,W),40°	Conf. 1 (15)	Conf. 2 (30)	Conf. 3 (30)
South facing roof area (m ²)	48	48	50	53	53
Ratio of annual electricity generation to Gable roof	1.17	1.15	1.25	1.27	1.29

Table 5.6, Energy Potential of the Multi-Faceted Roof Design Options

Roof Options		Annual Electricity generation (kWh/yr)	Heat generation (heating Period) (kWh/yr)	Combined generation (kWh/yr)	Electricity generation WDD (kWh/day)	Electricity generation SDD (kWh/day)	Heat generation (WDD) (kWh/day)	Average air change temperature ΔT (WDD)(°C)
Gable roof		7851	10068	17629	29.6	18.8	88.9	8.5
Split-surface	15°(E,W),40°	8815	11544	20358	33.6	22.3	101	9.5
	30°(E,W), 40°	8636	11169	19806	32	22.4	100	9
Folded Plates	Conf. 1 (15)	9460	12708	22168	37.6	23	113	10.2
	Conf. 2 (30)	9636	12974	22717	38	23.8	114.3	9.7
	Conf. 3 (30)	9743	12851	22486	38.2	24.3	115	9.7

Effect of Roof Design on Energy Performance of Units

The heating load of split-surface roof design is increased by 6% and 7% for configurations 1 and 2 (Fig. 5.10), respectively, relative to a hip roof with 45° side angle (reference case). The comparison to rectangular unit with a gable roof shows that the increase in heating load is not significant (2%). Cooling load is decreased by 6-7% as compared to the hip roof (45° side angle) and by approximately 10% as compared to the gable roof. Table 5.7 summarizes the results of the comparison of heating and cooling loads to rectangular units with a hip roof and with gable roof.

Heating load of rectangular units with folded plates roof is increased by 9% for configuration 1 and 10% for configurations 2 and 3 (Fig. 5.11), as compared to the rectangular unit with hip roof. Comparing these configurations to the unit with gable roof, the increase in heating load is less significant (5% and less). Results of these comparisons are presented in Table 5.7.

The increase in heating demand for rectangular housing units is correlated with the increase of the roof area. The larger the roof the higher the heating load. However, this increase in heating load is more than offset by the increased potential of such roofs, to generate both electricity and heat. The decrease in cooling load of multi-faceted roofs can be explained by the shade cast on the south façade by the overhang associated with these configurations.

5.4.2 Redesign of Units

The rectangle shape with multi-faceted roof is redesigned to conform to the perimeter of the roofs. Simulations are conducted to verify the effect of the redesigned shape on heating and cooling loads.

The results indicate that heating load for the redesigned units decreases as compared to the rectangular shapes with the same roof configurations. This decrease of heating load is not significant, however (a maximum of 5%). Comparing the redesigned units to the rectangle with gable roof shows that heating load is not significantly affected. A maximum increase of 5% is observed for the folded plate option (configurations 2 and 3 – Fig. 5.11).

The effect of redesign is to significantly increase cooling load. For instance, redesign that involves orientation of the south facing façade of 30° east and west increases cooling load by up to 45% (Table 5.7). This is due to the large window areas on the rotated facades (35% of the facade), which was originally intended for the true south facing facade (before redesigning the units). Results are presented in Table 5.7, in terms of the ratio of the heating and cooling loads of each configuration to that of the rectangular unit with 45° hip (reference) and to the unit with gable roof.

Table 5.7, Comparison of the Effect of Roof Shapes on Heating and Cooling, for the Rectangular Shape and the Redesigned Shapes

	Comparison to the 45° hip roof (reference case)				Comparison to gable roof			
	Rectangular unit		Redesigned units		Rectangular unit		Redesigned units	
	Heating	Cooling	Heating	Cooling	Heating	Cooling	Heating	Cooling
Split-surface								
Conf.1	1.06	0.94	1.06	0.97	1.02	0.89	1.01	0.92
Conf.2	1.07	0.93	1.02	1.17	1.02	0.89	0.97	1.11
Folded Plates								
Conf.1	1.09	1.01	1.04	1.03	1.04	0.96	0.99	0.98
Conf.2, 3	1.10	0.90	1.09	1.45	1.05	0.86	1.04	1.38

5.4.3 Evaluation of Energy Balance

In this section, energy consumption and generation are compared for the different roof configurations of rectangular layout.

Heat generation by air circulation is not considered in this analysis, and therefore energy generation/consumption balance is expected to be further enhanced once the heat generation for space and water heating is taken into consideration. Since the heat generation is directly proportional to electricity generation, increase of electricity generation has the twofold effect of increasing supply and reducing consumption of energy for space heating and hot water.

Figure 5.17 presents the total energy consumption alongside electricity production for rectangular shape units with different roof configurations. Energy consumption includes lighting, DHW and appliances, in addition to the computed heating and cooling energy consumptions.

The rectangle with gable roof produces some 2% more than it consumes. By comparison, electricity production of housing unit with hip roof of 45° side angle is some 35% less than consumption.

Housing units with split-surface roof options, generate as much as 17% more electricity than they consume, while the surplus of electricity generation in units with folded plate roofs reaches some 29%. Table 5.8 presents electricity production for the different roof configurations and plan layouts, including re-designed shapes. Energy balance is presented in terms of the ratio of energy production to energy consumption of the different configurations. It can be observed that the energy generation to energy consumption ratio of redesigned units is identical to that of the corresponding rectangular units. This allows the architect/engineer some flexibility of design, knowing that this energy performance is not significantly affected.

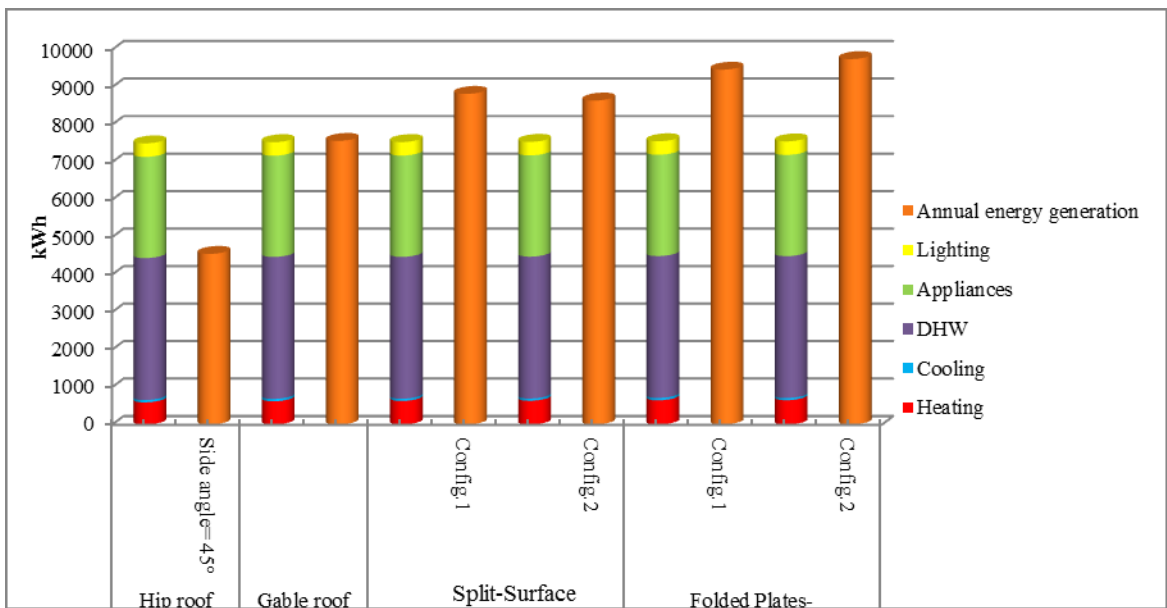


Figure 5.17, Energy consumption and production of rectangular units with different roof designs.

Table 5.8, Energy Production, Consumption and Energy Balance

		Hip roof	Gable roof	Split-surface roof		Folded Plate roof	
		Side angle= 45°		config.1	Config.2	Config.1	Config.2
Annual energy generation (kWh)		4848	7851	8814	8636	9460	9743
Rectangular shape	Annual energy consumption (kWh)	7496	7527	7530	7535	7551	7548
	Ratio of energy production to energy consumption	0.65	1.02	1.17	1.15	1.25	1.29
Redesigned units	Annual energy consumption (kWh)			7527	7517	7522	75742
	Ratio of energy production to energy consumption			1.17	1.15	1.26	1.29

CHAPTER VI: GUIDELINES FOR DESIGN OF SOLAR HOUSING UNITS AND NEIGHBORHOODS

This chapter summarizes the effects of design parameters on energy performance of housing units and neighborhoods investigated in the preceding chapters. The summary is presented as a matrix that relates design parameters to performance. A system is proposed for evaluating the performance of different designs, based on design parameters' effects and weights assigned to different performance. The evaluation system serves as a decision-aiding tool, which enables selection of design parameter values leading to optimal performance for the assumed performance criteria.

A heuristic methodology for the design of solar optimized housing units and neighborhoods is proposed, based on the systematic investigation of the key design parameters presented in previous chapters.

6.1. Summary of Design Parameters and their Effects

6.1.1. Shape Parameters

Parameters that govern convex and non-convex shapes are highlighted and their effects on energy performance are presented. These parameters are related to the configurations studied in this research (see Chapters II and III). Some of the effects can be generalized for application in the design of new building shapes.

Convex Shapes

Orientation Relative to South

Orientation of a dwelling unit relative to south affects solar radiation incident on the façades (and consequently heat gain by the windows), electrical/thermal energy generation from BIPV/T systems and energy consumption for heating and cooling. The main effects of this design parameter on the response variables are listed below.

- **Solar irradiation:** Solar irradiation incident on façades for the WDD is reduced by 20% with an orientation of 30° and by 40% with 60°, east or west of south (Chapter III). The irradiation increases significantly for SDD with an orientation of 30° and over.
- **Electricity generation:** Deviation of the orientation of the roof surface from the south by up to 45° west or east leads to an approximate reduction of 5% of the annual generation of electricity, as compared to a south facing BIPV system. A rotation of the system by 60°, west or east of south, results in a reduction of some 12% of the total annual electricity generation.
- **Energy demand:** The annual heating and cooling loads increase with increased angles of rotation. Heating load is increased by up to 30% with a rotation angle of 60° east or west from south, as compared to the south facing rectangular shape.

Aspect Ratio

Aspect ratio is another key parameter in the design of non-convex shape for increased solar potential:

- **Solar potential:** Radiation on façades, solar heat gain and BIPV electricity generation are all affected by the aspect ratio. They increase with a larger aspect ratio and vice versa. The increase in incident and transmitted radiation is proportional to the façade area and window size.
- **Energy demand:** Heating load increases sharply for an aspect ratio that is less than 1.3. For aspect ratio between 1.3 and 1.7 heating load decreases slightly (about 3%), cooling load increases by up to 14%. In heating dominated climate like in Canada, cooling is not an issue, and therefore an aspect ratio of up to 1.6-1.7 can be implemented.

Non-Convex Shapes

In the design of non-convex shapes, additional parameters influence the solar potential and the energy demand of dwellings. The major parameters are summarized below, and their effects are highlighted in Table 6.1.

Depth Ratio

- **Solar potential:** Depth ratio affects mainly solar radiation incident on façades, and transmitted by the windows of these façades. Energy generation is not significantly affected by the depth ratio because the tilt of the surface reduces shading.
- **Energy demand:** Heating and cooling load is significantly affected by depth ratio. L shape with DR of $\frac{1}{2}$ requires 9% less heating than L shape with DR of 1 (and about 7% more than the rectangle).

Number of Shading Façades

Number of shading façades affects the solar radiation on façades and on roofs, as well as heating and cooling demand, depending on the depth ratio and the angle between the wings. For 2 shading façades, such as in U shape, the reduction in radiation incident on façades is doubled, relative to L shape with a single shading façade (with the same depth ratio).

Angle Enclosed by Wings

The angle enclosed by the wings of a non-convex shape has significant effect on the solar potential and energy demand. Some of these effects are summarized below, and quantified in Table 6.1.

- **Solar irradiation:** A larger angle between the wings of L shape allows reducing the shade on the main wing (shaded façade), as well as the area of south projection of the façade, and therefore increasing transmitted radiation and windows heat gain.
- **Electricity generation:** Rotation of the wing in L variants (if the wing is south facing) allows increase of the south facing roof area, and consequently the potential to integrate a larger PV or PV/T system.
- **Shift of peak electricity:** A significant shift in the timing of peak electricity generation is obtained by the BIPV of different L variants units, due to variation in orientation of different roof surfaces. A maximum shift of 3 hours is obtained by the BIPV system of L variants with 60°-70° wing rotation, with respect to the solar noon.

- **Energy demand:** Heating load is not significantly affected by wing rotation. L shape with depth ratio of $\frac{1}{2}$ requires about 7% more heating than the rectangular shape. The increase of heating load for L variants over the rectangular shape (reference case) can reach 6%.

6.1.2. Neighborhood Parameters

Planar Obstruction Angle (POA) and Distance between Units

A major effect on solar potential of neighborhoods is the mutual shading by adjacent units. Two parameters define the relative position of the shaded and shading units: the angle of obstruction and the distance between the units.

These two parameters are defined by means of the line connecting the center of the south façade of the shaded unit and the closest corner of the shading unit. Planar Obstruction Angle (POA) is the angle between this line and the south, while the distance (d) is the length of the defining line. The effects of combinations of POA and distance (d) are presented in Table 6.2.

Site Layout

Site Layout can influence the shape of the units and the way they are positioned around the road. In curved road layouts the housing units are oriented along the curve. A number of scenarios are studied in this research. The study shows that when the position and design of the buildings respect the principles of passive design and the POA concepts (stated above), the site layout has no significant effect on energy performance.

Density

Two density effects are studied: spacing between units and row configurations.

Spacing – Attached Units

- **Solar potential:** Attaching the units (on the west-east axis) does not affect the electricity generation of convex shapes. The effect on convex shape is found only in curved layouts where shapes are changed to fit the layout of the streets (change of rectangle to trapezoid). For non-convex shapes, the density effect depends on the number of shading surfaces and their depth ratio as well as on the angle between them and the shaded surfaces.
- **Energy demand:** Heating and cooling load of attached units is lower than for the corresponding detached configurations. Doubling the space between detached units does not affect significantly the heating demand; however the cooling load increases with larger spacing between units.

Row Configurations

- **Solar irradiation:** Row configurations refer to scenarios where the south facing façades of a row of units are obstructed by another row. Distance between rows is of significant importance. It affects solar radiation incident/transmitted by the windows of the south façades.
- **Energy demand:** Heating load is affected significantly by the distance between the rows. The load of detached rectangular units of the obstructed row can increase by 50% as compared to the unobstructed row, for a distance of 5m. This effect is stronger for attached than for detached units (the increase in heating load can reach 70%).

6.1.3. Roof Parameters

Tilt Angle

The annual electricity generation of the BIPV/T system is not significantly affected by a tilt angle that ranges between 30° and 50°. In general, high slope roofs (>40°) are favored in climates such as those in most of Canada due to snow accumulation. Snow effect is not considered directly in this study.

Orientation Angle

Orientation of the roof surface affects the solar potential in two ways: the amount of generation and the time of peak generation.

- **Electricity generation and shift of peak generation:** Deviation of the orientation of the system from the south by up to 40° west or east leads to an approximate reduction of up to 5% of the annual electricity generation. A significant time shift of peak electricity generation can be obtained by orienting the BIPV/T system east or west of south (this is discussed above, section 6.1.1).
- **Useful heat generation:** The heat generation for the assumed heating period is reduced by up to 9%, for an orientation angle of 40° west or east. A rotation of the system by 60°, west or east of south, results in a reduction of some 12% of the total annual electricity generation and of 20% of the heat generation during the heating period.

Surface Area

The south facing roof surface area, for a given floor area is strongly dependent on the shape of a building. It is beneficial in some cases to manipulate the shape of the roof to maximize the south or near south facing roof area.

6.1.4. Tables of Performance

Tables of performance of housing units and neighborhoods are presented in this section, in terms of the range of values of design parameters and the maximum effects of these parameters.

Color shade concentration (tone) is employed in the tables to indicate the significance of effects. Yellowish colors indicate that there is no significant effect; shades of red represent undesirable effect, while a green tone indicates a positive effect. Figure 6.1 presents the key for shades associated with performance criteria of solar potential and of heating and cooling energy consumptions. The effects, expressed in percentage, are compared to the reference case. The reference cases are rectangular shape for shape effects, and rectangular detached units in site I for neighborhoods. It should be noted that for the evaluation of heating and cooling consumptions, a decrease of the value as compared to the reference case, expressed with negative sign (-), is a desirable effect and is represented by green colors in the Tables (Fig.6.1b).

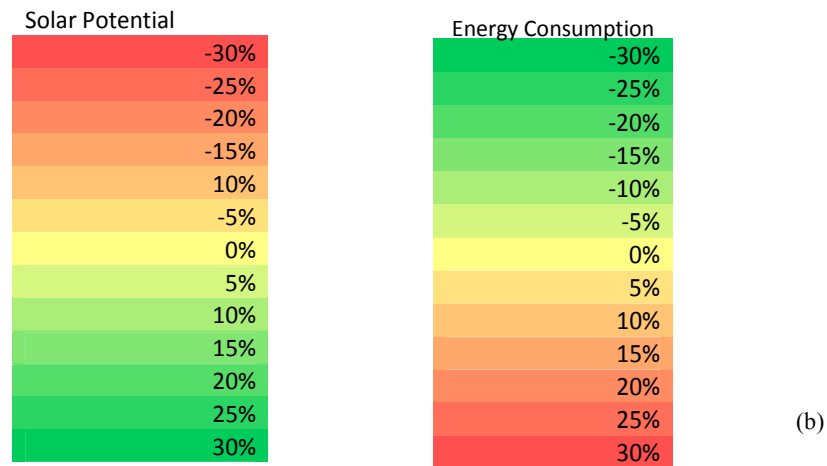
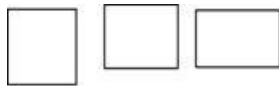

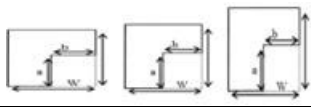
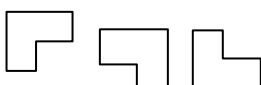
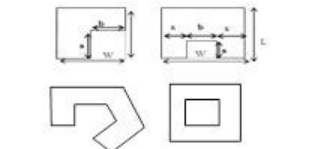



Figure 6.1, Keys for color shades expressing the performance of design parameters; (a) Solar potential, (b) Energy consumption.

Shape Effects

Table 6.1 shows the main effects associated with each of the design parameters on five performance criteria. The performance criteria are: heating energy consumption, cooling energy consumption, solar radiation incident on south and near south façades (and transmitted by their windows), solar energy generation by the BIPV system and shift of peak generation. Passive heat gain, represented by solar radiation incident on south façades and transmitted by south facing windows, is not accounted separately in the evaluation presented below (6.1.5), since this factor affects directly energy consumption for heating and cooling.

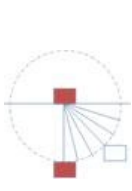
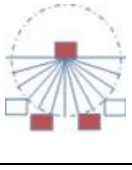
Table 6.1, Shape Parameters and their Effects

SHAPES		Energy consumption		Solar Potential							
		Heating	Cooling	Radiation on South Façades	South facing roof Electricity generation		Shift of Peak(hr)				
Values	Per m ²				per total area	AM	PM				
Convex Shapes	Aspect Ratio (AR)	2	-6%	38%	54%	0%	30%				
		1.6	-3%	14%	23%	0%	18%				
		1.3	0%	0%	0%	0%	0%				
		1	5%	-20%	-27%	0%	-13%				
		0.6	16%	-38%	-54%	0%	-38%				
		Orientation from south (O)	60 (E,W)	30%	65%	-8%	-12%	-12%	-2.5	2.5	
		45 (E,W)	19%	37%	-4%	-5%	-5%	-2	2		
		30(E,W)	7%	18%	-1%	-3%	-3%	-1.5	1.5		
		0	0%	0%	0%	0%	0%	0	0		
		Depth ratio (DR=a/b)	DR=1/2	7%	4%	-12%	-3%	21%			
Non-Convex shapes		DR=1	20%	3%	-20%	-6%	1%				
		DR=3/2	25%	3%	-25%	-6%	-16%				
		Wing Direction	DR=1/2	L-SW	7%	4%	-12%	-3%	21%		
		L-SE	7%	4%	-12%	-3%	20%				
		L-N	-3%	-3%	0%	0%	32%				
		Number of shading façades	South Direction; DR=1/2	n=1	7%	4%	-12%	-3%	21%		
		n=2	18%	1%	-24%	-6%	24%				
		Angle between the wing	DR=1/2;	β=0	7%	4%	-12%	-3%	21%	0	0
			β=30	7%	19%	-3%	-1%	26%	-1.5	1.5	
			β=45	6%	25%	-1%	0%	30%	-2	2	
β=60			6%	30%	0%	0%	35%	-2.5	2.5		
β=70			2%	36%	0%	0%	10%	-3	3		
South and near south facing windows : 35% of the corresponding façades All values are compared to the reference case (rectangular shape, south facing, AR=1.3, hip roof (45° side and tilt angles))											

Neighborhood Effects

Table 6.2 presents the effect of position of shaded and shading units with respect to each other. Effect of POA and of distance between units is shown. The effect is given for a single shading unit and for two shading units.

Table 6.2, POA and Distance




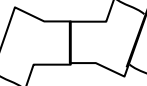

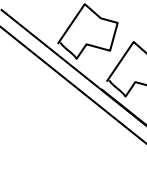
POA and distance associated with one and two shading units			Values d= POA= =	Energy consumption						Solar potential					
				Heating			Cooling			Radiation on south façades			Electricity generation		
				5m	10m	15 ⁺ m	5m	10m	15 ⁺ m	5m	10m	15 ⁺ m	5m	10m	15 ⁺ m
Obstruction angle	Obstruction by single unit		0-15	35%	17%	3%	-35%	-15%	-2%	-20%	-10%	-5%	-3%	0%	0%
		15-60	30%	15%	6%	-30%	-8%	3%	-20%	-8%	-5%	-3%	0%	0%	
		60+	20%	8%	1%	-25%	0%	5%	-17%	-7%	-2%	-3%	0%	0%	
	(POA) Obstruction by two units		15-30	70%	37%	20%	-55%	-25%	-25%	-45%	-20%	-12%	-3%	0%	0%
		30-60	60%	35%	20%	-60%	-35%	-40%	-40%	-20%	-20%	-3%	0%	0%	
		60+	50%	25%	15%	-60%	-30%	-25%	-35%	-15%	-8%	-3%	0%	0%	

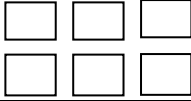
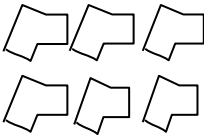
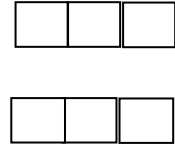
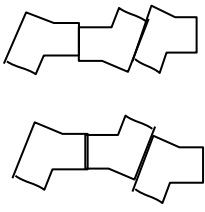
Various designs of neighborhoods are presented in Tables 6.3. The tables are divided according to different site layouts (straight road or curved road). The performance of layouts, associated with different densities and building shapes, is presented in terms of heating and cooling consumptions and electricity generation, as well as the approximate maximum shift of peak of electricity generation. The performance of each configuration is compared to that of a reference case. The reference configuration consists of detached rectangular units in a layout with straight road

(running East-West). The reference configuration itself is compared to the isolated rectangular unit in order to assess the effect of density on this configuration.

Tables 6.3, Neighborhood Patterns


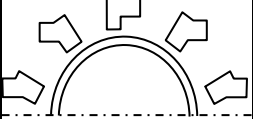
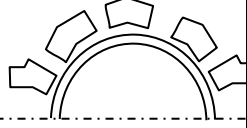
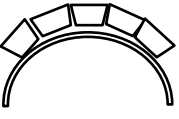

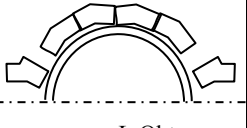
6.3 a- Straight Layout

				Energy consumption		Solar potential				
Site	Shape	Density	Examples of Neighborhood Configurations	Heating	Cooling	Electricity generation	Shift of Peak (hr)			
							AM	PM		
Straight road	E-W	Detached*		S1=4m	12%	-40%	0%			
				S2=2S1	6%	-3%	0%			
		Convex			-25%	-6%	0%			
				LN shape (R=1/2)	-12%	-17%	15%			
		Non-Convex	Attached		V-W30; (DR=1/2)	-13%	40%	22%	-1.5	1.5
	Inclined (SE-NW or SW-NE)	Convex	Detached		30°	13%	16%	-3%	-1.5	1.5
					45°	26%	36%	-5%	-2	2
					60°	35%	60%	-12%	-2.5	2.5
		Non Convex	Detached		V-WS30; (DR=1/2)	15%	-4%	26%	-1.5	1.5
					V-WS45; (DR=1/2)	16%	26%	30%	-2	2
			V-WS60; (DR=1/2)	26%	52%	35%	-2.5	2.5		
<p>*All values are compared to detached rectangle configuration in site I, for instance a configuration that has 15% heating demand (in green colored box) implies that the heat load of this configuration decreases by 15% as compared to the reference case. Detached rectangular configuration is compared to isolated rectangle</p>										

Site	Shape	Density	Examples of Neighborhood Configurations	Energy consumption		Solar potential					
				Heating	Cooling	Electricity generation	Shift of Peak (hr)				
							AM	PM			
Rows Straight/ E-W	Convex			r=5m	55%	-75%	-3%				
				r=10m	24%	-50%	0%				
				r=15m-20m	8%	-30%	0%				
			Non Convex	Detached		r=5m	32%	-14%	26%	-1.5	1.5
						r=10m	15%	4%	26%	-1.5	1.5
						r=15m-20m	3%	15%	26%	-1.5	1.5
	Convex			r=5m	26%	-80%	-3%				
				r=10m	-3%	-55%	0%				
				r=15m-20m	-20%	-40%	0%				
			Non Convex	Attached		r=5m	19%	-23%	26%	-1.5	1.5
						r=10m	1%	-6%	26%	-1.5	1.5
						r=15m-20m	-12%	2%	26%	-1.5	1.5

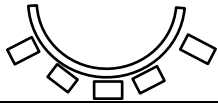
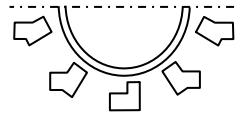

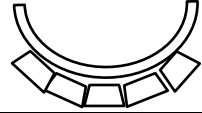
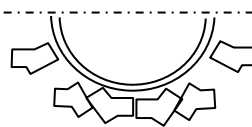
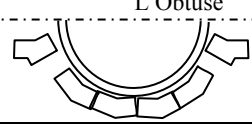
All values are compared to detached rectangle configuration in site I

6.3b- Layout with south facing curved road

	Shapes	Density	Examples of Neighborhood Configurations	Energy consumption		Solar potential			
				Heating	Cooling	Electricity generation	Shift of Peak(hr)		
							AM	PM	
Curved Road	South Facing	Convex	 Rectangles	2%	70%	-4%	-2	2	
			 L Variants	8%	100%	29%	-3	3	
		Non Convex	Detached	 L Obtuse	4%	100%	17%	-3	3
				 L Variants	-30%	-28%	-12%	-2	2
	Non Convex	Attached	 L Variants	5%	30%	29%	-3	3	
			 L Obtuse	-17%	-5%	15%	-3	3	

All values are compared to detached rectangle configuration in site I

6.3c- Layout with north facing curved road

	Shapes	Density	Examples of Neighborhood Configurations	Energy demand		Solar Potential		
				Heating	Heating	Electricity generation	Shift of Peak(hr)	
							AM	PM
Curved Road North Facing	Convex		Rectangles 	5%	73%	-3%	-2	2
			L Variants 	11%	60%	42%	-3	3
			L Obtuse 	7%	40%	30%	-3	3
	Non Convex		Trapezoids 	-3%	54%	7%	-2	2
			L Variants 	36%	52%	46%	-3	3
			L Obtuse 	7%	140%	31%	-3	3

All values are compared to detached rectangle configuration in site I

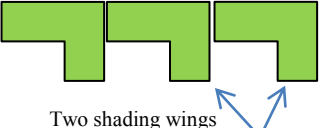
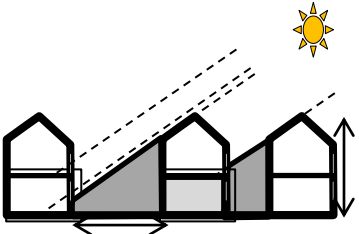
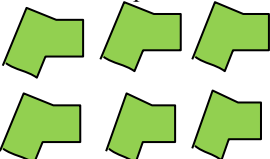
6.1.5 Design Considerations and Evaluation of Energy

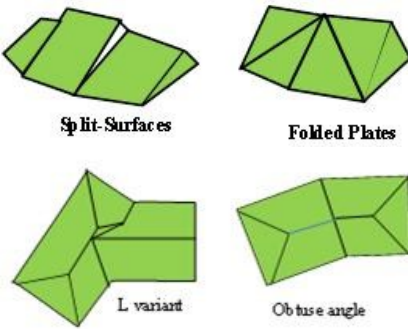
Performance

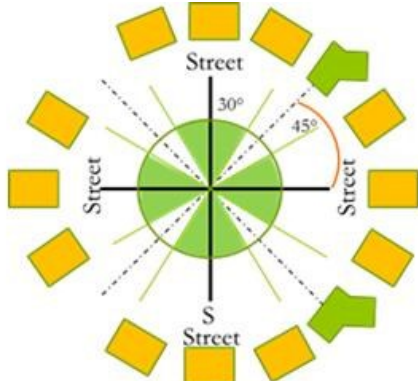
Design Considerations

Table 6.4 summarizes the main design considerations for solar optimized dwellings and neighborhoods. These design considerations are suggested based on various objectives, for instance minimizing heating and cooling consumptions, maximizing energy generation and enabling shift of peak energy generation.

Table 6.4, Considerations for solar neighborhood design

Site	Objective	Density		
		Low	Medium/High	Row Configuration
Straight E-W road	Minimize heating and cooling energy consumption	<p>Convex shape</p> <p>Aspect ratio, should be (1.3 to 1.6)</p> <ul style="list-style-type: none"> • South facing window: 35% is a good compromise to reduce heating load while not significantly increasing cooling load. • Orientation up to 30°, otherwise L variant should be used. <p>Non-convex shapes:</p> <ul style="list-style-type: none"> • $DR \leq 1/2$ • Wing oriented north more advantageous. <p>Use of L variants with:</p> <ul style="list-style-type: none"> • Rotation of the wings $\geq 30^\circ$ from south. • Windows on the rotated façade should be readjusted (from 35%) to reduce cooling load. 	<p>Attached units</p> <ul style="list-style-type: none"> • Rectangular shapes are optimal, for reduction of heating and cooling load/consumption; energy generation is enhanced when continuous roof surface is applied (gable roofs – see tables 5.3, 5.8 Chapter V). • Attached L variants (see recommended design of L variants) are good alternatives, enabling larger roof area, for increased potential electricity/heat generation. • Attached L shapes are advantageous when a small depth ratio is used. Otherwise, L shape with south branch should be avoided, to eliminate shading on south facade from the wings of the adjacent units. 	<p>Detached units:</p> <ul style="list-style-type: none"> • Distance between rows should be at least twice the height of the shading house, to avoid significant increase of heating load.  <ul style="list-style-type: none"> • L variants can be more beneficial especially when the land available is small. Due to the fact that the façades are not coplanar, a smaller distance between the rows is required.  <p>Attached units:</p> <p>Design recommendations for attached units should be followed, in addition to respecting the distance between rows.</p>

Site	Objective	Density		
		Low	Medium/High	Row Configuration
Straight E-W road	Maximize electricity generation	<p>Designing large south roof areas for the integration of PV systems, with appropriate tilt angle (which depends on the geographical location of the building) :</p> <ul style="list-style-type: none"> • Hip roofs: large side angle, or/and large aspect ratio should be used. Gable roofs (with side angle of 90°) can be recommended as simple solution to maximize the surface area. • In case of limited roof area (associated with a small floor plan) split-surface roofs that join different tilt, with different orientation may be considered. These can increase significantly the total roof area, in addition to optimize the tilt angle for summer and winter solar radiation. • L shape and L variants: Design the shapes to reduce shade on south roof (as detailed above).  <p>The diagrams show four types of roof configurations: 'Split-Surfaces' (a roof with two different tilt angles), 'Folded Plates' (a roof with multiple flat sections at different angles), 'L variant' (an L-shaped roof structure), and 'Obuse angle' (a roof with a non-right angle joint).</p>	<ul style="list-style-type: none"> • For rectangular shapes, it is recommended to use more advanced roof design for increased productions (as shown in Chapter V). • Gable roofs should be used instead of hip roofs, to increase roof area. • For L and L variants, recommendations for detached units apply to attached units. Careful design of the number of shading façades and the DR is suggested (see above). 	<ul style="list-style-type: none"> • For buildings with the same height, distance between rows does not affect electricity generation. • For attached units, careful design of the number of shading façades and the DR (same as for attached units).
	Peak shift	<ul style="list-style-type: none"> • For rectangular units, split-surface or folded plates are recommended to realize shift of peak. • L variants with various angle of orientation are recommended to obtain various peaks. • If the cooling load is large, orientation as much as 45°-60° west can be recommended, to produce energy at the time when the cooling load is large (i.e. in the afternoon hours). • Multiple orientations of the BIPV systems is advised especially in a neighborhood, since this enables counterbalance between winter and summer production, and shift of peak. 	Same as for detached.	Same as for detached.
Inclined road	Design recommendations for layout with E-W road can be applied to layouts with inclined roads, however a tradeoff should be made between the total orientation of rectangular units (if they are oriented to face the road) and partly oriented units (such as L variants). For instance, it is recommended to use L variants with $\beta \geq 45^\circ$ to replace a rectangular unit of orientation $\geq 45^\circ$. The POA and distances between units should be also taken into consideration.			

Site	Objective	The same design recommendations apply for sites with curved road facing south or north, however some configurations are more advantageous in one or the other site, as shown in the Tables of evaluation (Tables 6.6 and 6.7)	
	Density		
	Low	High	
Curved south and north	Minimize heating and cooling energy consumption	<ul style="list-style-type: none"> • In the case of convex shapes or non-convex shapes with orthogonal wings, the whole unit can be oriented along the curve provided that the orientation from south is still within the optimal range. • Beyond certain angle of orientation (30°), it is recommended to design partly oriented units, such as L variant (where only one wing is oriented toward the curve, while the main wing is south facing). For instance a rectangular shape with 45° orientation requires up to 20% more heating energy than an L variant where only the wing is oriented at 45°. 	<ul style="list-style-type: none"> • Rectangular shapes are modified to fit the curve into trapezoid. In south facing curve the trapezoid has the smallest faced south facing and therefore it is not an optimal design. Vice versa for north facing curve. • L variants configuration are optimal for minimizing heating load in south facing curve. • Obtuse angle configuration is optimal for minimizing heat load in north facing curve.
	Maximize electricity generation	<ul style="list-style-type: none"> • Avoid rectangular shape with high angle of orientation (e.g. $>45^\circ$). • Recommendations for straight road layout are valid. 	<ul style="list-style-type: none"> • Avoid trapezoid in south facing curve (see above). • Recommendations for attached units in straight road layout applies to curved layouts.
	Peak shift	<ul style="list-style-type: none"> • Recommendations for straight road layout are valid. • Combinations of orientation of the units and of the roofs, enables large shift of peak generation. 	<ul style="list-style-type: none"> • Recommendations for attached units in straight road layout applies to curved layouts.

Evaluation of Dwellings and Neighborhoods

The design process generally involves selection among design alternatives. A systematic selection procedure can be a useful tool in optimising the process. The evaluation system proposed in this section is based on assigning weights to energy performance criteria and numerical values (grades) to the response variables that represent the effects of design parameters. The procedure is illustrated in the examples of evaluation presented below.

Assignment of Weights

The assignment of weights should be based on a cost-benefit analysis, which depends on multiple considerations (context of designs, geographic location, cost of PV and HVAC systems vs. value and timing of generated electricity, as well as less quantifiable considerations such as flexibility of design and space utilization, etc.).

At the early design stages it is suggested to try several weight systems in order to assess the influence of the selection on the resulting design. Based on comparison of results between the weight systems a refinement can be made for the final selection.

The evaluation examples proposed hereunder relates only to energy considerations. It does not take into account other social, architectural (functional, daylight, etc.) and urban planning considerations. In a comprehensive design the evaluation methodology could be extended to include such additional objectives. For instance building integrated PV can serve as a high quality building envelope layer increasing thus value of a building (like high quality fenestration, granite kitchen counter

top etc). In addition, cost/benefit analysis should include issues such as initial cost, net revenue and interaction with a smart grid.

Evaluation Example

The criteria of performance employed in the example are consumption, energy generation and shift of peak generation timing.

Energy Consumption, Electricity Generation and Shift of Peak

The two criteria of electricity generation and shift of peak are related through the associated financial returns. The ultimate objective is to maximize the joint return rather than the individual values of these parameters. However, the financial returns associated with these two criteria are strongly dependent on time and location, as explained in what follows. The shift of peak as performance criteria is relevant when a variable pricing for electricity as a function of time is employed. Such a scheme imposes higher prices for a kilowatt-hour (kWh) of electricity at peak demand times and lower prices at off-peak times, as compared to flat-rate tariff (Borenstein, 2007).

The advantage of shift of peak is associated with the concept of time of use (TOU) tariffs. The value of electricity and heat produced by the PV/T system is increased in two ways if peak production can match peak demand. On the one hand the value of the electricity fed to the grid can be increased by up to 20% (Borenstein, 2005, 2008). On the other hand, the amount of electricity consumed at the high tariff rate is reduced (for space or/and water heating, etc.). Shift of time of peak generation should be however coupled with reducing the consumption at high rate timing. A BIPV/T system combined with heat pump for water heating and/or space heating can offer significant reduction in energy

consumption for heating and cooling , and economic benefits with short payback periods (4 - 7 years) (Kalogirou, 2004).

On the level of neighborhood, shifting peak generation toward peak demand and reducing energy consumption may be a step in achieving zero peak energy communities where the total energy needs for vehicles, thermal, and electrical energy within the community, is met by renewable energy (Carlisle, et al 2009).

Assignment of Weights and Grades

In view of the strong dependence on time and location of the financial value of electricity production and shift of peak generation, these two performance criteria should be considered separately and different weights assigned to them based on an expectation of the respective returns. It should be borne in mind that this assessment of returns should be for the whole lifetime of the structure. It is therefore recommended to perform separate evaluations based on different assignment of weights for these two criteria that reflect different expectations. In case the resulting performances differ widely, some compromise selection should be adopted. This approach is illustrated in the examples that follow.

Tables 6.5 a and b present two sets of weights of performance criteria and grading scales for the effects (response) of design criteria.

The grades, ranging from 0 to 10, are assigned according to the magnitude of the effect (as compared to the reference – Tables 6.1-6.3). For solar electricity generation potential as well as for shift of peak electricity generation higher grades are associated

with positive effects (increase). For energy use higher grades are associated with negative effects (decrease).

In the weighting schemes presented in Tables 6.5 heating consumption has a large weight relative to cooling consumption, since the design is for cold climate location. The two schemes differ in the weight assigned to the shift of peak performance criterion. Scenario 1 (Table 6.5a) represents a case where no TOU tariffs are applied and therefore shift of peak has no financial return, with a corresponding weight of zero. Scenario 2 (Table 6.5b) represents a case with high variability in TOU tariff, with a correspondingly high weight.

Table 6.5a, Scenario #1, Weights and grades of design objectives

Performance criteria weights		Ranges and grades of parameters' effects								
Criterion	Weight	Parameter	Ranges and grades of effects							
Heating consumption	2	Heating/cooling	Range (+ / -)	0-5%	5-10%	10-15%	15-25%	25-30%	30+	
Cooling consumption	1		Grade	(+)	5	4	3	2	1	0
				(-)	5	6	7	8	9	10
Electricity generation	3	Electricity generation	Range (+ or -)	0-5%	5-10%	10-15%	15-25%	25-30%	30+	
			Grade	(+)	5	6	7	8	9	10
				(-)	5	4	3	2	1	0
Shift of peak	0	Shift of peak	Range	0h	1h	1.5h	2h	2.5h	3h	
			Grade	0	1	1.5	2	2.5	3	

Table 6.5b, Scenario #2, Weights and grades of design objectives (including shift of peak timing generation as a performance criterion)

Performance criteria weights		Ranges and grades of parameters' effects								
Criterion	Weight	Parameter	Ranges and grades of effects							
Heating consumption	2	Heating/cooling	Range (+ / -)	0-5%	5-10%	10-15%	15-25%	25-30%	30+	
Cooling consumption	1		Grade	(+)	5	4	3	2	1	0
				(-)	5	6	7	8	9	10
Electricity generation	3	Electricity generation	Range (+ or -)	0-5%	5-10%	10-15%	15-25%	25-30%	30+	
			Grade	(+)	5	6	7	8	9	10
				(-)	5	4	3	2	1	0
Shift of peak	3	Shift of peak	Range	0h	1h	1.5h	2h	2.5h	3h	
			Grade	0	1	1.5	2	2.5	3	

Evaluation examples

Tables 6.6-6.7 present samples of evaluation of design alternatives of housing unit shapes and neighborhoods for the two scenarios presented above. The evaluation of design alternatives is based on the sum of products of performance criteria weights and the corresponding effect grades.

A value of the total points of within a margin of 25% less than the reference case is considered as acceptable (marked “!” in Tables 6.6 and 6.7), total points that are equal or above to the points gathered by the reference case are considered as good (marked “√”). Alternatives summing up to under 25% less than the reference case are rejected (marked “X”).

Tables 6.6a and 6.6b present examples of evaluation of dwelling shapes associated with scenarios 1 and 2. It can be noted that the total points gathered by the shapes do not change for the two scenarios. Shapes like L variants, which allow a shift of peak electricity generation timing, do not significantly increase heating energy consumption, while they enable a significant increase in electricity generation. These shapes therefore indicate a good energy performance, with or without potential benefits of shift of peak generation time as criteria of performance.

Table 6.6a, Evaluation of housing units' shapes- scenario 1

Shapes	Parameters	Values	Consumption		Electricity Generation	Total points		Ratio to reference case
			Heating	Cooling				
Convex Shapes	Aspect Ratio (AR)	2	12	0	30	✓	42	1.40
		1.6	10	3	24	✓	37	1.23
	Reference case	1.3	10	5	15	✓	30	1.00
		1	12	8	9	✓	29	0.97
		0.6	4	10	0	✗	14	0.47
	Orientation (O)	60° (E,W)	0	0	9	✗	9	0.30
		45° (E,W)	4	0	18	✗	22	0.73
		30° (E,W)	8	2	15	!	25	0.83
		0°	10	5	15	✓	30	1.00
	Non Convex Shapes	Depth Ratio	DR=1/2	8	5	24	✓	37
DR=1			4	5	15	!	24	0.80
DR=3/2			2	5	6	✗	13	0.43
Wing Direction		L-SW	8	5	24	✓	37	1.23
		L-SE	8	5	24	✓	37	1.23
		L-N	10	5	30	✓	45	1.50
Number of shading Facades		n=1	8	5	24	✓	37	1.23
		n=2	4	5	24	✓	33	1.10
Angle between the Wings		β=0°	8	5	24	✓	37	1.23
		β=30°	8	2	27	✓	37	1.23
		β=45°	8	1	30	✓	39	1.30
		β=60°	8	0	30	✓	38	1.27
		β=70°	10	0	21	✓	31	1.03

Table 6.6b, Evaluation of housing units' shapes- scenario 2

Shapes	Parameters	Values	Consumption		Electricity Generation	Shift of Peak	Total points	Ratio to reference case	
			Heating	Cooling					
Convex Shapes	Aspect Ratio (AR)	2	12	0	30	0	✓	42	1.40
		1.6	10	3	24	0	✓	37	1.23
	Reference case	1.3	10	5	15	0	✓	30	1.00
		1	12	8	9	0	✓	29	0.97
		0.6	4	10	0	0	✗	14	0.47
	Orientation (O)	60° (E,W)	0	0	9	9	✗	18	0.60
		45° (E,W)	4	0	18	6	!	28	0.93
		30° (E,W)	8	2	15	4.5	✓	29.5	0.98
		0°	10	5	15	0	✓	30	1.00
	Non Convex Shapes	Depth Ratio	DR=1/2	8	5	24	0	✓	37
DR=1			4	5	15	0	!	24	0.80
DR=3/2			2	5	6	0	✗	13	0.43
Wing Direction		L-SW	8	5	24	0	✓	37	1.23
		L-SE	8	5	24	0	✓	37	1.23
		L-N	10	5	30	0	✓	45	1.50
Number of shading Facades		n=1	8	5	24	0	✓	37	1.23
		n=2	4	5	24	0	✓	33	1.10
Angle between the Wings		β=0°	8	5	24	0	✓	37	1.23
		β=30°	8	2	27	4.5	✓	41.5	1.38
		β=45°	8	1	30	6	✓	45	1.50
		β=60°	8	0	30	9	✓	47	1.57
		β=70°	10	0	21	9	✓	40	1.33

Tables 6.7a and 6.7b present examples of evaluation of neighborhood designs associated with scenario 1 and 2 respectively. The results indicate that under scenario 2 – taking advantage of shift of peak generation (when available) offers significant improvement in energy performance of the majority of configurations. Some alternatives particularly rectangular shape configurations along inclined or curved roads are underperforming. This indicates that a tradeoff of building shape design should be performed, when the site is characterized by a curved road or an inclined road (with respect to east west direction).

Table 6.7a, Sample evaluation of neighborhood design- scenario 1

Site		Density	Shape	Consumption		Electricity Generation	Total Points		Ratio Reference Case	to
				Heating	Cooling					
Straight	E-W	Detached	Rectangles	15	5	15	✓	35	1.00	
		Attached	Rectangles	18	6	15	✓	39	1.11	
			L shape (R=1/2)	14	8	24	✓	46	1.31	
			V 30W; (DR=1/2)	14	0	24	✓	38	1.09	
Inclined Road	SE-NW or SW-NE	Detached	Rectangles (30°)	6	2	15	✗	23	0.66	
			Rectangles (45°)	2	1	12	✗	15	0.43	
			Rectangles (60°)	0	0	9	✗	9	0.26	
			V-30W; (DR=1/2)	4	5	27	✓	36	1.03	
			V-45W; (DR=1/2)	4	1	30	✓	35	1.00	
			V-60W; (DR=1/2)	2	0	30	✓	32	0.91	
Rows	E-W	Detached	Rectangles (5m)	0	10	15	✗	25	0.71	
			Rectangles (10m)	4	10	15	!	29	0.83	
			Rectangles (15-20m)	8	10	15	!	33	0.94	
			V-30W (5m)	0	3	27	!	30	0.86	
			V-30W (10m)	4	5	27	✓	36	1.03	
			V-30W (15-10m)	10	2	27	✓	39	1.11	
		Attached	Rectangles (5m)	2	10	15	!	27	0.77	
			Rectangles (10m)	20	10	15	✓	45	1.29	
			Rectangles (15-20m)	16	10	15	✓	41	1.17	
			V-30W (5m)	4	8	27	✓	39	1.11	
			V-30W (10m)	10	6	27	✓	43	1.23	
			V-30W (15-10m)	14	5	27	✓	46	1.31	
Curved Road	South Facing	Detached	Rectangle	10	0	15	✗	25	0.71	
			L Variants	8	0	27	✓	35	1.00	
			L Obtuse	10	0	24	!	34	0.97	
		Attached	Rectangle	20	9	9	✓	38	1.09	
			L Variants	10	1	27	✓	38	1.09	
			L Obtuse	16	5	24	✓	45	1.29	
	North Facing	Detached	Rectangle	10	0	15	✗	25	0.71	
			L Variants	6	0	30	✓	36	1.03	
			L Obtuse	8	0	30	✓	38	1.09	
		Attached	Rectangle	10	0	18	!	28	0.80	
			L Variants	0	0	30	!	30	0.86	
			L Obtuse	8	0	30	✓	38	1.09	

All Configurations are compared to detached rectangular shapes of the site with south facing straight road

Table 6.7b, Sample evaluation of neighborhood design- scenario 2

Site		Density	Shape	Consumption		Electricity Generation	Shift of Peak	Total Points		Ratio to Reference Case			
				Heating	Cooling								
Straight	E-W	Detached	Rectangles	15	5	15	0	✓	35	1.00			
		Attached	Rectangles	18	6	15	0	✓	39	1.11			
			L shape (R=1/2)	14	8	24	0	✓	46	1.31			
			V 30W; (DR=1/2)	14	0	24	4.5	✓	42.5	1.21			
Inclined Road	SE-NW or SW-NE	Detached	Rectangles (30°)	6	2	15	4.5	!	27.5	0.79			
			Rectangles (45°)	2	1	12	6	✗	21	0.60			
			Rectangles (60°)	0	0	9	9	✗	18	0.51			
			V-30W; (DR=1/2)	4	5	27	4.5	✓	40.5	1.16			
			V-45W; (DR=1/2)	4	1	30	6	✓	41	1.17			
			V-60W; (DR=1/2)	2	0	30	9	✓	41	1.17			
			E-W	E-W	Detached	Rectangles (5m)	0	10	15	0	✗	25	0.71
Rectangles (10m)	4	10				15	0	!	29	0.83			
Rectangles (15-20m)	8	10				15	0	!	33	0.94			
V-30W (5m)	0	3				27	4.5	!	34.5	0.99			
V-30W (10m)	4	5				27	4.5	✓	40.5	1.16			
V-30W (15-10m)	10	2			27	4.5	✓	43.5	1.24				
Attached	Rectangles (5m)	2			10	15	0	!	27	0.77			
	Rectangles (10m)	20			10	15	0	✓	45	1.29			
	Rectangles (15-20m)	16			10	15	0	✓	41	1.17			
	V-30W (5m)	4			8	27	4.5	✓	43.5	1.24			
	V-30W (10m)	10			6	27	4.5	✓	47.5	1.36			
	V-30W (15-10m)	14			5	27	4.5	✓	50.5	1.44			
	Curved Road	South Facing			Detached	Rectangle	10	0	15	6	!	31	0.89
						L Variants	8	0	27	9	✓	44	1.26
			L Obtuse	10		0	24	0	!	34	0.97		
Attached			Rectangle	20	9	9	6	✓	44	1.26			
			L Variants	10	1	27	9	✓	47	1.34			
			L Obtuse	16	5	24	9	✓	54	1.54			
North Facing		Detached	Rectangle	10	0	15	6	!	31	0.89			
			L Variants	6	0	30	9	✓	45	1.29			
			L Obtuse	8	0	30	9	✓	47	1.34			
		Attached	Rectangle	10	0	18	6	!	34	0.97			
L Variants	0	0	30	9	✓	39	1.11						
L Obtuse	8	0	30	9	✓	47	1.34						

All Configurations are compared to detached rectangular shapes of the site with south facing straight road

Sensitivity Analysis of the Weights

The above example illustrates the effect of varying the weight of a single performance criterion on energy performance. In a more general approach, a sensitivity

analysis was performed on the effect of weight assignment, in which the weights of all performance criteria are changed arbitrarily. Some of the alternatives studied are presented in Appendix C, as applied to housing units shape design. For instance, the heating consumption weight was decreased incrementally, while cooling consumption weight was increased. Weights of energy generation and shift of peak were also changed.

The sensitivity analysis indicates that the evaluation of shape alternatives is not highly sensitive to weight assignment. The results change significantly only when the weight for cooling energy consumption is much larger than that of the heating energy consumption (e.g. double the value), while the weight for energy generation is simultaneously reduced by about 20% (and over).

6.2. Solar Neighborhood Design Methodology

A heuristic methodology is presented to assist the design of near optimal solar neighborhoods, whereby initial designs are evaluated for energy performance (energy consumption versus generation) and selected designs are progressively modified for improved performance. The methodology outlines each step of the design process, highlighting alternatives that may offer good solar potential and presenting systematic methods for comparison and evaluation of these alternatives based on predetermined selection criteria. The design procedure allows for various site layouts and density levels. Stages of the design procedure are detailed below and illustrated in a flowchart in Figure 6.2. While the design stages are generally applicable, the details of implementation are related to the climatic conditions at the basis of this research – mid-latitude northern location.

1. Input

Input to the design process includes:

- Site layout (curve, straight, rows), density.
- Houses characteristics: passive solar/energy efficient houses, units' functional area, number of floors, total height, rooms, etc.
- Climatic data and location.
- Topographic data.

2. Design Alternatives

In a large community or neighborhood design, there may be several site layouts.

Following are guidelines for selecting initial design alternatives for each of the site layouts.

2.1 Low density – Detached units

2.1.1 Unit Design

For given units data (floors, area...) **Design** a number of housing shapes based on:

General Units and Site Considerations:

- Accessibility, functional convenience, shape of the site, its dimensions, layout of road.
- Minimizing total area for given functional area (minimizing passages and distributors in the interior space, minimizing wasted spaces etc.).

Energy Considerations:

Shape of dwelling units are suggested based on the study of shape analysis (chapter III) and summarized in Table 6.1. This study encompasses all basic shapes and their variants. Several other shapes can be obtained by the combination of these basic shapes. The main design guidelines for these shapes are detailed in the Table of design considerations (Table 6.4), and summarized below. For cases where the designer wishes to design different shapes not encompassed in this research, general guidelines principles of solar design, presented below, can be applied to any shape.

General

- Orientation: orientation of units should be within the optimal range (equatorial facing to 30° east or west). Otherwise, trade-offs in shape design should be made (see curved road, below).
- South facing window area: a 35% of the façade represents a good window size option that enables to reduce significantly heating load without a significant increase of cooling load.

Convex shapes

- Aspect ratio: ratio of south façade to lateral façade should be within the range of 1.3- 1.6 (for compromise between heating /cooling loads).
- Roof area: follow 2.4.

Non-convex shapes

- Depth ratio – the ratio of shading to shaded façade lengths: Ratio of ½ (or less) is suggested in cold climate design to reduce the effect of shade on heat gain by the

window. Larger ratios can be implemented in shapes with increased angle enclosed by the wings.

- Number of shading façades: It is suggested to reduce the number of shading façades. A larger number can be used when the angle between the wings is larger than 120°. Depth ratio is particularly critical with a larger number of shading façades (see Tables 6.1 and 6.5).
- Increase of the angle between shading and shaded façades: By increasing the angle enclosed between shading and shaded façades ($\geq 120^\circ$), self-shading can be controlled (See Tables 6.1 and 6.5).
- It is advisable to design options of L variants with the wing oriented toward south-east and south-west to facilitate spread of peak energy generation (if it is desirable), and to increase exploitable roof area. Some site layouts (such as cul-de-sac road scenario) require the implementation of L variant with south-west and south-east wings.

2.1.2. Placement and Orientation of Units in a Site

a) Housing units should first be placed with respect to roads, and in agreement with the bylaws and regulations of the specific location. Some regulations prefer that the principal façade would be parallel to the road.

b) Distances between units, distance from road and minimum length of backyards should be determined based on regulations of the specific location.

c) For improved energy performance, suggestions are presented in the following:

- The placement of units with respect to each other should take into consideration planar obstruction angle and distance between units. This is particularly relevant to sites with inclined straight roads (deviating from E-W direction), and in sites with curved road (especially tight curve such as in cul-de-sac).
 - POA (the angle between the normal to the south façade of the shaded unit and the closest corner of the shading unit) should be $\geq 60^\circ$.
 - The distance between the center of the south façade of shaded unit and the closest corner of the shading unit depends mainly on the height of the shading units. This distance can be determined based on the minimum distance between two aligned units (both south facing) to avoid shading (see row, 2.3). For two story units this distance should, ideally, be ≥ 15 m. This distance can be less for a single story house and larger for a higher building.
- Orientation: The dwelling unit can be wholly oriented toward the road, or it can be designed to have only a part (the entrance for instance) facing the road, such as in L variants. Trade-offs can be made between options (see Tables 6.1, 6.5, 6.6 and 6.7). For instance, in layouts that require a degree of orientation $\geq 45^\circ$, it is suggested to use L variant shapes.
- In cases where shift of peak of electricity generation is desirable, use of L variants with south-east and south-west facing wings, and/or units rotated east and west, to enable spread of electricity generation over the neighborhood.

2.2 High Density- Attached Units

2.2.1. Design of Units

Procedures of design of detached units applied in 2.1.1 should be followed in this section. Modify units as needed to enable the assemblage, for instance:

- Using L variants and their mirror images (see Table 6.3) and combinations of L variants with south and north facing wings to enable effective assemblage;
- Modify shapes, if required, around curved road (for instance rectangular shape to trapezoid along -Table 6.3).

2.2.2. Placement and Attachment of Units

- Distance from roads, backyards and orientation- trade-offs similar to 2.1.1.
- Reduce non -convex configuration effects:
 - Shading to shaded façade ratios (this applies also to whole units, in the case where units are staggered).
 - Number of shading façades (U shape effect for instance).

2.3 Row configurations

2.3.1 Detached units

- Follow design procedure as in 2.1.
- Distance between rows should be determined as function of the height of the shading units, where possible (≥ 2 times the height of shading units, or more precisely, based on the shadow length – for the 21st of December in the northern hemisphere).

2.3.2. Attached Units

- Follow procedure- concerning the design and attachment of the units- as in 2.2.
- Distance between rows should be determined as function of the height of the shading units.

2.4 Roof design

2.4.1 Detached Units

a) Default hip roof: For convex shapes a gable option can be the default, for non-convex, such as L and V a combination of hip and gable that maximizes effective roof area for PV or PV/T integration. A tilt angle that approximates the latitude of the location can be employed as default.

b) Define solar technologies characteristics: PV systems efficiency, thermal collectors, combined PV/T, preliminary area of integration of PV or PV/T.

c) To modify roof area and spread of peak electricity generation (in stage 4): consider multi-surface roof designs that join various tilt and orientation angles, such as split-surface and folded plate (presented in Chapter V).

2.4.2 Attached Units

Similar procedure as in 2.4.1 should be applied in this section.

- Roofs of attached units can be designed as continuous surfaces (e.g. continuous surface over hip roofs, in rectangular configurations). This enables the enlargement of roof area that can be employed for the integration of PV or PV/T systems.

3. Evaluation

3.1 Data generation for Simulation Software

- Run appropriate software for generating geometric data for whole building simulation program (for instance EnergyPlus) from given coordinates of housing units – e.g. Autocad or Google Sketchup or purpose developed tool.
- Provide data for whole building simulation software including weather data, building materials, glazing properties, HVAC, control systems, etc., as required by the relevant software.

3.2 Run Simulations

- Simulations should be performed at relatively small time step (≤ 1 hr).
- Raw data obtained from simulations (for instance hourly data in excel sheets, from EnergyPlus) should be processed to provide significant design related information. The processing can be automated. Relevant design data includes:
 - Computation of relevant information such as: total annual (and design days) heating and cooling loads;
 - Solar radiation on south facing and near south facing façades, heat gain from windows and thermal heat and electricity generation from BIPV/T systems (including peak generation time).

4. Selection

- Comparison of annual and design days results of the various design alternatives.
- Apply a selection procedure (e.g. weighted design procedure (section 6.1.5, and Table 6.4) for evaluation of design alternatives and selection.

- Pick best few alternatives, modify as seems suitable:
 - Shading/shaded façades in assemblages and in units;
 - Roof areas- roof designs (see roof design , 3.4.1 –b);
 - PV or PV/T efficiency, in stage 2.4.1. Efficiency of BIPV and BIPV/T is also related to the cost of PV. Higher efficiency implies a higher cost. This has to be taken into account in the decision analysis.
 - Orientations or partial orientations.
- Go back to step 3.2. – Simulation, and repeat selection process.
- If final selection go to step 5.

5. Output

Preparation of final documents (final plans and specifications for construction).

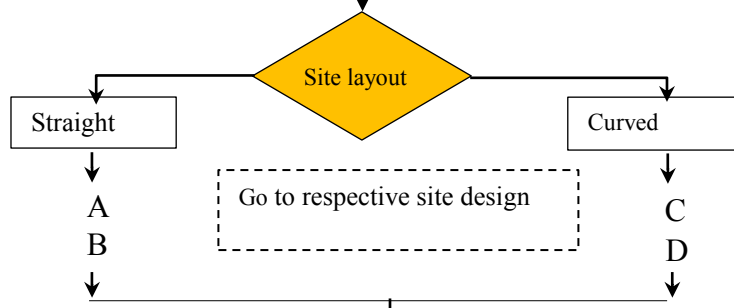
Final documents are supported by supplementary documents providing information of energy performance of individual units and neighborhoods, such as:

- Energy use for heating and cooling.
- Heat gain from windows of individual units.
- Potential of electricity and thermal generation by the BIPV or BIPV/T systems (in individual units and in neighbourhoods).
- Shift of peak / time of peak at various days of the year- Design Days.

Input (brief)



Initial design alternatives



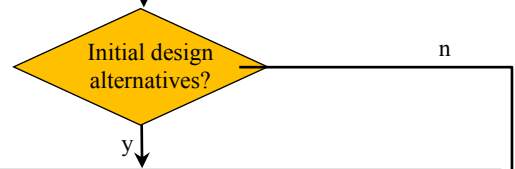
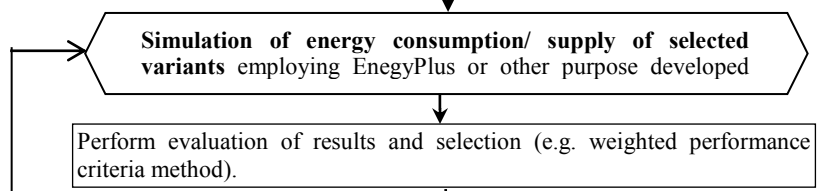
Roof

Default: Hip/gable roof and solar collectors' area

Generate geometric data for the design alternatives, based on drawings (coordinates, window locations and size, etc.). Provide data required for energy simulation software (e.g. weather data, auxiliary programs).

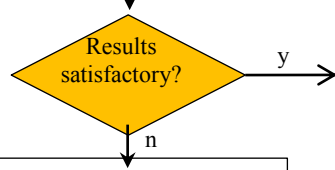
Develop an evaluation system (e.g. Assign weights to performance criteria - heating and cooling energy consumption, energy generation, time of peak electricity generation; and grades to values of design parameter effects).

Energy analysis and evaluation



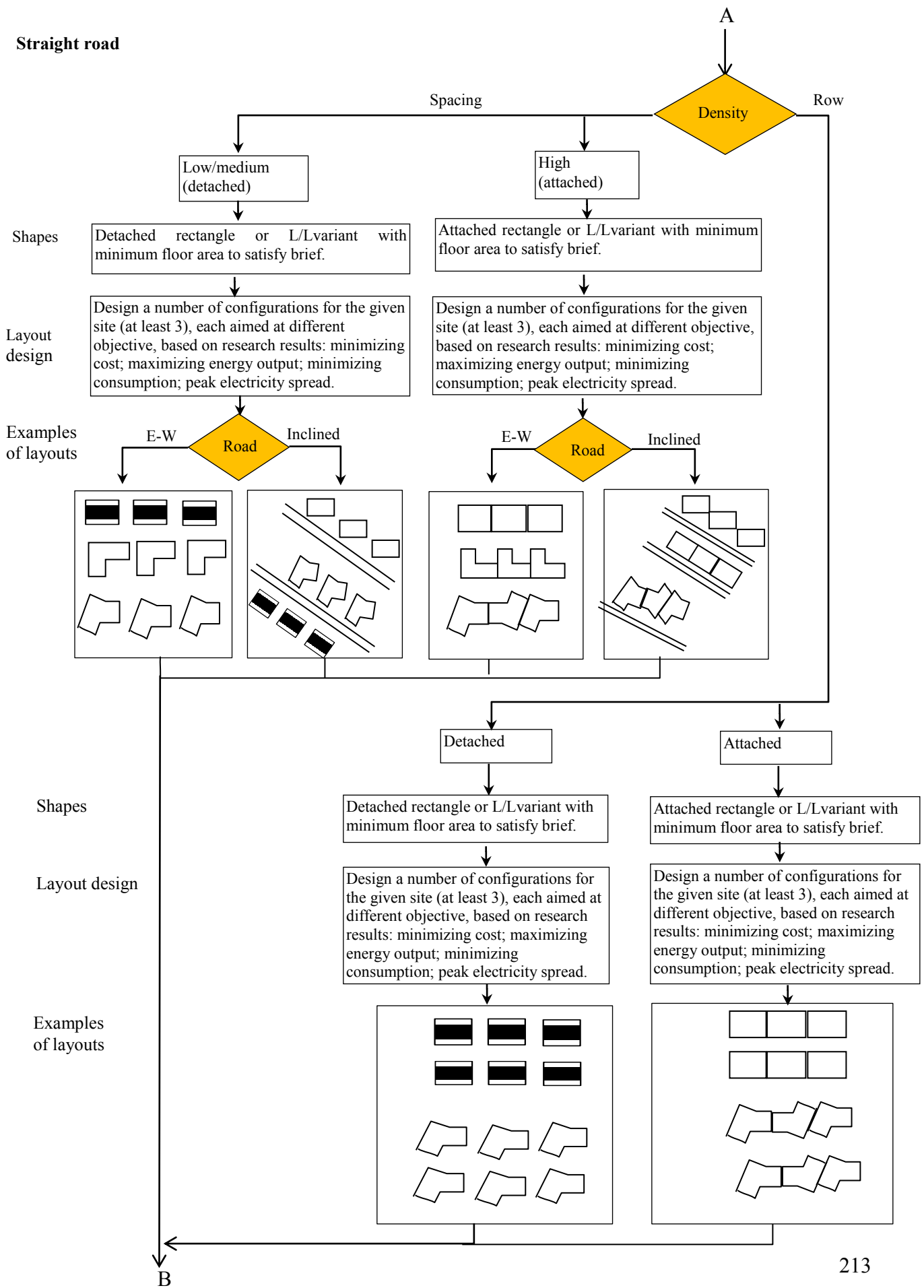
Modify best performing configurations to improve energy balance: multifaceted roofs (particularly on rect/trap. shapes), shapes variations for improved insolation, shapes orientation, tradeoff between shapes in some configurations.

Redesign of selected configurations



Output results (Final documents, energy analysis files, etc.)

Modify best performing configurations to improve energy balance (roof design, orientations...)



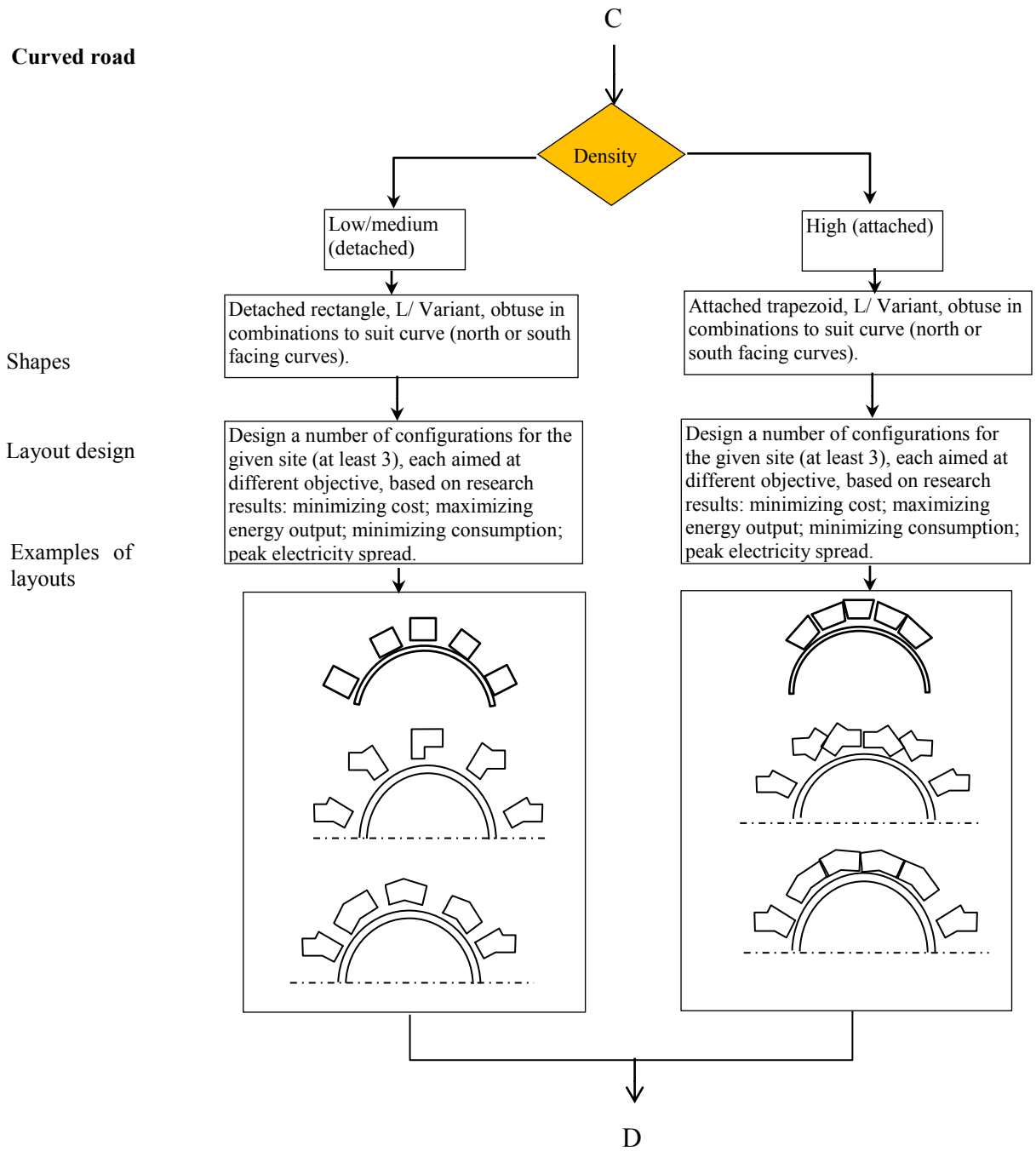


Figure 6.2, Flow chart illustrating the design process of solar energy efficient residential neighborhoods.

CHAPTER VII: CONCLUSION

This research presents an investigation of key design parameters of dwelling shapes and neighborhood patterns for increased solar potential. The investigation is conceived as an interface between architecture, building engineering and urban design. It aims at exploring maximum flexibility of design and maintaining functionality of the dwellings, while promoting energy conservation, and maximizing solar capture and utilization. The research highlights the importance of three interconnected parameters in the design of residential neighborhoods – building shape, density and site layout.

The ultimate goal of this and future research is to develop design methodology for solar optimized neighborhoods, based on effects of selected design parameters on energy performance of dwelling units and neighborhoods.

The effects of key parameters on response variables are evaluated by means of a parametric investigation. Response variables are solar potential and energy demand/consumption for heating and cooling. Design parameters are investigated separately and in combinations.

Dwelling units considered in this study are two-storied with a total floor area of 120 m². Dwelling units' shapes include basic shapes and variations on some of the basic shapes. Basic shapes are rectangle, which serves as a reference, and L, U, H and T shapes. Shape variations consist of varying values of the relative dimensions of shading and shaded façades of L and U shapes and variations to the angle enclosed by the wings of L shape. Roof design has a major influence on potential for energy generation by

housing units. In addition to the hip roof assumed as the basic design, a range of roof shape variations is investigated, from the simplest to more complex multi-faceted designs of varying tilt and orientation angles.

Neighborhood designs are characterized by the layouts of roads along which these neighborhoods are located, by the shape of dwelling units and their density. Three site layouts are considered: straight road, south-facing semi-circular road and north facing semi-circular road. The basic straight road site runs east-west, but deviations from this direction are also studied. Housing density is considered through detached configurations, representing lower density, and by attached configurations, representing higher density. Effect of rows of housing units is also considered for the straight road site. EnergyPlus building simulation program is used for estimating the response variables of energy solar potential and energy demand. Climatic, environmental and regulatory data employed in the simulations relate to northern regions and particularly to regions of Canada with similar climate to Montreal. While the specific results obtained are applicable to regions of similar climatic conditions, the methodology employed is generally applicable, and this forms the central focus of this chapter.

Summary of the Main Results

Dwelling Shape

The study shows that several parameters should be considered in the optimization of shapes for passive solar design of housing units. Rectangular layout is generally considered the optimal shape for energy efficiency. Non-rectangular and particularly non-convex shapes offer a wider flexibility in architectural as well as solar design, but due to

their complexity, their efficient design is influenced by several parameters. Some of the observed effects on different shapes are summarized below.

Convex Shapes

- **Aspect ratio** – ratio of equatorial facing to lateral façade dimensions – is the key parameter in the design of convex shape for increased solar potential: Radiation on façades, solar heat gain and BIPV electricity generation are all affected by the aspect ratio. Heating load increases significantly for an aspect ratio that is less than 1.3. Aspect ratio ranging between 1.3 and 1.6 -1.7 can offer a reasonable choice for reducing heating load, increasing south facing areas (especially roof), and maintaining the functionality of the plan.
- **Orientation:** A dwelling unit can be rotated by up to 30° east or west of south without significant effect on heating load (about 8%).
- **Window area:** it is advisable to design window area as percentage of the south façade, rather than a percentage of the floor area. A 35% of the façade can be a good option, to reduce heating load of convex shapes, while not compromising significantly their cooling load.

Non-convex Shapes

- Solar radiation on non-convex shapes is significantly affected by the *depth ratio* (DR) – the ratio of shading to shaded façade lengths, and by the number of shading façades. These two parameters control the extent of shading and consequently reduction of radiation incident on, and transmitted by windows of, the shaded façade. It is therefore desirable to reduce the depth ratio in order to

optimize the solar potential of façades. Difference of heating load between L shape with DR of 1 and DR of $\frac{1}{2}$ can reach about 10%.

- Depth ratio is particularly critical with a larger number of shading façades. For instance, the reduction of solar radiation on U shape, having two shading façades, is approximately double the values for L shape of the same depth ratio.
- Self- shading can be controlled and manipulated by variations of the basic geometry. By increasing the angle enclosed between the shading and shaded façades, the shading effect can be mitigated. The present study indicates that while such manipulations may not significantly affect the overall incident or transmitted radiation, it can alter the distribution of radiation between non-shaded and shaded façades.

Roof Design

- Solar optimized roof design requires optimal choice of orientation and tilt angle of roof surfaces. Both orientation and tilt angle of a building integrated photovoltaic/thermal (BIPV/T) system affect its overall energy generation. While the optimal tilt angle is equal to the latitude (45°), the annual electricity generation of the BIPV/T system is not significantly affected by a tilt angle that ranges between 30° and 50° .
- Deviation of the surface azimuth angle of the BIPV/T system from due south by up to 40° west or east leads to an approximate reduction of 5% in the annual generation of electricity while a rotation of 60° , west or east of south, results in a reduction of about 12% in the total annual electricity generation. The orientation

of a roof surface affects the time of peak generation. This can be of particular advantage in cases where the value of electricity varies with the time of day.

- Multi-faceted roofs, such as folded plate and split-surface configurations, can significantly increase electricity production and heat generation, primarily through increased effective surface area. Dividing the south part of the reference gable shaped roof surface of a rectangular unit into three plates with varying tilt/orientation angles can increase electricity generation by up to 17%. Replacing the gable roof with a folded plate surface increases electricity generation potential by up to 30%. Varying surface orientations in such roof designs enables spread of peak electricity generation over up to 3 hours, potentially improving the impact on the electric grid.
- The effect of roof design on heating and cooling demand is not significant. For rectangular units, increase of heating load with a split-surface roof reaches a maximum of 5%, as compared to the gable roof. Heating load increases slightly with increased roof area. This increase is, however, more than counterbalanced by the increase in electricity and heat generation.
- Redesigning the shape of units to match multi-faceted roof geometry results in a minor reduction of heating load as compared to the rectangular units with the same roof design. This approach allows for flexibility of design, whereby the designer can opt for a rectangular shape with a sophisticated roof design or a modified rectangular-based shape, where the façades follow the contour of the roofs.

Neighborhoods

Site Layout

- The positioning of units round the curved road causes, in addition to the surface rotation effect, some additional mutual shading of some detached units or some wings of attached units. This effect can lead to a significant reduction of irradiation on some surfaces. Two effects should be accounted for in the design, the relative position (angle and distance) between adjacent units in detached configurations, and the relative dimensions of adjacent, mutually shading façades of different units, in attached configurations (this is similar to the depth ratio effect in non-convex shapes).
- The main effect of site layout on electricity generation, other than the shape effect outlined above, is the shift in peak generation time on surfaces of different orientations of roof surfaces. In the straight road (east-west) site, where the different orientations are due exclusively to wing rotation of non-convex shapes, the time difference in peak generation (between main wing and branch) can reach 3 hours. In curved road sites, where rotation of whole units together with wing rotation produces a wide range of orientations, the difference in peak electricity generation time reaches 6 hours. Spread of peak generation time improves electricity supply efficiency by providing a more even electricity generation profile, thus imposing less demand on the electric grid. This can be economically beneficial, since the cost and price of electricity often vary with time of day. Shifting peak generation time towards peak demand time can lower net energy cost and also reduce net peak demand from the grid.

- Units in curved layouts have generally larger heating and cooling loads than in a straight road configuration. One reason of the increase of loads in curved roads is the mutual shading of units, as for instance in a north facing curve, where L variants may shade significantly each other. This shade can be reduced by more careful design of the relative ratio of self-shading surfaces. Cooling load is increased since the units are originally designed to be south facing, implying large window size on the south façades. In the curved layouts, some of these units are oriented towards west or east, resulting in increasing transmitted radiation in the morning and evening, when the sun is at low altitude during the summer period.

Density

- A higher residential density can be achieved by attaching units in multiplexes (up to 16 u/a maximum density), or/and designing row townhouse configurations (up to 35 u/a density). The effect of assembling units in multiplexes is to increase shading on some surfaces of non-rectangular shapes. Up to 25% reduction of incident irradiation on some façade surfaces of attached L shape and its variants is observed in the straight road site.
- Another effect on irradiation is shading by parallel rows of units. This effect is strongly dependent on the distance between rows of units and is most significant in winter. In the straight road site, at a row distance of 10m, incident radiation on rectangular units of the shaded row is reduced by up to 55%.
- Attaching units in multiplex configurations has the effect of increasing total active roof surface in some configurations. For instance, the substitution of rectangular with trapezoid shape in the attached configurations of a north-facing curved road,

results in 10% increase of electricity generation, as compared to the detached assemblage. On the other hand in a site with south-facing curved road there is a decrease in electricity generation of similar magnitude. Attaching some L configurations may produce some mutual shading.

- Row assemblage does not have significant effect on electricity generation for a row distance larger than 5m, due to the uniform height of all units assumed in this study. A maximum reduction of 7% is observed for a 5m row distance.
- Heating and cooling loads depend strongly on unit density in a site. Attaching units in multiplexes reduces heating loads by up to 30% and cooling load by up to 50% compared to the detached configurations of the same site. Heating and cooling loads of detached units are not highly sensitive to the spacing of units.
- Arranging the units in south facing rows affects significantly energy demand of the obstructed row, due to shading. The heating load is directly influenced by shading and is inversely related to the distance between rows, while the cooling load of both exposed and obstructed rows is significantly lower than for the single row configuration. For instance, with a distance of 10m between rows of rectangular units, the heating load of the obstructed row can increase by up to 25%, relative to single row configuration. At 20 m distance the effect is negligible.

Design Methodology and Recommendations

Heuristic design methodology of solar optimized neighborhood is developed to support designing solar optimized neighborhoods. Selection between design alternatives

in this thesis is based on a weighted objectives evaluation method. Following is a general description of the evaluation system and the design methodology.

Evaluation of Design Alternatives

Evaluation procedure of design alternatives of solar neighborhoods is proposed, as a decision-aiding tool, based on a set of performance criteria. The criteria included in this research are heating and cooling consumption (assuming the usage of a heat pump to supplement the active and passive solar heating) and solar potential (active and passive) of units and neighborhoods. These criteria can be expanded to include other parameters such as daylighting, cost, etc. The performance criteria are assigned weights and levels of performance of design alternatives, relative to a reference case, are assigned grades. The weights and grades can be manipulated according to climate conditions, objectives and priorities of the designer. Design alternatives are evaluated for their performance based on the sum of products of their performance grades by the weights of the corresponding performance criteria.

Weights can be assigned based on cost-benefit analysis, which depends on multiple considerations including geographic and climatic location such as cooling load in hot climate (see application to other climates below), cost of PV vs. value and timing of generated electricity, or cost if realizing economic houses is the main objective of the designer (see cost-benefit below).

Design Methodology

The design methodology details the stages of the design process, highlights alternatives to increase the overall solar potential and energy performance of neighborhoods. Following are the main steps of the design methodology:

- The design process starts with a brief that includes data on the site and on the housing units, such as road layout, density, number of units, number of stories of housing units, functional floor area, etc.
- The next step is, for the given site layout and density to prepare a number of design alternatives that fit the layout and have potential beneficial energy profile, based on the finding of this (or similar) investigation. Design alternatives should include different shapes and orientations.
- Each of the design alternatives is analysed for energy performance (consumption vs. generation) by means of a simulation program, such as EnergyPlus. Other performance criteria, such as cost, may also be included in the analysis.
- Design alternatives are evaluated and compared based on the weighted objectives procedure outlined above.
- A number of the most promising alternatives (depending on the size of the project) are selected for further analysis. Modifications are made to the original design, as appropriate, in an attempt to improve performance and simulations are performed again.
- The process of evaluation, selection, modification and re-analysis is repeated until the optimal design is reached for final preparation of documents.

Application to Other Climates

The effects studied in this research are specific to the climatic conditions – mid-latitude northern climate. However the nature of the design parameters, the evaluation system and the design methodology are generally applicable. While the nature of performance criteria – heating/cooling energy consumption, energy potential etc. does not change, their relative weights and grades are climate dependent. Similarly, the effects of design parameters, such as dwelling shapes, site layout, density, are similar in different climates, but the objectives change with climate. For instance, while mutual shading is undesirable in cold climate it may be desirable in hot climate and will have a positive effect on cooling load, which is a major performance criterion.

Design modifications for climatic zones include design of roof tilt and orientation, orientation of houses and façades, window properties, location and size, aspect ratio of houses, etc. These can be the subject of future investigations.

Cost-Benefit Considerations

This research does not include cost considerations. Cost estimates, which vary widely with time and place, need to be carried out on a case-by case basis. Following are some general observations. Opting for housing shapes that deviate from rectangular shape may increase cost. Some of the additional cost is due to additional building materials and labor that are associated with larger building envelope. For instance, H shape has a building envelope that is 60% larger than the rectangular case, while the building envelope of L shape is some 20% larger than the rectangular shape. Assuming that the cost of envelope material and labor is 20% of the total construction cost (Emrath, 2010), the increase in construction cost of most complex shapes would be less than 12%

as compared to the rectangular case (about 4% for L shape). This increase in cost may be more than compensated for by benefits that some shapes can provide. For instance, non-convex shapes enable penetration of daylight to northern zones due to the narrow width of some parts of the plan. In addition, some of these shapes have larger functional roof area, for the integration of BIPV/T systems. Enlarging roof area can be very beneficial especially in dense urban sites, where the ground area is limited. Additional non-material benefits of such shapes include flexibility of design, improved functionality, quality of life, improved neighborhood environment.

Complex roof systems, such as folded plate, are associated with increased cost due to increase of complexity in the manufacturing. However, the cost rise can be counterbalanced by an improved potential of BIPV/T system through increased electricity generation and spreading of peak generation time, which can increase the system value by up to 20% (Borenstein, 2008). Depending on the type of fuel employed in the dwelling, BIPV/T systems coupled with heat pump for water heating and/or space heating can offer significant economic benefits with short payback periods (between 4 years and 7 years) (Kalogirou, 2004). The economic benefit however, depends on different economic indices of a country including the inflation rate and fuel price.

Another beneficial characteristic of roof systems such as folded plates is that they can be designed as structural systems, saving therefore on the cost of structural elements required in the traditional roof systems, and freeing extra functional space.

Proposed Future Work

Future work proposed, based on this research includes:

- Extension of the methodology presented in this thesis to other representative climatic zones (e.g. hot and humid, temperate climates, etc.), and identification of optimal range of design parameters for each climate.
- Investigation of additional performance criteria such as daylighting, comfort, cooling strategies, and cost (initial cost, net revenue), cost of buying/selling electricity and interaction with the utility grid, etc. Considering such performance criteria enable optimization of design alternatives.
- Development of the methodology proposed in this research into an interactive design tool, initially for the same conditions but to be gradually developed to allow for more varied urban and climatic conditions.
- Extension of the methodology to include mix used neighborhoods and analyzing the interaction between site layouts, density, and building heights.

Contribution

The research presented in this thesis represents a novel holistic approach to the evaluation of energy performance of neighborhoods and to the design of solar optimized communities, through bridging the gap between engineering, architecture and urban planning. The research identifies key parameters in the design of solar dwellings and neighborhoods, quantifies the effects of these parameters on their energy performance, and presents a design methodology of residential neighborhoods with increased solar potential. Findings of the research have been published in four papers in prestigious journals (e.g. Solar Energy (Hachem et al, 2011a), Energy and Buildings (Hachem et al, 2011b; Hachem et al.,2012a), and ASHRAE Transactions (Hachem et al., 2012b)), as

well as in several conference proceedings, having gained the best paper award “Innovative directions in simulations”, in the e-Sim 2012 (IBPSA, Canada) conference.

The originality of the contribution derives from the following:

- Extensive design and analysis of non-rectangular building shapes aiming at exploring advantages and penalties of these shapes, while maintaining functional plans of dwellings. This innovative approach consists of the identification of parameters governing the design of such shapes and evaluation of their effects on different energy performance criteria. These parameters can be generalized to represent any building shape.
- Developing new roof concepts for increased solar potential of BIPV/T systems, which combines different tilt and orientation angles (Hachem et al, 2012b).
- A systematic approach for the design of neighborhoods for increased solar potential is developed, consisting of the following:
 - Identifying key parameters of neighborhood design and analyzing the effect of the interaction between these parameters and with the shape of buildings on overall energy performance of the neighborhoods.
 - Formulation of design considerations for solar optimized houses and neighborhoods, based on an investigation of a large number of dwelling shapes and neighborhood patterns. Although the specific design considerations are for design alternatives under the climatic conditions studied, the methodology can serve as template for other situations with suitable modifications.

- Formulation of a step-by-step design methodology for solar neighborhoods. The methodology incorporates an evaluation system of design alternatives, based on weighted objectives method, which enables comparison and selection among alternatives. This methodology is adaptable to any set of objectives, climatic and economic conditions, and can assist in shaping policies to reach net zero energy communities. A similar evaluation system of energy performance, where optimal weight schemes are determined according to priorities and targets of the design, can be applied to existing neighborhoods.

REFERENCES

1. Adamski, M. and Marks, W., 1993. Multicriteria optimization of shapes and structures of external walls of energy conservation buildings, *Archives of Civil Engineering* 39 (1), 77–91.
2. Adamski, M., 2007. Optimization of the form a building with an oval base, *Building and Environment* 42, 1632–1643.
3. Al Anzi, A., Seo, D. and Krarti, M., 2009. Impact of building shape on thermal performance of office buildings in Kuwait, *Energy Conversion and Management* 50(3): 822-828.
4. Ali-Toudert, F., 2009. Energy efficiency of urban buildings: significance of urban geometry, building construction and climate, *Proceedings of CISBAT conference*, Lausanne.
5. ANSI/ASHRAE Standard 62.2-2010, 2010. *Ventilation and Acceptable Indoor Air Quality in Low-Rise Residential Buildings*. Atlanta, GA: American Society of Heating, Refrigerating and Air-Conditioning Engineers.
6. Arasteh, D., Selkowitz, S. and Wolfe, J., 1989. The design and testing of a highly insulating glazing system for use with conventional window systems, *Journal of Solar Energy Engineering, Transactions of the ASME*, Vol. 3.
7. Armstrong, M., Swintona, M.C., Ribberink, H., Beausoleil-Morrison, I., Millette, J., 2009. Synthetically derived profiles for representing occupant-driven electric loads in canadian housing, *Journal of Building Performance Simulation* 2 (1) , 15-30.
8. Arumi, F., 1979. *Computer-aided energy design for buildings. Energy Conservation Through Building Design*, D. Watson (ed.), McGraw-Hill, NY.
9. ASHRAE, 2005. *Fenestration*, in: 2005 ASHRAE Fundamentals, Atlanta: American Society of Heating, Refrigerating and Air-Conditioning Engineers, Inc.
10. ASHRAE, 2007. *Solar Energy Use*, in : ASHRAE Handbook HVAC Applications (Chapter 33), ASHRAE, Atlanta, GA,.
11. ASHRAE, 2008. “ASHRAE Vision 2020.” www.ashrae.org/doclib/20080226_ashraevision2020.pdf. Last accessed 27, Sept., 2009.
12. Athienitis et al. 2010, *Design, Optimization, and Modelling Issues of Net-Zero Energy Solar Buildings*, EuroSun conference, Graz, Austria, Sep 28-Oct.1.
13. Athienitis, A., 2007. *Design of a solar home with BIPV-thermal system and ground source heat pump*, 2nd Canadian Solar Buildings Conference, June 10 – 14. Calgary, Canada.
14. Athienitis, A.K. and Santamouris, M., 2002. *Thermal Analysis and Design of Passive Solar Buildings*, London : James & James Ltd.

15. Athienitis, A.K., 1998. Building thermal analysis, second ed. Mathcad Electronic Book, Mathsoft Inc., Boston.
16. Athienitis, A.K., Bambara, J., O'Neil, B., Faille, J., 2011. A prototype photovoltaic/thermal system integrates with transpired collector, *Solar Energy* 85, 139-153.
17. Baker, N. and Steemers, K., 2000. *Energy and Environment in Architecture*, E&FN Spon, London.
18. Beccali, G., Cellura, M., Brano, V.L. and Orioli, A., 2005. Is the transfer function method reliable in a European building context? A theoretical analysis and a case study in the south of Italy, *Applied Thermal Engineering* 25(2-3): 341-357.
19. Borenstein, S., 2005. The Long-Run Efficiency of Real-Time Electricity Pricing, *Energy Journal*, 26(3).
20. Borenstein, S., 2007 *Electricity Rate Structures and the Economics of Solar PV: Could Mandatory Time-of-Use Rates Undermine California's Solar Photovoltaic Subsidies?* Center for the Study of Energy Markets (CSEM) University of California Energy Institute, Berkeley campus. <http://www.ucei.berkeley.edu/PDF/csemwp172.pdf>. Visited on 21 April, 2012.
21. Borenstein, S., 2008. The market value and cost of solar photovoltaic electricity production. Working paper, Center for the Study of Energy Markets (CSEM) University of California Energy Institute, Berkeley campus.
22. Breyer, Ch. and Gerlach, A., 2010. Global Overview on Grid-Parity Event Dynamics, 25th EUPVSEC/WCPEC-5, Valencia, September 6 – 10.
23. Burden, D., Wallwork, M., Sides K, and Bright H., 1999. Street design guidelines for healthy neighborhoods, Rue for Local Government Commission, Center for Livable Communities.
24. Canada Housing and Mortgage Corporation (CMHC), 2010. Photovoltaic (PV) Systems - Photovoltaic System Overview. http://www.cmhc-schl.gc.ca/en/co/maho/enefcosa/enefcosa_003.cfm. Visited on 25, Aug., 2011.
25. Capeluto, I.G. Shaviv, E., 2001. On the use of solar volume for determining the urban fabric, *Solar Energy* 70(3):275-280.
26. Carlisle, N., Geet, A. V. and Pless, P., 2009. Definition of a "Zero Net Energy" Community, Technical Report NREL/TP-7A2-46065. <http://www.nrel.gov/docs/fy10osti/46065.pdf>. Retrieved on 15, Jan. , 2011.
27. Center for Watershed Protection (CWP), 1998. Better site design: a handbook for changing development rules in your community, Ellicott City, MD.
28. Charron, R and Athienitis, A., 2006. Design and optimization of net zero energy solar homes, *ASHRAE Transactions* 112 (2): 286-295.

29. Charron, R., 2009. A Review of Low and Net-Zero Energy Solar Home Initiatives, CanmetENERGY, http://canmetenergy-canmetenergie.nrcan-mcan.gc.ca/eng/buildings_communities/buildings/pv_buildings/publications/2005133.html, visited on 14, Feb., 2011.
30. Charron, R., 2007. Development of a genetic algorithm optimisation tool for the early stage design of low and net-zero energy solar homes, PhD Thesis, Concordia University, Montréal.
31. Chen, Y., Athienitis, A. K., Galal K. E and, Poissant, Y., 2007. Design and Simulation for a Solar House with Building Integrated Photovoltaic-Thermal System and Thermal Storage, ISES Solar World Congress, Beijing, China, Vol. I, pp. 327-332.
32. Cheng, V., Steemers, K., Montavon, M. and Compagnon, R., 2006. Urban form, density and solar potential, Proceedings of the 23th Conference on PLEA, Geneva, Switzerland, 701–706.
33. Chiras, D., 2002. The solar house: passive heating and cooling, White River Junction, VT : Chelsea Green Publishing.
34. Christensen, C. and Horowitz, S., 2008. Orienting the neighborhood: a subdivision energy analysis tool, ACEEE Summer Study on Energy Efficiency in Buildings Pacific Grove, California, 17–22, August.
35. Christian, J., Pratsch, L., and Blazing T.J., 2007. Zero Peak Communities electric utility benefits. Retrieved from http://www.ornl.gov/sci/buildings/2010/Session%20PDFs/15_New.pdf, on 11, Jan., 2011.
36. Clarke, J.A., Cockroft, J., Conner, S., Hand, J.W., Kelly, N.J., Moore, R. et al., 2002. Simulation-assisted control in building energy management systems. *Energy and Buildings* 34 (9), 933–940.
37. Clarum Houses – Vista Montana, 2003. <http://www.pvdatabase.org/pdf/VistaMontana.pdf>. Visited on 9, Feb., 2011.
38. CMHC, 2011. The Fused Grid. <http://www.cmhc.ca/en/inpr/su/sucopl/fugr/index.cfm>. Visited on 12, Jan., 2011.
39. CMHC, 1998. Tap the Sun: Passive Solar Techniques and Home Designs. Ottawa: Canada Mortgage and Housing Corporation.
40. Cohen, A., 2000. Narrow Streets Database, Congress for the New Urbanism, www.sonic.net/abcaia/narrow.htm. Retrieved on 23, Oct., 2010.
41. Compagnon, R., 2004. Solar and daylight availability in the urban fabric. *Energy and Buildings* 36 (4), 321–328.
42. Crawley D., Pless, S., and Torcellini, P., 2009. Getting to Net Zero, ASHRAE Journal American Society of Heating, Refrigerating, and AirConditioning Engineers, Inc.
43. Crawley, D.B., 2001. EnergyPlus: the future of building energy simulation, US DOE replaces DOE-2 and BLAST. *HPAC Heating, Piping, Air Conditioning Engineering* 73 (11), 65–67.

44. Crawley, D.B., Hand, J.W., Kummert, M. and Griffith, B.T., 2008. Contrasting the capabilities of building energy performance simulation programs, *Building and Environment*, 43(4): 661-673.
45. Crawley, D.B., Pedersen, C.O., Lawrie, L.K., Winkelmann, F.C., 2000. Energy plus: energy simulation program. *ASHRAE Journal* 42 (4), 49– 56.
46. Curtright, A.E., Morgan, M.G., Keith, D.W., 2008. Expert Assessments of Future Photovoltaic Technologies, *Environ. Sci. Technol.*, 42, 9031-9038
47. Depecker, P., Menezes, C., Virgone, J. , and Lepers, S., 2001. Design of building shape and energetic consumption, *Building and Environment* 30(2): 201–222.
48. Duffie, J.A. and Beckman, W.A., 2006. *Solar engineering of thermal processes*, Wiley.
49. ECBCS Annex 29/ IEA task 21, IEA Energy Conservation in Buildings and Community systems and Solar Heating and Cooling Programme, 2011. Daylight in Buildings, http://www.ecbcs.org/docs/ECBCS_Annex_29_PSR.pdf. Visited on 13, March., 2012.
50. ECBCS News, Towards Net Zero energy Buildings, Energy Conservation in Buildings and Communities, issue 53, 2011. http://www.ecbcs.org/newsletters/ECBCS_1106_webversion.pdf. Retrieved on 16, Jan., 2012.
51. Emrath, P., 2010. Breaking Down House Price and Construction Costs, Report available to the public as a courtesy of HousingEconomics.com. <http://www.nahb.org/generic.aspx?sectionID=734&genericContentID=134543&channelID=311>. Retrieved on 5, Dec., 2011.
52. EN 15316-3-1, 2007. Heating systems in buildings – method for calculation of system energy requirements and system efficiencies, Part 3-1.
53. EnergyPlus. 2011. Version 6. 0. Lawrence Berkeley National Laboratory, Berkeley, CA.
54. Erley, D. and Jaffe M., 1979. Site planning for solar access. Washington D.C.: U.S. Department of Housing and Urban Development.
55. European Parliament, 2009. Press Release. www.europarl.europa.eu/sides/getDoc.do?pubRef=-//EP//TEXT+IM-PRESS+20090330IPR52892+0+DOC+XML+V0//EN&language=EN. Last accessed 27, Sept., 2009.
56. Foster, M. and Oreszczyn, T., 2001. Occupant control of passive systems: the use of Venetian blinds, *Building and Environment* 36(2): 149-155.
57. Gadsden, S., Rylatt, M., Lomas, K., Robinson, D., 2002, Predicting the urban solar fraction: a methodology for energy advisers and planners based on GIS, *Energy and Buildings*, 1458, p1-12.
58. Ghosh, S, and Vale R., 2006. The potential for solar energy use in a New Zealand residential neighbourhood: A case study considering the effects on CO₂ emissions and the possible benefits of changing roof form, *Australasian Journal of Environmental Management*, 13, 216-225.
59. Google SketchUp Plugins, 2011. <http://sketchup.google.com/intl/en/download/plugins.html>.

60. Green, M. A., Emery, K., Hishikawa, Y. and Warta, W., 2011. Solar cell efficiency tables (version 37), *Progress in Photovoltaics: Research and Applications* 19(1), 84–92.
61. Griffith B.T. and Ellis P.G., 2004. Photovoltaic and Solar Thermal Modeling with the EnergyPlus Calculation Engine, World Renewable Energy Congress VIII and Expo Denver, Colorado, 29Aug.– 3 Sep.
62. Groth, C.C., and Lokmanhekim, M., 1969. Shadow – A New Technique for the Calculation of Shadow Shapes and Areas by Digital Computer. Second Hawaii International Conference on System Sciences. Honolulu, HI, Jan. 22-24.
63. Hachem C., A. Athienitis, P. Fazio, 2011a, Parametric investigation of geometric form effects on solar potential of housing units, *Journal of Solar Energy*, Volume 85, Issue 9, Pages 1864-1877.
64. Hachem C., A. Athienitis, P. Fazio, 2011b, Investigation of Solar Potential of Housing Units in Different Neighborhood Designs, *Journal of Energy and Buildings*, Volume 43, Issue 9, Pages 2262-2273.
65. Hachem C., A. Athienitis, P. Fazio, 2012a. Evaluation of energy supply and demand in solar neighbourhoods, *Journal of Energy and Buildings*, DOI: 10.1016/j.enbuild.2012.02.021.
66. Hachem C., A. Athienitis, P. Fazio, 2012b. Design of roofs for increased solar potential of BIPV/T systems and their applications to housing units", *ASHRAE Transactions*, TRNS-00226-2011.R1.
67. Hagemann, I.B., 2007. Solarsiedlung am Schlierberg, Freiburg (Breisgau), Germany, PV Upscale. <http://www.pvupscale.org/IMG/pdf/Schlierberg.pdf>. Retrieved on Jan., 17, 2011.
68. Hamada, Y., Nakamura, M., Ochifuji, K., Yokoyama, S., Nagano, K., 2003. Development of a database of low energy homes around the world and analyses of their trends, *Renewable Energy* 28 (2), 321–328.
69. Hastings, R and Wall, M., 2007. Sustainable Solar Housing Strategies and Solutions, Vol. 1, Sterling, VA : Earthscan.
70. Heindl, W. and Grilli, P.V., 1991. On establishing standards for the overall heat transfer coefficient of buildings, CIB-W67-Workshop, Vienna.
71. Holbert, 2009. An analysis of utility incentives for residential photovoltaic installations in Phoenix, Arizona, 39th North American Power Symposium (NAPS 2007) Washington State University, Downloaded from IEEE Xplore on 10, Jan., 2010.
72. Holmberg, D.G., Bushby, S.T., 2009. "BACnet and the Smart Grid" "BACnet Today" Supplement to *ASHRAE Journal* 51(11), 8-12.
73. Hong, T., Chou, S.K., Bong, T.Y., 2000. Building simulation: an overview of developments and information sources, *Building and Environment* 35 (4), 347–361.
74. I.E.A., 2002. Potential for building integrated photovoltaics, Technical Report IEA –PVPS T7-4.

75. IEA PVPS Task 10: Urban – Scale Photovoltaic Applications. http://www.iea-pvps.org/products/download/flyer_t10.pdf. Visited on Jan., 17, 2011.
76. IEA PVPS-Task 10: Japan: Jo-Town Kanokodai. Community-scale pv: real examples of pv based housing and public developments. http://www.pvdatabase.org/projects_viewupscale.php. Visited on 15, Jan., 2011.
77. IEA- SHC Task 40/ECBCS Annex 52: Toward Net Zero Energy Solar Buildings. <http://www.iea-shc.org/task40/>. Visited on 18, Jan., 2011.
78. IEA Task 41, 2009. Solar Energy and Architecture, Solar Heating and Cooling Programme, International Energy Agency. <http://www.iea-shc.org/task41/>. Visited on 14, April, 2011.
79. IEA Task 7: Photovoltaic power systems in the built environment, Report IEA-PVPS 7-03: 2000, Photovoltaic Building Integration Concepts, Proceedings of the IEA PVPS Task VII Workshop, 11-12, Feb., 1999, EPFL, Lausanne, Switzerland.
80. Iqbal, M.T., 2004. A feasibility study of a zero energy home in Newfoundland, *Renewable Energy* 29 (2), 277–289.
81. Jabareen, Y. R., 2006. Sustainable urban forms: their typologies, models and concepts, *Journal of Planning Education and Research* 26(1), 38- 52.
82. Jedrzejuk, H. and Marks, W., 1994. Analysis of the influence of the service life and shape of buildings on the cost of their construction and maintenance, *Archives of Civil Engineering* 40 (3: 4), 507–518.
83. Jedrzejuk, H. and Marks, W., 2002. Discrete polyoptimization of energy-saving building, *Archives of Civil Engineering* 48 (3), 331–347.
84. Jones, P.J. et al, 1999. An energy and environmental prediction tool for planning sustainability in cities – a global model, *Proc. PLEA'99, Brisbane, Australia*, 789-794.
85. Kaan, H. and Reijenga, T., 2004. Photovoltaics in an architectural context. *Prog. Photovolt: Res. Appl.* 12: 395–408. doi: 10.1002/pip.554.
86. Kalogirou, S.A., 2004. Solar thermal collectors and applications, *Prog Energy Combust Sci*, 30, 231-295.
87. Kampf, J.H., Montavon, M., Bunyesc, J., Bolliger, R., and Robinson, D., 2010. Optimisation of buildings' solar irradiation availability. *Solar Energy* 84, 596–603.
88. Kemp, W.H., 2006. *The renewable energy handbook: a guide to rural energy independence, off-grid and sustainable living*, Tamworth, ON : Aztech Press.
89. Keoleian, G.A. and Lewis, G.M.D., 2003. Modeling the life cycle energy and environmental performance of amorphous silicon BIPV roofing in the US, *Renewable Energy* 28(2): 271-293.
90. Klein, S.A., Beckman, W.A., Duffie, J.A., 1976. TRNYSYS – a transient simulation program. *ASHRAE Transactions* 82 (1), 623–633.

91. Klingenberg, K., Kernagis, M. and James, M., 2008. Homes for a changing climate passive houses in the U.S., Larkspur, CA : Low Carbon Productions.
92. Knowles R. L., 1981. Sun Rhythm Form, The MIT Press, Cambridge, Massachusetts.
93. Knowles, R. L., 2003. The solar envelope: its meaning for energy and buildings, *Energy and Buildings* 35(1): 15-25.
94. Kolokotsa, D., Rovas, D., Kosmatopoulos, E. and Kalaitzakis, K., 2011. A roadmap towards intelligent net zero- and positive-energy buildings, *Solar Energy* 85 (12), 3067-3084.
95. Laouadi, A., Galasiu, A.D., Swinton, M.C., Armstrong, M., Szadkowski, F., 2009. Field performance of exterior solar shadings for residential windows: Summer results. 12th Canadian Conference on Building Science and Technology, Montréal, Quebec, May 6-8, 197-210.
96. Lechner, N., 2001. Heating, Cooling, Lighting : Design Methods for Architects, John Wiley & Sons, Inc. (US).
97. Leung, K. S. and Steemers, K., 2009. Exploring solar responsive morphology for high-density housing in the tropics, proceedings of CISBAT conference, Lausanne, Switzerland.
98. Leveratto, M.J., 2002. Urban planning instruments to improve winter solar access in open public spaces, *Environmental Management and Health* 13 (4), 366–372.
99. Liao, L., Athienitis, A. K., Candanedo, L. and Park, K.W., 2007. Numerical and experimental study of heat transfer in a BIPV–thermal system, *ASME Journal of Solar Engineering* 129 (4), 423–430.
100. Ling, C.S., Ahmad, M.H., Ossen, D.R., 2007. The effect of geometric shape and building orientation on minimising solar insolation on high-rise buildings in hot humid climate, *Journal of Construction in Developing Countries* 12 (1), 27–38.
101. Loutzenhiser, P. G., H. Manz, et al., 2007. Empirical validation of models to compute solar irradiance on inclined surfaces for building energy simulation, *Solar Energy* 81(2): 254-267.
102. Loutzenhiser, P. G., H. Manz, et al., 2009. An empirical validation of window solar gain models and the associated interactions, *International Journal of Thermal Sciences* 48(1): 85-95.
103. Mahdavi, A. and Gurtekin, B., 2002. Shapes, numbers, and perception: aspects and dimensions of the design performance space, *Proceedings of the 6th International Conference: Design and Decision Support Systems in Architecture*, The Netherlands, 291-300.
104. Mardaljevic, J. and Rylatt, M., 2000. An image-based analysis of solar radiation for urban settings, *PLEA*, Cambridge, UK, 442– 447.
105. Marks, W., 1997. Multicriteria optimisation of shape of energy-saving buildings, *Building and Environment* 32 (4), 331–339.
106. Minergie, 2011. <http://www.minergie.com>. Visited on 5 Jan. 2012.

107. Montavon, M., Scartezzini, J.-L. and Compagnon, R., 2004. Comparison of the solar energy utilisation potential of different urban environments, PLEA, Eindhoven, The Netherlands.
108. Morello et al., 2009. Sustainable urban block design through passive architecture, a tool that uses urban geometry optimisation to compute energy savings, proceedings of PLEA 2009, Quebec City, Canada.
109. Morello, E. and Ratti C., 2009. Sunscapes: 'Solar envelopes' and the analysis of urban DEMs, Computers, Environment and Urban Systems 33, 26–34.
110. Müller H.F.O., 2005. Integration of Photovoltaic in Low Energy Buildings, University of Sharjah. In: Journal of Pure & Applied Sciences 2 (2).
111. N. M. Pearsa L L, R. Hill, 2001. Photovoltaic Modules, Systems and Applications, edMA3.doc , ch. 15.
112. National Research council Canada: Institute of research in Construction (NRC-IRC), 2005. CBD-59. Principles of Solar Shading. <http://www.nrc-cnrc.gc.ca/eng/ibp/irc/cbd/building-digest-59.html>, visited on 29, Nov, 2010.
113. Natural Resources Canada (NRCan), Canadian Forest Service, 2011. Photovoltaic potential and solar resource maps of Canada, <https://glfc.cfsnet.nfis.org/mapserver/pv/pvmapper.phtml>. Visited on 3, Jan, 2012.
114. Natural Resources Canada (NRCan), Office of Energy Efficiency, 2008. Heating and cooling with a heat pump. <http://oee.nrcan.gc.ca/sites/oee.nrcan.gc.ca/files/pdf/publications/infosource/pub/home/heating-heat-pump/booklet.pdf>. Retrieved on 28, Jan, 2011.
115. Natural Resources Canada (NRCan), Office of Energy Efficiency, 2009a. About the R-2000 Standard, <http://oee.nrcan.gc.ca/residential/personal/new-homes/r-2000/standard/11018>. Visited on 14, March, 2012.
116. Natural Resources Canada (NRCan), Office of Energy Efficiency, 2010. Canada's Secondary Energy Use by Sector, End-Use and Sub-Sector. <http://oee.nrcan.gc.ca/corporate/statistics/neud/dpa/tableshandbook2>. Visited on 3, Jan, 2012.
117. Natural Resources Canada (NRCan), Office of Energy Efficiency, 2003. Comprehensive Energy Use Database (CEUD). http://oee.nrcan.gc.ca/corporate/statistics/neud/dpa/comprehensive_tables/index.cfm. Visited on 11, Oct., 2010.
118. Natural Resources Canada (NRCan): Office of Energy Efficiency, 2009b. How a heat recovery ventilator works. <http://oee.nrcan.gc.ca/residential/personal/new-homes/r-2000/standard/how-hrv-works.cfm?attr=4>. Retrieved on 5, April, 2009.
119. Neuhoff, K., 2005. Large-scale deployment of renewables for electricity generation, Oxford Review of Economic Policy 21 (1), 88–110.

120. Nikoofard S., Ugursal, I., and Beausoleil-Morrison, I., 2011. Effect of external shading on household energy requirement for heating and cooling in Canada. *Energy and Buildings*, 43(7):1627–1635.
121. Olgyay, V., 1963. *Design with Climate*, Princeton University press, Princeton NJ.
122. Ouarghi, R. and Krarti., M. , 2006. Building shape optimization using neural network and genetic algorithm approach, *ASHRAE Transactions* 112, 484-491.
123. Parker, D.S., 2009. Very low energy homes in the United States: perspectives on performance from measured data, *Energy and Buildings* 41 (5), 512–520.
124. Pearce, J.M., 2002. Photovoltaics: a path to sustainable futures, *Futures* 34 (7), 663–674.
125. Pelland S. and Poissant Y., 2006. An evaluation of the potential of building integrated photovoltaics in Canada, 31st Annual Conference of the Solar Energy Society of Canada (SESCI). Aug. 20-24th, Montréal, Canada.
126. Perez, D., Kämpf, J., Wilke, U., Papadopoulo, M. and Robinson, D., 2011. Citysim simulation: the case study of alt-wiedikon, a neighbourhood of Zürich city, *Proceeding CISBAT*, Lausanne, Switzerland, September 14-16.
127. Perez, R., Ineichen, P., Seals, R., Michalsky, J., and Stewart, R., 1990. Modelling daylight availability and irradiance components from direct and global irradiance, *Solar Energy* (44), 271-289.
128. Pessenlehner, W., and Mahdavi A., 2003. Building morphology, transparency, and energy performance, *Eighth International IBPSA Conference Proceedings*, Eindhoven, Netherlands.
129. Pietzcker, R., Manger, S. Bauer, N. Luderer, G. Bruckner, T., 2009. The Role of Concentrating Solar Power and Photovoltaics for Climate Protection, *Proceedings 10th IAEE European Energy Conference*, Vienna, September 7 – 10.
130. Pitts, A. C., 1994. Building design: Realising the benefits of renewable energy technologies, *Renewable Energy* 5(5-8): 959-966.
131. Pogharian, S. et al., 2008. Getting to a net zero energy lifestyle in Canada: the Alstonvale net zero energy house, *3rd European PV Solar Energy Conference*, Valencia, Spain.
132. Pogharian, S., Ayoub, J., Candanedo, J., and Athienitis, A.K., 2008. Getting to a net zero energy lifestyle in Canada: the Alstonvale net zero energy house. *The 3rd European PV Solar Energy Conference*, Valencia, Spain.
133. Poissant, Y. and Kherani, N.P., 2008. PV systems and components. Powerpoint Presentation, *SBRN BIPV Workshop*, 4th Canadian Solar Buildings Conference, Toronto, Canada, June 23.
134. Pol, O. and Robinson, D., 2011. Impact of urban morphology on building energy needs: a review on knowledge gained from modeling and monitoring activities, *Proceeding CISBAT*, Lausanne, Switzerland, 14-16 September.

135. Ratti, C., Baker, N. and Steemers, K., 2005. Energy consumption and urban texture, *Energy and Buildings* 37 (7), 762–776.
136. Ratti, C., Robinson, D., Baker, N., Steemers, K., 2000. LT Urban – the energy modelling of urban form, proceedings of PLEA, Cambridge.
137. RETScreen International, Clean Energy Project Analysis, 2005. Ministry of Natural Resources Canada.
138. Robertson and Athienitis, 2007. Solar energy for buildings: introduction: solar design issues, Canada Mortgage and Housing Corporation (CMHC). http://www.cmhc-schl.gc.ca/en/inpr/bude/himu/coedar/upload/OAA_En_aug10.pdf. Visited on 20, Oct., 2011.
139. Sartori, I., Candanedo J., Geier, S., Lollini R., Garde F., Athienitis, A., Pagliano, L., 2010. Comfort and energy efficiency recommendations for net zero energy buildings, EuroSun Conference, Graz, Austria, 28 Sep-1 Oct.
140. Scartezzini, J.-L., Montavon, M. and Compagnon, R., 2002. Computer evaluation of the solar energy potential in an urban environment, EuroSun, Bologna.
141. SECURE, Nieuwland solar energy Project, Benchmark Study, European Sustainable Urban Development Projects. http://www.secureproject.org/download/18.360a0d56117c51a2d30800078414/Nieuwland_Amersfoort_NL.pdf. Visited on 17, Jan., 2011.
142. Skoplaki, E., Palyvos, J. A., 2009. On temperature dependence of photovoltaic module electrical performances: A review of efficiency/power correlations, *Solar energy*, 83, 614- 624.
143. SolarBuzz: Solar Market Research and Analysis, 2011. <http://solarbuzz.com/facts-and-figures/retail-price-environment/module-prices>. Visited on April 16, 2011.
144. Stasinopoulos, T.N., 2002. Sunny walls vs sunnier roofs: a study on the advantages of roofs for solar collection, *Environmental Management and Health* 13 (4), 339–347.
145. Steemers, K., 2003. Energy and the city: density, buildings and transport. *Energy and Buildings* 35(1), 3-14.
146. Straube, J., 2009. Building Science Insights: The Passive House (Passivhaus) Standard—A comparison to other cold climate low-energy houses, <http://www.buildingscience.com/documents/insights/bsi-025-the-passivhaus-passive-house-standard>. Visited 17, Feb. 2011.
147. Teed, J., Condon, P., Muir, S., and Midgley, C., 2009. Sustainable urban landscape neighbourhood pattern typology, The University of British Columbia James, produced for the Sustainable Development Research Institute.
148. The Canadian Renewable Energy Network, Commercial Earth Energy Systems. <http://publications.gc.ca/collections/Collection/M92-251-2002E.pdf>. Retrieved June, 2011.

149. Threlkeld, J.L. and Jordan, R.C., 1958. Direct solar radiation available on clear days, ASHRAE Transactions, 64-45.
150. Torcellini, P.A. and Crawley, D.B., 2006. Understanding zero-energy buildings. ASHRAE Journal 48 (9), 62–64, 66–69.
151. Tripanagnostopoulos Y., Nousia Th., Souliotis M. and Yianoulis P., 2002. Hybrid Photovoltaic/Thermal solar systems, Solar Energy 72, 217-234.
152. TRNSYS, 2004. Manual, Solar Energy Laboratory, University of Wisconsin, USA.
153. Tsoutsos, T., Aloumpi, E., Gkouskos, Z., Karagiorgas, M., 2010. Design of a solar absorption cooling system in a Greek hospital, Energy and Buildings 42 (2), 265–272.
154. Tzempelikos, A. and Athienitis, A.K., 2007. The impact of shading design and control on building cooling and lighting demand, Solar Energy 81(3): 369-382.
155. U.S. Department of Energy: Energy Efficiency and Renewable Energy (EERE), 2011. Air Barriers, http://www.energysavers.gov/your_home/insulation_airsealing/index.cfm/mytopic=11300. Retrieved 19, Feb., 2011.
156. Vreenegoor, R.C.P., Hensen, J.L.M. and de Vries, B., 2008. Review of existing energy performance calculation methods for district use, proceedings of IBPSA-NVL, Event, Eindhoven, The Netherlands, 9th of October.
157. Walton, G.N., 1983. The Thermal Analysis Research Program Reference Manual. National Bureau of Standards. (now NIST).
158. Wang, L., Gwilliam, J., Jones, P., 2009. Case study of zero energy house design in UK, Energy and Buildings 41 (11), 1215–1222.
159. Watson, I.D. and Johnson GT., 1987. Graphical estimation of sky-view factors in urban environments, Journal of Climatology, 7, 193–197.
160. Whitaker, C.M., Townsend, T. U., Wenger, H. J., Illiceto, A., Chimento, G. & Paletta, F. 1991. Effects of Irradiance and Other Factors on PV Temperature Coefficients. Conference Record of the 22nd IEEE Photovoltaic Specialists Conference, (Las Vegas, NV 7-10.10.1991), pp. 608-613. ISBN 0-87942-635-7.
161. Whole Building Design Guide (WBDG), a program of National Institute of Building Sciences, 2011. Daylighting, <http://www.wbdg.org/resources/daylighting.php>. Retrieved on 18, Dec., 2011.
162. Wiginton, L.K., Nguyen, H.T., Pearce, J.M., 2010. Quantifying roof top solar photovoltaic potential for regional renewable energy policy, Computers, Environment and Urban Systems 34 (4), 345–357.
163. Winkelmann, F.C., 2001. Modeling windows in EnergyPlus. Proc. IBPSA, Building Simulation.
164. Yannas, S., 1994. Solar Energy and Housing Design, Vol. 1, Architectural Association, London.

165. Yi, Y.K. and Malkawi, A.M., 2009. Optimizing building form for energy performance based on hierarchical geometry relation, *Automation in Construction* 18(6): p. 825-833.

APPENDICES

Appendix A

Sensitivity analysis of insulation level of walls and windows

A sensitivity analysis is conducted to find the effect of different level of wall insulation on the heating load of the rectangular shape. The graph of Figure A-1 shows that increasing the insulation beyond the level of 6-7 RSI does not lead to a significant decrease in heating load.

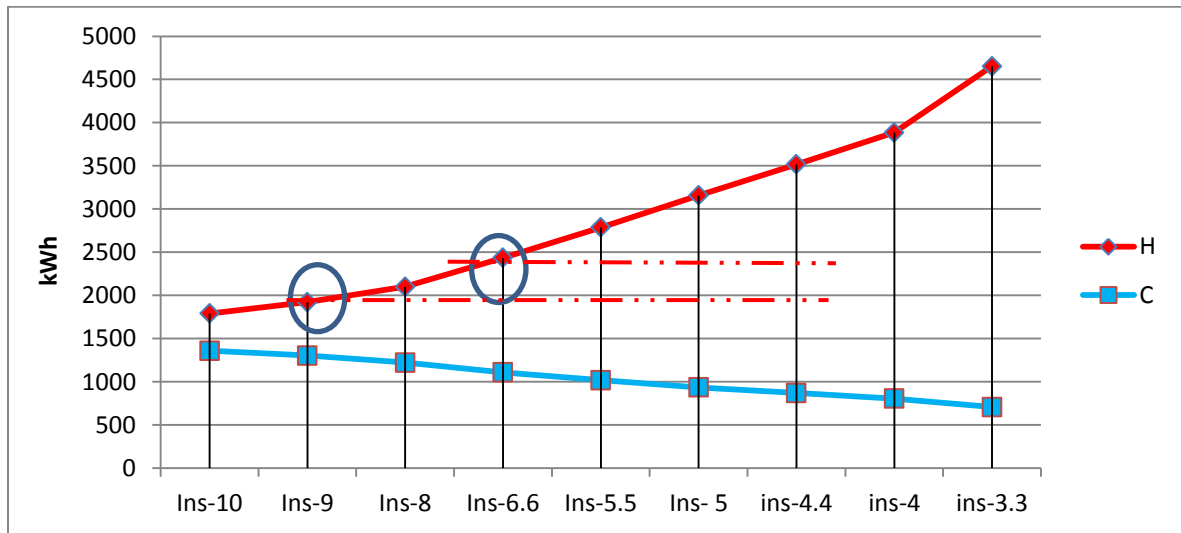


Figure A-1, effect of insulation on heating and cooling loads for the rectangular shape

Figure A-2 presents the analysis of window type effect on heating load. A double glazed low-e argon fill window can reduce the heating load by up to 40% as compared a double glazed window. A triple glazed low-e argon fill window can extend the energy saving for heating by about 16% as compared to the double glazed low-e, argon fill window.

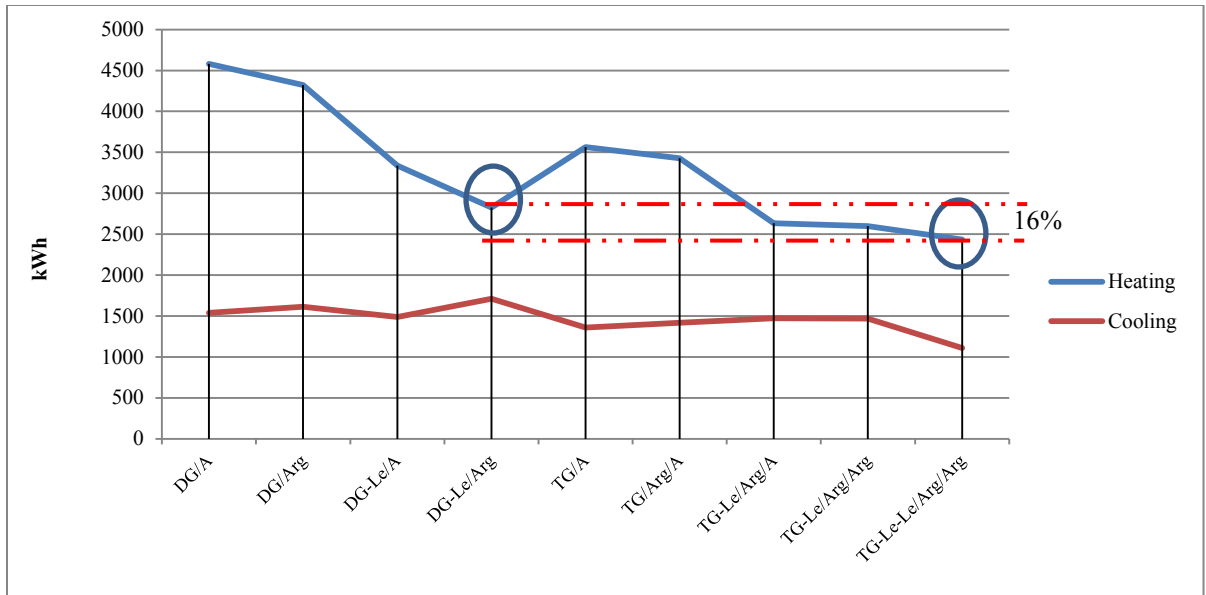


Figure A-2, effect of window characteristics on heating and cooling loads for the rectangular shape.

Figure A-3 is a sensitivity analysis conducted to find the coupled effect of insulation level of wall and the south facing window area, of a rectangular unit.

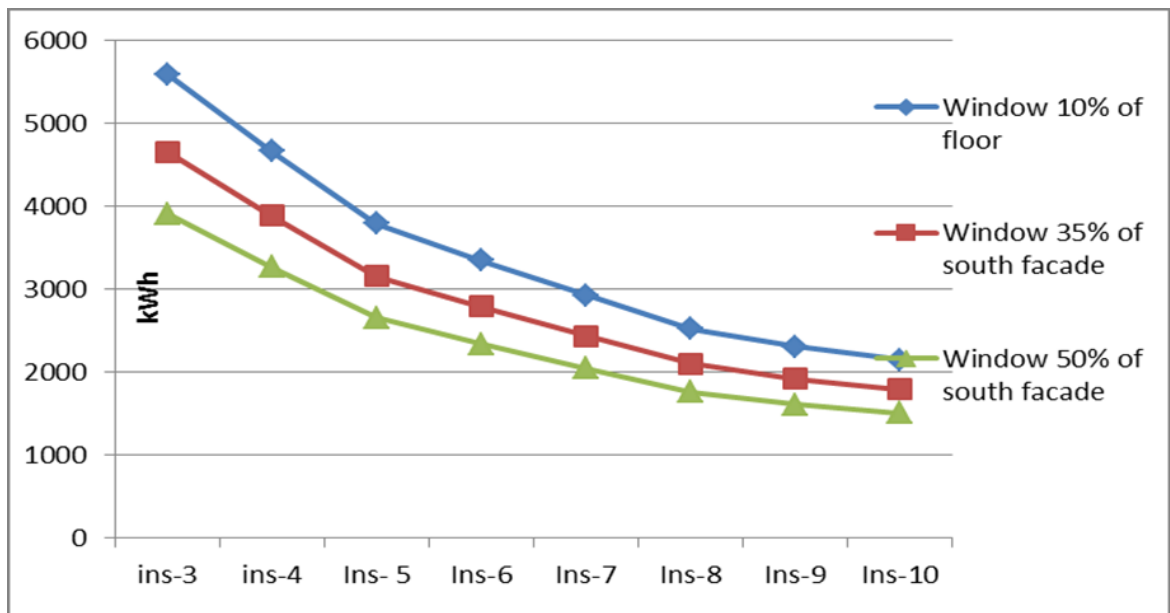


Figure A-3, Analysis of various insulation levels associated with different window size.

Appendix B

Roofs of L and L Variant Shapes

L shape and L variants are by their nature more complex than rectangular shape, and their roofs offer the possibility of design with various tilt angles and orientation (in the case of L variants)- as shown in previous chapters. The purpose of this section is only to illustrate possibilities and flexibility of design; however the extra complexity is probably not justified for small buildings such as housing units.

Split-surface roofs

An attempt is made to apply the concept of multifaceted roofs to L shape. Two possibilities are considered:

- 1) To consider a rectangular roof for the L shape. With small depth ratio it is possible to avoid cutting out the recess. This results in an overhang over the recessed part of the façade (Fig. B-1 a). For larger depth ratios the recess can be cut out (Fig. B-1b).
- 2) The second approach (which can be applied to L variants as well - Fig. B-3) is to consider the roof of the wing and of the main branch as two separate plate roofs. Each plate can be then designed at different tilt angle (see Fig. B-2).

First approach: Rectangular shape roof- with or without recess.

L shape roof can be designed in the same method as a rectangular roof. A part can serve as overhang (Fig. B-1a), or the recess can be cut out (Fig. B-1b).

In the case where a rectangular roof is used, the same principle of multifaceted roof used for the rectangular shape presented in Chapter V can be applied. In this case, it is recommended that the plate dimensions fit the dimensions of the façades of L shape, for better architectural design.

For the roof where the recess is cut out, three tilt angles are used: 35°, 40° and 45°. Each row of PV panels is characterized by a different tilt angle (see Fig. B-1). A disadvantage of this design is that it can result in a higher roof (compared to the rectangular shape) implying a large attic, and larger amount of materials as compared to the semi-hip roof design of L shape, employed throughout the research.

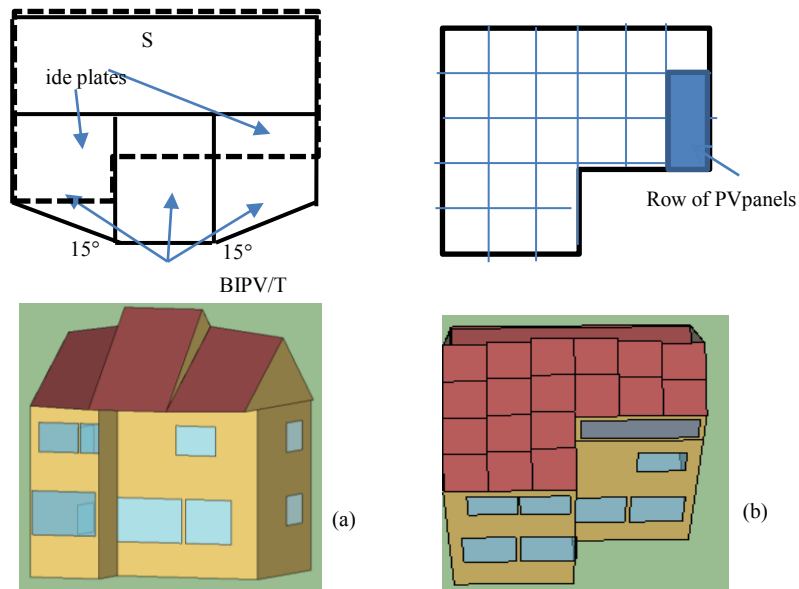


Figure B-1 , (a) rectangular roof, (b) roof with the recess cut out

Second Approach: Split Gable roofs

This part shows only few possibilities and not all the combinations that can be obtained. The focus is the type of roofs that can be designed for L and a few L variants.

In this approach, the wing and the main branch roofs are designed as separate gable roofs which may have the same or different tilt angles. This is shown in Figure B-2 a and b for L shape, and B-2 c for L variant (V-SW30).

The main problem in this design option is that with large tilt angle the wing roof may be considerably higher than the main branch roof, shading therefore its BIPV/T system (see figure B-2 b and c). This can be modified by reducing the surface area of the wing roof. But in this case an assessment should be done to find whether this option still beneficial (complexity / aesthetic/ energy generation).

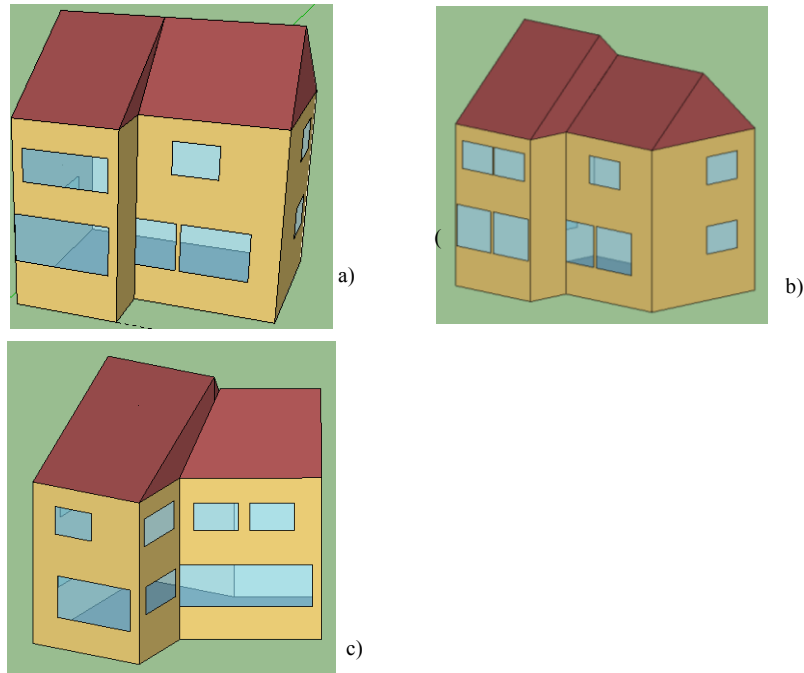


Figure B-2 , (a) rectangular roof, (b) roof with the recess cut out ; (c) L variant with a large wing surface

Folded Plate roofs

This is not easy to apply. An iterative design process needs to be applied that coordinates roof design with plan design to optimize both electricity generation and

functional space. Some attempts are made here at designs of selected L variants (V-SW30 and V-SW60), and L shape. The roof designs are limited only for plates with 30° orientations.

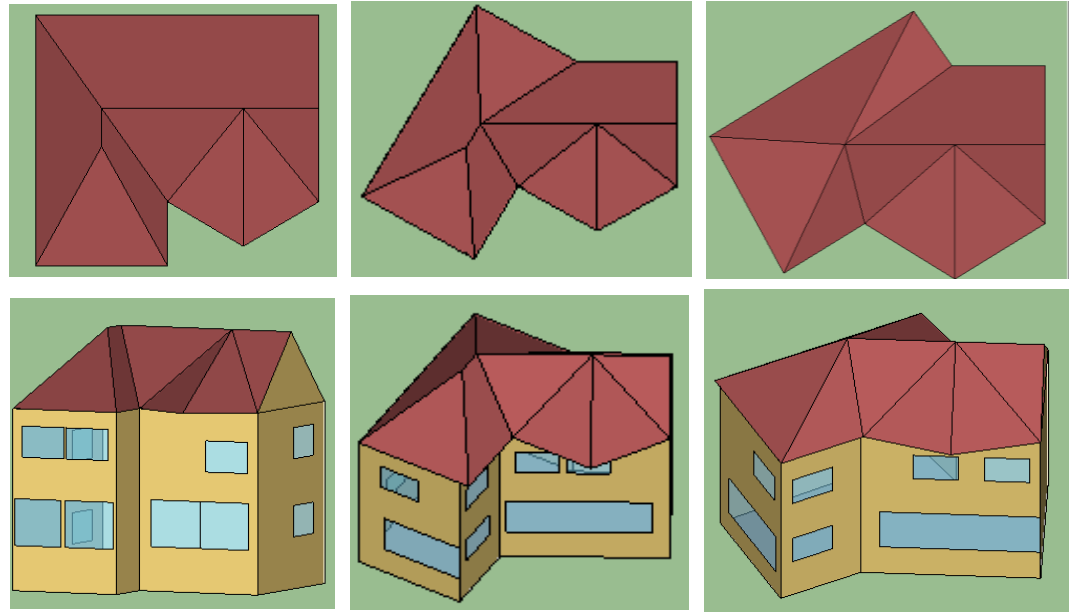


Figure B-3, folded plates L and L variants roof

Various additional possibilities of roofs of L and L variants are possible. Some of these are presented in Figure B-4.

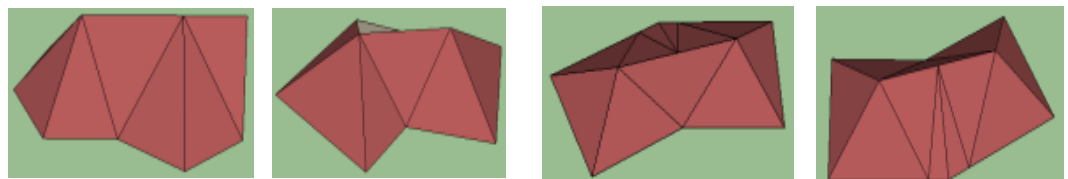


Figure B-4 – Additional possibilities of roof designs

Appendix C

Sensitivity Analysis of the Weight Assignment-Evaluation System

A sensitivity analysis is performed to identify the effect of weight assignment for the evaluation system of the design alternatives (proposed in chapter VI). Seven different alternatives, where weight of performance criteria is changed arbitrarily, and the evaluation of shape corresponding to these alternatives are presented below.

The results indicate that alternatives where heating consumption weight is lower than that of the cooling consumption (Alternatives 1, 2 and 3) or where there is no significant difference between the weights of these two criteria, the sum of the points gathered by the shapes is not significantly affected ($\leq 5\%$, as compared to the base case- the example presented in Chap VI- see Fig. C2). Alternatives (such as Alt.7- see Fig. C1) where cooling consumption is dominant (double the value of heating consumption), and where the weight of electricity generation criteria is reduced, favor shapes with small aspect ratio and large depth ratio (which cast shade on the south façade), which is expected. Some of the results of the sensitivity analysis are presented below, in tables of evaluation of shapes, and in Figures C1 and C2.

Table C1, Weight assignments for different alternatives

Alternatives	Weights			
	Heating Consumption	Cooling Consumption	Electricity generation	Shift of Peak Generation
Alt0	2	1	3	3
Alt1	2.2	1.3	2.9	0
Alt2	2.2	1.3	2.9	1.5
Alt3	1.9	1.5	2.5	2.5
Alt4	1.5	2	2.5	2.5
Alt5	1	2	2.3	2.3
Alt6	1	2	3	2.3
Alt7	1	3	2	1

Examples	Alternative 1					Total points
	Heating:	Cooling:	Generation:	Peak:		
	2.2	1.3	2.9	0		
AR	Heating	Cooling	Electricity	Shift of generation	Peak	
	2	13.2	0	29	0	42.2 ✓
	1.6	11	3.9	23.2	0	38.1 ✓
	1.3	11	6.5	14.5	0	32 ✓
	1	13.2	10.4	8.7	0	32.3 ✓
	0.6	4.4	13	0	0	17.4 ✗
Orientation		0	0	0	0	
60 (E,W)		0	0	8.7	0	8.7 ✗
45 (E,W)		4.4	0	17.4	0	21.8 ✗
30(E,W)		8.8	2.6	14.5	0	25.9 !
	0	11	6.5	14.5	0	32 ✓
Depth Ratio		0	0	0	0	
DR=1/2		8.8	6.5	23.2	0	38.5 ✓
DR=1		4.4	6.5	14.5	0	25.4 !
DR=3/2		2.2	6.5	5.8	0	14.5 ✗
Direction of the wing						
L-SW		8.8	6.5	23.2	0	38.5 ✓
L-SE		8.8	6.5	23.2	0	38.5 ✓
L-N		11	6.5	29	0	46.5 ✓
Number of shading facades						
n=1		8.8	6.5	23.2	0	38.5 ✓
n=2		4.4	6.5	23.2	0	34.1 ✓
Angle between the wings						
$\beta=0$		8.8	6.5	23.2	0	38.5 ✓
$\beta=30$		8.8	2.6	26.1	0	37.5 ✓
$\beta=45$		8.8	1.3	29	0	39.1 ✓
$\beta=60$		8.8	0	29	0	37.8 ✓
$\beta=70$		11	0	20.3	0	31.3 ✓

Alternative 2

Examples	Heating:	Cooling:	Generation:	Peak:	Total
AR	Heating	Cooling	Electricity generation	Shift of Peak	points
	2.2	1.3	2.9	1.5	
	2	13.2	0	29	0 ✓ 42.2
	1.6	11	3.9	23.2	0 ✓ 38.1
	1.3	11	6.5	14.5	0 ✓ 32
	1	13.2	10.4	8.7	0 ✓ 32.3
	0.6	4.4	13	0	0 ✗ 17.4
Orientation					0
60 (E,W)	0	0	8.7	4.5 ✗	13.2
45 (E,W)	4.4	0	17.4	3 !	24.8
30(E,W)	8.8	2.6	14.5	2.25 !	28.15
0	11	6.5	14.5	0 ✓	32
Depth Ratio					0
DR=1/2	8.8	6.5	23.2	0 ✓	38.5
DR=1	4.4	6.5	14.5	0 !	25.4
DR=3/2	2.2	6.5	5.8	0 ✗	14.5
Direction of the wing					0
L-SW	8.8	6.5	23.2	0 ✓	38.5
L-SE	8.8	6.5	23.2	0 ✓	38.5
L-N	11	6.5	29	0 ✓	46.5
Number of shading facades					0
n=1	8.8	6.5	23.2	0 ✓	38.5
n=2	4.4	6.5	23.2	0 ✓	34.1
Angle between the wings					0
$\beta=0$	8.8	6.5	23.2	0 ✓	38.5
$\beta=30$	8.8	2.6	26.1	2.25 ✓	39.75
$\beta=45$	8.8	1.3	29	3 ✓	42.1
$\beta=60$	8.8	0	29	4.5 ✓	42.3
$\beta=70$	11	0	20.3	4.5 ✓	35.8

Alternative 3

Examples	Heating : 1.9	Cooling: 1.5	Generation: 2.5	Peak: 2.5		
AR	Heating	Cooling	Electricity generation	Shift of Peak	Total points	
2	11.4	0	25	0	✓	36.4
1.6	9.5	4.5	20	0	✓	34
1.3	9.5	7.5	12.5	0	✓	29.5
1	11.4	12	7.5	0	✓	30.9
0.6	3.8	15	0	0	✗	18.8
Orientation						
60 (E,W)	0	0	7.5	7.5	✗	15
45 (E,W)	3.8	0	15	5	!	23.8
30(E,W)	7.6	3	12.5	3.75	!	26.85
0	9.5	7.5	12.5	0	✓	29.5
Depth Ratio						
DR=1/2	7.6	7.5	20	0	✓	35.1
DR=1	3.8	7.5	12.5	0	!	23.8
DR=3/2	1.9	7.5	5	0	✗	14.4
Direction of the wing						
L-SW	7.6	7.5	20	0	✓	35.1
L-SE	7.6	7.5	20	0	✓	35.1
L-N	9.5	7.5	25	0	✓	42
Number of shading facades						
n=1	7.6	7.5	20	0	✓	35.1
n=2	3.8	7.5	20	0	✓	31.3
Angle between the wings α						
$\beta=0$	7.6	7.5	20	0	✓	35.1
$\beta=30$	7.6	3	22.5	3.75	✓	36.85
$\beta=45$	7.6	1.5	25	5	✓	39.1
$\beta=60$	7.6	0	25	7.5	✓	40.1
$\beta=70$	9.5	0	17.5	7.5	✓	34.5

Alternative 4

Examples	Heating :	Cooling:	Generation:	Peak:		
	1.5	2	2.5	2.5		
AR	Heating	Cooling	Electricity generation	Shift of Peak	Total points	
	2	9	0	25	0	✓ 34
	1.6	7.5	6	20	0	✓ 33.5
	1.3	7.5	10	12.5	0	✓ 30
	1	9	16	7.5	0	✓ 32.5
	0.6	3	20	0	0	! 23
Orientation						
		0				
60 (E,W)		0	0	7.5	7.5	✗ 15
45 (E,W)		3	0	15	5	! 23
30(E,W)		6	4	12.5	3.75	! 26.25
	0	7.5	10	12.5	0	✓ 30
Depth Ratio						
		0				
DR=1/2		6	10	20	0	✓ 36
DR=1		3	10	12.5	0	! 25.5
DR=3/2		1.5	10	5	0	✗ 16.5
Direction of the wing						
L-SW		6	10	20	0	✓ 36
L-SE		6	10	20	0	✓ 36
L-N		7.5	10	25	0	✓ 42.5
Number of shading facades						
n=1		6	10	20	0	✓ 36
n=2		3	10	20	0	✓ 33
Angle between the wings						
$\beta=0$		6	10	20	0	✓ 36
$\beta=30$		6	4	22.5	3.75	✓ 36.25
$\beta=45$		6	2	25	5	✓ 38
$\beta=60$		6	0	25	7.5	✓ 38.5
$\beta=70$		7.5	0	17.5	7.5	✓ 32.5























Alternative 5

Examples	Heating : 1	Cooling: 2	Generation 2.3	Peak: 2.3		
AR	Heating	Cooling	Electricity generation	Shift of Peak	Total points	
	2	6	0	23	0	✓ 29
	1.6	5	6	18.4	0	✓ 29.4
	1.3	5	10	11.5	0	! 26.5
	1	6	16	6.9	0	✓ 28.9
	0.6	2	20	0	0	✗ 22
Orientation						
60 (E,W)		0	0	6.9	6.9	✗ 13.8
45 (E,W)		2	0	13.8	4.6	✗ 20.4
30(E,W)		4	4	11.5	3.45	! 22.95
	0	5	10	11.5	0	! 26.5
Depth Ratio						
DR=1/2		4	10	18.4	0	✓ 32.4
DR=1		2	10	11.5	0	! 23.5
DR=3/2		1	10	4.6	0	✗ 15.6
Direction of the wing						
L-SW		4	10	18.4	0	✓ 32.4
L-SE		4	10	18.4	0	✓ 32.4
L-N		5	10	23	0	✓ 38
Number of shading facades						
n=1		4	10	18.4	0	✓ 32.4
n=2		2	10	18.4	0	✓ 30.4
Angle between the wings						
$\beta=0$		4	10	18.4	0	✓ 32.4
$\beta=30$		4	4	20.7	3.45	✓ 32.15
$\beta=45$		4	2	23	4.6	✓ 33.6
$\beta=60$		4	0	23	6.9	✓ 33.9
$\beta=70$		5	0	16.1	6.9	! 28

Alternative 6

Examples	Heating : 1 Heating	Cooling: 2 Cooling	Generation: 3 Electricity generation	Peak: 2.3 Shift of Peak	Total points		
	2	6	0	30	0	✓	36
	1.6	5	6	24	0	✓	35
	1.3	5	10	15	0	✓	30
	1	6	16	9	0	✓	31
	0.6	2	20	0	0	✗	22
Orientation					0		
60 (E,W)		0	0	9	6.9	✗	15.9
45 (E,W)		2	0	18	4.6	!	24.6
30(E,W)		4	4	15	3.45	!	26.45
	0	5	10	15	0	✓	30
Depth Ratio					0		
DR=1/2		4	10	24	0	✓	38
DR=1		2	10	15	0	!	27
DR=3/2		1	10	6	0	✗	17
Direction of the wing					0		
L-SW		4	10	24	0	✓	38
L-SE		4	10	24	0	✓	38
L-N		5	10	30	0	✓	45
Number of shading facades					0		
n=1		4	10	24	0	✓	38
n=2		2	10	24	0	✓	36
Angle between the wings					0		
$\beta=0$		4	10	24	0	✓	38
$\beta=30$		4	4	27	3.45	✓	38.45
$\beta=45$		4	2	30	4.6	✓	40.6
$\beta=60$		4	0	30	6.9	✓	40.9
$\beta=70$		5	0	21	6.9	✓	32.9

Alternative 7

Examples	Heating : 1	Cooling: 3	Generation 2	Peak: 1		
AR	Heating	Cooling	Electricity generation	Shift of Peak	Total points	
	2	6	0	20	0	26 
	1.6	5	9	16	0	30 
	1.3	5	15	10	0	30 
	1	6	24	6	0	36 
	0.6	2	30	0	0	32 
Orientation						
60 (E,W)		0	0	6	3	9 
45 (E,W)		2	0	12	2	16 
30(E,W)		4	6	10	1.5	21.5 
	0	5	15	10	0	30 
Depth Ratio						
DR=1/2		4	15	16	0	35 
DR=1		2	15	10	0	27 
DR=3/2		1	15	4	0	20 
Direction of						
L-SW		4	15	16	0	35 
L-SE		4	15	16	0	35 
L-N		5	15	20	0	40 
Number of shading faca						
			0	0	0	
n=1		4	15	16	0	35 
n=2		2	15	16	0	33 
Angle between the wings						
$\beta=0$		4	15	16	0	35 
$\beta=30$		4	6	18	1.5	29.5 
$\beta=45$		4	3	20	2	29 
$\beta=60$		4	0	20	3	27 
$\beta=70$		5	0	14	3	22 

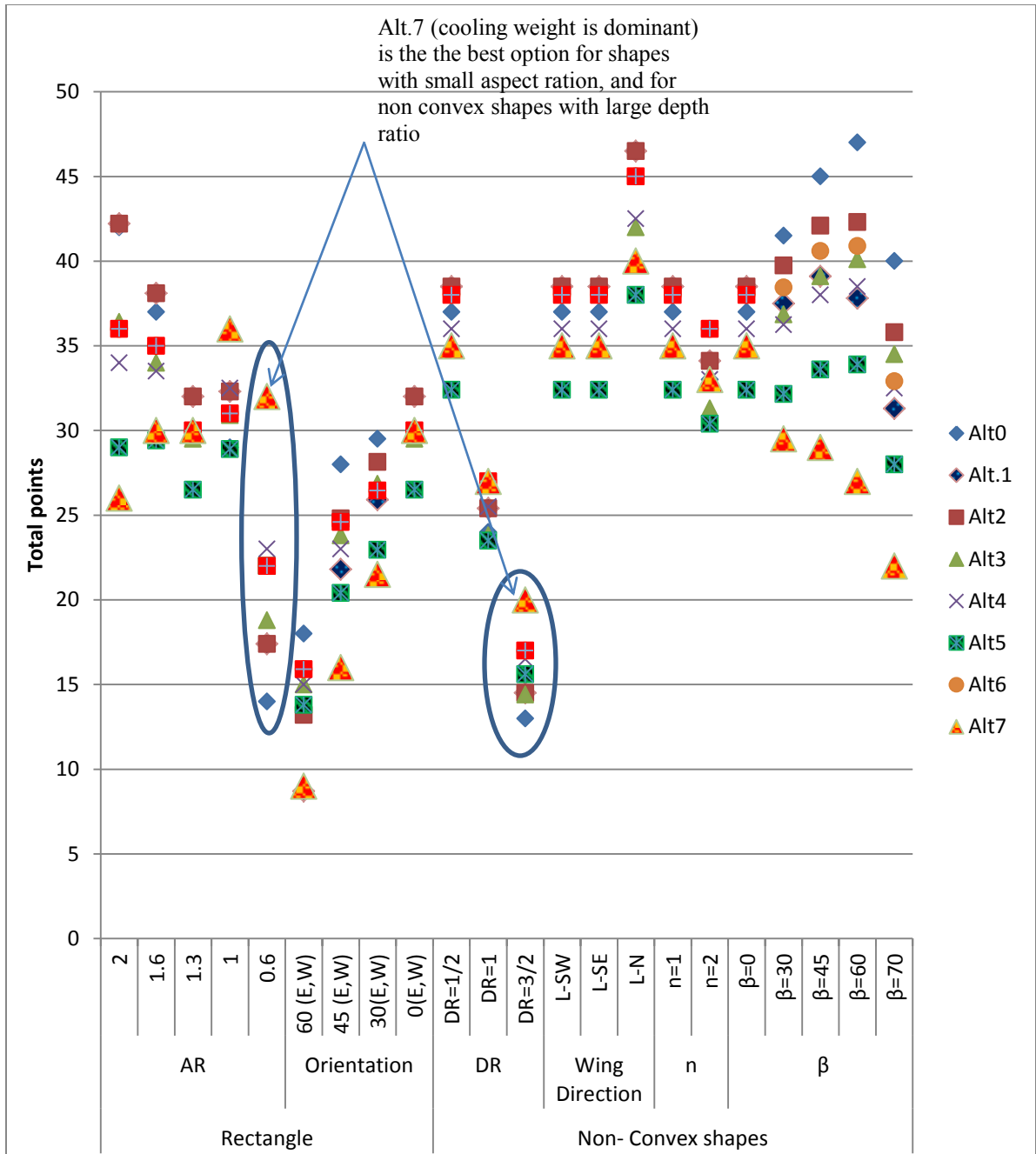


Figure C1, representation of all points accumulated by each shapes, for each alternative of weight assignment

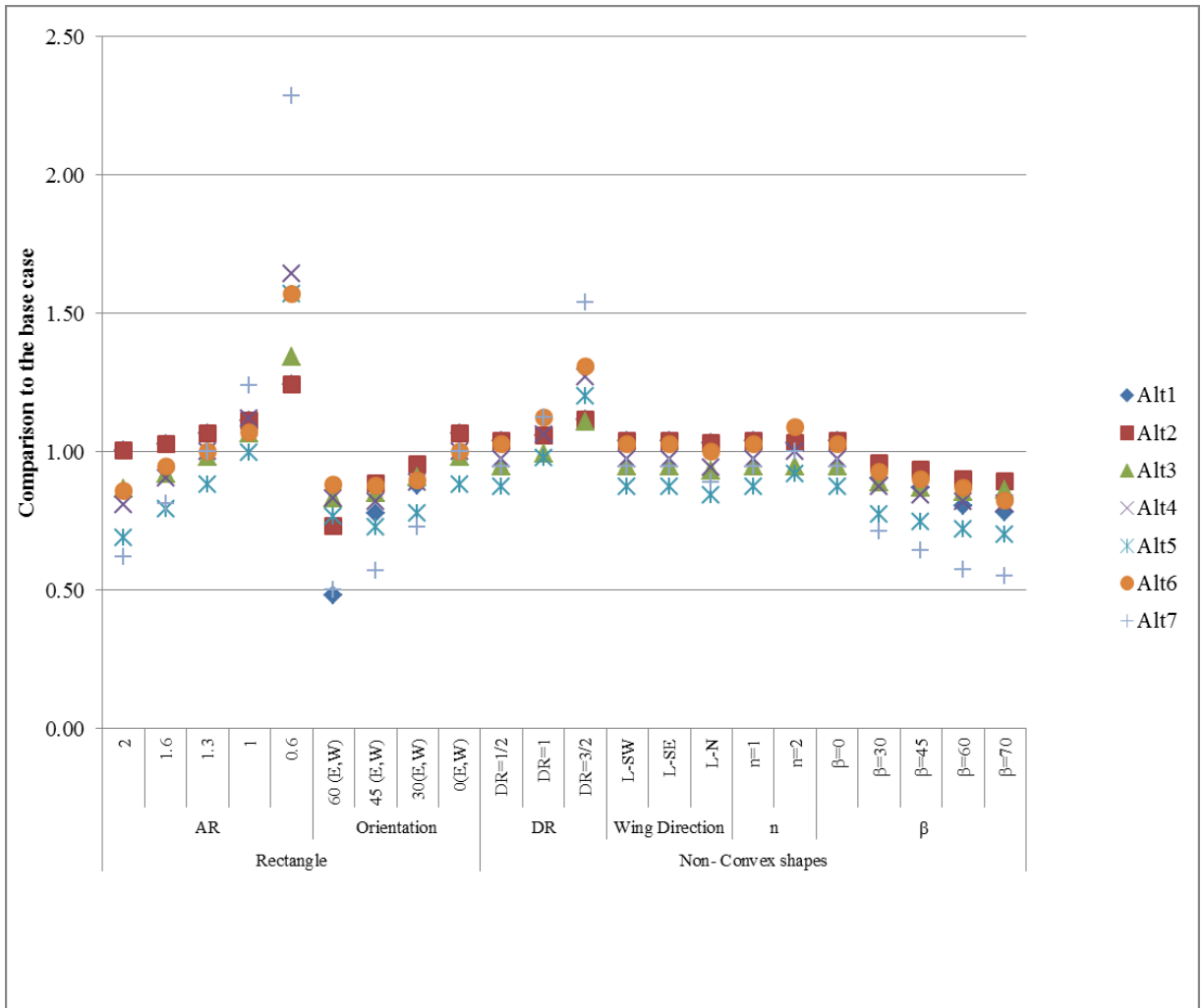


Figure C2, comparison of all alternatives of weight assignments to the base case (the example presented in Chapter VI)

GLOSSARY

Aspect Ratio: Ratio of equatorial facing façade to the perpendicular façade.

Building-Integrated: A component that is designed to be part of a façade or roof. In this work, it refers to solar collectors (photovoltaic or thermal or both).

Coefficient of performance (COP)-Heat pump: The ratio of the rate of energy output of the heat pump to the rate of energy input, under specific operating conditions (ASHRAE Standard, 90.1, 2007).

Design Day (DD): A day having representative climatic conditions for specific objectives design. In this document two design days are selected to represent sunny winter and summer days (Hong et al, 1999).

Depth Ratio: In non-convex housing unit shapes having two or more wings, where wings are mutually shading, the depth ratio is the ratio of the width of the shade-casting façade (non-equatorial facing) to the width of the shaded façade (equatorial facing).

Energy performance: Energy performance criteria of buildings and neighborhood includes total annual energy consumption, energy generation (electricity and heat) and time spread of peak electricity generation

Exposed facade: In a non-convex shapes exposed façade refers to the equatorial or near-equatorial façade of a shading wing that is perpendicular to the shade casting façade.

L Variations: L shapes with different angles between the wings.

Non-convex Shape: A shape where at least one line segment connecting two points along the boundary lies outside the shape.

Net-zero energy homes (NZEH): Houses which, on an annual basis, produce as much energy from renewable sources as they consume.

Obtuse Angle: Special L variant with large value of the angle β between the wings ($\beta=70^\circ$ is adopted in the study).

Orientation Angle: The orientation angle of a surface is defined as the angle between equatorail and the projection on a horizontal plane of the normal to this surface.

Passive solar strategy: The act of collecting solar energy and storing it within a building's structure to offset energy demand without dependence on active systems.

Planar Obstruction Angle (POA): POA concept represents the angle between the center of the equatorial façade of the shaded unit and the closest corner of the shading unit.

Shaded facades: Facade in non-convex geometries that are shaded by other facades. In this research they refer to the equatorial facing facades, shaded by the adjacent one.

Solar Potential: Passive potential involves irradiation and transmission of heat and daylighting by fenestration of near-equatorial-facing facades. Active potential consists of generation of both electricity and thermal energy employing building integrated photovoltaic thermal systems (BIPV/T).

Space load (heating and cooling): The amount of energy that must be added to or extracted from a space to maintain thermal comfort (ASHRAE, 2005).

Summer Design Day (SDD): Represents an extreme hot sunny day.

Tilt Angle: Tilt angle of a surface is the angle between the normal to the surface and the vertical direction.

Winter Design Day (WDD): Represents an extreme cold sunny day.